COMPARISON OF KYRIAZIS AND ANTICANCER MODELS WITH CLINICAL PATTERN OF METASTASIS

Tumor Type	Cell Line	Kyriazis (19)	AntiCancer MetaMouse	Clinical Pattern of Metastasis
Bladder (Transitional cell carcinoma)	RT-4	No metastasis	Liver, pancreas, diaphragm, omentum, iliac lymph nodes, superficial inguinal lymph nodes, gastric lymph nodes (1).	Regional lymph nodes, liver, lung, pancreas, diaphragm, spleen (2, Chapter 107).
Bladder (Transitional cell carcinoma)	RT-10		Liver, lung, pancreas, spleen, diaphragm, lymph nodes (21).	
Bladder (Transitional cell carcinoma)	SW-800	Submaxillary lymph node, salivary gland, diaphragm		
Bladder (Transitional cell carcinoma)	SW-780	Pectoral and intercostal muscles, mediastinal lymph nodes.		
Bladder (Mucinous adenocarcinoma)	13678	Inconsistent finding		

Exhibit 2 RMH

COMPARISON OF KYRIAZIS AND ANTICANCER MODELS WITH CLINICAL PATTERN OF METASTASIS

Tumor Type	Cell Line	Kyriazis (19)	AntiCancer MetaMouse	Clinical Pattern of Metastasis
Colon	SW-480 (Well differentiated adenocarcinoma)	Lymph node and lungs		Liver, mesenteric lymph nodes, omentum, peritoneum, lung, abdominal wall, disseminated carcinomatosis (2, Chapter 103).
Colon	Co-3 (Well differentiated adenocarcinoma)		Liver, peritoneum, mesenteric lymph nodes, lung, omentum, abdominal wall, ileum (6-8).	
Colon	AC-1935 (Moderately differentiated adenocarcinoma)		Liver, peritoneum, mesenteric lymph nodes, lung, abdominal wall (9).	
Colon	COL-2-JCK (Poorly differentiated adenocarcinoma)		Liver (10,11).	
Colon	COL-3-JCK (Poorly differentiated adenocarcinoma)		Liver (11). Mesenteric lymph nodes (7).	
Colon	COL-5-JCK (Well differentiated adenocarcinoma)		Liver (11).	
Colon	Patient colon cancer specimens		Liver, lymph nodes, local invasion, disseminated carcinomatosis (12).	

COMPARISON OF KYRIAZIS AND ANTICANCER MODELS WITH CLINICAL PATTERN OF METASTASIS

Tumor Type	Cell Line	Kyriazis (19)	AntiCancer MetaMouse	Clinical Pattern of Metastasis
Pancreas	(Mia)PaCa (Well differentiated adenocarcinoma)	Axillary lymph nodes, lung.	Liver, spleen, portal lymph nodes, stomach, mediastinum, lung, retroperitoneum (13, 16, 20).	Liver, spleen, portal lymph nodes, colon, stomach, mediastinum, lung, kidney, retroperitoneum, diaphragm, small intestine (2, Chapter 101).
Pancreas	Capan-1	Lymph nodes, lung.		
Pancreas	Patient specimens		Liver, stomach, duodenum, regional lymph nodes, adrenal gland, diaphragm, mediastinal lymph nodes (14).	
Pancreas	Panc-4		Liver, peritoneal, duodenum (15).	
Pancreas	BxPC-3		Portal lymph nodes, retroperitoneum, spleen, liver, diaphragm, small intestine, colon, liver, kidney, mediastinum, lung, omentum (13, 16,20).	
Pancreas	Pan-12-JCK		Liver, kidney, regional and distant lymph nodes, lung, adrenal gland (17,18).	

COMPARISON OF KYRIAZIS AND ANTICANCER MODELS WITH CLINICAL PATTERN OF METASTASIS

Tumor Type	Cell Line	Kyriazis (19)	AntiCancer MetaMouse	Clinical Pattern of Metastasis
Breast	BrCa	Lymph nodes		Axillary lymph nodes, lung, liver, bone (2, Chapter 118).
Breast	MDA-MB-435		Axillary lymph nodes, lung, liver (3). Bone (4).	
Breast	AC-2468 (Patient breast cancer specimen)		Lung (5).	

REFERENCES:

1. Fu, X., and Hoffman, R.M. Human RT-4 bladder carcinoma is highly metastatic in nude mice and comparable to *ras*-H-transformed RT-4 when orthotopically onplanted as histologically intact tissue. Int. J. Cancer **51**, 989-991, 1992.

2. Holland, James E., and Frei, Emil III (eds.), Cancer Medicine, 5th Edition. Hamilton, Ontario, Canada: B.C. Decker, Inc., 2000.

3. Li, X-M., Wang, J-W., An, Z., Yang, M. Baranov, E., Jiang, P., Sun, F-X., Moossa, A.R., and Hoffman, R.M. Optically-imageable metastatic model of human breast cancer. Clinical & Experimental Metastasis, in press.

4. An, Z., et al., unpublished.

5. Fu, X., Le, P., and Hoffman, R.M. A metastatic orthotopic-transplant nude-mouse model of human patient breast cancer. Anticancer Res. **13**, 901-904, 1993.

6. Fu, X., Herrera, H., Kubota, T., and Hoffman, R.M. Extensive liver metastasis from human colon cancer in nude and scid mice after orthotopic onplantation of histologically-intact human colon carcinoma tissue. Anticancer Res. **12**, 1395-1398, 1992.

7. Togo, S., Shimada, H., Kubota, T., Moossa, A.R., Hoffman, R.M. Host organ specifically determines cancer progression. Cancer Res. **55**, 681-684, 1995.

8. An, Z., Wang, X., Willmott, N., Chander, S.K., Tickle, S., Docherty, A.J.P., Mountain, A., Millican, A.T., Morphy, R., Porter, J.R., Epemolu, R.O., Kubota, T., Moossa, A.R., and Hoffman, R.M. Conversion of highly malignant colon cancer from an aggesssive to a controlled disease by oral administration of a metalloproteinase inhibitor. Clinical & Experimental Metastasis **15**, 184-195, 1997.

9. Wang, X., Fu, X., Brown, P.D., Crimmin, M.J., and Hoffman, R.M. Matrix metalloproteinase inhibitor BB-94 (Batimastat) inhibits human colon tumor growth and spread in a patient-like orthotopic model in nude mice. Cancer Res. **54**, 4726-4728, 1994.

10. Furukawa, T., Kubota, T., Watanabe, M., Kuo, P.H., Kase, S., Saikawa, Y., Tanino, H., Teramoto, T., Ishibiki, K., Kitajima, M., and Hoffman, R.M. Immunochemotherapy prevents human colon cancer metastasis after orthotopic onplantation of histologically-intact tumor tissue in nude mice. Anticancer Res. **13**, 287-291, 1993.

11. Kuo, T-H., Kubota, T., Watanbe, M., Furukawa, T., Teramoto, T., Ishibiki, K., Kitajimi, M., Moossa, A.R., Penman, S., Hoffman, R.M. Liver colonization competence governs colon cancer metastasis. Proc. Natl. Acad. Sci. USA **92**, 12085-12089, 1995.

12. Fu, X., Besterman, J.M., Monosov, A., and Hoffman, R.M. Models of human metastatic colon cancer in nude mice orthotopically constructed by using histologically intact patient specimens. Proc. Natl. Acad. Sci. USA **88**, 9345-9349, 1991.

13. Bouvet, M., Yang, M., Nardin, S., Wang, X., Jiang, P., Baranov, E., Moossa, A.R., Hoffman, R.M. Chronologically-specific metastatic targeting of human pancreatic tumors in orthotopic models. Clinical & Experimental Metastasis **18**, 213-218, 2000.

14. Fu, X., Guadagni, F., and Hoffman, R.M. A metastatic nude-mouse model of human pancreatic cancer constructed orthotopically from histologically intact patient specimens. Proc. Natl. Acad. Sci. USA **89**, 5645-5649, 1992.

15. Furukawa, T., Kubota, T., Watanabe, M., Kitajima, M., and Hoffman, R.M. A novel "patient-like" treatment model of human pancreatic cancer constructed using orthotopic transplantation of histologically intact human tumor tissue in nude mice. Cancer Res. **53**, 3070-3072, 1993.

16. Lee, N.C., Bouvet, M., Nardin, S., Jiang, P., Baranov, E., Rashidi, B., Yang, M., Wang, X., Moossa, A.R., and Hoffman, R.M. Antimetastatic efficacy of adjuvant gemcitabine in a pancreatic cancer orthotopic model. Clinical & Experimental Metastasis **18**, 379-384, 2001.

17. An, Z., Wang, X., Kubota, T., Moossa, A.R., Hoffman, R.M. A clinical nude mouse metastatic model for highly malignant human pancreatic cancer. Anticancer Res. **16**, 627-632, 1996.

18. Tomikawa, M., Kubota, T., Matsuzaki, S.W., Takahasi, S., Kitajima, M., Moossa, A.R., and Hoffman, R.M. Mitomycin C and cisplatin increase survival in a human pancreatic cancer metastatic model. Anticancer Res. **17**, 3623-3626, 1997.

19. Kyriazis, A.P., Kyriazis, A.A., McCombs, William B. III, and Kereiakes, J.A. Biological behavior of human malignant tumors grown in the nude mouse. Cancer Res. **41**, 3995-4000, 1981.

20. Bouvet, M., Wang, J-W., Nardin, S.R., Nassirpour, R., Yang, M., Baranov, E., Jiang, P., Moossa, A.R., and Hoffman, R.M. Real-time optical imaging of primary tumor growth and multiple metastatic events in a pancreatic cancer orthotopic model. Cancer Research **62**, 1534-1540, 2002.

21. Fu, X., Theodorescu, D., Kerbel, R.S., and Hoffman, R.M. Extensive multi-organ metastasis following orthotopic onplantation of histologically-intact human bladder carcinoma tissue in nude mice. Int. J. Cancer **49**, 938-939, 1991.

Int. J. Cancer: 51, 989–991 (1992)

Publication of the International Union Against Cancer
Publication de l'Union Internationale Contre le Cancer

LETTER TO THE EDITOR

Dear Sir,

Human RT-4 bladder carcinoma is highly metastatic in nude mice and comparable to *ras*-H-transformed RT-4 when orthotopically onplanted as histologically intact tissue

It has been estimated that 5–10% of human transitional-cell carcinomas (TCCs) of the bladder contain a mutated ras *gene (Theodorescu* et al., *1990). This raises the question of whether activated* ras *genes are causal to acquisition of the metastatic program of bladder tumors. Theodorescu* et al. *(1990) observed that the RT-4 human bladder carcinoma line is not invasive in nude mice, even after orthotopic injection of disaggregated cells. However, when a mutated human H-*ras *gene was transfected into RT-4 so that over-expression of the gene occurred in selected cell lines such as RT-4-mr-10 (RT-10), the selected cell line was able to locally invade the bladder after transurethral orthotopic inoculation of disaggregated cells. However, no contiguous or metastatic spread by RT-10 was found in other organs. The parental cell lines and the* ras*-transfectants all produced tumors when inoculated s.c. However, the tumors grew in the s.c. site as pseudoencapsulated masses without any evidence of tissue invasion (Theodorescu* et al., *1990).*

We have developed an intact-tissue onplant method of orthotopic transplantation of human tumors in nude mice (Fu et al., *1991*a,b*). This method, first developed with colon cancer (Fu* et al., *1991*a*), allows surgical patient tissue to be directly grafted onto the orthotopic organ of the nude mouse with resulting local growth and subsequent extensive regional metastases, lymph-node and liver metastases (Fu* et al., *1991*a*). The method utilized harvested, s.c.-grown tissue of RT-10 as a tissue source, and showed that the orthotopically-onplanted RT-10 was highly metastatic to many organs in the nude mouse (Fu* et al., *1991*b*). These results contrasted with findings obtained by injection of disaggregated cells of RT-10, which were invasive but not metastatic (Theodorescu* et al., *1990). We have now applied the orthotopic onplant method to histologically intact tissue of the parental RT-4 itself and found that it, too, was highly metastatic.*

RT-4 human bladder cells were obtained from the ATCC (Rockville, MD) and grown s.c. in 4-week-old outbred female nude mice. The s.c. grown tumors were excised and cut into 2-mm^3 pieces and orthotopically onplanted as previously described (Fu et al., *1991*a,b*). Briefly, the nude mice were anesthetized with isofluorene inhalation and the lower abdomen was sterilized with iodine and alcohol swabs. A small midline incision was made and the urinary bladder was exposed. The surgical adhesive 2-cyanoacrylic acid ester was applied on one side of the 2-mm^3 tumor xenograft tissue and the piece of tumor was subsequently glued on top of the urinary bladder. The abdominal incision was closed with 7-0 silk surgical sutures in one layer. The animals were then kept in a sterile environment. When the animals were moribund they were sacrificed and full autopsies were performed. At autopsy all major organs were grossly examined. Each organ was fixed in 10% formalin, dehydrated, embedded in paraffin, sectioned and stained with hematoxylin and eosin.*

After orthotopic transplantation of RT-4 to the nude-mouse bladder, extensive local growth occurred (over 2 cm × 2 cm) along with invasion of the bladder with metastases to the lymph nodes, diaphragm, abdominal wall, omentum, pancreas and liver (Table I). These results are similar to those with the ras*-H-transformed RT-4 tumor RT-10 after orthotopic onplantation of intact tissue (Fu* et al., *1991*b*). Figure 1*a *shows a nude mouse bladder in which RT-4 had grown orthotopically for 83 days. As can be seen, the tumor formed large masses in the abdominal area and became much larger than the bladder itself (also shown). Figure 1*b *shows the nude mouse bladder after orthotopic onplantation of normal human-bladder tissue which did not result in tumor formation, thus emphasizing the tumor-forming ability of RT-4. Figure 1*c *shows the pathohistology of the locally-growing RT-4 tumor in the nude mouse which is a typical transitional-cell carcinoma. Figure 1*d *shows a greatly enlarged nude-mouse iliac lymph node involved with tumor. Figure 1*e *shows the pathohistology of the tumor-involved lymph node in the nude mouse, indicating typical transitional-cell carcinoma. Figure 1*f *shows the human RT-4 bladder tumor which has metastasized to the pancreas, liver serosa and lymph nodes in the nude mouse. The metastatic tumor growth on the liver serosa did not invade the parenchymal tissue. Therefore, the possibility of transcoelomic spread cannot be ruled out. Figure 1*g *shows the histopathology of the pancreatic metastasis in the nude mouse. Figure 1*h *shows tumor-involved gastric lymph nodes. Figure 1*i *shows the pathohistology of the tumor-involved gastric lymph node of the nude mouse, indicating transitional-cell carcinoma. Figure 1*j *shows the excised nude mouse diaphragm fully involved with bladder tumor. Figure 1*k *shows the pathohistology of the tumor-involved diaphragm of the nude mouse indicating transitional-cell carcinoma. The entire diaphragm was replaced by*

TABLE I – GROWTH AND METASTASIS OF THE RT-4 BLADDER CARCINOMA IN NUDE MICE AFTER ORTHOTOPIC ONPLANTATION

Onplantation strategy	Mouse number	Primary tumor growth	Local invasion	Lymph-node metastasis[1]	Organ metastasis[2]
Orthotopic onplantation of intact RT-4 tumor tissue	8	8/8	8/8	5/8	3/8
Orthotopic onplantation of intact normal human bladder specimen	4	0/4	0/4	0/4	0/4
Orthotopic onplantation of intact normal mouse bladder specimen	3	0/3	0/3	0/3	0/3

[1]Lymph nodes include: iliac lymph node, superficial inguinal lymph node, gastric lymph node, pancreatic lymph node.–[2]Organs include: liver, pancreas, diaphragm, omentum.

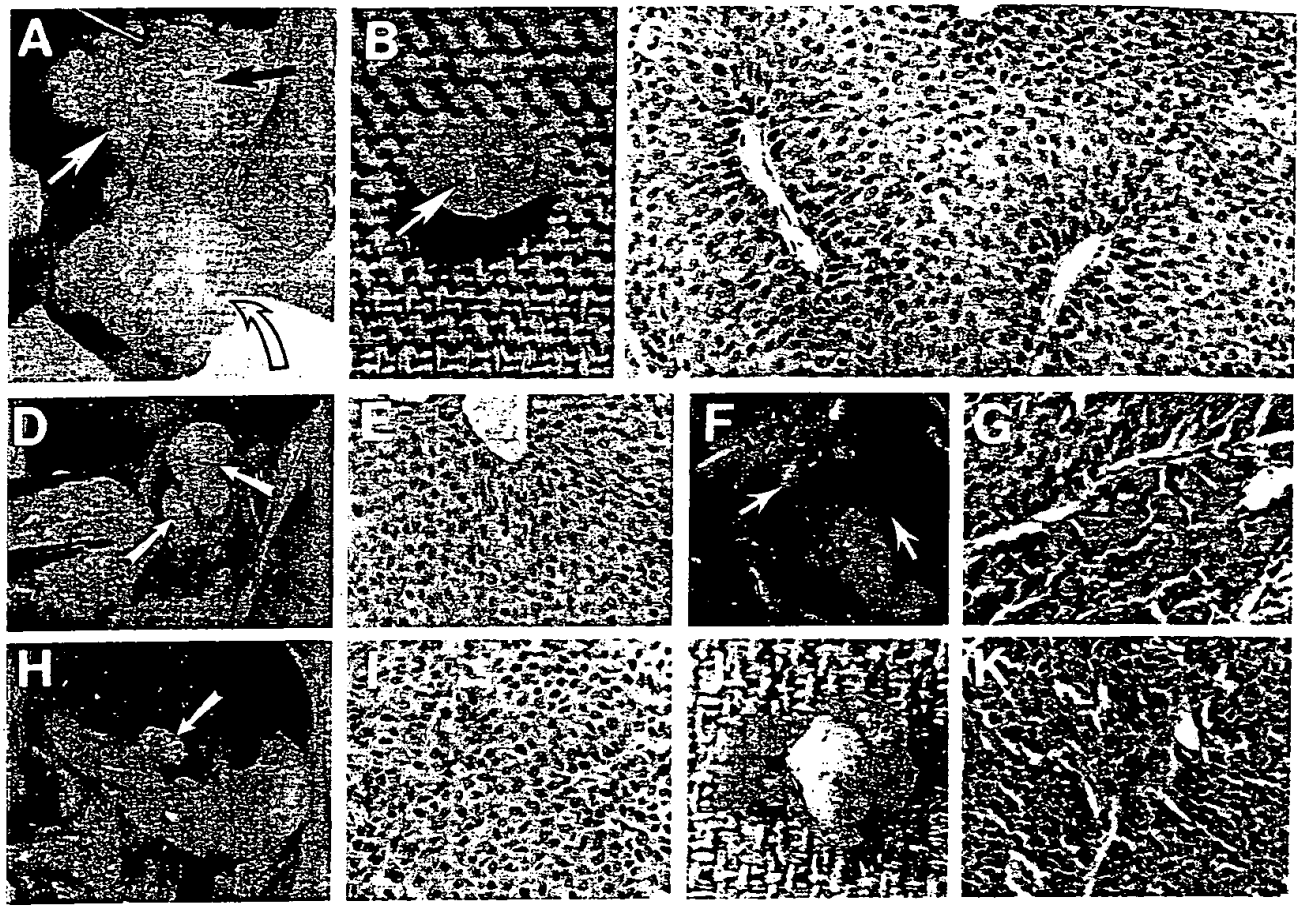

FIGURE 1 – *(a)* Tumor growth and invasion of human bladder RT-4 tumor after orthotopic onplantation to nude mouse bladder (83 days). Black arrow indicates tumor growing on nude mouse bladder. White arrow indicates nude mouse bladder. Curved arrow indicates abdominal wall tumor metastasis. *(b)* Nude mouse bladder after onplantation of normal intact human bladder tissue (73 days). Arrow indicates the residue of the onplanted tissue. *(c)* Histopathology of human-bladder RT-4 tumor growth on nude mouse bladder. *(d)* Nude mouse iliac lymph-node metastases after orthotopic onplantation of human bladder RT-4 tumor on nude mouse bladder (arrows). *(e)* Histopathology of nude mouse iliac lymph-node metastasis after human bladder RT-4 tumor orthotopic onplantation. *(f)* Nude mouse liver, pancreas and lymph-node metastases after orthotopic onplantation of human bladder RT-4 tumor. Blue arrow indicates a metastatic deposit on nude mouse liver. Black arrow indicates pancreatic metastasis. White arrows indicate lymph-node metastases. *(g)* Histopathology of nude-mouse pancreatic metastases after orthotopic onplantation of human bladder RT-4 tumor. The area above the arrow indicates tumor growth. The area below the arrow indicates normal pancreas of the nude mouse. *(h)* Nude mouse gastric lymph-node metastasis after orthotopic onplantation of human bladder RT-4 tumor. *(i)* Histopathology of nude mouse gastric lymph-node metastasis after orthotopic onplantation of human bladder RT-4 tumor. *(j)* Nude mouse diaphragm metastasis after orthotopic onplantation of human bladder RT-4 tumor. *(k)* Histopathology of nude mouse diaphragm metastasis after orthotopic onplantation of human bladder RT-4 tumor.

the metastatic growth, its normal structure being completely destroyed.

The spread of RT-4 to lymph nodes and other specific sites on a repeatable basis makes it unlikely that the distant tumor growth is due to non-specific seeding from the onplant procedure. These results contrast with findings obtained when disaggregated RT-4 cells are injected transurethrally, in which case neither invasion nor metastases can be observed (Theodorescu et al., *1990). Similarly, when RT-4 was implanted s.c., only encapsulated tumors were formed (Theodorescu* et al., *1990). The results, however, are consistent with the invasive behavior of the original tumor in the patient (Rigby and Franks, 1970). Therefore, it seems that the orthotopic onplant method using histologically-intact tissue allows fuller expression of the tumor's metastatic capability, possibly as a result of the maintenance of the native tissue architecture of the tumor and site of onplantation.*

Thus, for bladder tumors and possibly others it may be critical for the tissue to remain histologically intact in the orthotopic xenografting process so that its metastatic potential may be fully expressed. Thus, it is quite possible that native cell–cell interactions are necessary for the full expression of metastatic potential in these tumors. The use of such a model may give a more realistic picture of the effects of individual genes on the metastatic program.

Yours sincerely,

Xinyu FU and Robert M. HOFFMAN

AntiCancer, Inc., 5325 Metro Street, San Diego, CA 92110; and Laboratory of Cancer Biology, Department of Pediatrics, 0609F, University of California, San Diego, La Jolla, CA 92093-0609, USA.

January 9, 1992.

REFERENCES

FU, X., BESTERMAN, J.M., MONOSOV, A. and HOFFMAN, R.M., Models of human metastatic colon cancer in nude mice orthotopically constructed by using histologically-intact patient specimens. *Proc. Nat. Acad. Sci. (Wash.)*, **88**, 9345–9349 (1991*a*).

FU, X., THEODORESCU, D., KERBEL, R.S. and HOFFMAN, R. M., Extensive multi-organ metastasis in nude mouse of orthotopically onplanted human bladder carcinoma cell line tissue. *Int. J. Cancer*, **49**, 938–939 (1991*b*).

RIGBY, C.C. and FRANKS, L.M., A human tissue culture cell line from a transitional-cell tumour of the urinary bladder: growth, chromosome pattern and ultrastructure. *Brit. J. Cancer*, **24**, 746–754 (1970).

THEODORESCU, D., CORNIL, I., FERNANDEZ, B. and KERBEL, R., Over-expression of normal and mutated forms of H-*ras* induce orthotopic bladder invasion in a human transitional cell carcinoma. *Proc. Nat. Acad. Sci. (Wash.)*, **87**, 9047–9051 (1990).

ANTICANCER RESEARCH *13*: 901-904 (1993)

A Metastatic Orthotopic - Transplant Nude-Mouse Model of Human Patient Breast Cancer

XINYU FU[1], PHUONG LE[1] and ROBERT M. HOFFMAN[1,2]

[1]*AntiCancer Inc., 5325 Metro Street, San Diego, CA 92110;* [2]*Laboratory of Cancer Biology, Department of Pediatrics, 0609F, School of Medicine, University of California, San Diego, La Jolla, CA 920930609, U.S.A.*

Abstract. *We report here the development of an orthotopic-transplant model of human patient breast cancer in nude mice. Histologically-intact patient breast tumor tissue was transplanted as intact tissue to the mammary fat pad of nude mice where the tumor tissue grew extensively and metastasized to the lung. This is the first orthotopic-transplant metastatic model of human breast cancer. The potential clinical and basic-science uses of the model are discussed.*

Breast cancer is one of the most devastating diseases to women and, in the Western world, affecting one out of nine women in their lifetime. Metastatic breast cancer has a poor prognosis, especially if the tumor is hormone-independent.

A number of animal models of breast cancer have been developed over the past years, especialy using cell lines. Metastasis of xenografted tumors can occur if human breast cancer cell lines such as MCF-7 injected in the mammary fat pad of female nude mice supplemented with estrogen. These orthotopically-injected breast cancer cell lines can metastasize to the lungs and lymph nodes (1, 2, 3, 4). One estrogen-receptor (ER)-negative cell line, MDA - MB - 231, has been reported to form lung metastases after i.v. injection (5). Price et al (6) have reported that another ER-negative cell line, MDA-MB-435, after injection in the mammary fat pad, produces metastases in several different organs in the nude mice. The orthotopic injection model of murine breast cancer cell lines was also shown by Elliott *et al* (7,8) to allow both local growth and metastases as well, for example, to the lung of the nude mouse.

However, human breast carcinoma patient specimens have previously had a low tumor take rate in nude mice (9). Although Outzen and Custer (10) orthotopically implanted human breast cancer-patient surgical specimens and local growth occurred, no metastases were observed. In the other experiments reported above only cell lines were used. Thus, there is a critical need for metastatic rodent models of human patient breast cancer. In this light, we have developed orthotopic-transplant nude-mouse models of human cancers of the colon (11, 12), stomach (13), pancreas (14), bladder (15, 16), prostate (17) and lung (18, 19, 20) that utilized microsurgery for transplantation of intact tissue, including patient specimens. In at least bladder cancer (15, 16), lung cancer (18, 19, 20), and stomach cancer (13) intact-tissue orthotopic transplants seem to result in considerably more metastatic potential than orthotopic injections of cell suspensions. We describe here the orthotopic transplantation of a human breast cancer patient specimen to the nude mouse mammary fat pad which subsequently led to orthotopic growth and metastases to the lung of the nude mice. The results described here demonstrate it is possible to develop metastatic models for breast - cancer patient tumors in immunodeficient mice for basic and treatment studies.

Correspondence to: Prof. R.M. Hoffman, Anticancer Inc., 5325 Metro Street, San Diego, CA 92110, USA. Tel. 619-2993250, Fax 619-2992435.

Key Words: Metastatic orthotopic transplant, nude mouse model, breast cancer, human.

Materials and Methods

Four-week old outbred female nu/nu mice were used for tumor transplantation. All nude mice were bred and maintained in a separated specific pathogen-free facility with controlled light/dark cycle, temperature and humidity. Cages, bedding, food and water were all autoclaved. A surgical specimen of a poorly-differentiated ductal carcinoma of human breast (AntiCancer #2468) was used for tumor transplantation. The tumor specimen was inspected, and grossly necrotic and suspected necrotic tissue was first removed. The tumor specimen was then equally divided into six parts, and each part was subsequently cut into small pieces about 1 mm^3. Tumor pieces for each transplantation were taken from each of the six parts of the specimen equally. In this way, different areas of the heterogeneous cancer tissue can be equally selected, and the chance for viable tissue to be transplanted is also maximized.

For orthotopic transplantation, nude mice were anesthetized with isofluarane inhalation before surgery. After a proper state of anesthesia was induced, the nude mice were put in a supine position. The second right mammary gland was chosen for orthotopic transplantation because it has anatomical resemblance to the anatomical position of the human breast. The surgical region was sterilized with iodine and alcohol swabs.

0250-7005/93 $2.00+.40

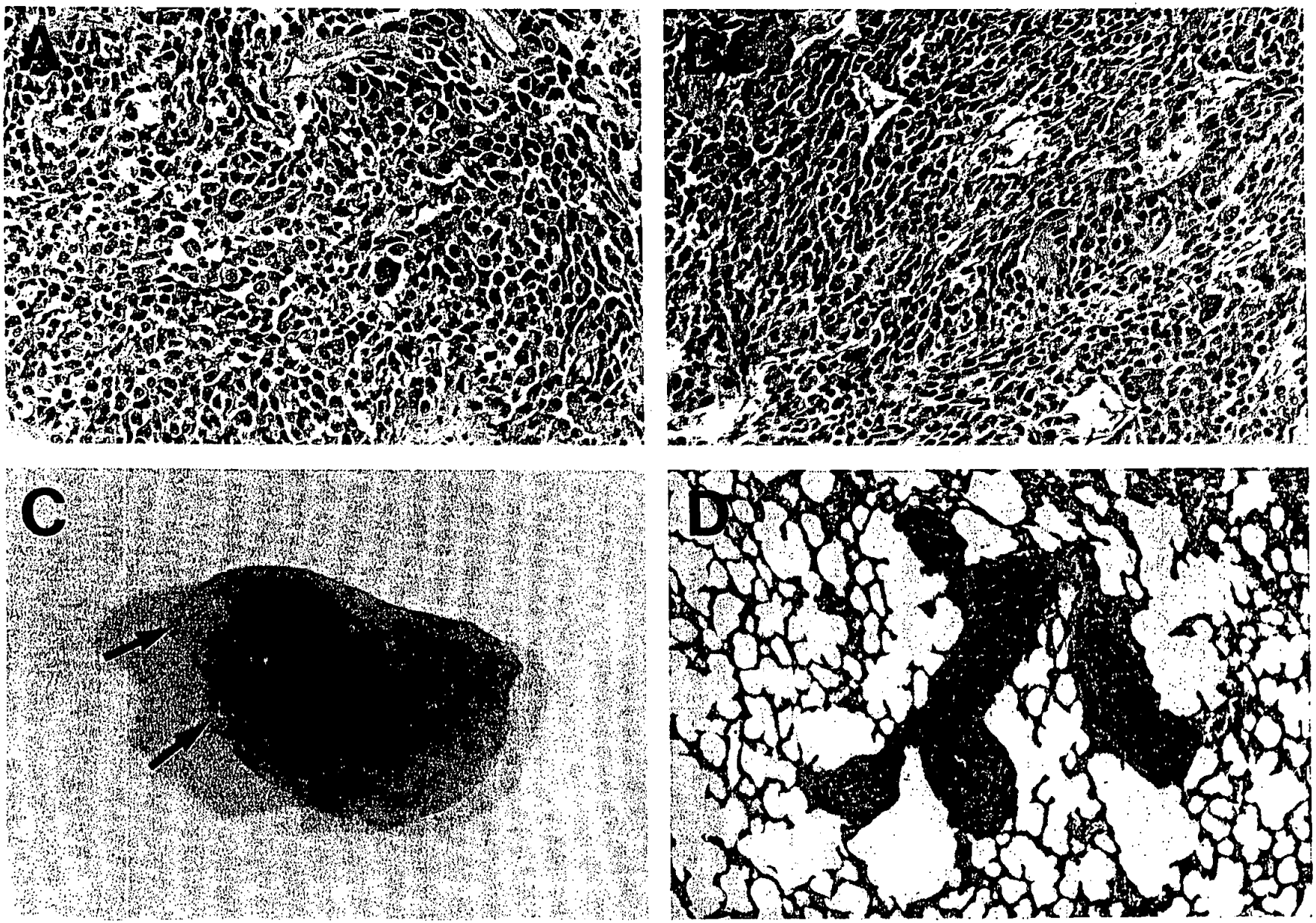

Figure 1. *A. Histopathology of the human breast cancer surgical specimen before transplantation.*
B. Histopathology of human breast cancer grown on the fat pad of nude mouse as seen in Figure 1A. Note the similarity to the pre-transplantation specimen.
C. Tumor metastases in nude mouse lung after orthotopic transplantation of the human breast cancer. Note the multiple nodules as indicated by arrows.
D. Histopathology of nude mouse lung metastasis after orthotopic transplantation of human breast cancer. Note the similarity to the pre-transplantation specimen, and the tumor grown locally in the nude mouse after orthotopic transplantation of the patient specimen.

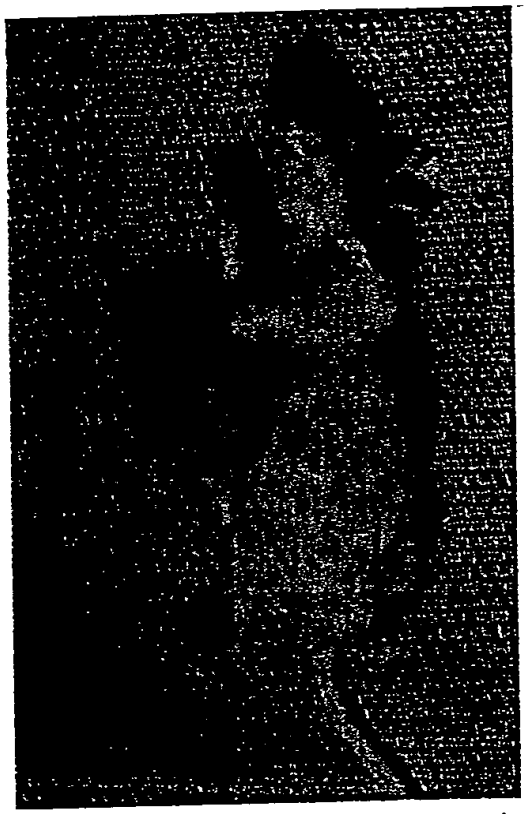

Figure 2. *Nude mouse bearing human breast cancer after orthotopic transplantation of histologically-intact surgical specimens from patient (AC # 2468). The histologically-intact human breast cancer tissue was transplanted to the right second mammary gland fat pad of the nude mouse and was allowed to grow for three months.*

Table I. *Comparison of growth and metastasis in nude mice of orthotopically-transplanted and subcutaneously-transplanted histologically-intact surgical specimens of human breast cancer.*

Transplantation route	No. of mice	No. of mice with primary tumor	No. of mice with lung metastasis
Orthotopic transplantation	8	8	6
Subcutaneous transpantation	7	7	0

Histologically-intact human-patient breast cancer specimens from patient AC # 2468 were transplanted orthotopically to the 2nd mammary fat pad of nude mice or subcutaneously in the flank of nude mice and were allowed to grow for three months. (For details, see text).

An incision of about 1.5 cm was made along the medial side of the nipple. After blunt dissection, the fat pad was exposed. A small incision was made on the fat pad and a small pocket was formed. Six pieces of tumor tissue, previously prepared as described above, were transplanted into the pocket and a 8-0 suture was made to close the pocket. The skin layer was closed by 6-0 sutures.

For subcutaneous transplantation, after the nude mice were anesthetized and the surgical region sterilized, six pieces of tumor specimen were transplanted into the flank of the nude mice. Incisions were closed with 6-0 surgical sutures.

For histological studies at the time of sacrifice, primary tumors grown in the nude mice were removed, major organs and lumph nodes were inspected and removed and put into 10% formalin. All the tissues were subsequently processed through alcohol dehydration, chlorate and paraffinization. Tissues were embedded in paraffin and sectioned at 5 μm. All slides were stained by hematoxylin-eosin and examined microscopically.

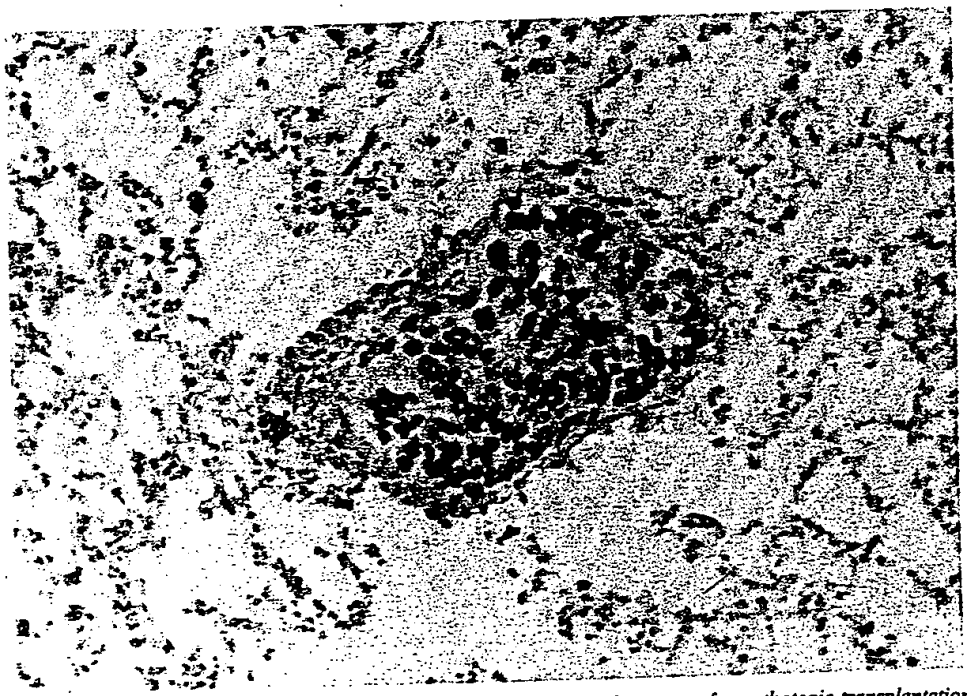

Figure 3. *In situ hybridization of human genomic DNA probe to lung metastasis in nude mouse after orthotopic transplantation of human breast cancer. Brown stain indicates positive probe hybridization and human origin of cells.*

For *in situ* hybridization studies to demonstrate the presence of human genes in the breast tumors growing in the nude mice, paraffin-embedded tissue blocks were sectioned at 4 μm and mounted on silanized slides. After deparaffinization and enzymatic protein digestion, a biotinylated human DNA probe (Oncor, Gaithersburg, MD 20877) was used for hybridization. Avidin and anti-avidin-antibody, along with avidin-horseradish peroxidase and 3-3′-diamine-benzidine tetrahydro-chloride (DAB) as the substrate, were subsequently applied for the detection of the hybridization which was visualized by brown staining. Hematoxylin and eosin were used for counterstaining.

Results and Discussion

Eight mice were used for orthotopic transplantation and seven mice were used for subcutaneous transplantation of the breast cancer specimen. All 15 mice had primary tumor growth after transplantation. The subcutaneously-growing tumors were encapsulated with no local invasion or distal organ metastasis observed. For mice with orthotopic transplantation, the local tumor grew in the mammary gland into a very large mass (Figure 2). The locally-growing tumor was anaplastic and poorly differentiated (Figure 1B) and was very similar to the pretransplantation patient's tumor (Figure 1A). No local invasion and infiltration of the tumor, and no axillary lymph node metastasis were observed. However, six out of eight (75%) mice in the orthotopic transplantation group had multiple metastatic nodules in the lung (Table I, Figure 1C).

The metastatic nodules in the lung, when examined histopathologically, were seen also to be poorly differentiateed and (Figure 1D) very similar to the locally-growing tumor. *In situ* hybridization experiments with a human genomic-wide probe were positive for the locally-growing tumor and lung-metastasis demonstrating their human origin (Figure 3). Thus, the results described here demonstrate that human breast cancer obtained directly from surgery can grow orthotopically in nude mice and metastasize to a clinically-important organ, in this case the lung. This model opens the way toward achieving the goal of being able to transplant, as standard procedure, human breast cancer patient specimens, to obtain clinically-relevant models in an appropriate animal system. Achievement of this goal should greatly enhance our understanding of breast cancer and lead to more effective treatment.

Acknowledgements

This work was supported by U.S. National Cancer Institute Small Business Innovation Research Grants R43 CA53963 and R43 CA58139. We thank Ms. Polly Jayne Pomeroy for expert word processing of the manuscript and for many years of devoted service.

References

1 Shafie SM and Liotta LA: Formation of metastasis by human breast carcinoma cells (MCF-7) in nude mice. Cancer Lett *11:* 81-87, 1980.

2 Ozzello L and Sordat M: Behavior of tumors produced by transplantation of human mammary cell lines in athymic nude mice. Eur J Cancer *16:* 553-559, 1980.

3 Miller FR, Medina D, and Heppner GH: Preferential growth of mammary tumors in intact mammary fatpads. Cancer Res *41:* 3863-3867, 1981.

4 Miller FR: Comparison of metastasis of mammary tumors growing in the mammary fatpad versus the subcutis. Invasion Metastasis *1:* 220-226, 1981.

5 Fraker LD, Halter SA, Forbes JT: Growth inhibition by retinol of a human breast carcinoma cell line in vitro and in athymic mice. Cancer Res *44:* 5757-5763, 1984.

6 Price JE, Polyzos A, Zhang RD and Dantels LM: Tumorigenicity and metastasis of human breast-carcinoma cell lines in nude mice. Cancer Res *50:* 717-721, 1990.

7 Elliott BE, Maxwell L, Arnold M, Wei, WZ and Miller FR: Expression of epithelial-like markers and class-I major histocompatibility antigens by a murine carcinoma growing in the mammary gland and in metastases: orthotopic site effects. Cancer Res *48:* 7237-7245 1988.

8 Elliott BE, TAM SP, Dexter D, Chen ZQ: Capacity of adipose tissue to promote growth and metastasis of a murine mammary carcinoma. Effect of estrogen and progesterone Int J Cancer *51:* 416-424 1992.

9 Giovanella BC and Fogh J: The nude mouse in cancer research. Adv Cancer Res *44:* 69-120, 1985.

10 Outzen HC and Custer RP: Growth of human normal and neoplastic mammary tissues in the cleared mammary fat pad of the nude mouse. J Natl Cancer Inst *55:* 1461-1466, 1975.

11 Fu X, Besterman JM, Monosov A and Hoffman RM: Models of human metastatic colon cancer in nude-mice orthotopically constructed by using histologically-intact patient specimens. Proc Natl Acad Sci USA *88:* 9345-9349, 1991a.

12 Fu X, Guadagni F and Hoffman RM: A metastatic nude-mouse model of human pancreatic cancer constructed orthopically from histologically-intact patient specimens. Proc Natl Acad Sci USA *89:* 5645-5649, 1992a.

13 Furukawa T, Fu X, Kubota T, Watanaba M, Kitajima M, Hoffman RM: Nude mouse metastatic models of human stomach cancer constructed using orthotopic implantation of histologically-intact tissue, Cancer Res *53:* 1204-1208, 1993.

14 Fu X, Herrera H, Kubota T and Hoffman RM: Extensive liver metastasis from human colon cancer in nude and scid mice after orthotopic onplantation of histologically-intact human colon carcinoma tissue. Anticancer Res *12:* 1395-1398, 1992b.

15 Fu X, Theodorescu D, Kerbel RS and Hoffman RM: Extensive multi-organ metastasis following orthotopic onplantation of histologically-intact human bladder carcinoma tissue in nude mice. Int J Cancer *49:* 938-939, 1991b.

16 Fu X and Hoffman RM: Human RT-4 bladder carcinoma is highly metastatic in nude mice and comparable to ras-H-transformed RT-4 when orthotopically onplanted as histologically-intact tissue. Int J Cancer *51:* 989-991, 1992.

17 Fu X, Herrera H, and Hoffman RM: Orthotopic growth and metastasis of human prostate carcinoma in nude mice after transplantation of histologically-intact tissue. Int J Cancer *52:* 987-990, 1992c.

18 Wang X, Fu X and Hoffman RM: A new patient-like metastatic model of human lung cancer constructed orthotopically with intact tissue via thoracotomy in immunodeficient mice. Int J Cancer *51:* 992-995, 1992a.

19 Wang X, Fu X and Hoffman RM: A new patient-like metastatic model of human small-cell lung cancer constructed orthotopically with intact tissue via thoracotomy in nude mice. Anticancer Res *12:* 1403-1406, 1992b.

20 Wang X, Fu X and Hoffman RM: A patient-like metastasizing model of human lung adenocarcinoma constructed via thoracotomy in nude mice. Anticancer Res *12:* 1399-1402, 1992c.

Received February 23, 1993
Accepted March 30, 1993

ANTICANCER RESEARCH *12:* 1395-1398 (1992)

Extensive Liver Metastasis from Human Colon Cancer in Nude and Scid Mice after Orthotopic Onplantation of Histologically-Intact Human Colon Carcinoma Tissue

XINYU FU[1], HECTOR HERRERA[1], TETSURO KUBOTA[2] and ROBERT M. HOFFMAN[1,3]

[1]*AntiCancer, Inc., 5325 Metro Street San Diego, California 92110, U.S.A.;*
[2]*Department of Surgery, School of Medicine, Keio University, 35 Shinanomachi, Shinjuku-ku, Tokyo 160, Japan;*
[3]*Laboratory of Cancer Biology, Department of Pediatrics, 0609F, University of California, San Diego, School of Medicine, La Jolla, California 92093-0609, U.S.A.*

Abstract. *Clinically-relevant animal models of human cancer are greatly needed for the study of human cancer biology and the development of new cancer therapeutics and diagnostics. We report here that by orthotopically transplanting histologically-intact human colon cancer to the colon of the immunodeficient nude and scid mouse mutants that extensive local growth and liver metastases occur consistently even after extensive* in vivo *orthotopic passage. We demonstrate that the liver metastases arise by hematogenous spread. The models described in this report for human colon cancer should prove useful for individual cancer patients as well as for basic and applied studies to develop improved treatment.*

The development of better animal models for human cancer are important for improved treatment for this disease. Subcutaneous or intra-muscular xenografts of immunodeficient mice have low or non-existent metastatic capability even from tumors that were highly metastatic in the patients from whom the tissue were derived (1-5).

A number of studies have indicated that implanting human tumor cells orthotopically in the corresponding organ of nude-mice resulted in much higher metastatic rates. For example, human colon cancer cells, when dissociated, grown in culture, and subsequently injected into the cecum of nude mice can produce tumors that eventually metastasize to the liver (5-9). Similar results also have been achieved for orthotopic implantation of cell lines of other cancers (5).

Our approach is to avoid disruption of tissue integrity and to orthotopically implant histologically-intact tumor tissue directly. With this overall strategy, we have constructed models of human colon cancer in nude mice (10) and human bladder cancer in nude mice (11, 12), human pancreatic cancer in nude mice (13) and human lung cancer in nude and severe combined immunodeficient (scid) mice (14) that demonstrate the variety of clinical behavior that occurs in human subjects. We report here that this approach can allow the development of very extensive liver metastases in nude and scid mice after transplantation of human colon cancer tissue to the mouse colon.

Correspondence to: Dr. R.M. Hoffman, Tel: (619) 299-3250, FAX: (619) 299-2435; Tel: (619) 534-3907, FAX: (619) 534-6032.

Key Words: Colon cancer, human, liver metastasis, orthotopic onplantation, nude unice, scid mice.

Materials and Methods

Four-week-old outbred *nu/nu* mice and scid mice of both sexes were used for tumor transplantation. All animals were maintained in a sterile environment. Cages, bedding, food and water were all autoclaved. All animals were maintained on a daily 12-hr light/12-hr dark cycle. Bethaprim Pediatric Suspension (containing sulfamethoxazole and trimethoprim) was added to the drinking water.

Specimens were then inspected, and grossly necrotic and suspected necrotic tissue was removed. Each specimen was equally divided into four to six separated parts, and each part was subsequently cut into small pieces of about 1 mm^3. Tumor pieces for each transplantation were taken from each of the four to six parts of the specimen equally. In this way, the chance for viable tissue to be transplanted was maximized.

For transplantation, nude mice were anesthetized, and the abdomen was sterilized with iodine and alcohol swabs. A small midline incision was made and the cecal part of the intestine was exteriorized. Serosa of the site where tumor pieces were to be transplanted was removed. Eight to 15 pieces of 1-mm^3 size tumor were implanted on the top of the animal intestine; an 8-0 surgical suture was used to penetrate these small tumor pieces and suture them on the wall of the intestine. The intestine was returned to the abdominal cavity, and the abdominal wall was closed with 7-0 surgical sutures. Animals were kept in a sterile environment.

Results and Discussion

As can be seen in Table I and Figure 1, in three of five nude mice in which the human colon tumor Co-3 xenograft line was transplanted as intact tissue to the mouse colon, liver metastases have resulted, in some cases larger than a centimeter (Figure 1A). Figure 1B demonstrates the adenocarcinoma histopathology of the human colon-tumor metastases growing into the nude-mouse liver. Figure 1C also shows the histopathology of the human colon tumor metastases growing in the nude mouse liver after seven passages, demonstrating the stability during passage of the tumor. This same line, when transplanted to the scid mouse colon, also resulted in liver metastases in four of five mice. Figure 1D shows the histo-

0250-7005/92 $2.00+.40

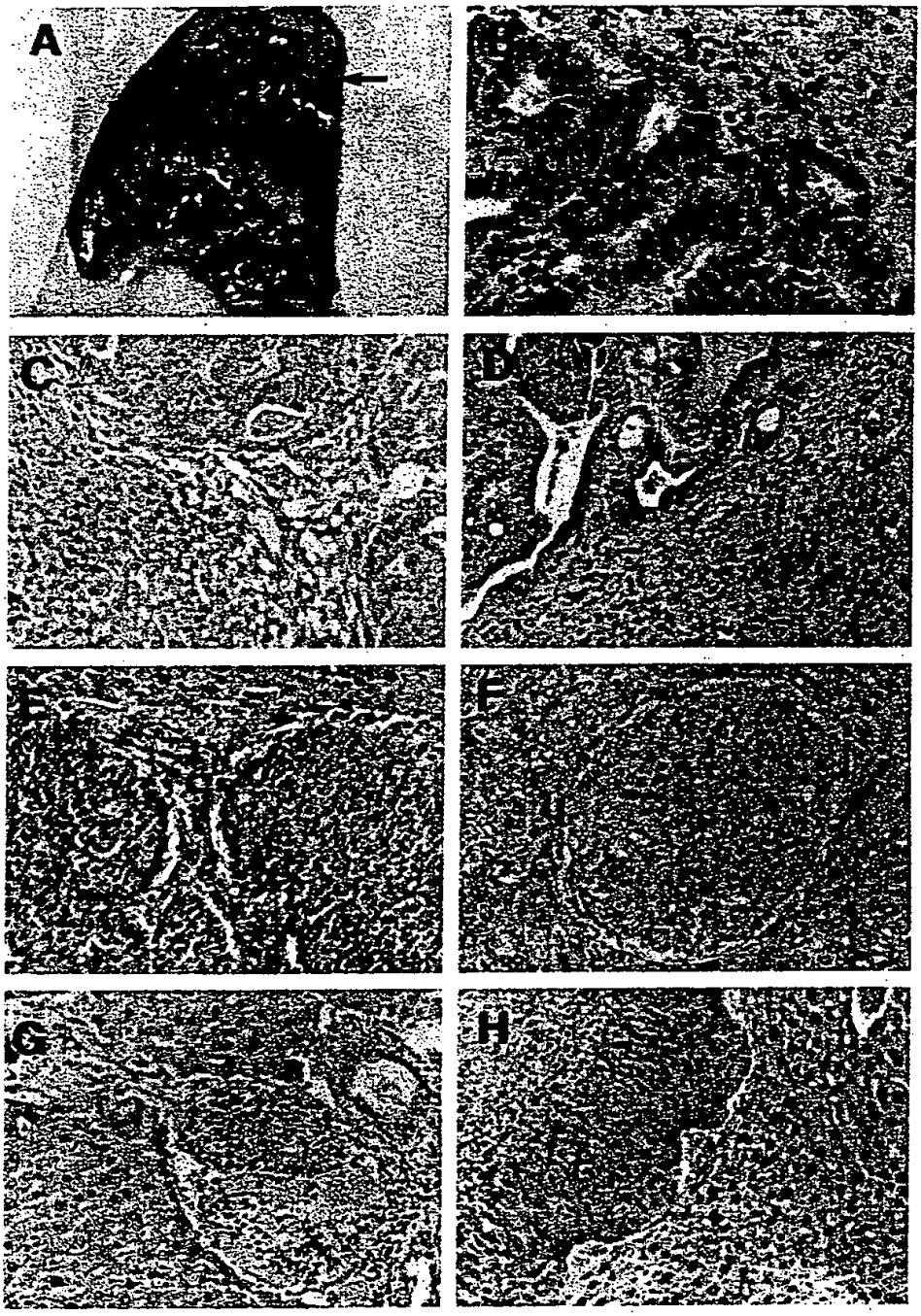

Figure 1. *Liver metastases of human colonic tumors in immunodeficient mice after orthotopic onplantation.*

A. Very large liver metastasis in nude mouse of human colonic tumor Co-3 after orthotopic onplantation to mouse colon (arrow).
B. Histopathology of human colon tumor Co-3 metastasis in nude-mouse liver after orthotopic onplantation.
C. Histopathology of human colon tumor Co-3 metastasis in nude-mouse liver after seven passages and orthotopic onplantation.
D. Histopathology of human colon tumor Co-3 metastasis in scid-mouse liver after orthotopic onplantation.
E. Histopathology of liver metastases of human colon tumor #1594 after orthotopic onplantation to nude mouse colon.
F. Same as E. Please note isolated micrometastasis of human colonic tumor #1594 in nude-mouse liver.
G. Same as E. Please note isolated metastasis of human colonic tumor #1594 in nude-mouse liver blood vessel indicating hematogenous spread.
H. Histopathology of human colon tumor #1594 metastasis in nude-mouse liver after second passage and orthotopic onplantation.

Table I. *Growth and liver metastasis of human colon Co-3 tumor after orthotopic onplantation of intact tissue.*

Mouse type	Number of mice transplanted	Number of mice with local tumor growth	Number of mice with liver metastasis
Nude	5	5	3
Scid	5	5	4

pathology of the human colon tumor metastasis in the scid-mouse liver, again demostrating the adenocarcinoma nature of the tumor. Figure 1E shows a micrometastasis of the poorly-differentiated adenocarcinoma of the human colon cancer from patient #1594 in the liver of the nude mouse. Figure 1F shows an isolated micrometastasis of the human colon cancer in the nude-mouse liver. Note in Figure 1G the human colon tumor in a vessel entering the nude mouse liver, demonstrating the hematogenous spread of the human tumor in the nude mouse. Figure 1 H demonstrates a metastasis of the human colon tumor in the nude mouse liver two passages later, demonstrating stability of the tumor during passage. Thus, the results presented here indicate that the onplant method of orthotopic transplantation can result in very extensive repeatable metastatic behavior of particular colon tumors in immunodeficient mice such as nude and scid. This system should prove very useful for the study of human tumor biology, in particular metastasis, and the evaluation of potential anti-metastatic agents.

Acknowledgements

This study was supported by the Small Business Innovation Research grant R43 CA53963.

References

1 Sordat B, Fritsche R, Mach JP, Carrel S, Ozzello L, Cerotini, JC: Proceedings of the First Intrnational Workshop on Nude Mice. pp 269-277, (eds.) Rygaard J & Povlsen, CO. Gustav Fischer Verlag, Stuttgart, Germany (1973).

2 Povlsen CO and Rygaard J: *In:* B.B. Bloom and J.R. David (eds.), In Vitro Methods, of Cell Mediated in Tumor Immunity, : pp 701-711, Academic Press, New York (1976).

3 Kyriazis AP, DiPersio L, Michael GJ, Pesce AJ, Stinnett JD: Growth patterns and metastatic behavior of human tumors growing in athymic mice. Cancer Res *38:* 3186-3190, 1978.

4 Fidler IJ: Rationale and methods for the use of nude mice to study the biology and therapy of human cancer metastasis. Cancer Metastasis REv *5:* 29-49, 1986.

5 Fidler IJ: Critical factors in the biology of human cancer metastasis: Twenty-eighth G.H.A. Clowes Memorial Award Lecture. Cancer Res *50:* 6130-6138, 1990.

6 Giavazzi R, Jessup JM, Campbell DE, Walker SM, Fidler IJ: Experimental nude mouse model of human colorectal cancer liver metastases. J Natl Cancer Inst *77:* 1303-1308, 1986.

7 Bresalier S, Raper SE, Hujanen ES, Kim YS: A new animal model for human colon cancer metastasis. Int J Cancer *39:* 625-630, 1987.

8 Morikawa K, Walker S, Nakajima M, Pathak S, Jessup JM, Fidler IJ: Influence of organ environment on the gorwth, selection, and metastasis of human colon carcinoma cells in nude mice. Cancer Res *48:* 6863-6871, 1988a..

9 Morikawa K, Walker SM, Jessup JM, Fidler IJ: *In vivo* selection of highly metastatic cells from surgical specimens of different primary human colon carcinomas implanted into nude mice. Cancer Res *48:* 1943-1948, 1988b.

10 Fu X, Besterman JM, Monosov A, Hoffman RM: Models of human metastatic colon cancer in nude-mice orthotopically constructed by using histologically-intact patient specimens. Proc Natl Acad Sci USA *88:* 9345-9349, 1991a.

11 Fu X, Theodeorescu D, Kerber RS, Hoffman RM: Extensive multiorgan metastasis following orthotopic onplantation of histologically-intact human bladder carcinoma tissue in nude mice Int J Cancer *49:* 938-939, 1991b.

12 Fu X and Hoffman, RM: Human RT-4 bladder carcinoma is highly metastatic in nude mice and comparable to *ras*H-transformed RT-4 when orthotopically onplanted as histologically-intact tissue. Int J Cancer in press.

13 Fu X, Guadagni F and Hoffman RM: A metastatic nude-mouse model of human pancreatic cancer constructed orthotopically with histologically-intact patient specimens. Proc Natl Acad Sci USA, in press.

14 Wang X, Fu X and Hoffman RM: A new patient -like metastatic model of human lung cancer constructed orthotopically with intact tissue *via* thoracotomy in immunodeficient mice. Int J Cancer, in press.

Received April 6, 1992
Accepted May 5, 1992

[CANCER RESEARCH 55, 681–684, February 1, 1995]

7

Host Organ Specifically Determines Cancer Progression

Shinji Togo, Hiroshi Shimada, Tetsuro Kubota, A. R. Moossa, and Robert M. Hoffman[1]

Second Department of Surgery, Yokohama City University School of Medicine, Yokohama, Japan [S. T., H. S.]; Department of Surgery, Keio University School of Medicine, Tokyo, Japan [T. K.]; Department of Surgery, University of California, San Diego Medical Center, San Diego, California [S. T., A. R. M.]; Laboratory of Cancer Biology, University of California, San Diego School of Medicine, La Jolla, California [S. T., R. M. H.]; and AntiCancer Incorporated, San Diego, California [R. M. H.]

ABSTRACT

In order to further understand the role of the host organ in tumor progression, we have transplanted into nude mice histologically intact human colon cancer tissue on the serosal layers of the stomach (heterotopic site) and the serosal layers of the colon (orthotopic site). Xenograft lines Co-3, which is well differentiated, and poorly differentiated COL-3-JCK were used for transplantation. After orthotopic transplantation of the human colon tumors on the nude mouse colon, the growing colon tumor resulted in macroscopically extensive invasive local growth in 4 of 10 mice, serosal spreading in 9 of 10 mice, musclaris propria invasion in 1 of 10 mice, submucosal invasion in 3 of 10 mice, mucosal invasion in 3 of 10 mice, lymphatic duct invasion in 4 of 10 mice, regional lymph node metastasis in 4 of 10 mice, and liver metastasis in 1 of 10 mice. In striking contrast, after heterotopic transplantation of the human colon tumor on the nude mouse stomach, a large growing tumor resulted but with only limited invasive growth and without serosal spreading, lymphatic duct invasion, or regional lymph node metastasis. It has become clear from these studies that the orthotopic site, in particular the serosal and subserosal transplant surface, is critical to the growth, spread, and invasive and metastatic capability of the implanted colon tumor in nude mice. These studies suggest that the original host organ plays the same critical role in tumor progression.

INTRODUCTION

An important but incompletely understood process in cancer biology is the role of the host organ in cancer progression. In this light, orthotopic implantation using histologically intact cancer tissue has been shown to produce "patient-like" mouse models of cancer progression and metastasis (1, 2). In the last 10 years, it has become clear that the orthotopic site of transplantation allows much higher and more physiological expression of tumor progression and metastatic capability of the transplanted tumor than s.c. transplantation in nude mice. For instance, with regard to colon carcinoma, when the cecum was used as the site of implantation of colon cancer tissue, metastasis occurred, including that to the liver, as opposed to the s.c. site, which allowed primary growth to occur but not metastasis (3). Thus, the advantages of orthotopic transplantation were determined by comparison between orthotopic transplantation and s.c. implantation. However, the difference of two similar visceral transplantation sites has not been noted with respect to supporting growth, spread, invasion, and metastasis. In this report, we have compared orthotopic implantation of human colon cancer tissue on the serosal layers of the stomach, which is the heterotopic site, and the serosal layers of the colon, which is the orthotopic site using histologically intact cancer tissue. Tumor growth, spread, extent of invasion, and metastasis between the two sites were compared, and striking differences were found. We have concluded that the host organ is highly specific with respect to tumor progression.

MATERIALS AND METHODS

Mice. Four-week-old outbred *nu/nu* mice of both sexes were used for tumor implantation. All animals were maintained in a sterile environment: cages, bedding, food, and water were all autoclaved. All animals were maintained on a daily 12-h light/12-h dark cycle. Bethaprim pediatric suspension (containing sulfamethoxazole and trimethoprim) was added to the drinking water. NIH guidelines were followed for all animal experimentation.

Human Colonic Cancer Xenografts. Two human colonic cancer xenografts (COL-3-JCK, poorly differentiated adenocarcinoma established in 1980; and Co-3, well differentiated adenocarcinoma established in 1976) were used in the study (4).

Orthotopic Tumor Tissue Implantation. Subcutaneously growing tumors at the exponential phase in nude mice were resected aseptically, necrotic tissues were cut away, and the remaining healthy tumor tissues were scissor minced into pieces about 1–2 mm^3 in size in Hanks' balanced salt solution (2, 3).

Nude mice were anesthetized with isoflurane (Forane) inhalation. An incision was made through the left upper abdominal pararectal line and perito-

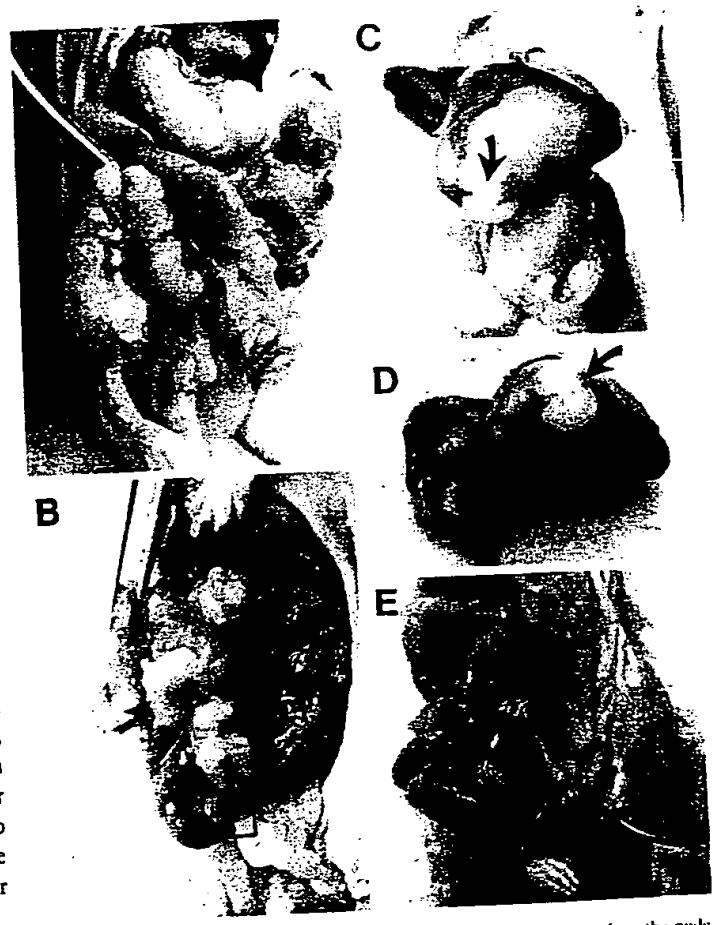

Fig. 1. Tumor growth and progression of human colon tumor implanted on the nude mouse colon. The human colon tumors (Co-3 and COL-3-JCK) were transplanted to the nude mouse colon serosal layers by a surgical procedure described in "Materials and Methods." The tumor tissue grew for 36 or 37 days before the animals were sacrified. *A*, tumor growth (*black arrow*) and serosal spreading (*open arrow*) on colon (COL-3-JCK). *B*, tumor growth (*black arrow*) and serosal spreading (*open arrow*) on colon (Co-3). *C* and *D*, liver metastasis (*black arrow*). *E*, lymphnode metastasis (*black arrow*).

Received 8/15/94; accepted 11/21/94.

The costs of publication of this article were defrayed in part by the payment of page charges. This article must therefore be hereby marked *advertisement* in accordance with 18 U.S.C. Section 1734 solely to indicate this fact.

[1] To whom requests for reprints should be addressed, at AntiCancer Incorporated, 7917 Ostrow Street, San Diego, CA 92111.

Fig. 2. Tumor growth and progression of human colon tumor implanted on the stomach. The human colon tumor Co-3 was transplanted to the nude mouse stomach serosal layers by a surgical procedure described in "Materials and Methods." The tumor tissue (*black arrow*) grew for 37 days before the animal was sacrified. *Open arrow*, normal, uninvolved stomach.

neum. The stomach wall was carefully exposed, and a part of serosal membrane, about 3 mm in diameter, in the middle of the greater curvature of the glandular stomach was mechanically injured using forceps. Seven to 10 pieces of 1–2 mm^3 size were implanted on the nude mouse stomach where the serosa had been injured. An 8-0 suture was used to penetrate these small pieces and suture them onto the wall of the stomach (2). Subsequently, the colocecal part of the intestine was exteriorized. The same suturing procedure described above was performed on the cecum to affix the colon cancer tissue. The stomach and colocecal part of the intestine were then returned to the peritoneal cavity, and the abdominal wall and skin were closed with 6-0 black silk sutures.

Evaluation of Growth and Metastasis of Orthotopically Implanted Tumors. When the palpable tumor reached about 1 cm, the animals were sacrificed and autopsied. The gross tumor growth was observed, and all major organs were fixed in formalin and prepared for sectioning and staining with hematoxylin and eosin by standard procedures.

RESULTS

Figs. 1 and 2 show macroscopic findings of the growing human colon cancer tissue (xenograft lines Co-3, which is well differentiated, and poorly differentiated COL-3-JCK) implanted as histologically intact tissue on the serosal layers of the stomach and the serosal layers of the colon of nude mice. An expansive growth of the colon tumor resulted with no serosal spreading observed on the stomach in all animals (Fig. 2). In striking contrast, when the colon tumor was transplanted on the serosal layers of the colon, growth resulting in extensive gross invasion was observed in 4 of 10 animals, multifocal serosal spreading (Fig. 1, *A* and *B*) occurred in 9 of 10 animals, and lymph node metastasis (Fig. 1*E*) occurred in 4 of 10 animals.

With regard to orthotopic transplantation of the human colon tumor on the nude mouse colon, Fig. 3 shows microscopic findings of musclaris propria invasion in 1 of 10 animals, submucosal invasion in 3 of 10 animals, and mucosal invasion in 3 of 10 animals. In striking contrast, heterotopic site transplantation of the human colon tumor on the nude mouse stomach resulted in musclaris propria invasion in 1 of 10 animals and no submucosal or mucosal invasion (Fig. 4). Orthotopic transplantation resulted in lymphatic duct invasion (Fig. 3) in 4 of 10 animals; heterotopic transplantation on the stomach did not result in lymphatic duct invasion by the colon tumor. Although the nature of tumor progression was radically different at the orthotopic

Table 1 *Effect of the host organ on colon tumor progression*

Histologically intact human colon carcinoma tissue (Co-3 and COL-3) was surgically transplanted to the serosal layers of the nude mouse colon and stomach and analyzed grossly and microscopically as described in "Materials and Methods."

Mouse no.	Tumor[a]	Days after operation	Growing form	Depth of invasion[b]	Serosal spreading	Lymphtic duct invasion	Lymph node metastasis	Comment[c]
Stomach as host organ								
1	Co-3	17	Expansive	ss	–	–	–	
2	Co-3	37	Expansive	ss	–	–	–	
3	Co-3	37	Expansive	ss	–	–	–	
4	Co-3	37	Expansive	ss	–	–	–	
5	Co-3	13	Expansive	ss	–	–	–	
6	Co-3	21	Expansive	ss	–	–	–	
7	Co-3	35	Expansive	ss	–	–	–	
8	COL-3	36	Expansive	ss	–	–	–	
9	COL-3	36	Expansive	pm	–	–	–	
10	COL-3	21	Expansive	ss	–	–	–	
Colon as host organ								
1	Co-3	17	Invasive	ss	+	–	–	
2	Co-3	37	Expansive	sm	+	+	–	Liver meta.
3	Co-3	37	Expansive	sm	+	+	+	
4	Co-3	37	Expansive	pm	++	–	–	Nodule on oment.
5	Co-3	13	Invasive	ss	++	–	–	
6	Co-3	21	Invasive	ss	+	–	–	
7	Co-3	35	Expansive	m	+	+	+	
8	COL-3	36	Invasive	m	+	–	+	Ascites, cecal obst.
9	COL-3	36	Expansive	m	–	+	+	
10	COL-3	21	Expansive	sm	+	–	–	Cecal obst.

[a] COL-3, COL-3-JCK.
[b] ss, subserosa; pm, muscularis propria; sm, submucosa; m, mucosa.
[c] meta., metastasis; oment., omentum; obst., obstruction.

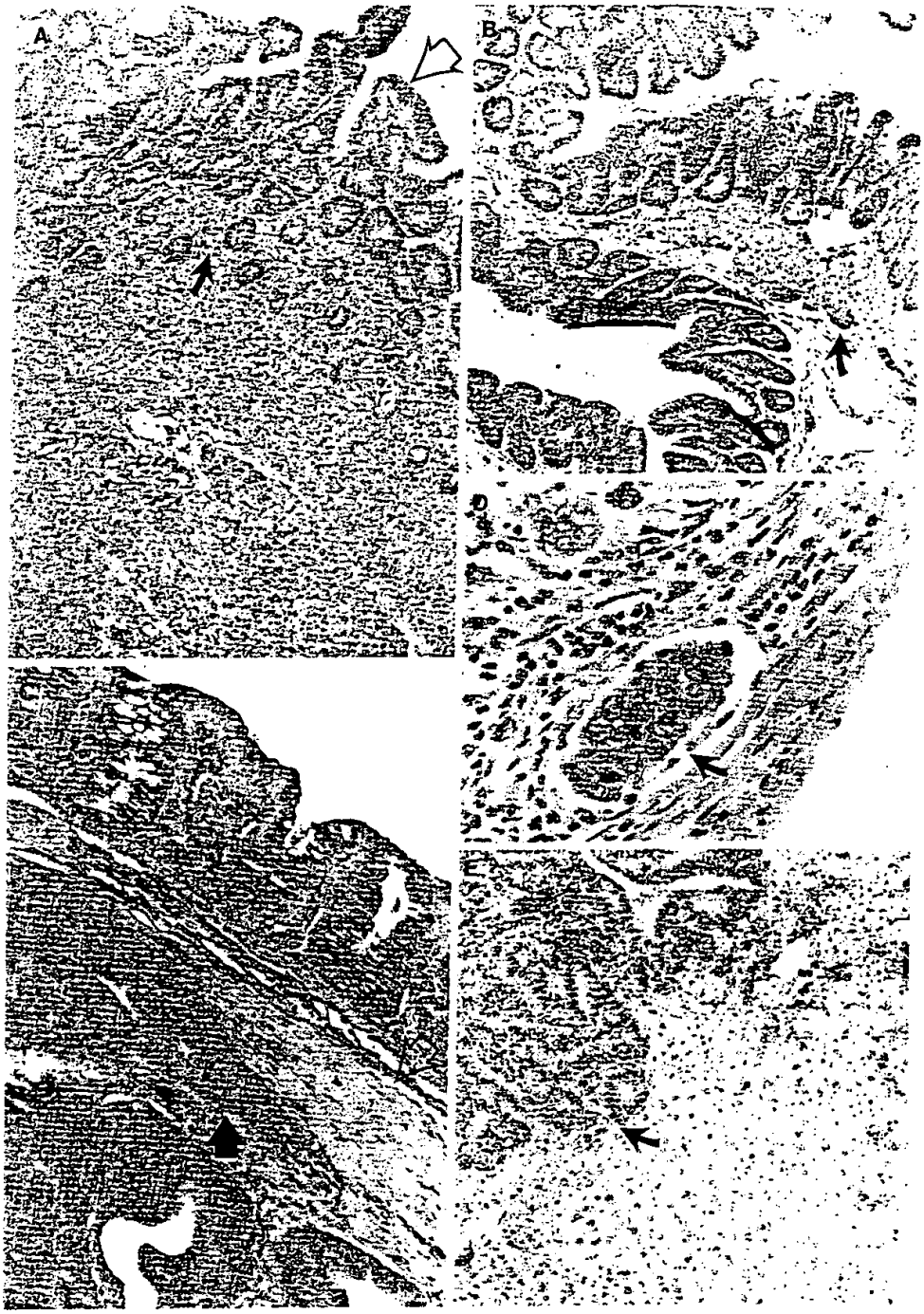

Fig. 3. Extensive invasive properties of human colon tumor implanted on the nude mouse colon. See Fig. 1 for details. Five-μm sections of tissue were made and stained with hematoxylin and eosin. *A*, invasion into the mucosa (COL-3-JCK colon tumor, *black arrow;* mouse colon mucosa, *open arrow*). *B*, invasion into the submucosa (COL-3-JCK colon tumor, *black arrow*). *C*, invasion into muscularis propria (Co-3 colon tumor, *black arrow;* muscularis propria, *open arrow*). *D*, invasion into the lymphtic duct (*black arrow*). *E*, liver metastasis (*black arrow*).

and heterotopic sites, the overall growth rates were similar, emphasizing the difference between tumor growth and tumor progression.

Tables 1 and 2 summarize tumor growth, depth of tumor invasion, serosal spreading, lymphatic duct invasion, regional lymph node metastasis, and distant metastasis for the colon cancer xenografts Co-3 and COL-3-JCK when implanted into the stomach and colon of the nude mice as histologically intact tissue. As described above, expansive growth with limited invasion with no submucosal and mucosal invasion, no serosal spreading, and no regional lymph node metastasis resulted from the human colon cancer-implanted tumor on the stomach. However, grossly extensive invasive growth, serosal spreading, lymphatic duct invasion, and regional lymph node metastasis resulted from the human colon tumor transplanted on the serosal surface of the nude mouse colon. Macroscopic and microscopic exploration did not reveal other sites of metastases. It should be noted that Co-3 is well differentiated and COL-3-JCK is poorly differentiated, but both grew similarly in the experiments described above, suggesting the possibility of the generality of the results.

DISCUSSION

In 1889, Paget (5) analyzed 735 autopsy records of women with breast cancer. The nonrandom pattern of visceral metastasis suggested to him that certain tumor cells (the "seed") had a specific affinity for the milieu of certain organs (the "soil"). Paget suggested that metastases resulted only when the seed and soil were matched.

Work from a number of laboratories has indicated that implanting human tumor cells orthotopically in the corresponding organ of nude

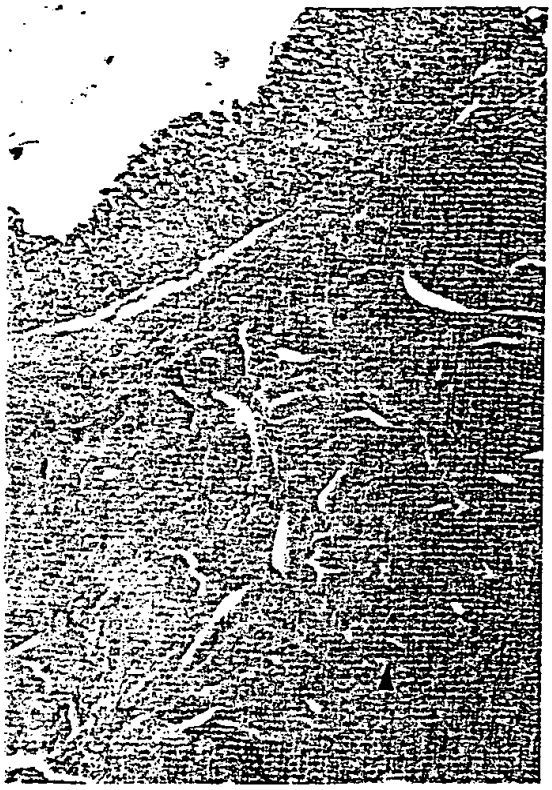

Fig. 4. Limited invasive growth of human colon tumor on the nude mouse stomach. The human colon tumor Co-3 was transplanted to the nude mouse stomach serosal layers by a surgical procedure described in "Materials and Methods" and was grown for 37 days. Five-μm sections of tissue were made and stained with hematoxylin and eosin. *Black arrow,* tumor. *Open arrow,* uninvolved muscularis propria.

Table 2 *Summary of the effect of the host organ on colon tumor progression*

Histologically intact human colon carcinoma tissue (Co-3 and COL-3) was surgically transplanted to the serosal layers of the nude mouse colon and stomach and analyzed grossly and microscopically as described in "Materials and Methods."

	Orthotopic site (colon)	Heterotopic site (stomach)
Gross extensive invasiveness	4	0
Serosal spreading	9	0
Lymphatic duct invasion	4	0
Lymph node metastasis	4	0
Microscopic tissue invasion:		
to musclaris propria	1	1
to submucosa	3	0
to mucosa	3	0
Liver metastasis	1	0

mice resulted in much higher metastatic rates and take rates than s.c. transplantation (6). Recent work has indicated that orthotopic transplantation of histologically intact tissue allowed patient-like expression of metastatic capability, as opposed to orthotopic injection of cell suspensions (2, 3).

However, the usefulness of orthotopic implantation was determined only by the comparison between the orthotopic site and the subcutis. In this report, we compared the growth of human colon tumor implanted as histologically intact tissue on the serosal layers of the orthotopic site and the heterotopic site (stomach). After heterotopic transplantation on the stomach serosal layers, expansive growth resulted with limited gross invasion, no submucosal and mucosal invasion, no lymphatic duct invasion, no serosal spreading, and no regional lymph node metastasis. In striking contrast, extensive gross invasion, submucosal or mucosal invasion, serosal spreading, lymphatic duct invasion, and regional lymph node metastasis resulted when the human colon tumor was implanted on the nude mouse colon. Liver metastasis occured in one animal, also presumably from the orthotopically growing and extensively invasive tumor growing on the colon (Fig. 1, *C* and *D*).

It is interesting to note that, despite radically different growth patterns at the orthotopic and heterotopic sites, the overall growth rates seemed similar. However, while the heterotopically transplanted tumors grew very extensively, they still demonstrated limited growth, suggesting that even after even a greater growth period, heterotopic growth would remain limited with regard to progression. Although the stomach is a heterotopic site for the colon tumor transplantation, it is related somewhat to the colon. We suggest the term "paratopic" for a related site of transplantation.

Fidler (6) has suggested that the facilitation factors of the host for metastasis are: (*a*) neovascularization; (*b*) paracrine and endocrine growth factors; (*c*) platelets and their products; and (*d*) immune cells and their products affecting the implanted tumor. The data presented in this paper suggested that the host environment, in particular the serosal surfaces, are also critical for growth and progression of the transplanted tumor. Similar results were observed with both a well differentiated and poorly differentiated tumor, suggesting the possibility of generality of the phenomena observed in this report. Perhaps as in embryonic development, the specific intersection of two tissue types, in this case the tumor and the orthotopic serosal layers, influences the subsequent behavior of at least one of the tissues, in this case the tumor. Studies of the properties of the specific organ serosal layers allowing tumor progression are imperative.

REFERENCES

1. Hoffman, R. M. Patient-like models of cancer in mice. Curr. Perspect. Mol. Cell. Oncol., *1:* 311–326, 1992.
2. Furukawa, T., Fu, X., Kubota, T., Watanabe, M., Kitajima, M., and Hoffman, R. M. Nude mouse metastatic models of human stomach cancer constructed using orthotopic transplantation of histologically intact tissue. Cancer Res., *53:* 1204–1208, 1993.
3. Fu, X., Besterman, J. M., Monosov, A., and Hoffman, R. M. Models of human metastatic colon cancer in nude mice orthotopically constructed by using histologically-intact patient specimens. Proc. Natl. Acad. Sci. USA, *88:* 9345–9349, 1991.
4. Kuo, T., Kubota, T., Watanabe, M., Fujita, S., Furukawa, T., Teramoto, T., Ishibiki, K., Kitajima, M., Hoffman, R. M. Early resection of primary orthotopically-growing human colon tumor in nude mouse prevents liver metastasis: further evidence for patient-like hematogeneous metastatic route. Anticancer Res., *13:* 293–298, 1993.
5. Paget, S. The distribution of secondary growths in cancer of the breast. Lancet, *1:* 571–573, 1889.
6. Fidler, I. J. Critical factors in the biology of human cancer metastasis. Cancer Res., *50:* 6130–6138, 1990.

Clin. Exp. Metastasis, 1997, 15, 184–195

8

Conversion of highly malignant colon cancer from an aggressive to a controlled disease by oral administration of a metalloproteinase inhibitor

Zili An,* Xiaoen Wang,* Neville Willmott,† Surinder K. Chander,† Simon Tickle,† Andrew J. P. Docherty,† Andrew Mountain,† Andrew T. Millican,† Richard Morphy,† John R. Porter,† R. Ola Epemolu,† Tetsuro Kubota,‡ A. R. Moossa§ and Robert M. Hoffman*§

**AntiCancer Inc., 7917 Ostrow St., San Diego, CA, USA; †Celltech Therapeutics Ltd, 216 Bath Road, Slough, Berkshire, UK; ‡Department of Surgery, School of Medicine, Keio University, 35 Shinanomachi, Shinjuku-ku, Tokyo, Japan; §Department of Surgery, School of Medicine, University of California, San Diego, 402 Dickinson Street, San Diego, CA, USA*

(Received 18 September 1996; accepted in revised form 7 December 1996)

In this study, we describe the activity of CT1746, an orally-active synthetic MMP inhibitor that has a greater specificity for gelatinase A, gelatinase B and stromelysin than for interstitial collagenase and matrilysin, in a nude mouse model that better mimics the clinical development of human colon cancer. The model is constructed by surgical orthotopic implantation (SOI) of histologically-intact tissue of the metastatic human colon tumor cell line Co-3. Animals were gavaged with CT1746 twice a day at 100 mg/kg for 5 days after the SOI of Co-3 for 43 days. In this model CT1746 significantly prolonged the median survival time of the tumor-bearing animals from 51 to 78 days. Significant efficacy of CT1746 was observed on primary tumor growth (32% reduction in mean tumor area at day 36), total spread and metastasis (6/20 treated animals had no detectable spread and metastasis at autopsy compared to 100% incidence of secondaries in control groups). Efficacy of CT1746 could also be seen on reducing tumor spread and metastasis to individual organ sites such as the abdominal wall, cecum and lymph nodes compared to vehicle and untreated controls. We conclude that chronic administration of a peptidomimetic MMP inhibitor via the oral route is feasible and results in inhibition of solid tumor growth, spread and metastasis with increase in survival in this model of human cancer, thus converting aggressive cancer to a more controlled indolent disease.

Keywords: CT1746, matrix metalloproteinase inhibitors, MMPs, tumor growth

Introduction

Malignancy is most often a very aggressive disease with a rapid course leading to the demise of the patient. However the present therapeutic modalities can not successfully control most solid tumors with rapid local invasive growth and metastasis, contributing to the poor 5-year survival rate. An alternative measure to this enormous problem is to convert human malignancy from a highly aggressive to a more controlled indolent disease that allows the patient to survive longer with minimum symptoms.

Targets for this therapeutic approach include the matrix metalloproteinases (MMPs), which are a family of zinc-dependent endopeptidases frequently found in and around the more invasive and metastatic human tumors [1]. They possess proteo-

Address correspondence to: Robert M. Hoffman, 7917 Ostrow Street, San Diego, CA 92111, USA. Tel: (+1) 619 654 2555; Fax: (+1) 619 268 4175; E-mail: antica@ix.netcom.com

lytic activity for components of the extracellular matrix such as collagen and proteoglycans and are thought to promote the growth and spreading of tumor tissue, possibly through degradation of basement membranes, the modulation of sites of cell adhesion, and by facilitating tumor angiogenesis [1, 2]. Genetic manipulation of MMP expression, or studies involving one or other of the recombinant tissue inhibitors of metalloproteinases (TIMP1 and TIMP2), have demonstrated the involvement of these enzymes in the process of tumor growth and metastasis [3–5]. More recently, efficacy has been demonstrated with synthetic MMP inhibitors in animal models of tumor growth and spread [6, 7]. Further more, it has been recognized since early this century that solid tumors possess an abnormal blood supply [8] and it is of considerable interest that synthetic MMP inhibitors are also inhibitors of angiogenesis [9, 10].

Targeting tumor vasculature is an example of an approach to cell control as opposed to the traditional approach of cell kill [11]: as such, the pharmacology of this type of therapeutic agent is completely different from that of conventional agents. For example, chronic dosage regimes maintained for long periods appear necessary and in consequence orally active compounds are mandatory.

One of our laboratories (AntiCancer Inc.) has developed a nude mouse model that better mimics the clinical development of human colon cancer by surgical orthotopic implantation (SOI) of histologically intact human tumor tissue [12, 13]. Orthotopic transplantation of histologically intact tissue enables the model to reflect the clinical behavior of human cancer including primary tumor growth, invasion and metastasis [14, 15]. Using this model, the present study examined the anti-tumor and anti-metastatic efficacy on chronic administration of an MMP inhibitor, CT1746, which is known from screening studies [16] to be absorbed after oral administration. The results described here demonstrate that malignant colon cancer, treated chronically by oral administration with CT1746 in the model, could be converted from a highly aggressive to a more controlled indolent disease with significant increase in survival.

Materials and methods

Animals

A total of 55 male 3- to 4-week-old, nu/nu CD-1 outbred mice (Charles River Laboratory, Wilmington, MA), were used in the study. They were kept under specific pathogen-free conditions. The animal diets were obtained from Harlan Teklad (Madison, WI) and 0.15% (v/v) HCl was added to the drinking water.

Colon carcinoma xenograft

A metastatic human colon cancer cell line, Co-3, was used in this study. This well-established cell line was kindly provided by Dr Tetsuro Kubota (Keio University, Tokyo, Japan). It is a well-differentiated adenocarcinoma of the colon and was obtained from a metastatic lesion in the lung of a 39-year-old female patient in 1975. Co-3 has a rapid yet stable growth rate and has shown no changes in histology from the original tumor, even after repeated transfers [17]. The cell line has been maintained subcutaneously in nude mice in Keio University as well as our animal facility. The specimen for orthotopic implantation was derived from tumor stock growing subcutaneously in nude mice.

Gelatinolytic activity was detected in cytosols prepared by disrupting pieces of normal caecum, or orthotopically grown tumor tissue, with a Mikro-Dismembrator U (B. Braun Biotech, Melsungen, Germany). This machine disrupts frozen tissue by shaking it rapidly in a flask with a tungsten ball. Each piece of tissue was weighed and similar amounts were disrupted by the flask being shaken at 1600 rpm for 2 min. The tissue was allowed to thaw before the addition of 0.1 M Tris base, 0.1 M NaCl, 0.05% Tween 20, pH 7.4, to give a final ratio of 1:5 tissue to buffer (w/v). The solution was then centrifuged in an Eppendorf microfuge for 2 min, the supernatant was removed and the protein content determined using the Coomassie Protein Reagent (Pierce and Warriner). The gelatinolytic content was evaluated by analysing equal amounts of total protein by gelatin zymography [18]. The sensitivity of any gelatinase activity to inhibition by CT1746 was determined by including the inhibitor at a concentration of 1–100 nM during the incubation step.

Construction of orthotopic model

The stock tumor tissue was derived from subcutaneously-growing tumors when they were in the log phase. Fresh tumor tissue was harvested from the periphery of the tumor masses. The tumor tissues were then minced in RPMI-1640 culture medium with antibiotics into $1 \times 1 \times 1$ mm^3 fragments. The resulting fragments were then randomized. Orthotopic implantation of Co-3 human colon cancer tissue was carried out using micro-surgical procedures we have developed previously [12–15].

Briefly, mice were anesthetized by isoflurane inhalation and immobilized in a supine position. With the aid of a dissecting microscope (×7) a small midline incision was made in the abdomen and the colocecal portion of the colon was exposed. A small piece of serosa was then removed from the site where the tumor fragments were to be implanted and 10 fragments were implanted on the top of the intestine using 8-0 nylon sutures. The intestine was returned to the abdominal cavity and the abdomen was closed with 6-0 surgical sutures.

The tumor fragments were randomized such that quantitatively and qualitatively equal amounts of tumor were implanted in each mouse so as to limit the mouse to mouse variability in subsequent tumor growth within a statistically acceptable range.

The mortality rate of surgical procedure is approximately 5%, which was mainly due to anesthesia overdose. The other cause of postsurgical death is abdominal wall rupture. Routinely several extra mice are transplanted to compensate for possible postsurgical loss.

Synthetic inhibitor of MMP

CT1746 (N1-[2-(S)-(3,3-dimethylbutanamidyl)]-N4-hydroxy-2-(R)-[3-(4-chlorophenyl)-propyl]-succinamide) is a recently described orally active peptidomimetic MMP inhibitor which incorporates a zinc chelating hydroxamic group within a structure that resembles a peptide substrate [6, 16, 19–21]. Selectivity towards gelatinase was obtained by including an arylpropyl group at the P_1' position, which mimics the aromatic amino acid usually found at the S_1' position in the MMP propeptide that is cleaved during autoactivation [22]. Cleavage at this position by collagenase does not readily occur [23] and as a result CT1746 exhibits a significantly greater selectivity for gelatinase than for collagenase.

The compound is insoluble in aqueous solution and for kinetic analysis was dissolved in methanol before dilution in assay buffer. For *in vivo* experiments it was formulated in propylene glycol as described below. The K_i values using a quenched fluorescent peptide substrate [16, 18] against human gelatinase-A, gelatinase-B, stromelysin 1, collagenase, and matrilysin are 0.04, 0.17, 10.9, 122 and 136 nM, respectively. Against other classes of metalloproteinases such as neprilysin (EC 24.11), meprin, peptidyl-dipeptidase A (ACE), and aminopeptidase N, CT1746 exhibits negligible activity with IC_{50} values against peptide substrates that are greater than 40 μM (unpublished observations). We confirmed *in vitro* that the compound could inhibit the gelatin degrading activity of gelatinase A; and when administered orally to mice at 100 mg/kg in a volume of 0.2 ml, a single dose could inhibit gelatin degradation *in vivo* in a time-dependent fashion, with 50% inhibition being recorded after 12 h [16].

Acetonitrile precipitation of plasma extracted at various time points from mice that had been dosed as described above, followed by HPLC analysis, revealed a peak plasma concentration of 25 μM at 20–40 min, after which the concentration declined to approximately 2.5 μM. This concentration was maintained for at least 8 h, and we conclude that the propylene glycol facilitates a slow absorption rate, resulting in the maintenance of circulating levels of inhibitor for long periods of time. This conclusion is supported by the biodistribution of ^{14}C-labeled CT1746 which was found to exhibit a long residency time in the stomach and intestines, with relatively lower levels in other tissues. Confirmation that the CT1746 detected by HPLC was active was obtained by methanol precipitation of plasma followed by its titration against gelatinase A in the quenched fluorescent peptide assay.

No evidence of any CT1746-associated cytotoxicity in assays of clonogenicity, thymidine incorporation, or measurement of cell viability by MTT (3-[4,5-dimethylthiazol-2-yl]-2,5-diphenyltetrazolium bromide) staining was observed. Colorectal cell lines of both murine (COLO26) [24] and human (SW1222) [25] origin were tested, and inhibitor concentrations ranging from 0.08 to 10 μM over 3–7 days were employed. In the MTT assay, exposure to 25 μM CT1746 for 4 days had no measurable effect on HT1080 [3] cell viability.

Less favorable pharmacokinetics were achieved at a lower dose of 10 mg/kg, with the compound being undetectable in the plasma after 30 min by these methods. A dose of 100 mg/kg was therefore selected for the efficacy studies.

Experimental design

Fifty-five mice were randomly assigned to the following three groups on day 2 after surgical orthotopic implantation (SOI) of the human colon tumor: untreated control (15 mice); CT1746 (100 mg/kg bd; 20 mice); vehicle (propylene glycol) control (0.2 ml bd; 20 mice).

The vehicle and drugs were administered orally by gavage using an animal feeding needle (22 guage, Pro Vet Inc., City of Industry, CA). CT1746 was administered at a dosage of 100 mg/kg in propylene glycol twice a day with a 12-h interval. Each mouse received a volume of 0.2 ml of drug suspension in a single dose. Administration of compound started 5 days after SOI.

All mice were kept under close observation for symptoms of tumor growth and spread. Body weight, tumor size and survival information were collected during the course of the experiment. With regard to the compound and vehicle groups, gavage and data collection were conducted in a blinded fashion.

All mice, when found dead, were immediately immersed in 10% neutral buffered formalin for subsequent macroscopic and microscopic examination. Tissue samples derived from the primary tumor, the spread found on the colon, the cecum, the ileum and the abdominal wall, as well as the tissues of the lung, the liver and the regional lymph nodes were processed for histopathology study from all the groups. Standard H&E staining was used for microscopic examination of all the tissue sections.

Measurement of primary tumor size and animal body weight

Primary tumor size during the course of the experiment was measured with calipers by abdominal wall palpation and the tumor area was calculated by multiplying the two largest diameters. Body weight of the animals was measured by an electrical balance.

Evaluation of tumor spread and metastasis

The term 'spread' here stands for spontaneous implantation and direct invasion of the peritoneal surface of the adjacent organs such as the abdominal wall, the cecum and the ileum in the abdominal cavity (Figure 3). Any visible tumor deposit in the abdominal cavity other than the primary tumor was considered as spread, which was determined macroscopically under a dissecting microscope (×7) and confirmed microscopically.

The liver, lung and para-aortic and mesentery lymph nodes were routinely serially sectioned and stained for microscopic examination of metastasis. In this study, when lymph node metastasis was considered together with spread upon evaluation, they were defined as the 'secondary tumor deposits'.

Statistical analysis

Differences in median survival, and in mean size of the primary tumors at defined time points, between the three groups were assessed for significance using the Wilcoxon Rank-Sum test and Student's *t*-test, respectively. Incidence of survivors at defined time points and incidence of secondary tumor deposits per group as a whole as well as the incidence of secondary tumor deposits per organ site in different groups on autopsy were assessed using the Fisher Exact test. The comparison of the average number of sites of secondary tumor deposits (spread and lymph node metastasis) per mouse between groups was assessed using the Mann-Whitney *U*-test. As used here all tests of significance were two-tailed.

Results

In situ *MMP expression by the Co-3 tumor*

The gelatinolytic activity of orthotopically grown Co-3 tumor tissue and normal cecum from non-tumor-bearing mice was compared. Frozen explants of each type of tissue were used to prepare cytosols which were analysed by gelatin zymography. Normal cecum generated two major bands of approximately 45 and 55 kDa, whereas the tumor-bearing tissue had additional higher molecular weight bands including a predominant band corresponding in size to murine progelatinase-B. On incubation of the zymograms in the presence of 1, 10, or 100 nM CT1746, it was found that only the additional gelatinolytic bands associated with the tumor samples were inhibited, partially at 1 nM, and completely at 10 and 100 nM, thereby demonstrating selective inhibition of the tumor-associated gelatinase.

Effect of CT1746 on survival

Tumor was palpable in mice of all three groups 13 days after implantation (8 days after initiation of treatment). At this point, animals were observed closely and when clearly symptomatic (showing signs of cachexia and declining or restricted physical activity) due to effects of progressive tumor, or if having succumbed, were assigned a survival time.

By day 41 (36 days of treatment) it was apparent that CT1746 was exerting an effect. Thus, by this time, the incidence of survivors (Figure 1) in the compound-treated group was significantly greater than in control groups (CT1746 vs untreated, $P = 0.04$; CT1746 vs vehicle, $P = 0.03$ by the Fisher Exact test). Consequently, response to treatment was consolidated for a further 7 days before gavage was stopped.

The last animal was sacrificed on day 136 and the survival curve, accounting for all subjects in the study, is shown in Figure 1. The median survival time in the three groups is as follows: untreated, 51 days; CT1746, 78 days; vehicle, 43 days. There was no significant difference between control groups; however, there were highly statistically significant differences in median survival between the compound-treated group and control group (CT1746 vs untreated, $P = 0.0002$; CT1746 vs vehicle, $P = 0.0001$).

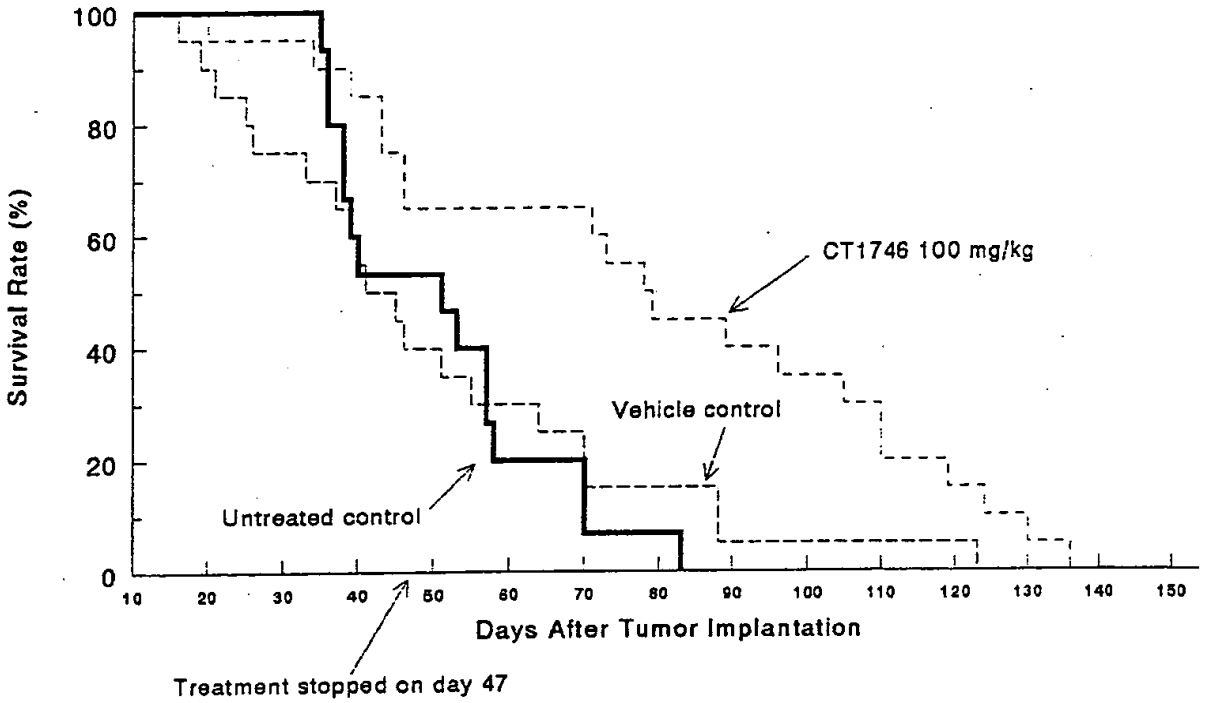

Figure 1. Survival of mice orthotopically implanted with Co-3 tumor after treatment with CT1746. Fifty-five nude mice were surgically implanted with Co-3 colon carcinoma at the orthotopic site. After 5 days animals were randomized into three groups: CT1746, 100 mg/kg bd ($n = 20$); vehicle (propylene glycol) bd ($n = 20$); untreated ($n = 15$). Treatment with compound or vehicle was continued over the next 43 days. Survival was assigned either as the day at which animals were severely symptomatic (criteria of which were mainly signs of cachexia and declining or restricted physical activity) or had succumbed to the effects of tumor. Median survival: CT1746, 78 days; vehicle, 43 days; untreated, 51 days. See text for statistical analysis.

The early demise of two to three mice in the vehicle control group (as shown in Figure 1) might have been due to the gavage procedure, which the untreated control group was not subjected to. It should be noted that despite the gavage procedure the CT1746-treated group had a much greater survival, further indicating the strong efficacy of CT1746.

Effect of CT1746 on primary tumor growth, spread and metastasis

The rate of primary tumor growth was serially assessed over 56 days by palpation and measurement of abdominal tumor. Figure 2 shows growth delay curves for the CT1746-treated group versus untreated and vehicle-treated groups: for clarity, the comparisons are shown separately. In both cases it can be seen that CT1746 treatment produces a marked growth delay relative to both control groups. At each time point the number of tumors used to calculate each mean tumor size is quoted and it can be seen in the case of the comparison of CT1746-treated with untreated animals that the number of subjects decreases rapidly from day 36 onwards, making statistical comparisons less secure at later time points. Nevertheless, at day 36 CT1746 treatment reduced tumor size by 32% relative to the untreated group ($P = 0.0001$) and by 39% relative to the vehicle-treated group ($P = 0.002$). There was no significant difference between the control groups.

Table 1 shows that in both control groups secondary tumor deposits (including spread to the abdominal wall, cecum and the ileum and metastasis to the mesenteric lymph node) were seen in all evaluable animals whereas in six animals treated with CT1746 lesions they were restricted to the site of implantation. The difference in the total incidence of secondary lesions was statistically significant when the CT1746-treated group was compared with both control groups (Table 1). Quantitative evaluation of the average number of sites of tumor spread and metastasis per mouse also showed advanced tumor development with statistical significance in the control groups compared with the treated group ($P = 0.0021$, untreated control vs CT1746; $P = 0.0031$, vehicle control vs CT1746; see

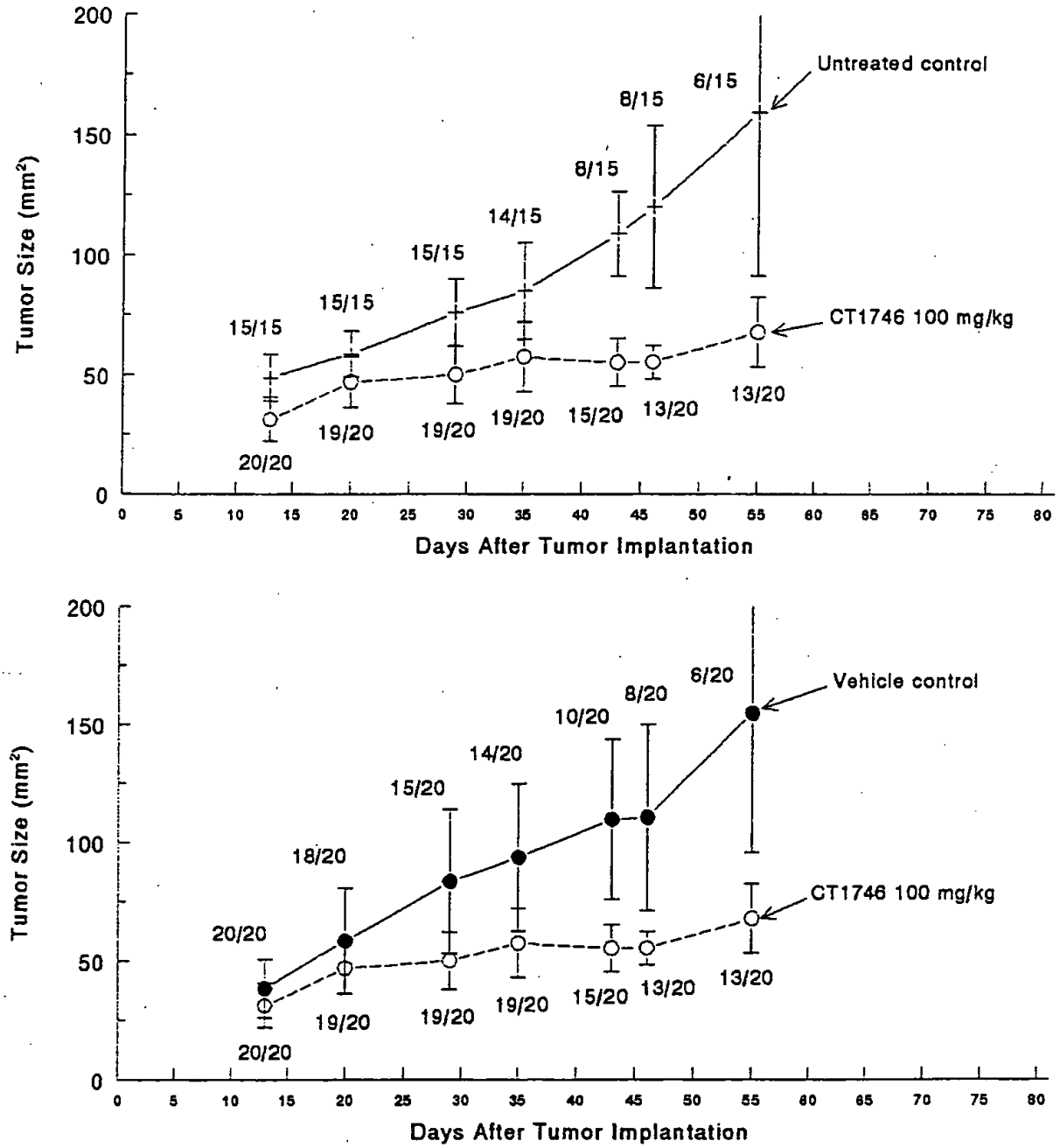

Figure 2. Growth delay of mice orthotopically implanted with Co-3 tumor after treatment with CT1746. Same experiment as Figure 1. Growth of primary tumor was assessed serially by caliper measurement after abdominal palpation: tumor size was computed from the product of two diameters. Data expressed as mean ± 1 SD. See text for statistical analysis. For clarity, comparisons of primary tumor growth after CT1746 treatment with the control groups are shown separately.

Table 1. Effect of CT1746 on tumor spread and metastasis

Treatment (no. of mice)	No. of mice available for autopsy[a]	No. of mice without secondary deposit[b]	Significance relative to untreated[c]
Untreated control (15)	14	0/14	-
Vehicle[d] bd[e] control (20)	19	0/19	NS
CT1746 100 mg/kg bd (20)	20	6/20	$P = 0.028$

[a] One animal in the untreated control and one in the vehicle group were unavailable due to tissue changes post mortem.
[b] See Table 2 for details concerning sites of tumor spread and metastasis.
[c] Differences in the incidence of secondary tumor deposits relative to the untreated control assessed by two-tailed Fisher's-exact test. Significance of difference between compound and vehicle control, $P = 0.012$.
[d] Vehicle was neat propylene glycol (0.2 ml/dose).
[e] bd = twice daily (at approx. 12 h interval).

Table 2. Effect of CT1746 on the incidence of tumor spread and metastasis at different organ sites

Group	Organ sites and incidence/percentage of tumor spread and metastasis				
	Abdominal[a] wall	Cecum[b]	Ileum[c]	Mesenteric[d] lymph nodes	Median with range[e] for no. of sites of spread and metastasis per mouse
Untreated control	13/14 (92.9%)	11/14 (78.6%)	1/14 (7.1%)	4/14 (21.42%)	2(1–3)
Vehicle control	14/19 (73.7%)	18/19 (94.7%)	2/19 (10.5%)	4/19 (21.1%)	2(1–3)
CT1746, 100 mg/kg	12/20 (60.0%)	8/20 (40.0%)	1/20 (5.0%)	0/20 (0.0%)	1(0–2)

[a] $P = 0.0504$, CT1746 vs untreated control; $P = 0.5006$, CT1746 vs vehicle control; all by Fisher's exact test.
[b] $P = 0.0382$, CT1746 vs untreated control; $P = 0.0004$, CT1746 vs vehicle control; all by Fisher's exact test.
[c] $P = 0.99$, CT1746 vs untreated control; $P = 0.605$, CT1746 vs vehicle control; all by Fisher's exact test.
[d] $P = 0.0216$, CT1746 vs untreated control; $P = 0.047$, CT1746 vs vehicle control; all by Fisher's exact test.
[e] $P = 0.0021$, CT1746 vs untreated control; $P = 0.0031$, CT1746 vs vehicle control; all by Mann–Whitney U-test. See Table 3 for the number of mice under different categories regarding the number of sites of secondary tumor deposit in the three groups.

Table 3. Effect of CT1746 on the number of secondary tumor deposits per mouse

Group	Number of sites of tumor spread and metastasis			
	0	1	2	3
	Number of mice			
Untreated control	0	2	9	3
Vehicle control	0	5	9	5
CT1746 (100 mg/kg)	6	6	8	0

Tables 2 and 3 for details). Separate analysis of the incidence of secondary tumor deposits on different organs (the abdominal wall, the cecum, the mesenteric lymph nodes) in the different groups also showed statistically-significant differences between the CT1746-treated vs both untreated control groups (see Table 2 for details).

Histopathology studies of the primary tumor in both the CT1746-treated group and the control groups did not show different cytotoxicity (Figure 3). Also no differences were observed in histologic morphology.

Effect of CT1746 on animal body weight

The mean body weight (Figure 4) in the untreated control group increased until day 21, from 17.7 to 21.0 g, while both the CT1746-treated and vehicle control groups showed a slight drop in body weight (from 19.2 to 18.4 g and from 20.0 to 18.1 g, respectively), which may have been due to the gavage procedure. By day 29, mean body weights in all three groups had stabilized at 18–19 g and remained at this level for a further 10 days, by which time treatment effects were impossible to separate from tumor cachexia.

Discussion

Models of surgical orthotopic implantation (SOI) of histologically-intact human tumor tissue in nude mice provide a unique opportunity for assessing activity of new anticancer agents against a variety of tumor types. This model, compared with orthotopic inoculation of cell suspensions and subcutaneous models, can reveal more clinical characteristics of malignant tumors, such as invasive local growth, spread and distant metastasis [12, 13]. Therefore the model can provide a clinical profile that helps in the evaluation of new therapeutic modalities.

The immunodeficient nude mouse has been used in the field of cancer research since the 1960s. Although they have severely reduced numbers of mature functional T lymphocytes, which are critical in tumor immunity, it has been shown that T-cell-like activity can be induced [26, 27], especially when the nude mouse encounters a microbial infection. Also it is believed that the older the mice are, the stronger the residual T-cell function is. Moreover, the activities of other cell types in the nude mouse defense system, such as NK cells and macrophages, are reported to be at normal or even higher levels [28, 29]. These cells are suggested to play an important role in inhibiting tumor xenograft growth in nude mice [30, 31]. Based on these properties, mice of the same strain, same sex and the same age were used for all the groups in this study to eliminate any possible variables in this aspect. Also, mice of young age (3–4 weeks old in this study) were chosen to facilitate tumor growth and to avoid the possible variability of residual T-cell function in older mice.

The salient points emerging from this evaluation of CT1746 are that a non-cytotoxic peptidomimetic compound, administered orally in a chronic fashion, exerts a degree of control on tumor growth, spread and metastasis. That CT1746 is not generally cytotoxic is suggested by the lack of compound-related toxicity as assessed by body weight over the period of administration. In addition, we have found that it has no effect on cell viability *in vitro* at a concentration as high as 25 μM (see Materials and Methods).

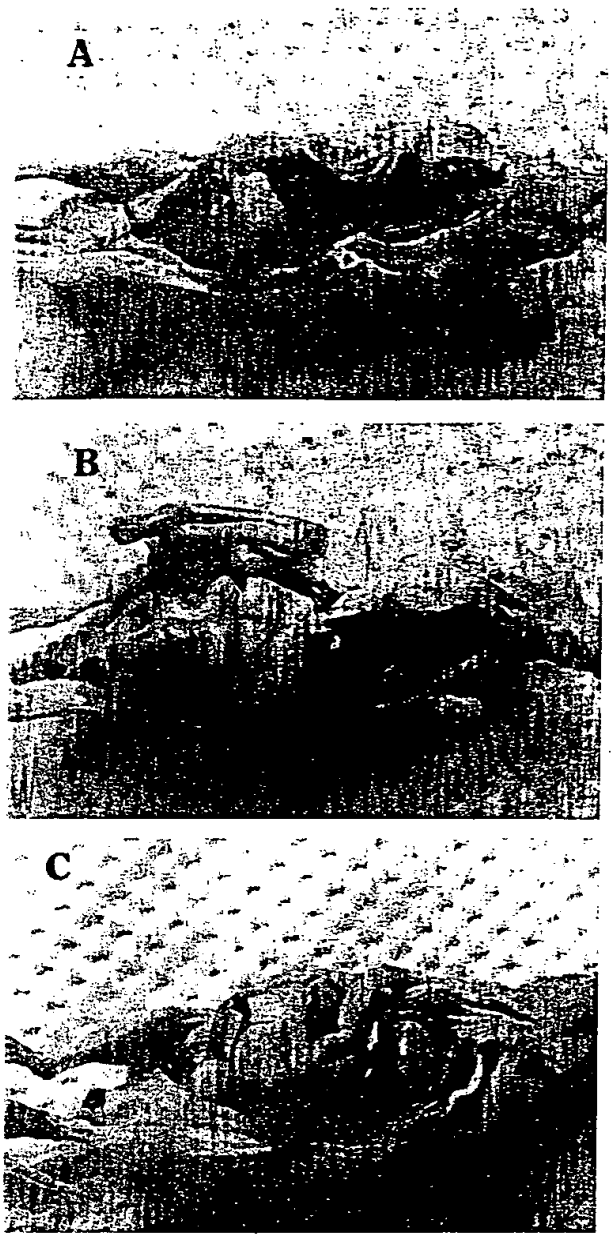

Figure 3. (A) Gross picture of the primary tumor in the CT1746-treated group. (B) Gross picture of the primary tumor in the untreated control group. (C) Gross picture of the primary tumor in the vehicle control group.

The results herein are noteworthy because, so far as we are aware, this is the first published demonstration of anti-tumor activity using an orally active, synthetic MMP inhibitor. This is important for two reasons: first, although it is frequently possible to synthesize potent peptidomimetic

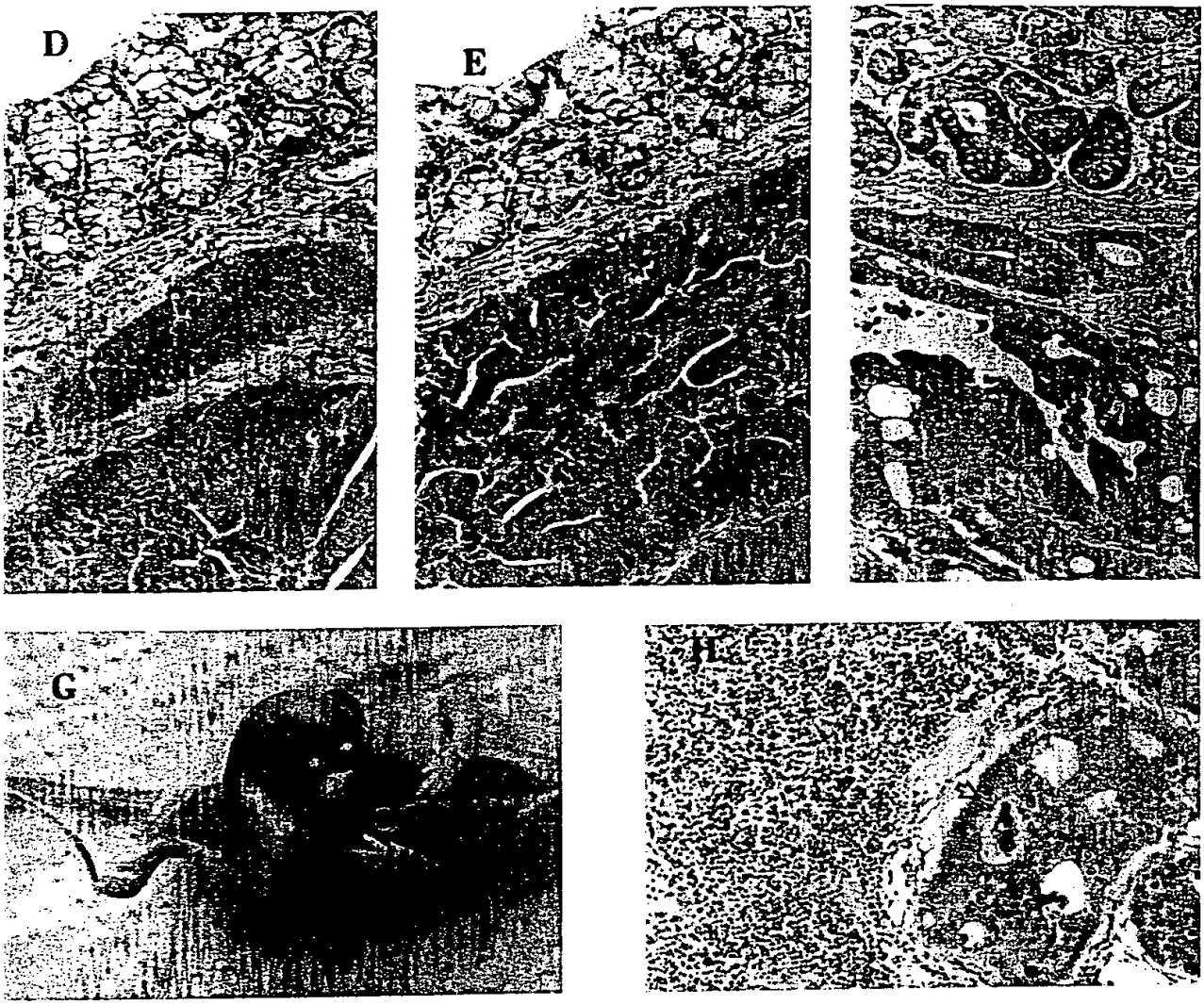

Figure 3. *Continued*
(D) Histopathology of the primary tumor in the CT1746-treated group. (E) Histopathology of the primary tumor in the untreated control group. (F) Histopathology of the primary tumor in the vehicle control group. (G) Gross picture of cecum spread in the untreated control group. (H) Histopathology of lymph node metastasis in the untreated control group.

inhibitors [19–21, 32], they are generally found to possess little or no oral activity. Building this into the molecule is unpredictable and may militate against potency [33]. Second, pharmaceuticals designed to exert cell control rather than cell kill will require chronic administration and this is only feasible with compounds that are absorbed from the gastrointestinal tract.

The tumor response recorded here is manifested as an increase in survival (Figure 1), which is presumably a reflection of reduced primary tumor growth (Figure 2) and lower incidence of secondary tumors (Tables 1–3). The compound is about three orders of magnitude less potent at inhibiting interstitial collagenase and matrilysin than gelatinase A or B, and we found that the gelatinase activity associated with the tumor tissue, but not normal cecum, could be selectively inhibited by CT1746, *ex vivo*, on zymograms. However, we do not know what concentrations of CT1746 are actually required to inhibit each of the MMPs *in vivo*, and the blood levels of CT1746 achieved in the model greatly exceed the concentration required to inhibit pure preparations of all four types of MMPs. It is therefore noteworthy that tumor growth inhibition, analogous to that previously described for broad spectrum inhibitors that effectively inhibit collagenase and matrilysin, is observed [7], but with better apparent survival efficacy achieved with CT1746. We cannot rule out the possibility that

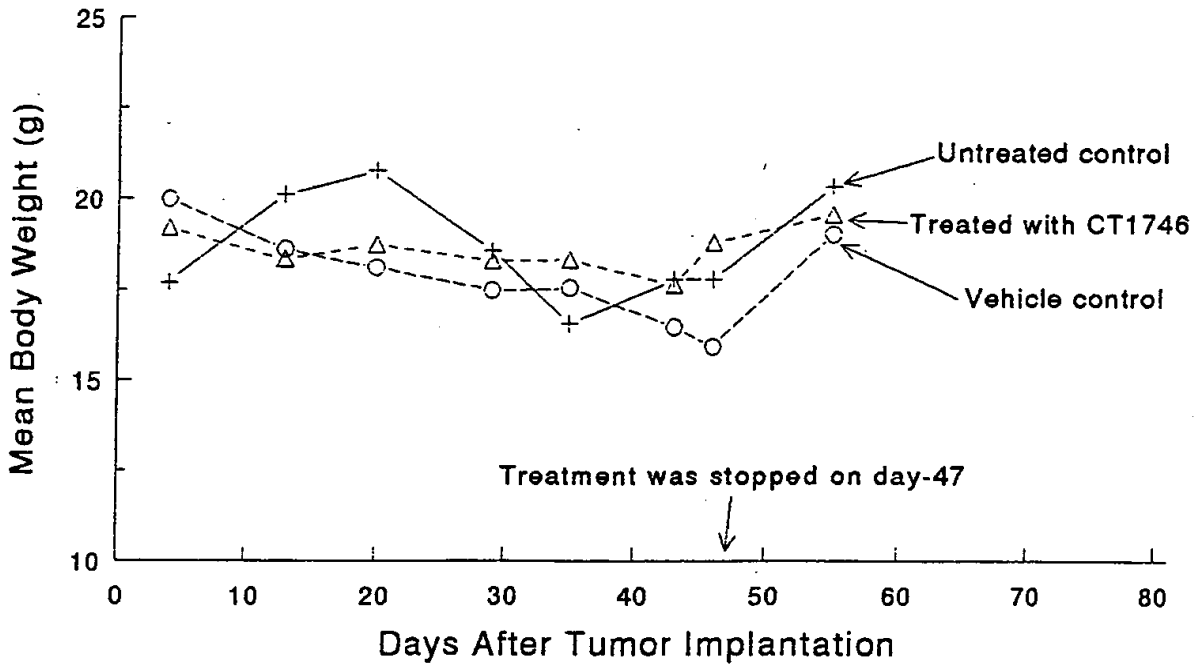

Figure 4. Mean body weight in the three groups of mice orthotopically implanted with human colon tumor Co-3. Same experiment as Figure 1. Body weights were measured with an electrical balance. See text for details.

inhibition of one or more of the newly described MT-MMPs, or an unknown metalloproteinase, may also contribute to the effect.

Given the lack of evidence for any CT1746-associated cytotoxicity we do not believe the tumor response involves cell death, at least not as a direct consequence of the compound. MMPs or related MPs are thought to be responsible for a wide variety of molecular processing events, many of which could be considered to be pro-inflammatory [21, 34]. Although a number of publications have demonstrated the inhibition of TNFα release from inflammatory cells by MMP inhibitors [21, 34 and references therein], the selectivity of CT1746 is such that its IC_{50} value for TNFα release *in vitro* is in excess of 10 μM. Furthermore, *in vivo* studies confirmed that at doses ranging from 7 to 700 mg/kg, CT1746 does not inhibit TNFα release following LPS stimulation in immunocompetent BALB/C mice (unpublished observations). It is therefore most unlikely that CT1746 exerts its effects in tumor models through inhibition of a TNFα-mediated inflammation pathway.

The control of tumor growth and spread described here may be at least in part due to an anti-angiogenic effect. Hydroxamic acid-based MMP inhibitors have been reported to inhibit angiogenesis [9, 10] and evidence that CT1746 can inhibit angiogenesis comes from our observation that when administered under identical conditions to those described here, it inhibited the rate of neovascularization of sponges implanted in the flanks of mice [35 and manuscript in preparation]. The effect is dose-dependent and occurs over a period of at least 25 days following sponge implantation.

A further mechanism via which CT1746 may be exerting its effect may be related to the recently published observation that gelatinase functions to modulate cell attachment, and hence cell migration and invasion [2]. To date, however, this has only been demonstrated for melanoma cells, where gelatinase A activity was shown to have a direct effect on adhesion and spreading.

It has been suggested that cytotoxic chemotherapy has reached the limit of efficacy [11, 36] and that approaches based on cell control, rather than cell kill, are becoming a credible alternative. The prototype compound of this general class is the anti-oestrogen tamoxifen [37], that has activity in breast cancer. More recently, vitamin A acid has demonstrated activity in acute promyelocytic leukemia [38]. MMP inhibitors and other anti-angiogenic agents are currently undergoing evaluation in patients with solid tumors. This study suggests that if tumor

control, in the absence of tumor cell kill, can be achieved then a survival advantage will accrue.

Acknowledgements

We warmly acknowledge the contributions of Mary Birch, Jimi O'Connell, Barbara Janczynski, Andy Nesbitt, Ted Parton, Amanda Suitters, Karen Zinkewich-Peotti and Liz Beaumont at Celltech Therapeutics, and Paul Elvin at Zeneca Pharmaceuticals to this study.

References

1. Liotta LA, Steeg PS and Stetler-Stevenson W, 1991, Cancer metastasis and angiogenesis: an imbalance of positive and negative regulation. *Cell*, **64**, 327–36.
2. Ray JM and Stetler-Stevenson WG, 1995, Gelatinase A activity directly modulates melanoma cell adhesion and spreading. *EMBO J*, **14**, 908–17.
3. Frisch SM, Reich R, Collier IE, Genrich LT, Martin G and Goldberg GI, 1990, Adenovirus E1A represses protease gene expression and inhibits metastasis of human tumor cells. *Oncogene*, **5**, 75–83.
4. Schultz RM, Silberman S, Persky B, Bajkowski AS and Carmichael DF, 1988, Inhibition by human recombinant tissue inhibitor of metalloproteinases of human amnion invasion and lung colonization by murine B-16 F10 melanoma cells. *Cancer Res*, **48**, 5539–45.
5. DeClerk YA, Perez N, Shimada H, *et al.* 1992, Inhibition of invasion and metastasis in cells transfected with an inhibitor of metalloproteinases. *Cancer Res*, **52**, 701–8.
6. Anderson IA, Shipp MA, Docherty AJP and Teicher BA, 1996, Combination therapy including a gelatinase inhibitor and cytotoxic agent reduces local invasion and metastasis of murine Lewig lung carcinoma. *Cancer Res*, **56**, 715–8.
7. Wang X, Fu X, Brown PD, Crimmin MJ and Hoffman RM, 1994, Matrix metalloproteinase inhibitor BB-94 (Batimastat) inhibits human colon tumor growth and spread in a patient-like orthotopic model in nude mice. *Cancer Res*, **54**, 4726-28.
8. Goldmann E, 1907, The growth of malignant disease in man and the lower animals with special reference to the vascular system. *Lancet*, **2**, 1236–40.
9. Galardy RE, Grobelny D, Foellmer HG and Fernandez LA, 1994, Inhibition of angiogenesis by the matrix metalloproteinase inhibitor N-[2R-2-(hydroxamidocarbonymethyl)-4-methylpentonyl)]-L-tryptophan methylamide. *Cancer Res*, **54**, 4715–18.
10. Taraboletti G, Garofalo A, Bellotti D, *et al.* 1995, Inhibition of angiogenesis and murine hemangioma growth by Batimastat, a synthetic inhibitor of matrix metalloproteinases. *J Natl Cancer Inst*, **87**, 293–8.
11. Braverman AS, 1993, Chemotherapeutic failure: resistance or insensitivity. *Ann Int Med*, **118**, 630–2.
12. Hoffman RM, 1992, Patient-like models of human cancer in mice. *Curr Perspec Molec Cell Oncol*, **1(B)**, 311–29.
13. Hoffman RM, 1994, Orthotopic is orthodox: why are orthotopic-transplant metastatic models different from all other models? *J Cell Biochem*. **56**, 1–3.
14. Fu X, Guadagni F and Hoffman RM, 1992, A metastatic nude-mice model of human pancreatic cancer constructed orthotopically from histologically-intact patient specimens. *Proc Natl Acad Sci, USA*, **89**, 5645–9.
15. Furukawa T, Fu X, Kubota T, Watanabe M, Kitajima M and Hoffman RM, 1993, Orthotopic transplantation of histologically-intact clinical specimens of stomach cancer to nude mice: correlation of metastasis sites in mouse and human. *Int J Cancer*, **53**, 608–12.
16. Chander SK, Antoniw P, Beeley NRA, *et al.* 1995, An *in vivo* model for screening peptidomimetic inhibitors of gelatinase A. *J Pharm Sci*, **84**, 404–9.
17. Kubota T, Shimosato Y and Nagai K, 1978, Experimental chemotherapy of carcinoma of the human stomach and colon serially transplanted in nude mice. *Gann*, **68**, 299–309.
18. Murphy G, Willenbrock F, Ward RV, *et al.* 1992, The C-terminal domain of 72 kDa gelatinase A is not required for catalysis, but is essential for membrane activation and modulates interactions with tissue inhibitors of metalloproteinases. *Biochem J*, **283**, 637–41.
19. Henderson B, Docherty AJP and Beeley NRA, 1990, Design of inhibitors of cartilage destruction. *Drugs Future*, **15**, 496–508.
20. Beeley NRA, Ansell PRJ and Docherty AJP, 1994, Inhibitors of matrix metalloproteinase (MMPs). *Curr Opinion Ther Patents*, **4**, 7–16.
21. Beckett RP, Davidson AH, Drummond AH, Huxley P and Whittaker M, 1996, Recent advances in matrix metalloproteinase inhibitor research. *DDT*, **1**, 16–26.
22. Nagase H, Okada Y, Suzuki K, Enghild JJ and Salvesen G, 1991, Substrate specificities and activation mechanisms of the precursors of matrix metalloproteinases. *Biochem Soc Trans*, **19**, 715–18.
23. Crabbe T, O'Connell JP, Smith BJ and Docherty AJP, 1994, Reciprocated matrix metalloproteinase activation: a process performed by interstitial collagenase and progelatinase A. *Biochemistry*, **33**, 14419–25.
24. Tsuruo T, Yamori T, Naganuma K, Tsukagoshi S, and Sakurai Y, 1983, Characterisation of metastatic clones derived from a metastatic variant of mouse colon adenocarcinoma 26. *Cancer Res*, **43**, 5437–42.
25. Richman PI and Bodmer WF, 1988, Control of differentiation in human colorectal carcinoma cell lines: epithelial–mesenchymal interactions. *J Pathol*, **156**, 197–211.
26. Wortis HH, 1971, Immunological responses of "nude" mice. *Clin Exp Immunol*, **8**, 305–17.
27. Huning T and Bevan MJ, 1980, Specificity of cytotoxic T cells from athymic mice. *J Exp Med*, **152**, 688–702.
28. Minato N, Reid L, Neighbour A, Bloom BR and Holland J, 1980, Interferon, NK cells and persistent virus infection. *Ann NY Acad Sci*, **350**, 42–52.
29. Sharp AK and Colston MJ, 1984, The regulation of macrophage activity in congenitally athymic mice. *Eur J Immunol*, **14**, 102–5.
30. Benomar A, Gerlier D and Doré JF, 1986, Interaction with host macrophages and ability of human melanoma cell lines to grow in nude mice. *Int J Cancer*, **38**, 419.

31. Herberman RB, Nunn ME, Holden HT, Staal S and Djeu JY, 1977, Augmentation of natural cytotoxic reactivity of mouse lymphoid cells against syngeneic and allogeneic large T cells. *Int J Cancer*, **19**, 555.
32. Porter JR, Beeley NRA., Boyce BA, *et al.* 1994, Potent and selective inhibitors of gelatinase A I. Hydroxamic acid derivatives. *Bioorg Med Chem Lett*, **4**, 2741–6.
33. Kleinwert HD, Baker WR and Stein HH, 1993, Orally-active peptide-like molecules: a case history. *Biopharmacology*, **6**, 36–41.
34. Goetzl EJ, Banda MJ and Leppert D, 1996, Matrix metalloproteinases in immunity. *J Immunol*, **156**, 1–4.
35. Mahadevan V, Hart IR and Lewis GP, 1989, Factors influencing blood supply in wound granuloma quantified by a new *in vivo* technique. *Cancer Res*, **49**, 415–19.
36. Schipper H, Goh CR and Wang TL, 1995, Shifting the cancer paradigm: must we kill to cure? *J Clin Oncol*, **13**, 801–7.
37. Furr BJ and Jordan VC, 1984, The pharmacology and clinical uses of tamoxifen. *Pharmacol Ther*, **25**, 127–205.
38. Warrell RP, Frankel SR, Miller WH, *et al.* 1991, Differentiation therapy of acute promyelocytic leukemia with tretinoin (all-*trans*-retinoic acid). *New Engl J Med*, **324**, 1385–93.

[CANCER RESEARCH 54, 4726–4728, September 1, 1994]

9

Matrix Metalloproteinase Inhibitor BB-94 (Batimastat) Inhibits Human Colon Tumor Growth and Spread in a Patient-like Orthotopic Model in Nude Mice

X. Wang, X. Fu, P. D. Brown, M. J. Crimmin, and R. M. Hoffman

AntiCancer, Inc., San Diego, California 92111 [X. W., X. F., R. M. H.], and British Bio-technology, Ltd., Watlington Road, Cowley, Oxford, OX4 5LY, United Kingdom [P. D. B., M. J. C.]

ABSTRACT

Matrix metalloproteinases have been implicated in the growth and spread of metastatic tumors. This role was investigated in an orthotopic transplant model of human colon cancer in nude mice using the matrix metalloproteinase inhibitor BB-94 (batimastat). Fragments of human colon carcinoma (1–1.5 mm) were surgically implanted orthotopically on the colon in 40 athymic *nu/nu* mice. Administration of BB-94 or vehicle (phosphate buffered saline, pH 7.4, containing 0.01% Tween 80) commenced 7 days after tumor implantation (20 animals/group). Animals received 30 mg/kg BB-94 i.p. once daily for the first 60 days and then 3 times weekly. Treatment with BB-94 caused a reduction in the median weight of the primary tumor from 293 mg in the control group to 144 mg in the BB-94 treated group ($P < 0.001$). BB-94 treatment also reduced the incidence of local and regional invasion, from 12 of 18 mice in the control group (67%) to 7 of 20 mice in the treated group (35%). Six mice in the control group were also found to have metastases in the liver, lung, peritoneum, abdominal wall, or local lymph nodes. Only two mice in the BB-94 group had evidence of metastatic disease, in both cases confined to the abdominal wall. The reduction in tumor progression observed in the BB-94-treated group translated into an improvement in the survival of this group, from a median survival time of 110 days in the control group to a median survival time of 140 days in the treated group ($P < 0.01$). Treatment with BB-94 was not associated with any obvious toxic effect, and these results suggest that such agents may be effective as adjunctive cancer therapies.

INTRODUCTION

Previous studies with the native matrix metalloproteinase inhibitors, TIMP-1[1] and TIMP-2, have demonstrated the potential of these inhibitors to block specific steps in the processes of tumor growth and metastatic progression. In a study of B16 mouse melanoma in mice TIMP-1 was shown to inhibit lung colonization by blood-borne melanoma cells, one of the final steps in the metastatic process (1). Results from a separate study of malignant 4R rat embryo fibroblasts, transfected with the natural matrix metalloproteinase inhibitor TIMP-2, suggested that TIMP-2 can inhibit solid tumor growth (2). Recently, transfection of B16-F10 cells with TIMP-1 has been shown to be associated with inhibition of both the primary tumor growth and metastatic potential of these cells (3).

Collectively, these studies support the hypothesis that matrix metalloproteinase inhibitors can restrict malignant progression by blocking the breakdown of matrix structure that is required for metastasis and tumor expression. However, these studies have examined tumor growth in syngeneic models with mouse and rat tumors. The current study was designed to allow the process of malignant progression to be examined as a whole, in a model that resembled as closely as possible the clinical situation. In this model fragments of metastatic human colorectal carcinoma are surgically implanted on the colon of nude mice. These fragments grow rapidly in the colon environment to form large primary colon tumors. The tumors invade locally and subsequently metastasize to sites common in metastatic human colorectal cancer, namely, the lymph nodes, liver, peritoneum, and lung (4, 5). The objective of the study was to test the synthetic low molecular weight matrix metalloproteinase inhibitor, BB-94 (batimastat), for its ability to inhibit primary tumor growth, local invasion, and metastatic spread. The effect of BB-94 treatment on the survival of the tumor bearing mice was also examined.

BB-94 (batimastat) ([4-*N*-hydroxyamino)-2*R*-isobutyl-3*S*-(thienylthiomethyl)succinyl]-L-phenylalanine-*N*-methylamide, M_r, 478) is a peptide-like analogue of the collagen substrate. IC_{50}s were determined for BB-94 *in vitro* against the following metalloproteinases: interstitial collagenase, 3 nM; stromelysin, 20 nM; M_r 72,000 type IV collagenase, 4 nM; M_r 92,000 type IV collagenase, 4 nM; and matrilysin, 6 nM. The inhibitor shows little detectable inhibitory activity against other metalloproteinases such as angiotensin converting enzyme (0% inhibition at 1000 nM) (6).

MATERIALS AND METHODS

Animals. Male and female athymic *nu/nu* mice 4–6 weeks of age were used for the study. The animals were maintained in a sterile environment and cages, food, and bedding were autoclaved. The animal diets were obtained from Harlan Teklad (Madison, WI) and 0.15% (v/v) HCl was added to the drinking water. Forty mice were used for the study, 20 each in the treatment and control groups.

Colon Carcinoma Xenograft. The human colon mucinous adenocarcinoma was obtained from colon cancer patient AC1935. The tumor was in the 5th passage when used in the study. Before implantation the tumor was harvested from the colon of a nude mouse, cut into 1–1.5-mm fragments, and placed in Earle's minimal essential medium.

Surgical Orthotopic Implantation. The animals were anesthetized with isoflurane and the abdomens were sterilized with iodine and alcohol. A small midline incision was made in the abdomen and the colocecal portion of the colon was exposed. The serosa was removed from the site where the tumor fragments were to be implanted and 8-10 fragments were implanted on the top of the animal intestine. An 8-0 surgical suture was used to penetrate these small tumor fragments and suture them on the intestine wall. The intestine was returned to the abdominal cavity and the abdominal wall was closed with 7-0 surgical sutures. The animals were maintained in the sterile environment after surgery.

Pharmacokinetics of BB-94. The dosing regimen used in the current study was based on a pharmacokinetic analysis performed prior to the study in BALB/c mice (6–8 weeks of age). The concentration of BB-94 in the blood was determined by *ex vivo* bioassay. Briefly, 0.5 ml of blood was taken by cardiac puncture at appropriate times and placed in a polypropylene tube containing 3 ml of methanol. The precipitated proteins were separated by centrifugation and 2.5-ml portions of the methanol extract were dried under vacuum. The extracted BB-94 was resolubilized in 200 μl of dimethyl sulfoxide and added to tubes containing radiolabeled type I collagen and collagenase. The concentration of inhibitor in the blood extracts was determined by comparison with the degree of inhibition of collagenase in parallel incubations that contained known concentrations of BB-94. Separate experiments in which BB-94 was added directly to whole blood revealed that the extraction efficiency of the methanol process was approximately 50%.

The blood levels of BB-94 following a single 30-mg/kg dose ranged between 30 and 12 ng/ml over 24 h. These values, when corrected for extraction efficiency (~50%), are over 10-fold higher than the IC_{50} of this inhibitor for collagenase (1.5 ng/ml) and the M_r 92,000 and M_r 72,000 type IV

Received 3/23/94; accepted 7/5/94.

The costs of publication of this article were defrayed in part by the payment of page charges. This article must therefore be hereby marked *advertisement* in accordance with 18 U.S.C. Section 1734 solely to indicate this fact.

[1] The abbreviation used is: TIMP, tissue inhibitor of metalloproteinases.

collagenases (2 ng/ml). On the basis of these results a dose of 30 mg/kg i.p. once daily was selected. However, in view of the length of the experiment this was reduced to 30 mg/kg three times weekly after 60 days in order to reduce any morbidity associated with the i.p. injection. Administration of the metalloproteinase inhibitor BB-94 or vehicle (phosphate buffered saline, pH 7.4, containing 0.01% Tween 80) began 1 week after surgery.

Evaluation of Response. During the course of the study, both primary tumor size and the performance status of each animal were followed. On autopsy the weight of the primary tumor was calculated as

$$\text{Weight} = \frac{\text{width}^2 \times \text{length}}{4}$$

The extent of both local and distant tumor spread was also assessed. Tissue samples were also processed for histology by fixation in 10% formalin followed by paraffin embedding and sectioning. The sections were stained with hematoxylin and eosin.

The sizes of primary tumors in the two groups were compared using the Mann-Whitney two-tailed test and the differences in survival were compared using the log rank test.

RESULTS

Effect of BB-94 on Primary Tumor Growth. Tumors developed on the colon in all of the animals, although two animals in the control group were lost following death and post-mortem data were not obtained. Treatment with BB-94 caused a significant reduction in the median weight of the primary tumor from 293 mg (range, 1141 to 124 mg) in the control group to 144 mg (range, 424 to 38 mg) in the BB-94 treated group ($P < 0.001$).

Effect of BB-94 on Local/Regional Invasion. Treatment with BB-94 caused a marked reduction in the incidence of tumor invasion of adjacent tissue, from 12 of 18 mice in the control group (67%) to 7 of 20 mice in the BB-94 treated group (35%) (Table 1). In the control group there were 8 cases of invasion of adjacent abdominal wall and 4 cases of invasion of the peritoneal surface. In the BB-94 treated group there were 6 cases of abdominal wall invasion and 1 case of peritoneal invasion.

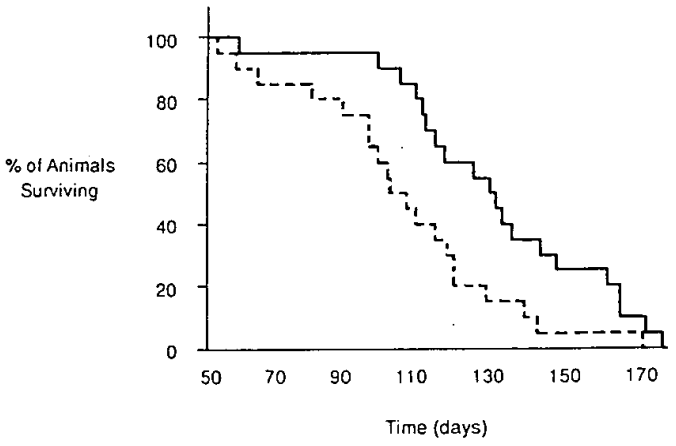

Fig 1. Survival curve for mice bearing orthotopically transplanted human colon carcinoma. Animals were treated with BB-94 (——) or vehicle (– – –) once daily from day 7 to day 60 and three times weekly thereafter.

Table 1 *Effect of BB94 on tumor progression*

	Primary Tumor size (mg)		Survival time (days)		Incidence of	
Group	Mean ± SD	Median	Mean ± SD	Median	Invasion	Metastasis
Control	362 ± 246	293	112 ± 33	110	12/18	6/18
BB-94	147 ± 91	144	140 ± 33	140	7/20	2/20

Effect of BB-94 on Metastasis. Treatment with BB-94 caused a reduction in the incidence of metastasis. In the control group 3 mice had metastases at a distant site on the abdominal wall, 1 mouse had metastases on the parietal peritoneum; 1 mouse had malignant ascites; and 1 mouse had extensive metastatic disease with metastases in the cecum, liver, and mesentery lymph nodes. In addition, another mouse in this group had a possible lung metastasis. In contrast, only 2 mice in the BB-94 treated group showed signs of distant tumor spread, in both cases to the abdominal wall (Table 1).

$P < 0.01$ for total invasion and metastases comparing the treated and control group.

Effect of BB-94 on Survival. Treatment with BB-94 resulted in a modest improvement in survival. On day 138, 50% of the BB-94 treated animals remained alive compared with only 15% of the control animals. The median survival time of the control group was 110 days (range, 187–59 days) compared to 140 days (range, 193-60 days) for the BB-94 treated group ($P < 0.01$) (Fig. 1).

$P < 0.025$ for survival probability difference between the treated and control group at day 138 using the Mantel-Haenszel test (7).

Effect of BB-94 on Tumor Histology. Although it has not been possible to quantitate differences in histological appearance, the tumors in the control group showed high degrees of viability and cellularity, whereas those from the BB-94 treated animals appeared less viable, with lower cell densities and often increased amounts of mucin (Fig. 2).

Effect of BB-94 on Animal Weight. Treatment with BB-94 caused no significant changes in animal weight when compared to the control group, indicating that BB-94 was not overtly toxic (data not shown).

DISCUSSION

The current model of orthotopic implantation of a human colon carcinoma provides a unique opportunity to study a human malignancy in a context that is as close as possible to the clinical condition. In this study, treatment with BB-94 resulted in inhibition of primary tumor growth, local/regional spread, and distant metastasis. Since the implanted tumor was in direct contact with BB-94 it is possible that some of the antitumor activity might be the result of direct toxicity. However, studies with two other human colorectal carcinoma cell lines, AP-5 and C170HM2, and the mouse melanoma cell line B16-BL6 have shown that BB-94 does not inhibit proliferation of these cells, even at concentrations approaching saturation (6 μM).[2] It has not been possible to examine *in vitro* the effect of BB-94 on the colorectal carcinoma used in the current study. However, direct cytotoxic effect seems unlikely, particularly in view of the lack of overt toxicity during the 193-day study.

A large body of correlative data now exists supporting the involvement of matrix metalloproteinases in the malignant progression of many common tumors (for review see Ref. 8). In the case of human colorectal carcinoma, fibrillar collagenolytic activity has been shown to correlate with histological grade (9) and expression of the M_r 72,000 gelatinase has been correlated with tumor progression (10). *In situ* RNA hybridization studies have shown the source of the M_r 72,000 gelatinase in colorectal carcinoma to be the tissue stroma adjacent to the invasive front of the tumour (11). The antitumor effects observed in the current study are consistent with the established action of a matrix metalloproteinase inhibitor such as BB-94. The model has allowed the action of this inhibitor to be studied on the process of malignant progression as a whole. By blocking matrix degradation

[2] S. Watson and R. Giavazzi, personal communication.

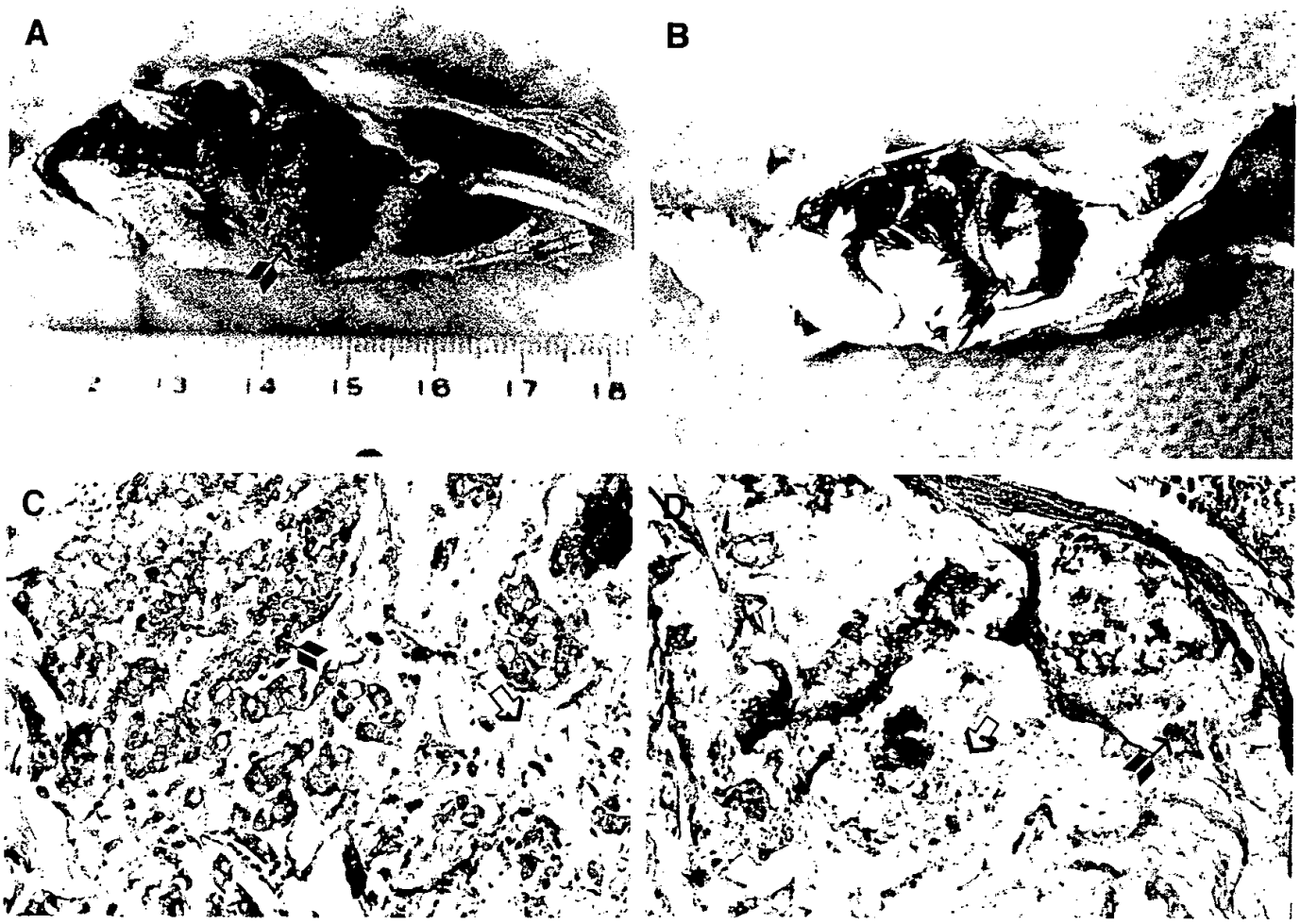

Fig 2. *A*, gross picture of the orthotopically implanted human colon tumor in an untreated mouse. The implanted tumor is 10 x 13.4 mm at day 126 (*arrow*). *B*, gross picture of the orthotopically implanted human colon tumor in a BB-94 treated mouse. The implanted tumor is 5.2 × 5.6 mm at day 180 (*arrow*). The tumor appears more firm than the tumor in the untreated mice. *C*, histopathology of primary human colon tumor of an untreated mouse shown in *A*. *Solid arrow*, tumor cells; *open arrow*, mucin. *D*, histopathology of primary human colon tumor of a BB-94 treated mouse shown in *B*. The tumor seems to have more mucin (*open arrow*) and less tumor cells (*solid arrow*) than the untreated mice.

BB-94 was able to inhibit not only metastatic spread but also "primary" tumor growth.

This effect on the growth of a solid tumor has important implications for the possible therapeutic use of matrix metalloproteinases. The prevention of metastasis has always been of more interest to academic scientists than to practicing oncologists. The latter are acutely aware of the fact that the patients in need of more effective therapy are those whose tumors have already metastasized. Following surgery, chemotherapy remains the most effective way to check the relentless growth and spread of metastatic tumors. Provided agents such as BB-94 show in the clinic the low toxicity profile seen in preclinical studies, it would be possible to envision their use as adjunctive agents to complement more toxic chemotherapies. Used in this way it is possible that matrix metalloproteinase inhibitors could contain both tumor growth and spread between cycles of cytotoxic agents. The results from this study indicate that i.p. BB-94 should be investigated in the clinic as a therapy for inhibiting malignant progression in colon carcinoma.

REFERENCES

1. Schultz, R. M., Silberman, S., Persky, B., Bajkowski, A. S., and Carmichael, D. F. Inhibition by human recombinant tissue inhibitor of metalloproteinases of human amnion invasion and lung colonization by murine B16-F10 melanoma cells. Cancer Res., *48:* 5539–5545, 1988.
2. DeClerck, Y. A., Perez, N., Shimada, H., Boone, T. C., Langley, K. E., and Taylor, S. M. Inhibition of invasion and metastasis in cells transfected with an inhibitor of metalloproteinases. Cancer Res., *52:* 701–708, 1992.
3. Khokha, R. Suppression of tumorigenic and metastatic abilities of murine B16-F10 melanoma cells *in vivo* by the overexpression of the tissue inhibitor of metalloproteinases-1. J. Natl. Cancer Inst., *86:* 299–304, 1994.
4. Fu, X., Besterman, J. M., Monosov, A., and Hoffman, R. M. Models of human metastatic colon cancer in nude mice orthotopically constructed by using histologically intact patient specimens. Proc. Natl. Acad. Sci. USA, *88:* 9345–9349, 1991.
5. Furukawa, T., Fu, X., Kubota, T., Watanabe, M., Kitajima, M., and Hoffman, R. M. Nude mouse metastatic models of human stomach cancer constructed using orthotopic implantation of histologically intact tissue. Cancer Res., *53:* 1204–1208, 1993.
6. Chirivi, R., Garofalo, A., Crimmin, M., Bawden, L., Stoppacciaro, A., Brown, P., and Giavazzi, R. Inhibition of the metastatic spread and growth of B16-BL6 murine melanoma by a synthetic matrix metalloproteinase inhibitor. Int. J. Cancer, *58:* 1–5, 1994.
7. Pagano, M., and Gauvreau, K. Principles of Biostatistics. North Scituate MA: Duxbury Press, 1992.
8. Brown, P. D. Section review—matrix metalloproteinase inhibitors: a new class of anticancer agent. Curr. Opin. Invest. Drugs, *2:* 617–626, 1993.
9. van der Stappen, J. W. J., Hendriks, T., and Wobbes, T. Correlation between collagenolytic activity and grade of histological differentiation in colorectal tumours. Int. J. Cancer, *45:* 1071–1078, 1990.
10. D'Errico, A., Garbisa, S., Liotta, L. A., Castronovo, V., Stetler-Stevenson, W. G., and Grigioni, W. F. Augmentation of type IV collagenase, laminin receptor, and Ki67 proliferation antigen associated with human colon, gastric and breast carcinoma progression. Mod. Pathol., *4:* 239–246, 1991.
11. Poulsom, R., Pignatelli, M., Stetler-Stevenson, W. G., Liotta, L. A., Wright, P. A., Jeffery, R. E., Longcroft, J. M., Rogers, L., and Stamp, G. W. Stromal expression of 72 kDa type IV collagenase (MMP-2) and TIMP-2 mRNAs in colorectal neoplasia. Am. J. Pathol., *141:* 389–396, 1992.

[CANCER RESEARCH 53, 3070–3072, July 1, 1993]

A Novel "Patient-like" Treatment Model of Human Pancreatic Cancer Constructed Using Orthotopic Transplantation of Histologically Intact Human Tumor Tissue in Nude Mice[1]

Toshiharu Furukawa, Tetsuro Kubota,[2] Masahiko Watanabe, Masaki Kitajima, and Robert M. Hoffman

Department of Surgery, School of Medicine, Keio University, 35 Shinanomachi, Shinjuku-ku, Tokyo 160, Japan [T. F., T. K., M. W., M. K.]; AntiCancer, Inc., San Diego, California 92110 [R. M. H.]; and Laboratory of Cancer Biology, School of Medicine, University of California, San Diego, La Jolla, California 92093–0609 [R. M. H.]

ABSTRACT

Pancreatic cancer is a disease with essentially no effective treatment. To increase the potential for discovering effective treatment, we have developed a new treatment model whereby a human pancreatic cancer line, PANC-4, was orthotopically transplanted to the pancreas of nude mice as histologically intact tumor tissue. The tumor grew with subsequent invasive local tumor growth and liver and peritoneal metastases. The antitumor activity of 5-fluorouracil (5-FU) and mitomycin C (MMC) against PANC-4 was initially determined in the *in vitro* collagen-sponge-gel supported histoculture drug-response assay with the 3-(4,5-dimethylthiazol-2-yl)-2,5-diphenyltetrazolium bromide end point. Inhibition rates were 5.6% for 5-FU and 39.4% for MMC indicating higher efficacy of MMC than 5-FU against PANC-4. When the antitumor activities of 5-FU and MMC against PANC-4 were determined *in vivo* using the nude mouse orthotopic transplant treatment model, slight local tumor growth inhibition with equivalent incidence of metastases to the liver and the peritoneum as the control were observed in the mice treated with 5-FU, while those treated with MMC had considerably reduced local tumor growth without liver and peritoneal metastases. Thus the histoculture drug-response assay in combination with the orthotopic transplant metastatic models provides for the first time a paradigm for evaluation of agents which may be effective against not only locally growing human pancreatic cancer but resulting metastases as well.

INTRODUCTION

Pancreatic cancer is extremely aggressive and very resistant to currently known systemic treatment. Most patients are found to have metastatic lesions, and for the majority of patients, even with early disease removed surgically, there is no prospect for cure or even effective palliation because of almost inevitable metastases observed soon after surgery (1, 2). New treatment strategies are necessary against metastases of pancreatic cancer and require appropriate models for their development. Transgenic rodent models of pancreatic cancer as well as chemically induced pancreatic cancer in rodents have been useful to study this disease, including possible models of growth control (3). It is important, however, to study clinically relevant metastases and their treatment. Metastases of human pancreatic cancer after s.c. transplantation in nude mice have only occasionally been reported, however (4, 5). Vezeridis *et al.* (6) reported a metastatic model using splenic injection of a fast-growing variant of human pancreatic cancer. Although this was a valuable model for the study of certain steps of the metastatic process, it bypasses invasion and in essence generates colonization rather than metastases (7).

Recently, Tan and Chu (8) and Marnicola *et al.* (9, 10) reported a metastatic model of human pancreatic cancer using orthotopic implantation of tumor-cell suspensions, which resulted in invasive local tumor growth and subsequent metastases. Moreover, Vezeridis *et al.* (7) used tumor tissue for orthotopic transplantation, resulting in extensive local growth, metastases to liver, lung, and lymph nodes. Furthermore, Fu *et al.* (11) used histologically intact patient specimens of pancreatic cancer for orthotopic transplantation to nude mice to construct a metastatic model of human pancreatic cancer. We report here that this orthotopic transplant approach to pancreatic cancer utilizing histologically intact tissue can be utilized to test treatment efficacy against local and metastatic growth allowing the design of treatment effective against metastases.

MATERIALS AND METHODS

Mice. Male BALB/c nu/nu mice, which originated from the Central Institute for Experimental Animals (Kawasaki, Japan), were obtained from CLEA Japan, Inc. (Tokyo Japan). Animals which were 6–8 weeks old and weighed 20–22 g were used.

Drugs. 5-FU[3] and MMC were purchased from Kyowa Hakko Kogyo, Co., Ltd. (Tokyo, Japan).

Human Pancreas Cancer Xenograft. PANC-4, a human pancreatic carcinoma xenograft, was provided by Dr. T. Nomura, the Central Institute for Experimental Animals, and was maintained by serial s.c. transplantation into nude mice at Keio University School of Medicine.

Orthotopic Transplantation of Histologically Intact Tumor Tissue. Pancreatic tumor tissues were transplanted orthotopically in nude mice using the method of Fu *et al.* (11) with some modifications. Tumors at the exponential growth phase in nude mice were resected aseptically, necrotic tissues were cut away and the remaining healthy tumor tissues were cut with scissors and were minced into approximately 3 × 3 × 3 mm pieces in Hanks' balanced salt solution containing 100 units/ml penicillin and 100 μg/ml streptomycin. Each piece was weighed and adjusted with scissors to be 50 mg.

Mice were anesthetized by i.p. administration (0.3 ml/mouse) of 2.5% solution of a mixture of 2,2,2-tribromoethanol (Aldrich Chemical Company, Inc., Milwaukee, WI) and *tert*-amylalcohol (Wako Pure Chemical Industries, Ltd., Osaka, Japan) (1:1). An incision was then made through the left upper abdominal pararectal line and peritoneum. The pancreas was carefully exposed and a tumor piece was transplanted on the middle of the pancreas with a 6–0 Dexon (Davis-Geck, Inc., Manati, Puerto Rico) surgical suture. The pancreas was then returned into the peritoneal cavity, and the abdominal wall and the skin were closed with 6–0 Dexon sutures. Animals were kept in a sterile environment.

Experimental Chemotherapy. On day 7 after orthotopic transplantation, mice were randomized into control and treated groups. 5-FU and MMC, dissolved in 0.2 ml of physiological saline solution, were administered i.p. as boluses. The doses of the drugs used were 180 mg/kg for 5-FU and 6 mg/kg for MMC, which were determined as maximum tolerated doses in nude mice in our previous studies (12). On the 90th day after orthotopic transplantation, the tumors growing in the peritoneal cavity and the liver were removed from each mouse, weighed, and then examined histologically after careful macroscopic examination. Since it required at least 90 days in the initial experiments for PANC-4 to express its metastatic potential after orthotopic transplantation (data not shown) some mice died in this period due to extensive local tumor growth. Therefore, only the mice which survived 90 days were evaluable.

Histoculture Drug Response Assay with the MTT End Point. The HDRA was performed using the MTT end point as reported previously (13). The MTT end point is a simple and convenient colorimetric method. The

Received 1/25/93; accepted 4/21/93.

The costs of publication of this article were defrayed in part by the payment of page charges. This article must therefore be hereby marked *advertisement* in accordance with 18 U.S.C. Section 1734 solely to indicate this fact.

[1] This study was supported in part by U.S. National Cancer Institutes Small Business Innovative Research Grants R43CA56192 and R43CA53963.

[2] To whom requests for reprints should be addressed.

[3] The abbreviations used are: 5-FU, 5-fluorouracil; HDRA, histoculture drug-response assay; MMC, mitomycin C; MTT, 3-(4,5-dimethylthiazol-2-yl)-2,5-diphenyltetrazolium bromide; DMSO, dimethyl sulfoxide.

inhibition of the number of viable tumor cells correlates well with inhibition of total succinate dehydrogenase activity. Succinate dehydrogenase activity is measured by optical density at A_{540} resulting from the DMSO-extracted formazan crystals produced by MTT reduction (14, 15). Special collagen gels manufactured from pig skin were purchased from Health Design, Inc. (Rochester, NY). The gels were removed from their sterile packages and cut with scissors into 1-cm^3 pieces, and 1 piece was placed in each well of several 24-well plates. The antitumor drugs were dissolved in RPMI 1640 (Nissui Pharmaceutical Co., Ltd., Tokyo, Japan) containing 20% fetal calf serum (GIBCO, Grand Island, NY), 100 units/ml penicillin and 100 μg/ml streptomycin. One ml/well of the solutions was added to each well which reached but did not cover the upper part of the gel. The cutoff concentrations of the drugs used, or concentrations that allowed *in vitro* evaluation of tumor drug response, were 300 μg/ml for 5-FU and 7.5 μg/ml for MMC since these concentrations allowed high correlation with *in vivo* response (12).

Tumor pieces divided into 50-mg units as described above were further scissor-minced into pieces about 1 mm in diameter. The tissue was further minced into 5–10 pieces about 0.5 mm in diameter, which were then placed on each of the prepared collagen surfaces in 24-well plates. The plates were incubated for 7 days at 37°C in a humidified atmosphere containing 95% air/5% CO_2.

After incubation, 100 μl of Hanks' balanced salt solution containing 0.1 mg/ml collagenase (Worthington Biochemical Co., NJ) and 100 μl of MTT (Dojindo Laboratories, Kumamoto, Japan) solution, dissolved in 5 mg/ml phosphate-buffered saline containing 0.1 mol/l of sodium succinate and filtered through a 0.45-μm membrane filter (Millipore, Bedford, MA), were added to each well and incubated for an additional 8 h. The medium was then aspirated completely from each well by careful use of micropipets. One ml of DMSO (Nacalai Tesque, Inc., Kyoto, Japan) per well was added to dissolve the formazan product. After 2 h the solutions were transferred to 96-well microtiter plates (100 μl/well) and the absorbance of the solution in each well was read at 540 nm on a Model EAR 340 AT reader (SLT-Labinstruments). The absorbance/g of each tumor was calculated from the mean absorbance of 4 wells and the initial tumor weight which was estimated prior to the culture.

The inhibition rate was calculated using the formula:

$$\text{Inhibition rate (\%)} = \left(1 - \frac{\text{Mean } A_{540} \text{ of DMSO-extracted formazan of treated tumors/g}}{\text{Mean } A_{540} \text{ of DMSO-extracted formazan of control tumors/g}}\right) \times 100$$

Each drug concentration was tested in triplicate wells and the experiment was repeated three times. The *in vitro* test was considered to be evaluable for tumor drug response at the cutoff drug concentrations which were determined as 300 μg/ml for 5-FU and 7.5 μg/ml for MMC in our previous study, since these concentrations allowed high correlation with *in vivo* response (13). The concentration of each drug which lowered tumor cell MTT reduction activity by 50% was calculated using concentration effect data with the steepest slope determined by linear regression.

RESULTS

Orthotopically transplanting PANC-4 human pancreatic cancer to the pancreas of nude mice resulted in local invasive growth (Fig. 1*A*), invasion of the duodenum (Fig. 1*B*), and liver metastasis (Fig. 1*C*). The incidence of metastases observed in the untreated control mice were 6 and 7 of 18, for liver and peritoneal metastases, respectively (Table 1).

Table 2 shows the *in vitro* results of antitumor activity of 5-FU and MMC against PANC-4 determined in the HDRA with the MTT end point. The mean concentrations of 5-FU and MMC which lowered tumor cell MTT reduction activity by 50% were over 10- and 3-fold above the cutoff drug concentrations, respectively, and the mean inhibition rates at the cutoff concentrations were 5.6 and 39.4%, respectively, indicating higher efficacy of MMC than 5-FU against PANC-4.

Table 1 shows the *in vivo* results of antitumor activity of 5-FU and MMC against PANC-4 after orthotopic transplantation in nude mice. Local tumor growth was slightly inhibited in mice treated with 5-FU, resulting in 80% of the mean actual tumor weight in treated mice relative to that in control mice (T/C). The incidence of metastases to the liver and the peritoneum in the mice treated with 5-FU was 2 of 6 each, equivalent to that observed in the control mice. On the other hand, MMC demonstrated a considerable antitumor activity on local tumor growth, resulting in a 46% T/C value in actual tumor weight, with a statistically significant difference from the control. Most importantly, none of 8 mice treated with MMC developed liver or peritoneal metastases. A loss of body weight was observed for the majority of the mice which correlated with tumor growth (data not shown).

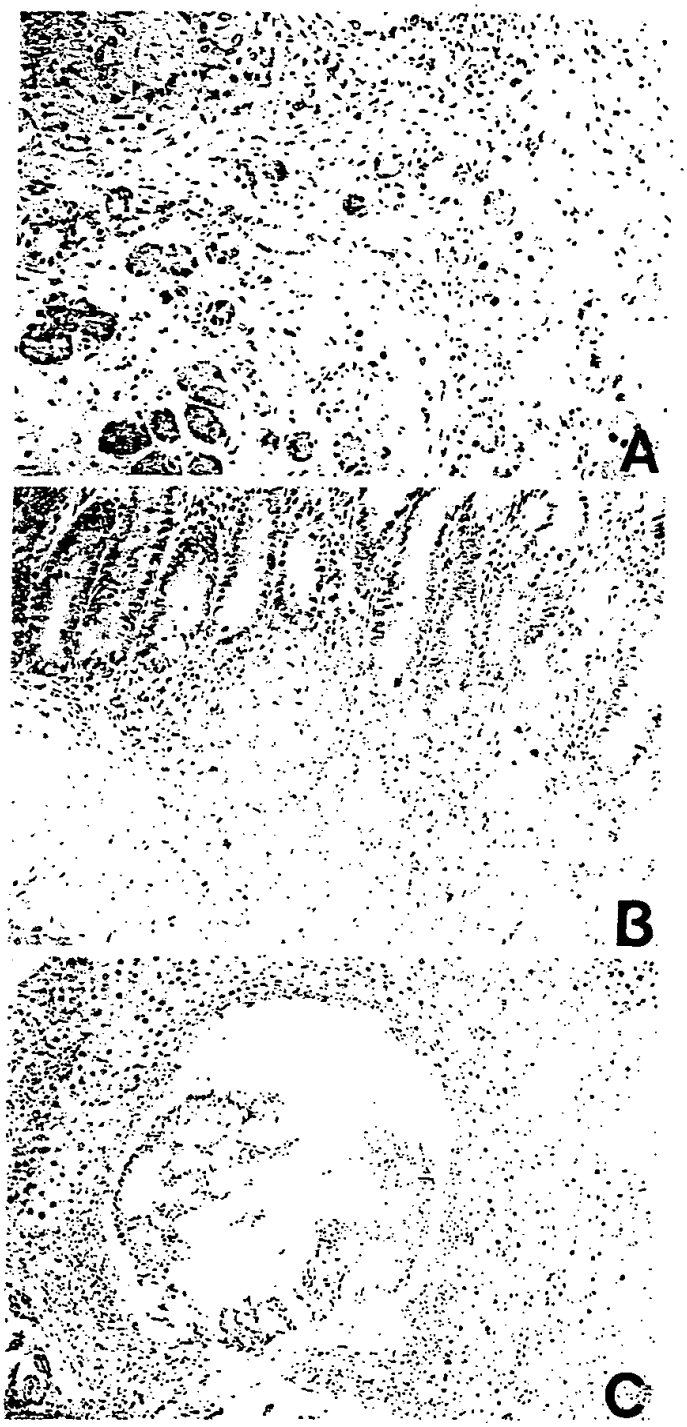

Fig. 1. Microscopic views of local invasive growth into the pancreatic ducts (*A*), invasion to the duodenal submucosal layer (*B*), and liver metastasis of the PANC-4 human pancreatic cancer observed after orthotopic transplantation of histologically intact tumor tissue in nude mice (*C*). Mice were transplanted with PANC-4 on day 0 and then examined on day 90.

Table 1 *Metastases observed after orthotopic transplantation of PANC-4 and in vivo antitumor effects of 5-FU and MMC against PANC-4*

PANC-4 was transplanted into nude mice on day 0 and maximum tolerated doses of 5-FU or MMC were administered i.p. bolus on day 7. Three separate control groups were run at different times. On day 90, only the surviving mice were evaluated.

Treatment	Survivors after 90 days	Actual[a] tumor weight	T/C value of local tumor (%)	Liver metastases	Peritoneal metastases
Control 1	7/13	1.687[b]		2/7	3/7
Control 2	7/9	(0.614) [0.232]		3/7	2/7
5-FU	6/8	1.353[b] (0.652) [0.266]	80.2	2/6	2/6
Control 3	4/8	1.945[c] (0.306) [0.153]		1/4	2/4
MMC	8/8	0.894[c] (0.751) [0.266]	46.0	0/8	0/8
Control (total)[d]	18/30			6/18	7/18

[a] Data are shown as mean tumor weight in grams. Numbers in parens, SD. Numbers in brackets, SEM.
[b] Not significant.
[c] $P < 0.025$ by Student's t test.
[d] Summary of control 1, 2, and 3.

Table 2 *In vitro chemosensitivity of PANC-4 determined by the histoculture drug-response assay with the MTT end point*

The inhibition rate (%) was calculated as shown in "Materials and Methods." The IC_{50} values of drugs was calculated using concentration effect date with the steepest slope determined by linear regression. Cutoff concentration used were 300 and 7.5 μg/ml for 5-FU and MMC, respectively (please see text for details). Data are shown as mean (SD) from triplicate determinations.

Drug	IC_{50}[a] (μg/ml)	Inhibition rate (%) at cutoff
5-FU	>3000	5.6 (2.8)
MMC	21.6 (4.2)	39.4 (8.8)

[a] IC_{50}, concentration of each drug which lowered tumor cell MTT reduction by 50%.

DISCUSSION

Orthotopic transplantation of histologically intact PANC-4 tumor tissue resulted in extensive local growth, invasion to surrounding organs, and metastases to liver and peritoneum. In other orthotopic transplant models developed by us for colon (16, 17), stomach (18, 19), bladder (20, 21), lung (22), and prostate (23), transplantation of histologically intact tissue results in greater metastatic potential in immunodeficient mice than injection of cell suspensions (17, 18, 20). In this study, we applied this model to experimental treatment, which seemed advantageous compared with other nude mouse models of metastatic human pancreatic cancer.

In routine *in vivo* chemosensitivity assays using s.c. tissue transplantation in nude mice (12), both 5-FU and MMC demonstrated only negligible effects against PANC-4 (data not shown). In the model using orthotopic transplantation, both drugs failed to score positive effects against the local tumor, according to currently used criteria which determine a positive effect as that lowering the mean local tumor weight by 42% (12). However, MMC showed preventive effects against liver and peritoneal metastases, which might be produced from more rapidly growing and therefore possibly more chemosensitive cell subpopulations of this line (24), possibly resulting in an improved survival rate of the mice treated with MMC. In contrast, 5-FU showed only minimal antitumor effect on local tumor growth, resulting in 80% of control growth in terms of actual tumor weight, and mice treated with 5-FU had essentially an equivalent incidence of liver and peritoneal metastases in comparison with the control mice. Therefore, drugs selected according to the results of the *in vitro* HDRA seemed to have potential to prevent metastasis of human pancreatic cancer in our orthotopic transplant model. This response could not have been evaluated with the currently used s.c. implantation nude mouse models, where metastasis rarely occurs.

Thus, the metastatic model of human pancreatic cancer using orthotopic transplantation of histologically intact tumor tissue in conjunction with the HDRA *in vitro* model provides a paradigm for treatment of pancreatic cancer both at the level of local growth and metastasis.

REFERENCES

1. Warshaw, A. L. Progress in pancreatic cancer. Introduction. World J. Surg., *8:* 801–802, 1984.
2. Moertel, C. G. Current concepts in cancer: chemotherapy of gastrointestinal cancer. N. Engl. J. Med., *299:* 1049–1052, 1978.
3. Zhou, W., Povoski, S. P., Longnecker, D. S., and Bell, R. H. Novel expression of gastrin (cholecystokinin-B) receptors in azaserine-induced rat pancreatic carcinoma: receptor determination and characterization. Cancer Res., *52:* 6905–6911, 1992.
4. Kyriazis, A. P., Kyriazis, A. A., McCombs, W. B., and Kereiakes, J. A. Biological behavior of human malignant tumors grown in the nude mouse. Cancer Res., *41:* 3995–4000, 1981.
5. Kajii, S. M., Meitner, P. A., Bogaars, H. A., Dexter, D. L., Calabresi, P., and Turner, M. D. Metastasis of human pancreatic adenocarcinoma (RWP-1) in nude mice. Br. J. Cancer, *46:* 970–975, 1982.
6. Vezeridis, M. P., Turner, M. D., Kajiji, S. M., Yankee, R. M., and Meitner, P. A. Metastasis of a human pancreatic cancer (HPC) to liver in nude mice (Abstract). Proc. Am. Assoc. Cancer Res., *26:* 53, 1985.
7. Vezeridis, M. P., Doremus, C. M., Tibbetts, L. M., Tzanakakis, G., and Jackson, B. J. Invasion and metastasis following orthotopic transplantation of human pancreatic cancer in the nude mouse. J. Surg. Oncol., *40:* 261–265, 1989.
8. Tan, M. H., and Chu, T. M. Characterization of the tumorigenic and metastatic properties of a human pancreatic tumor cell line (AsPC-1) implanted orthotopically into nude mice. Tumor Biol., *6:* 89–98, 1985.
9. Marincola, F., Taylor-Edwards, C., Drucker, B., and Holder, W. D., Jr. Orthotopic and heterotopic xenotransplantation of human pancreatic cancer in nude mice. Curr. Surg., *44:* 294–297, 1987.
10. Marincola, F. M., Drucker, B. J., Siao, D. Y., Hough, K. L., and Holder, W. D, Jr. The nude mouse as a model for the study of human pancreatic cancer. J. Surg. Res., *47:* 520–529, 1989.
11. Fu, X., Guadagni, F., and Hoffman, R. M. A metastatic nude mouse model of human pancreatic cancer constructed orthotopically from histologically intact patient specimens. Proc. Natl. Acad. Sci. USA, *89:* 5645–5649, 1992.
12. Kubota, T., Ishibiki, K., and Abe, O. The clinical usefulness of human xenografts in nude mice. Prog. Clin. Biol. Res., *276:* 213–225, 1988.
13. Furukawa, T., Kubota, T., Watanabe, M., Takahara, T., Yamaguchi H., Takeuchi, T., Kase, S., Kodaira, S., Ishibiki, K., Kitajima, M., and Hoffman, R. M. High *in vitro-in vivo* correlation of drug response using sponge-gel-supported three-dimensional histoculture and the MTT end point. Int. J. Cancer, *51:* 489–498, 1992.
14. Mosmann, T. Rapid colorimetric assay for cellular growth and survival: application to proliferation and cytotoxicty assays. J. Immunol. Methods, *65:* 55–63, 1983.
15. Carmichael, J., DeGraff, W. G., Gazdar, A. F., Minna, J. D., and Mitchell, J. B. Evaluation of a tetrazolium-based semiautomated colorimetric assay: assessment of radiosensitivity. Cancer Res., *47:* 936–942, 1987.
16. Fu, X., Besterman, J. M., Monosov, A., and Hoffman, R. M. Models of human metastatic colon cancer in nude mice orthotopically constructed by using histologically intact patient specimens. Proc. Natl. Acad. Sci. USA, *88:* 9345–9349, 1991.
17. Furukawa, T., Kubota, T., Watanabe, M., Kuo, T-H., Saikawa, Y., Kase, S., Tanino, H., Teramoto, T., Ishibiki, K., and Kitajima, M. A metastatic model of human colon cancer constructed using cecal implantation of cancer-tissue in nude mice. Surg. Today, Jpn. J. Surg., *23:*420–423, 1993.
18. Furukawa, T., Fu, X., Kubota, T., Watanabe, M., Kitajima, M., and Hoffman, R. M. Nude mouse metastatic models of human stomach cancer constructed using orthotopic implantation of histologically intact tissue. Cancer Res., *53:* 1204–1208, 1993.
19. Furukawa, T., Kubota, T., Watanabe, M., Kitajima, M., and Hoffman, R. M. Orthotopic transplantation of histologically-intact clinical specimens of stomach cancer to nude mice: correlation of metastatic sites in mouse and human. Int. J. Cancer, *53:* 608–612, 1993.
20. Fu, X., Theodorescu, D., Kerbel, R. S., and Hoffman, R. M. Extensive multi-organ metastasis following orthotopic onplantation of histologically-intact human bladder carcinoma tissue in nude mice. Int. J. Cancer, *49:* 938–939, 1991.
21. Fu, X., and Hoffman, R. M. Human RT-4 bladder carcinoma is highly metastatic in nude mice and comparable to *ras*-H-transformed RT-4 when orthotopically onplanted as histologically-intact tissue. Int. J. Cancer, *51:* 989–991, 1992.
22. Wang, X., Fu, X., and Hoffman, R. M. A new patient-like metastatic model of human lung cancer constructed orthotopically with intact tissue via thoracotomy in immunodeficient mice. Int. J. Cancer, *51:* 992–995, 1992.
23. Fu, X., Herrera, H., and Hoffman, R. M. Orthotopic growth and metastasis of human prostate carcinoma in nude mice after transplantation of histologically intact tissue. Int. J. Cancer, *52:* 987–990, 1992.
24. Kubota, T., Nakada, M., Tsuyuki, K., Inada, T., Asanuma, F., Ishibiki, K., and Abe, O. Cell kinetics and chemosensitivity of human carcinomas serially transplanted into nude mice. Jpn. J. Cancer Res. (Gann), *77:* 502–507, 1986.

Proc. Natl. Acad. Sci. USA
Vol. 92, pp. 12085–12089, December 1995
Medical Sciences

Liver colonization competence governs colon cancer metastasis

(liver metastasis/nude mouse/orthotopic implantation/intrahepatic implantation)

TSONG-HONG KUO*, TETSURO KUBOTA*†, MASAHIKO WATANABE*, TOSHIHARU FURUKAWA*, TATUSO TERAMOTO*, KYUYA ISHIBIKI*, MASAKI KITAJIMA*, A. RAHIM MOOSSA‡, SHELDON PENMAN§, AND ROBERT M. HOFFMAN‡¶

*Department of Surgery, School of Medicine, Keio University, 35 Shinanomachi, Shinjuku-ku, Tokyo 160, Japan; ‡Laboratory of Experimental Oncology, Department of Surgery, University of California, San Diego, CA 92103-8400; §Department of Biology, Massachusetts Institute of Technology, Cambridge, MA 02139; and ¶AntiCancer, Inc., 7917 Ostrow Street, San Diego, CA 92111

Contributed by Sheldon Penman, August 31, 1995

ABSTRACT **Tumors that metastasize do so to preferred target organs. To explain this apparent specificity, Paget, >100 years ago, formulated his seed and soil hypothesis; i.e., the cells from a given tumor would "seed" only favorable "soil" offered by certain organs. The hypothesis implies that cancer cells must find a suitable "soil" in a target organ—i.e., one that supports colonization—for metastasis to occur. We demonstrate in this report that ability of human colon cancer cells to colonize liver tissue governs whether a particular colon cancer is metastatic. In the model used in this study, human colon tumors are transplanted into the nude mouse colon as intact tissue blocks by surgical orthotopic implantation. These implanted tumors closely simulate the metastatic behavior of the original human patient tumor and are clearly metastatic or nonmetastatic to the liver. Both classes of tumors were equally invasive locally into tissues and blood vessels. However, the cells from each class of tumor behave very differently when directly injected into nude mouse livers. Only cells from metastasizing tumors are competent to colonize after direct intrahepatic injection. Also, tissue blocks from metastatic tumors affixed directly to the liver resulted in colonization, whereas no colonization resulted from nonmetastatic tumor tissue blocks even though some growth occurred within the tissue block itself. Thus, local invasion (injection) and even adhesion to the metastatic target organ (blocks) are not sufficient for metastasis. The results suggest that the ability to colonize the liver is the governing step in the metastasis of human colon cancer.**

A metastatic colony is the end result of a complex series of processes resulting from tumor–host interactions (1, 2). These include angiogenesis and intravasation of tumor cells (3), circulation and extravasation (4), and adhesive interactions with other cells, including endothelial and target cells (5–7), as well as colonization of the target organ. Adhesion molecules and proteolytic enzymes seem to play a role in this process (5–8). However, only some tumors metastasize and there is no clear understanding of the key properties and events that lead to metastatic colony formation.

Tumors can have enormously different characteristic metastatic rates. In contrast to the variability in rates, there is a surprising degree of specificity in the target organs colonized by metastases from a particular type of tumor (e.g., colon tumors most often target the liver). Over 100 years ago, Paget (9) noted the highly nonrandom spread of cancer to specific target organs. From these observations, he formulated the "seed" (primary cancer) and "soil" ("target organ") hypothesis of metastasis. A corollary of this hypothesis is that cancer cells must find a suitable "soil" in a target organ, one supporting colonization, for metastasis to occur. We demonstrate in this report that ability of cells from a particular human colon cancer to colonize liver tissue (i.e., to use it as "soil") directly reflects whether that cancer is metastatic.

These experiments were made possible by the recently developed, "patient-like" models of human cancer in nude mice. These models are the first in which animal-implanted human tumors closely replicate the complex behaviors of the original tumor while still in the human host. The implanted tumors parallel the original tumor's characteristic growth and local invasiveness, its drug sensitivity and, most important, the tumor's rate of metastases to corresponding target tissues (10–35). These models are created in nude mice by surgical orthotopic implantation (SOI) (i.e., implantation to the organ or tissue corresponding to the original human tumor site) of histologically intact tumor blocks. Both the use of an orthotopic site of implantation and the use of tissue blocks rather than dispersed cells are critical to the accuracy of the model. Metastatic models of human colon cancer (10–16), stomach cancer (17–20), pancreatic cancer (21, 22), bladder cancer (23, 24) lung cancer (25–33), ovarian cancer (34), breast cancer (35), and prostate cancer (36) have been established with SOI. In every case, the implanted tumors show patterns of metastasis that closely resemble the patterns in the patient donors with regard to rates and the targeting of corresponding mouse tissue.

In this study we have utilized the realistic model of metastasis afforded by the SOI nude mouse model of colon cancer. The model accurately classifies human colon tumors as to whether they metastasize (M) or do not metastasize (non-M) to liver as the target tissue. Cells taken from M and non-M tumors were assayed for their ability to directly colonize the liver when implanted in liver tissue either by injection or by affixation of a block of tumor tissue. Cells from the M tumors colonized the liver when implanted by either method. In sharp contrast, cells derived from the non-M colon tumors were unable to colonize liver under either procedure. This radical difference suggests that the ability of the tumor cells to colonize the liver is critical for the metastasis of human colon cancer.

MATERIALS AND METHODS

Transplantable Human Colon Tumors. Eight human colon cancer strains transplantable into BALB/cA *nu/nu* mice were used for the experiments described in this report. COL-2-JCK, COL-3-JCK, and COL-5-JCK were established at Tokai University (Atsugi, Japan) and supplied by T. Nomura (Central Institute for Experimental Animals, Kawasaki, Japan). Co-3 and Co-4 were established at the Pathology Division, National Cancer Center Research Institute (Tokyo). Co-6 was established at the Department of Surgery, Keio University School

The publication costs of this article were defrayed in part by page charge payment. This article must therefore be hereby marked "*advertisement*" in accordance with 18 U.S.C. §1734 solely to indicate this fact.

Abbreviations: H/E, hematoxylin and eosin; NK, natural killer; SOI, surgical orthotopic implantation.

†To whom reprint requests should be addressed.

Table 1. Human colon cancer xenografts

Name	Description
COL-2-JCK	Poorly differentiated adenocarcinoma
COL-3-JCK	Poorly differentiated adenocarcinoma
COL-5-JCK	Well-differentiated adenocarcinoma
Co-3	Well-differentiated adenocarcinoma
Co-4	Mucinous carcinoma
Co-6	Poorly differentiated adenocarcinoma
WiDr	Well-differentiated adenocarcinoma
COLO-205	Poorly differentiated adenocarcinoma

See text for derivation of the colon tumor xenografts.

of Medicine (37). COLO-205 was established as a cell line by Semple *et al.* (38), and was provided from the Pathology Division, National Cancer Research Institute (Tokyo). WiDr was provided by H. Ishitsuka (Nippon Roche Research Center, Tokyo). The histological types of these cancer lines are listed in Table 1. All strains were maintained by serial transplantation into nude mice (39, 40). Tumors in the exponential growth phase were used for the experiments.

Nude Mice. Male nude mice with a BALB/cA genetic background were purchased from CLEA Japan (Tokyo). They were maintained under specific pathogen-free conditions with an Isorack and were fed sterile food and water *ad libitum*. Six- to eight-week-old mice weighing 20–22 g were used for the experiments.

SOI. Human colon tumors growing subcutaneously in nude mice were harvested and transplanted as intact tissue by SOI onto the cecum of nude mice with microsurgical procedures (10–16). In brief, subcutaneously growing human colon tumors in nude mice were resected aseptically and the tumor tissues were minced with scissors into pieces about 4 mm in diameter, weighing about 75 mg each. Mice were anesthetized with a 2.5% solution of a 1:1 (vol/vol) mixture of 2,2,2-tribromoethanol (Aldrich) and *tert*-amyl alcohol (Wako Pure Chemical, Osaka).

An incision was made through the left lower abdominal pararectal line and peritoneum. The cecal wall was exposed and a part of the serosal membrane was scraped with a 27-gauge needle. Care was exercised to prevent the rupture of the cecal wall. One tumor piece was then fixed on each scraped site of the serosal surface with a 6-0 Dexon (Davis–Geck, Manatai, PR) transmural suture. The cecum was then returned into the peritoneal cavity, and the abdominal wall and the skin were closed with 6-0 Dexon sutures.

The mice were kept in a sterile environment and were sacrificed by cervical dislocation 12 weeks after SOI or earlier if they developed signs of distress. Upon autopsy, all organs, including the cecum and liver, were processed for routine histological examination using hematoxylin and eosin (H/E) staining after careful macroscopic examination.

Intrahepatic Injection. For intrahepatic injection, dissociated tumor cells were obtained after harvest of human colon tumors growing subcutaneously in nude mice. Mice were anesthetized and a midline incision was made through the upper abdomen and peritoneum. A part of the liver was exposed and 50 μl of the tumor-cell suspension per mouse, containing 5×10^6 viable tumor cells, was injected intrahepatically via a 27-gauge needle. Briefly, subcutaneous tumors in the exponential growth phase in nude mice were resected aseptically, necrotic tissues were cut away, and the remaining intact tumor tissues were minced with scissors as finely as possible in Hanks' balanced salt solution containing 100 units of penicillin and 100 μg of streptomycin per ml (Hanks' solution). After incubation for 30 min at 37°C with a mixture of 0.02% collagenase (Boehringer Mannheim) and 0.02% DNase (Boehringer Mannheim), the homogenates were passed through a stainless steel mesh (200 pores per cm^2). The filtrates were washed once in RPMI-1640 medium (Nissui Seiyaku, Tokyo) containing 10% fetal bovine serum. The filtered homogenate was then centrifuged for 5 min at 516 × g.

The dissociated tumor cells were then suspended in Hanks' solution, and the concentration of viable cells in the suspension was determined by trypan blue dye exclusion. After centrifugation, the tumor cells were suspended at 10^8 viable cells per ml. Mice were anesthetized by the same method as mentioned previously. A scissors incision was made on the left lateral flank through the peritoneum. The liver was carefully exposed as mentioned above and 50 μl of the tumor cell suspension per mouse, equivalent to 5×10^6 viable tumor cells, was carefully injected intrahepatically via a 27-gauge needle.

Hepatic Affixation of Colon Tumors. Two human colon carcinoma strains, COL-2-JCK (metastatic, M) and Co-4 (nonmetastatic, non-M) were used in this experiment. Mice were anesthetized and a midline incision was made through the upper abdomen and peritoneum. One tumor piece, about 6 mm, was then fixed on the surface of the liver with a 6-0 Dexon suture. The abdominal wall and the skin were closed with 6-0 Dexon sutures. The mice were kept in a sterile environment and were sacrificed 6 weeks after transplantation.

Suppression of Natural Killer (NK) Cells. Anti-asialo-GM1 antibody, an immunosuppressive agent against NK cell activity (41), was purchased from Wako Pure Chemical. The anti-asialo-GM1 antibody, containing 10 mg/ml per vial, was diluted

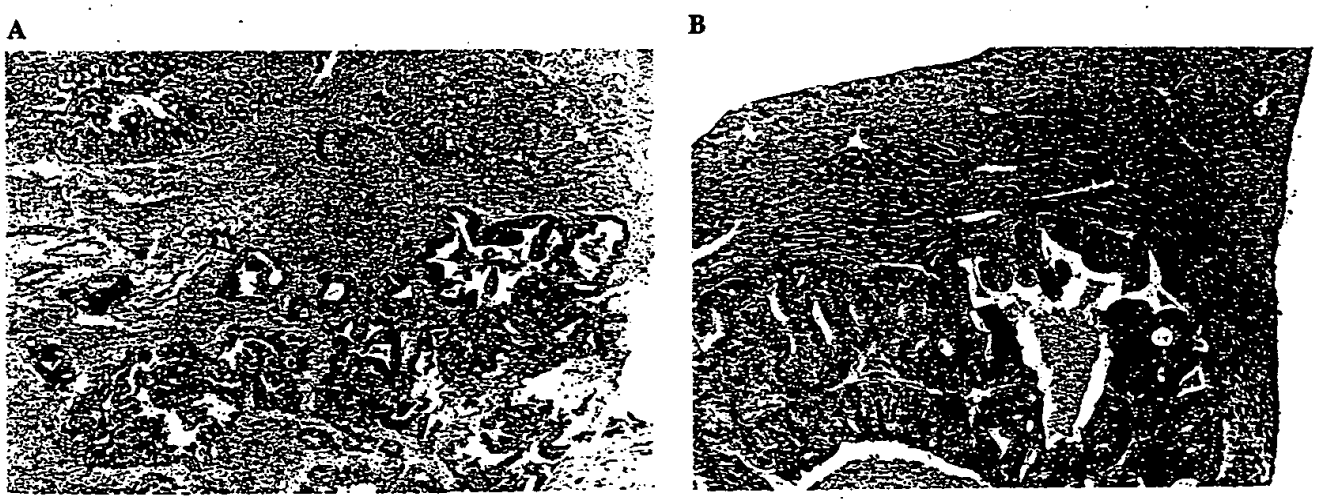

FIG. 1. (*A*) Local growth of human colon tumor Co-3, a well-differentiated adenocarcinoma, in the cecum of a nude mouse at 4 weeks after SOI. Arrows indicate the tumor cells. (H/E: ×100.) (*B*) Liver metastasis of Co-3 at 4 weeks after SOI. (H/E; ×100.)

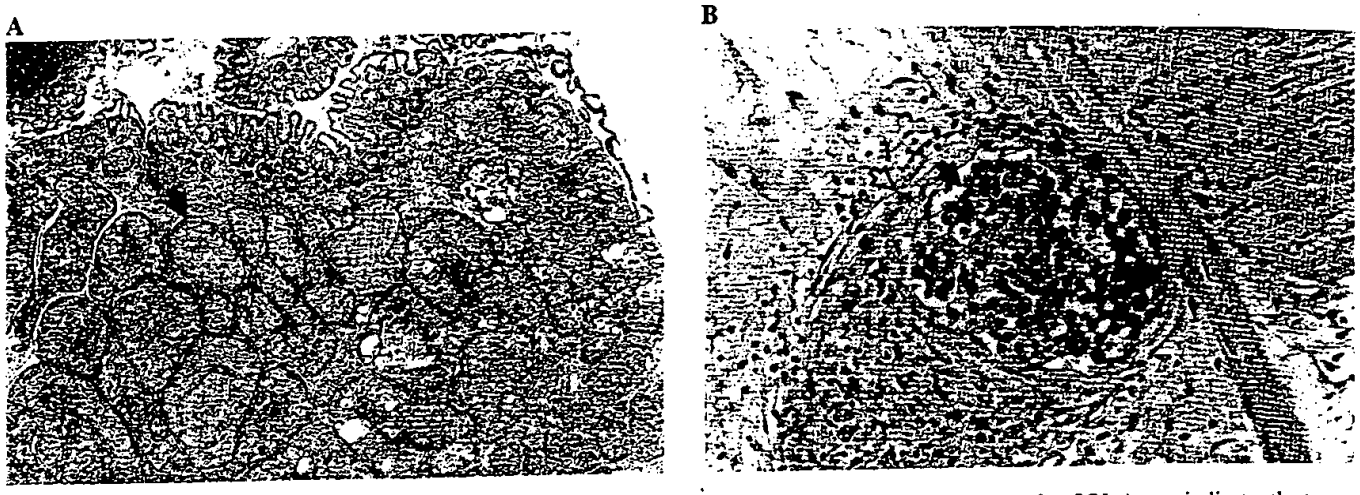

FIG. 2. (*A*) Extensive local growth of COLO-205, a non-M strain, in the cecum of a nude mouse at 7 weeks after SOI. Arrow indicates the tumor. (H/E; ×100.) (*B*) Pathohistology of growing COLO 205, a poorly differentiated adenocarcinoma, in the nude mouse cecum at 7 weeks after SOI. Black arrow indicates invasive tumor cells and the open arrow identifies the blood vessel wall. (H/E; ×100.)

in 0.9% NaCl to a total volume of 10 ml. To suppress NK cells the anti-asialo-GM1 antibody was administered intraperitoneally to the mice of the treated group on days −1, 0, 7, 14, and 21 at a dose of 200 μg per mouse, equivalent to 0.2 ml of the dissolved antibody. This was done to determine whether NK cells are a factor in liver colonization.

Analysis of Primary Tumor and Metastatic Growth. The liver and other organs were removed after sacrifice and processed for histological examination in H/E-stained sections by standard techniques.

RESULTS AND DISCUSSION

Metastatic and Nonmetastatic Tumor Strains. The data in Table 1 show the metastatic behavior of the two groups of tumors used here. Human colon tumors COL-2-JCK, COL-3-JCK, COL-5-JCK, and Co-3 gave rise to liver metastases in more than half of the nude mice after SOI of intact tumor tissue into the mouse cecum. These tumors were therefore classified as M (metastatic). The histological section in Fig. 1*A* shows the local growth of Co-3, a well-differentiated adenocarcinoma, at 4 weeks after implantation in the cecum. The histological section in Fig. 1*B* shows a typical metastasis in the liver arising from Co-3.

Table 2. Liver colonization competence correlates with metastatic potential

Human colon carcinoma strain	Tumor growth in cecum*	Liver metastasis	Tumor growth after intrahepatic injection†
COL-2-JCK	12/12	9/12	4/4
COL-3-JCK	12/12	7/12	5/5
COL-5-JCK	15/15	8/15	4/4
Co-3	14/14	7/14	4/4
Co-4	8/8	0/8	0/6
Co-6	5/5	0/5	0/5
WiDr	8/8	0/8	0/6
COLO-205	8/8	0/8	0/6

Data are shown as no. of mice with tumor growth or liver metastasis after SOI and tumor growth after intrahepatic injection/no. of mice evaluated.

*Human colon tumors growing subcutaneously in nude mice were harvested and transplanted as intact tissue by SOI onto the cecum of nude mice. One tumor piece was then fixed on each scraped site of the serosal surface with a 6-0 Dexon transmural suture.

†For intrahepatic injection, dissociated tumor cells were obtained after harvesting human colon tumors growing subcutaneously in nude mice. A part of the liver was exposed and 50 μl of the tumor-cell suspension per mouse, containing 5×10^6 viable tumor cells, was injected intrahepatically via a 27-gauge needle.

A second group of colon tumors, Co-4, Co-6, COLO-205, and WiDr, gave rise to no detectable liver metastases even 12 weeks after implantation and were classified as non-M (non-metastatic). Fig. 2*A* shows a histological section of COLO-205, a poorly differentiated adenocarcinoma, at 7 weeks after implantation in the mouse cecum. Fig. 2*B* is a higher-power view of COLO-205 showing tumor cells invading a blood vessel. Although non-M, this tumor is clearly highly invasive locally.

Apart from their different metastatic behavior, the M and non-M tumors appeared to be quite similar. Both M and non-M tumors showed similar extensive local growth and invasion of cancer cells into vessels of the cecal wall within 4–7 weeks after orthotopic transplantation. However, a major difference between the M and non-M tumors emerged when dissociated cells from the tumors were directly seeded on the liver.

Intrahepatic Injection of Colon Tumor Cells. Table 2 shows that dissociated cells from the M tumors were completely effective in originating tumors in the liver after intrahepatic injection of the dissociated tumor cells. These growths closely resembled spontaneously arising metastases from the same tumors (Fig. 3). In contrast, the cells from non-M tumors showed no detectable tumor growth in the liver after direct

FIG. 3. Pathohistology of a growing colony of COL-5-JCK, a well-differentiated adenocarcinoma, at 4 weeks after intrahepatic injection into a nude mouse liver. (H/E: ×100.)

Table 3. Hepatic colonization of human colon carcinoma after liver affixation of tissue block

Strain	Tumor growth	Adhesion to liver	Liver colonization	Metastasis to liver
COL-2-JCK	5/5	5/5	5/5	9/12
Co-4	5/5	5/5	0/5	0/8

Two human colon carcinoma strains, COL-2-JCK (M strain) and Co-4 (non-M strain), were used in this experiment. Mice were anesthetized and a midline incision was made through the upper abdomen and peritoneum. One tumor piece, about 6 mm, was then fixed on the surface of the liver with a 6-0 Dexon suture. The abdominal wall and the skin were closed with 6-0 Dexon sutures. Mice were kept in a sterile environment and were sacrificed 6 weeks after transplantation. Data are shown as no. of mice with tumor growth, adhesion to liver, or liver colonization/no. of mice evaluated.

intrahepatic injection. As a further test, the cells from the non-M tumors showed no tumor growth in the liver even when NK cell activity of the mice was suppressed by anti-asialo-GM1 antibody (data not shown). Therefore, local immune mechanisms in the liver are not likely to be the cause of the marked difference between the M and non-M tumor cells.

Intrasplenic Injection of Colon Tumor Cells. A previous test for metastatic capability injected dissociated tumor cells into the mouse spleen (2). Intrasplenic injection of cells from the M tumors, COL-2-JCK, COL-3-JCK, COL-5-JCK, and Co-3, resulted in development of splenic tumors and metastases to the liver. In contrast, no tumor growth in the spleen was observed after intrasplenic injection of cells from non-M tumors Co-4, Co-6, COLO-205, and WiDr. Moreover, no mice developed liver metastases even 10 weeks after the intrasplenic injection (data not shown). Cells from non-M tumors did not develop tumor growth in the spleen or metastasize to the liver even when NK cell activity was suppressed by the anti-sialo-GM1 antibody.

Affixing Intact Colon Tumor Tissue Blocks to the Liver. The intrahepatic injection experiments necessarily employed dissociated cells. Cells from M and non-M tumors might have behaved differently under the stress due to the procedure. Colonization was therefore also measured by affixing tissue blocks from the tumors to the liver. Histologically intact tumor tissue from two of the human colon carcinoma strains, COL-2-JCK (M strain) and CO-4 (non-M strain), were affixed to the liver surface as a tissue block of ≈6-mm diameter with a 6-0 Dexon suture. Table 3 shows that tumor growth adjacent to liver occurred for both strains. However, the M tumor, COL-2-JCK, showed extensive invasion and colonization of the liver

Table 4. Liver colonization competence is essential for the metastatic process

Process	Presence in M strains	Presence in non-M strains
Growth	+	+
Invasion	+	+
Lymphatic/hematogenous spread	+	+
Adhesion to distant organ	+	+
Liver colonization capability	+	−

(Fig. 4*A*). In contrast, the tissue from the non-M tumor, Co-4, did not colonize the liver by invasion even after adhesion to liver for 6 weeks (Fig. 4*B*). In the latter case, the border delimiting liver tissue from the affixed tumor remained remarkably regular and sharply defined despite extensive external growth by the tumor cells. The results support those of the injection experiments.

Colonization Competence Governs Metastasis. The experimental results show that although non-M tumors can grow locally on the colon and invade surrounding tissue, including blood vessels, their cells cannot colonize the metastatic target organ even when they are injected directly or are affixed to the liver as a tissue block. Only cells from tumors that can actually metastasize from the primary site can also colonize the liver after direct implantation (Table 4). The inability of cells from non-M tumors to grow in the liver when directly injected or affixed to the liver as a tissue block suggests that an essential event in metastasis is the successful seeding and growth of colon cells in the liver. Simple adhesion of the tumor cells to the liver is clearly insufficient for colonization. Since both non-M and M tumors are locally invasive at the primary site, such local invasion is clearly insufficient to result in distant metastasis to the liver. In this realistic model of tumor metastasis the ability of the colon cancer cells to colonize the liver appears to govern the metastatic process.

The animal models of human cancer described here make possible further study of metastatic process of colon cancer in general and, in particular, the critical step of liver colonization. Most important, the SOI model avoids trivial obstacles to metastasis such as the encapsulation characteristic of ectopic implantation (e.g., subcutaneous tumors). The models can be used for evaluating drugs and biologicals which may directly prevent colon tumors from colonizing the liver. Also, study of the basic mechanisms underlying metastasis will be greatly facilitated by selecting metastatic variants (2) on the basis of their ability to directly colonize the liver.

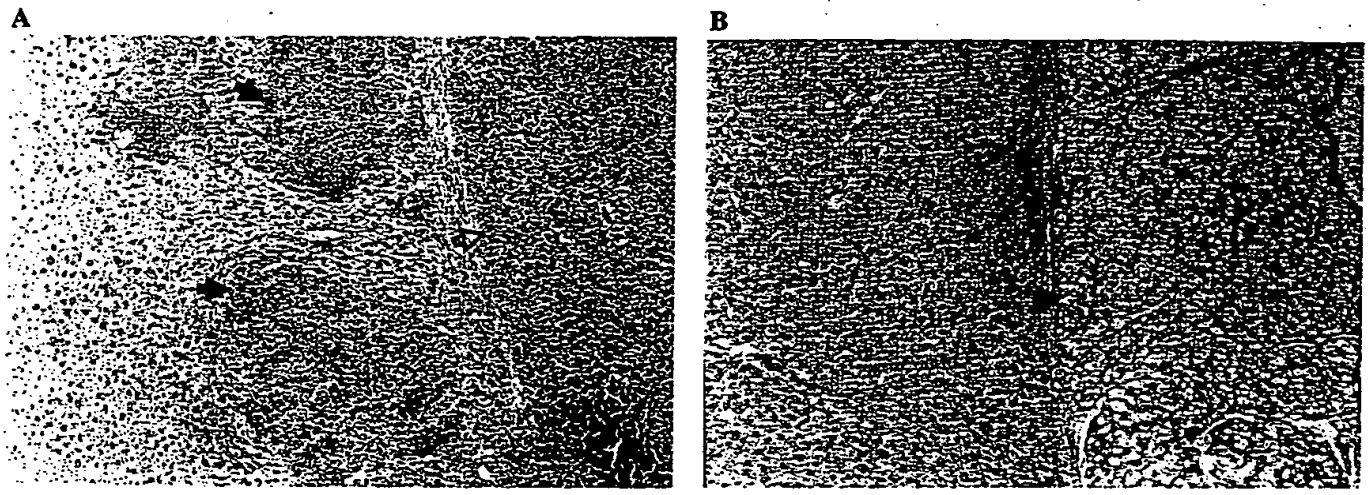

FIG. 4. (*A*) Junction of normal liver and a tissue block from the M tumor COL-2-JCK. Note the extensive invasion and colonization of the liver. (H/E; ×100.) (*B*) Junction of normal liver and a tissue block from the non-M tumor Co-4. (H/E; ×100.)

1. Liotta, L. A., Stetler-Stevenson, W. G. & Steeg, P. S. (1991) *Cancer Invest.* **9**, 543–551.
2. Fidler, I. J. (1990) *Cancer Res.* **50**, 6130–6138.
3. Liotta, L. A., Kleinerman, J. & Saidel, G. (1974) *Cancer Res.* **34**, 997–1004.
4. Lapis, K., Paku, S. & Liotta, L. A. (1988) *Clin. Exp. Metast.* **6**, 73–89.
5. Hynes, R. O. (1992) *Cell* **69**, 11–25.
6. Ruoslahti, E. (1991) *J. Clin. Invest.* **187**, 1–5.
7. Taraboletti, G., Belotti, D., Giavazzi, R., Sobel, M. & Castronovo, V. (1993) *J. Natl. Cancer Inst.* **85**, 235–240.
8. Nakajima, M., Morikawa, K., Fabra, A., Bucana, C. D. & Fidler, I. J. (1990) *J. Natl. Cancer Inst.* **19**, 1890–1898
9. Paget, S. (1889) *Lancet* **i**, 571–573.
10. Fu, X., Besterman, J. M., Monosov, A. & Hoffman, R. M. (1991) *Proc. Natl. Acad. Sci. USA* **88**, 9345–9349.
11. Fu, X., Herrera, H., Kubota, T. & Hoffman, R. M. (1992) *Anticancer Res.* **12**, 1395–1398.
12. Kuo, T., Kubota, T., Watanabe, M., Fujita, S., Furukawa, T., Teramoto, T., Ishibiki, K., Kitajima, M. & Hoffman, R. M. (1993) *Anticancer Res.* **13**, 293–298.
13. Furukawa, T., Kubota, T., Watanabe, M., Kuo, T., Kase, S., Saikawa, Y., Tanino, H., Teramoto, T., Ishibiki, K., Kitajima, M. & Hoffman, R. M. (1993) *Anticancer Res.* **13**, 287–291.
14. Kuo, T., Kubota, T., Nishibori, H., Watanabe, M., Furukawa, T., Fujita, S., Kase, S., Tanino, H., Saikawa, Y., Teramoto, T. & Kitajima, M. (1993) *Jpn. J. Surg.* **23**, 420–423.
15. Wang, X., Fu, X., Brown, P. D., Crimmin, M. J. & Hoffman, R. M. (1994) *Cancer Res.* **54**, 4726–4728.
16. Togo, S., Wang, X., Shimada, H., Moossa, A. R. & Hoffman, R. M. (1995) *Cancer Res.* **55**, 681–684.
17. Furukawa, T., Kubota, T., Watanabe, M., Nishibori, H., Kuo, T., Ishibiki, K. & Kitajima, M. (1992) *J. Jpn. Surg. Soc.* **93**, 561.
18. Furukawa, T., Kubota, T., Watanabe, M., Kitajima, M., Fu, X. & Hoffman, R. M. (1993) *Int. J. Cancer* **53**, 608–612.
19. Furukawa, T., Fu, X., Watanabe, M., Kitajima, M., Kubota, T. & Hoffman, R. M. (1993) *Cancer Res.* **53**, 1204–1208.
20. Furukawa, T., Kubota, T., Watanabe, M., Kitajima, M. & Hoffman, R. M. (1993) *Int. J. Cancer* **54**, 397–401.
21. Fu, X., Guadagni, F. & Hoffman, R. M. (1992) *Proc. Natl. Acad. Sci. USA* **89**, 5645–5649.
22. Furukawa, T., Kubota, T., Watanabe, M., Kitajima, M. & Hoffman, R. M. (1993) *Cancer Res.* **53**, 3070–3072.
23. Fu, X., Theodorescu, D., Kerbel, R. S. & Hoffman, R. M. (1991) *Int. J. Cancer* **49**, 938–939.
24. Fu, X. & Hoffman, R. M. (1992) *Int. J. Cancer* **51**, 989–991.
25. Kuo, T., Kubota, T., Watanabe, M., Furukawa, T., Kase, S., Tanino, H., Nishibori, K., Saikawa, Y., Teramoto, T., Ishibiki, K., Kitajima, M. & Hoffman, R. M. (1992) *Anticancer Res.* **12**, 1407–1410.
26. Wang, X., Fu, X. & Hoffman, R. M. (1992) *Int. J. Cancer* **51**, 992–995.
27. Wang, X., Fu, X. & Hoffman, R. M. (1992) *Anticancer Res.* **12**, 1399–1402.
28. Wang, X., Fu, X., Kubota, T. & Hoffman, R. M. (1992) *Anticancer Res.* **12**, 1403–1406.
29. Kuo, T.-H., Kubota, T., Watanabe, M., Furukawa, T., Kase, S., Tanino, H., Nishibori, H., Saikawa, Y., Ishibiki, K., Kitajima, M. & Hoffman, R. M. (1993) *Anticancer Res.* **13**, 627–630.
30. Astoul, P., Colt, H. G., Wang, X. & Hoffman, R. M. (1993) *Anticancer Res.* **13**, 1999–2002.
31. Astoul, P., Wang, X. & Hoffman, R. M. (1993) *Int. J. Oncol.* **3**, 713–718.
32. Astoul, P., Colt, H. G., Wang, X. & Hoffman, R. M. (1994) *Anticancer Res.* **14**, 85–92.
33. Astoul, P., Colt, H. G., Wang, X., Boutin, C. & Hoffman, R. M. (1994) *J. Cell. Biochem.* **57**, 1–7.
34. Fu, X. & Hoffman, R. M. (1993) *Anticancer Res.* **13**, 283–286.
35. Fu, X., Le, P. & Hoffman, R. M. (1993) *Anticancer Res.* **13**, 901–904.
36. Fu, X., Herrera, H. & Hoffman, R. M. (1992) *Int. J. Cancer* **52**, 987–990.
37. Kase, S., Kubota, T., Furukawa, T., Yamaguchi, H., Takeuchi, T., Takahara, T., Suto, A., Kodaira, S. & Ishibiki, K. (1991) *Jpn. J. Cancer Chemother.* **18**, 2247–2253.
38. Semple, T. U., Quinn, L. A., Woods, L. K. & Moore, G. E. (1978) *Cancer Res.* **38**, 1345–1355
39. Shimosato, Y., Kameyaa, T., Nagai, K., Hirohashi, S., Koide, T., Hayashi, H. & Nomura, T. (1976) *J. Natl. Cancer Inst.* **56**, 1251–1260
40. Kubota, T., Ishibiki, K. & Abe, O. (1988) in *Prediction of Response to Cancer Therapy*, ed. Hall, T. C. (Liss, New York), pp. 213–225.
41. Habu, S., Fukui, H., Shimamura, K., Kasai, M., Nagai, Y., Okumura, K. & Tamaoki, N. (1981) *J. Immunol.* **127**, 34–38.

Proc. Natl. Acad. Sci. USA
Vol. 88, pp. 9345–9349, October 1991
Medical Sciences

12

Models of human metastatic colon cancer in nude mice orthotopically constructed by using histologically intact patient specimens

(histologically intact colon tumor specimens/nude-mouse implant/orthotopic growth/carcinomatosis/metastasis)

XINYU FU*, JEFFREY M. BESTERMAN†, ANN MONOSOV*, AND ROBERT M. HOFFMAN*‡§

*AntiCancer, Inc., 5325 Metro Street, San Diego, CA 92110; †Department of Cell Biology, Glaxo, Inc., Five Moore Drive, Research Triangle Park, NC 27709; and ‡Laboratory of Cancer Biology, University of California San Diego, La Jolla, CA 92093-0609

Communicated by I. M. Gelfand, July 12, 1991

ABSTRACT **There is an important need for clinically relevant animal models for human cancers. Toward this goal, histologically intact human colon-cancer specimens derived surgically from patients were implanted orthotopically to the colon or cecum of nude mice. We have observed extensive orthotopic growth in 13 of 20 cases of implanted patient colon tumors. These showed various growth patterns with subsequent regional, lymph-node, and liver metastasis, as well as general abdominal carcinomatosis. Thus, models for human colon cancer have been developed that show (*i*) local growth, (*ii*) abdominal metastasis, (*iii*) general abdominal carcinomatosis with extensive peritoneal seeding, (*iv*) lymph-node metastasis, (*v*) liver metastasis, and (*vi*) colonic obstruction. These models permit the passage of the tumors to form large cohorts. They will facilitate research into the biology of colon cancer metastatic capability and the development of new drugs active against metastatic cancer. These models may also predict the clinical course and the *in vivo* response to drugs of the cancer of individual patients.**

There is a need for the development of better animal models for human cancer. Models based on athymic nude mice have been used for this purpose. However, metastatic rates from subcutaneous or intramuscular xenografts have been low or nonexistent even from tumors that were highly metastatic in the patient from whom the tissue was derived (1–5).

Recent work from a number of laboratories has indicated that implanting human tumor cells orthotopically in the corresponding organ of nude mice resulted in much higher metastatic rates. For example, a human renal-cell carcinoma obtained from a surgical specimen was dissociated by enzymatic treatment and subcutaneously injected into the renal capsule of nude mice as well as other sites. The injection of human renal-cell carcinoma cells into the kidney of nude mice produced the highest incidence of tumor establishment and of metastasis to the lungs and other peritoneal organs. The nude-mouse renal capsule appears to be a most advantageous site for implantation of human renal-cell carcinoma (6–8). However, the subrenal capsule may be an advantageous implant site for other tumor types also (9). Human colon-cancer cells were dissociated, grown in culture, and subsequently injected into the cecum of nude mice to produce tumors that eventually metastasized to the liver, demonstrating that orthotopic implantation can enhance the metastatic capability of human tumor cells in nude mice (5, 10–13). Similar results also have been achieved for orthotopic implantation of cell lines of human lung cancer (14), human pancreatic cancer (15), bladder cancer (16, 17), melanoma (18, 19), breast cancer (20–22), and head and neck cancer (23). It should be noted, however, that the effects of orthotopicity have not been fully evaluated in that, at least in some cases, metastasis may arise from nonorthotopic sites.

Our approach is to avoid disruption of tumor integrity and to orthotopically implant histologically intact tumor tissue directly. Such a model should better reflect the original properties of human cancer and could be of great value in development of new drugs and treatment strategies of cancer. With this overall strategy, we have constructed a model of human colon cancer in nude mice that can show the variety of clinical behaviors that occur in human subjects. These include (*i*) local growth, (*ii*) abdominal metastasis, (*iii*) general abdominal carcinomatosis with extensive peritoneal seeding, (*iv*) lymph-node metastasis, (*v*) liver metastasis, and (*vi*) colonic obstruction. A very high tumor-establishment rate of 13 cases of 20 attempts was observed.

MATERIALS AND METHODS

Mice. Four-week-old outbred *nu/nu* mice of both sexes were used for tumor implantation. All animals were maintained in a sterile environment. Cages, bedding, food, and water were all autoclaved. All animals were maintained on a daily 12-hr light/12-hr dark cycle. Bethaprim Pediatric Suspension (containing sulfamethoxazole and trimethoprim) was added to the drinking water.

Colon Cancer Specimens. Fresh surgical specimens were obtained as soon as possible, but no later than 24 hr after surgery, from local San Diego hospitals and kept in Earl's minimal essential medium (MEM) at 4°C. Before implantation, specimens were washed twice with antibiotic-containing Earl's MEM, at least 10 min each time, to prevent possible contamination and infection. The formulation, in 500 ml of Earl's MEM, was: 70 ml of fetal bovine serum, 75.2 mg of penicillin, 125 mg of streptomycin, 10 ml of fungizone, 5 mg of tetracycline, 50 mg of amikacin, 75 mg of chloramphenicol, and 50 mg of gentamycin.

Specimens were then inspected, and grossly necrotic and suspected necrotic tissue was removed. Each specimen was equally divided into four to six separated parts, and each part was subsequently cut into small pieces of about 1 mm^3. Tumor pieces for each implantation were taken from each of the four to six parts of the specimen equally. In this way, the chance for viable tissue to be implanted was maximized.

Surgical Microprocedures. For direct implantation, nude mice were anesthetized, and the abdomen was sterilized with iodine and alcohol swabs. A small midline incision was made and the colocecal part of the intestine was exteriorized. Serosa of the site where tumor pieces were to be implanted was removed. Eight to 15 pieces of 1-mm^3 size tumor were implanted on the top of the animal intestine; an 8-0 surgical

The publication costs of this article were defrayed in part by page charge payment. This article must therefore be hereby marked "*advertisement*" in accordance with 18 U.S.C. §1734 solely to indicate this fact.

§To whom reprint requests should be addressed.

suture was used to penetrate these small tumor pieces and suture them on the wall of the intestine. The intestine was returned to the abdominal cavity, and the abdominal wall was closed with 7-0 surgical sutures. Animals were kept in a sterile environment.

For induction of a vascular bed prior to tumor implantation, gelfoam (Upjohn) was preimplanted, first being hydrated with Earle's MEM, cut into approximately $5 \times 5 \times 3$ mm^3 pieces, and stored in a CO_2 incubator. Mice were anesthetized with isoflurane inhalation, and the abdomen was sterilized with iodine and alcohol swabs. A small midline incision was made and the colocecal part of the intestine was exteriorized. Hydrated gelfoam was either implanted to the cecum or to the ascending colon 1 cm away from the cecum. Serosa was removed from the part where gelfoam was to be implanted. A $5 \times 5 \times 3$ mm^3 piece of hydrated gelfoam was implanted on the top of the colon or cecum. Two or three stitches of 8-0 surgical suture were applied to very small bits of the intestinal wall so as not to penetrate it. The intestine was returned to the abdominal cavity, and the wound was closed in one layer. Animals were maintained in a sterile environment. After 20 days, mice bearing the gelfoam preimplantation (now vascularized) were anesthetized and sterilized in exactly the same way as during the gelfoam implantation. The abdomen was reopened in the midline. The part of the intestine where the gelfoam had been implanted was exteriorized, and a small pocket was made into the vascularized gelfoam. About 8–15 pieces of the 1-mm^3 tumor, depending on the amount of tumor available, were implanted into the pocket. The pocket was closed with a stitch of 8-0 surgical suture. The intestine was then returned to the abdominal cavity. The wound was closed with 7-0 surgical sutures in one layer, and the animals were kept in a sterile environment.

A skin flap was induced into the abdominal cavity of nude mice to create a "sandwich-style" implantation. The main idea for doing so is because the tumor may have a better chance of growing in the subcutaneous environment. The nude mouse was anesthetized and the abdomen sterilized in the same way as in the gelfoam implantation. Tumor pieces were implanted between the skin flap and the cecum serosa.

For tumor and normal-surrounding-tissue coimplantation, the mice were anesthetized and the colocecal part of intestine was exposed in the same way as in direct implantation. After removing the serosa of the implantation site, 8–15 pieces of tumor together with 8–15 pieces of normal surrounding tissue were penetrated with 8-0 surgical sutures and sutured on the wall of the intestine. The intestine was returned to the abdominal cavity, and the abdominal wall was closed with 7-0 surgical sutures. Animals were kept in a sterile environment.

For tumor coimplantation with mouse embryonic tissue and gelfoam, anesthesia of the nude mice and the surgical approach to expose the colocecal part of the intestine were the same as in direct implantation. After removal of the serosa on the implantation site, a piece of $5 \times 5 \times 3$ mm^3 size gelfoam was implanted on the site. A pocket was made on the pieces of gelfoam, and 8–15 pieces of tumor and 8–15 pieces of mouse embryonic liver tissue were planted in the pocket; 8-0 surgical sutures were used to close the pocket. The intestine was then returned to the abdominal cavity, and the abdominal wall was closed with 7-0 surgical sutures. Animals were kept in a sterile environment.

RESULTS AND DISCUSSION

Twenty different cases of colon cancer surgical specimens were implanted orthotopically directly or with the use of gelfoam, an internal skin flap or the coimplantation of human normal and tumor tissue or coimplantation of tumor with mouse embryonic tissue and gelfoam. Thirteen of 20 individual patient specimens showed local orthotopic growth, with different specimens showing subsequent regional, lymph-node, and liver metastasis. These can serve as models for human colon cancer, including a model for (*i*) local growth, (*ii*) abdominal metastasis, (*iii*) general abdominal carcinomatosis with extensive peritoneal seeding, (*iv*) lymph-node metastasis, (*v*) liver metastasis, and (*vi*) colonic obstruction.

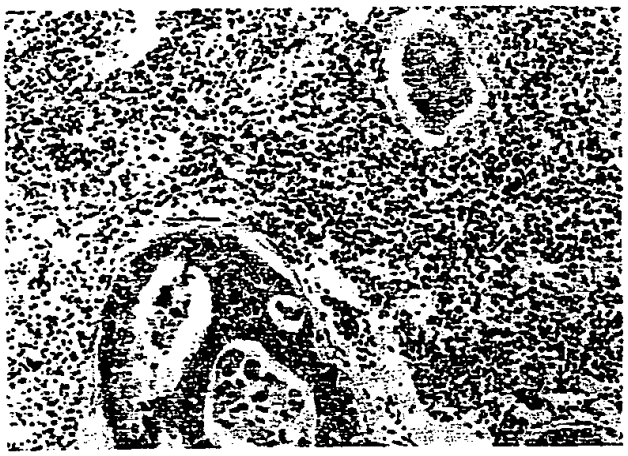

FIG. 1. Pathohistology of nude-mouse mesenteric lymph node involved with human-colon tumor metastases. (×130.)

Local Growth and Abdominal Metastasis. An example is specimen case 1701, an infiltrating mucinous adenocarcinoma of the right colon (modified Duke's classification C2). Two nude mice with preimplanted gelfoam were used for tumor implantation, two nude mice were used for tumor implantation with an internal skin flap, and two nude mice were used for direct implantation of tumor tissue to the cecum. Two of the six mice suffered early death (one with direct tumor implantation, one with gelfoam preimplantation) and were not available for assessment of tumor growth. All of the remaining mice demonstrated extensive primary growth ranging from 8 mm × 5.7 mm to 13 mm × 13 mm as well as abdominal-wall metastases ranging from 8 mm × 11 mm to 22 mm × 15 mm. All of the remaining mice showed visible tumor growth in the abdomen. Autopsies were performed 113–139 days after implantation.

Local Growth, Abdominal Metastasis, and Lymph-Node Metastasis. An example is specimen case 1707, an infiltrating adenocarcinoma of the right colon, moderately differentiated (modified Duke's classification D). Two nude mice were used

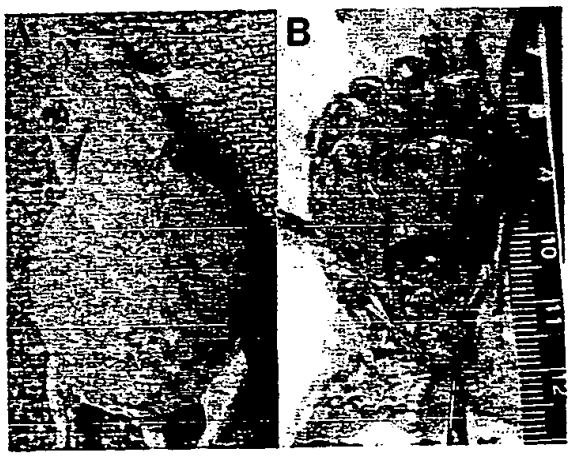

FIG. 2. (*A*) Nude mouse bearing orthotopically implanted human colon carcinoma. (*B*) Intraoperative view: Carcinomatosis growing extensively in nude-mouse abdominal organs and peritoneum after orthotopic implantation.

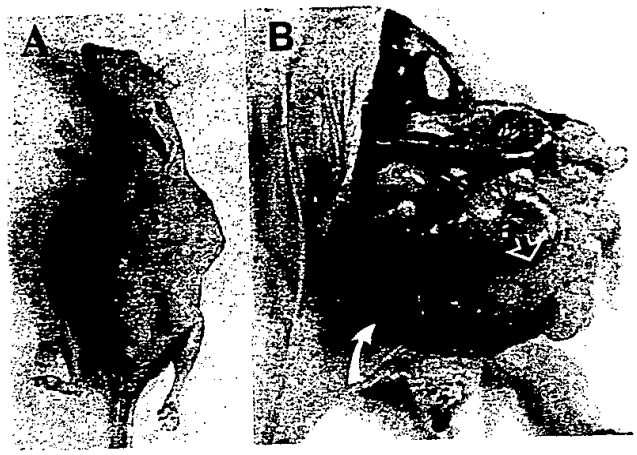

FIG. 3. (*A*) Nude mouse bearing orthotopically implanted human colon carcinoma. (*B*) Intraoperative view. Curved arrow indicates nude-mouse cecum. Hollow arrow indicates the site of implantation and tumor growth from there.

for tumor and normal-surrounding-tissue coimplantation to the cecum, and two nude mice were used for tumor direct implantation to the cecum. One mouse (direct implantation) was lost with no assessment of the tumor's growth. Orthotopic growth and abdominal metastasis occurred in the other three mice. A 10 × 10 mm primary tumor and 12 × 14 abdominal-wall metastasis were found at day 175 after implantation in one of the mice (tumor and normal surrounding tissue coimplanted). Lymph-node metastases were noted in this animal (Fig. 1). The histology of the original tumor and the orthotopically growing tumor both indicated adenocarcinoma. In the mouse with direct tumor implantation and in the other mouse with coimplantation of tumor and normal surrounding tissue, only local tumor growth occurred when observed at autopsy on days 159 and 230 after implantation, respectively.

General Abdominal Carcinomatosis with Extensive Peritoneal Seeding. An example is specimen case 1935, infiltrating mucinous adenocarcinoma moderately differentiated. Tumors were found to be growing in two mice after direct implantation. In one mouse 127 days after implantation, the primary tumor measured 19 × 16 mm. An abdominal mass measured 20 × 14 mm, and a mass on the pancreas, which was easily peeled off, measured 21 × 17 mm. In addition, extensive carcinomatosis was found with small tumors growing all over the peritoneum and abdominal organs (Figs. 2 *A* and *B*).

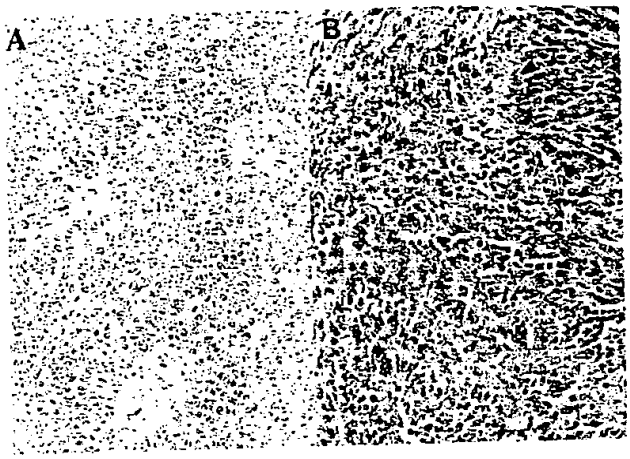

FIG. 5. (*A*) Pathohistology of original human-colon carcinoma prior to implantation. (×130.) (*B*) Pathohistology of primary tumor growth on nude-mouse colon as shown in Fig. 3*B*. (×130.)

Liver Metastasis. Specimen case 1594 is a high-grade poorly differentiated adenocarcinoma of the colon (modified Duke's classification B_2). Tumor pieces were implanted in two mice with preimplanted gelfoam (20 days after gelfoam implantation), and two mice were implanted with the internal skin-flap technique. Forty-eight days after implantation, one mouse (with skin-flap implantation) was found to have a palpable mass in the abdomen. The animal was examined and extensive tumor growth measuring approximately 25 × 25 mm was found. There was no liver or other distal organ metastasis. The animal died during surgery. Another animal (with skin-flap implantation) was found moribund 79 days after implantation. Autopsy showed the implanted tumor grew extensively in the colorectal area. Three tumor nodules measuring 9 × 9 mm, 11 × 7.5 mm, and 13 × 9 mm respectively were found, but no distal organ metastasis was observed. The animals with the internalized skin flaps overlaying the tumor implanted on the colon grew more extensively than those with gelfoam implantations. One mouse with gelfoam implantation was examined 56 days after tumor implantation. Primary tumor growth of approximately 12 × 9 mm was found, but no regional or distal organ metastasis was observed. The animal was sacrificed for pathohistology study of the abdominal masses that indicated adenocarcinoma. The other nude mouse with gelfoam implantation was moribund 160 days after tumor implantation (Fig. 3*A*). Autopsy was

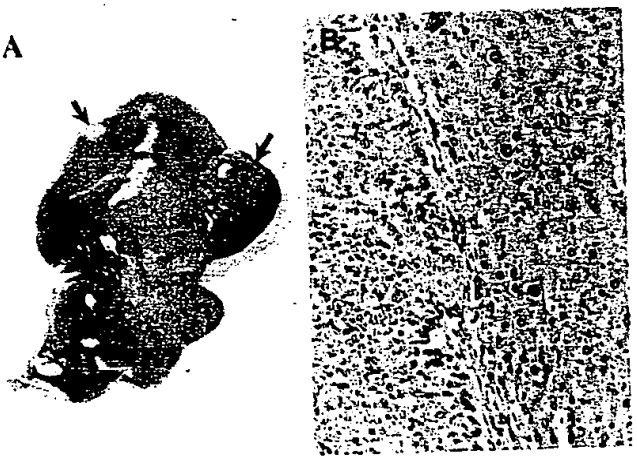

FIG. 4. (*A*) Nude-mouse liver involved with tumor metastases (arrows). (*B*) Pathohistology of tumor-involved nude-mouse liver as shown in *A*. (×130.)

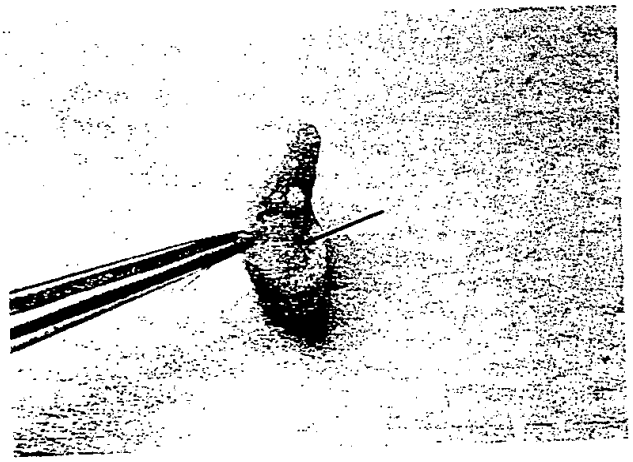

FIG. 6. Tumor-infiltrated nude-mouse cecum. Arrow indicates extremely narrowed lumen.

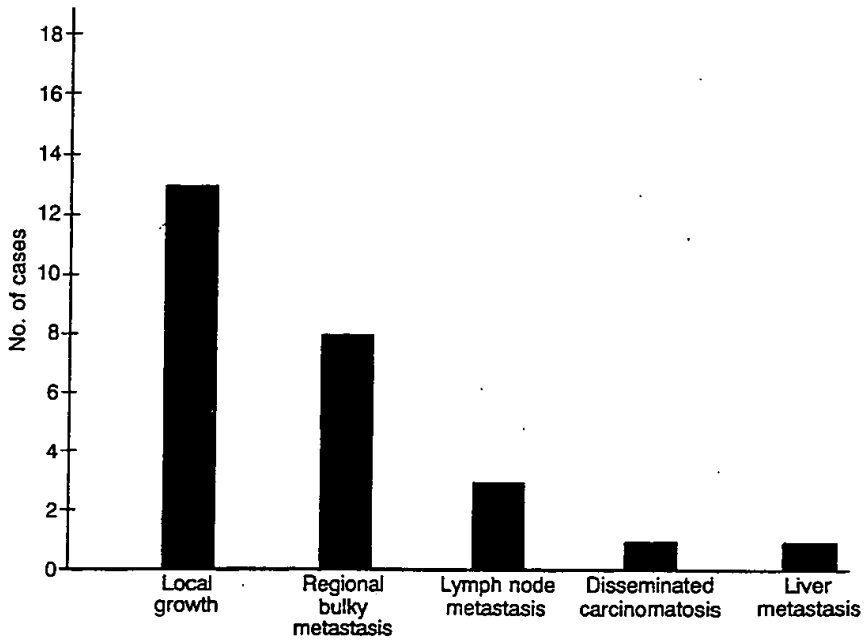

FIG. 7. Modes of growth and spread of human cancer specimens in nude mice after orthotopic implantation.

done, and the mouse was found to have extensive primary tumor growth measuring approximately 37 × 30 mm (Fig. 3*B*) and multiple liver metastases ranging from 1.5 × 1.5 mm to 9 × 9 mm (Fig. 4*A*). Pathohistology studies on the original tumor tissue (Fig. 5*A*), abdominal masses (Fig. 5*B*), and multiple liver lesions (Fig. 4*B*) indicated adenocarcinoma.

Colonic Obstruction. An example is specimen case 1701, infiltrating mucinous adenocarcinoma of the right colon. Fig. 6 shows the cecum to be infiltrated and obstructed 127 days after direct implantation of the specimen.

Cohort Construction. To utilize the models for testing treatment modalities, it is necessary to construct cohorts. We have now orthotopically passaged tumor from mouse 1594 six times and have developed a cohort of 12–20 animals with growing tumors, some of which have metastasized to the liver as occurred in the first group of animals implanted.

Sequential Appearance of Primary Tumor and Metastasis. Laparotomy was performed on day 26 on the nude mouse implanted with patient tumor 1594. Primary tumor growth was observed. No local or distal organ metastases were observed. The animal was returned for further observation on day 78 when the second laparotomy was performed. Primary growth was found. No liver or other distal organ metastasis was found. On day 160, the mouse was sacrificed. Primary tumor growth, local invasion, and liver metastasis were found at autopsy.

The results we have presented show that histologically intact surgical specimens of human colon cancer can be implanted in the nude-mouse colon, grow locally, regionally spread to lymph nodes and abdominal organs, result in peritoneal carcinomatosis, and distally metastasize to the liver. Fig. 7 summarizes the frequency of occurrences of these modes of tumor growth and spread in the implant model in our experiments. Results obtained indicate that tumor alone may be sufficient for orthotopic tumor growth and metastasis. Further experimentation is necessary to ascertain this. Thus, we have developed models where the human colon cancer derived directly from the patient mimics in the nude mouse many aspects of the natural history in a series of typical human colon-cancer patients. The models should be superior to existing animal models, which use highly deviated tumors to study new treatment modalities. The model may also be useful in predicting drug response or clinical course for individual patients (24).

Significance of These Findings. Subcutaneous tumor implantation had been a standard methodology for establishing animal models for human cancer research for years (4, 5). Although such a model has helped us to understand the nature and therapeutic treatment for human cancer, major problems still remain unresolved. One of them is that the tumor that is derived from a patient and subsequently put into immunodeficient animals subcutaneously no longer behaves as it did in the human patient—i.e., although the tumor can grow subcutaneously, the tumor is encapsulated and fails to metastasize either regionally or distally.

Recently a new strategy of what is called "orthotopic implantation" had been used for developing human tumor animal models (4, 5). Cell lines or disaggregated cells are injected to the corresponding organ of the mouse where the human tumor was derived. It was shown that this method of implantation allows metastasis to occur. However, the cell lines and disaggregated cells used for orthotopic implantation were obtained from breaking the original structure of human tumor tissue, which may lead to a change in the nature and the biological behavior of the tumor (25).

The model of orthotopic implantation of fresh histologically intact human tumor specimens avoids the drawbacks of previous animal models. Such an animal model of individual human tumors can facilitate optimal individual therapy.

The development of new cancer therapeutics and protocols require animal models that closely resemble the human patient. The model of orthotopic implantation of fresh histologically-intact human-tumor specimens seems to meet this need.

This paper is dedicated to the 70th birthday of Professor Sun Lee for his founding role in the field of experimental microsurgery. We are grateful for the expert word processing of Ms. Polly Jayne Pomeroy. This study was supported in part by a contract from Glaxo, Inc., to AntiCancer, Inc.

1. Sordat, B., Fritsche, R., Mach, J. P., Carrel, S., Ozzello, L. & Cerottini, J. C. (1973) in *Proceedings of the First International Workshop on Nude Mice*, eds. Rygaard, J. & Povlsen, C. O. (Fischer, Jena, F.R.G.), pp. 269–278.
2. Povlsen, C. O. & Rygaard, J. (1976) in *In Vitro Methods in Cell*

Mediated and Tumor Immunity, eds. Bloom, B. B. & David, J. R. (Academic, New York), pp. 701–711.
3. Kyriazis, A. P., DiPersio, L., Michael, G. J., Pesce, A. J. & Stinnett, J. D. (1988) *Cancer Res.* **38**, 3186–3190.
4. Fidler, I. J. (1986) *Cancer Metastasis Rev.* **5**, 29–49.
5. Fidler, I. J. (1990) *Cancer Res.* **50**, 6130–6138.
6. Naito, S., Giavazzi, R., Walker, S. M., Itoh, K., Mayo, J. & Fidler, I. J. (1987) *Clin. Exp. Metastases* **5**, 135–146.
7. Naito, S., von Eschenback, A. C. & Fidler, I. J. (1987) *J. Natl. Cancer Inst.* **78**, 377–385.
8. Naito, S., von Eschenback, A. C., Giavazzi, R. & Fidler, I. J. (1986) *Cancer Res.* **46**, 4109–4115.
9. Bodgen, A. E. & Von Hoff, D. D. (1984) *Cancer Res.* **44**, 1087–1090.
10. Giavazzi, R., Jessup, J. M., Campbell, D. E., Walker, S. M. & Fidler, I. J. (1986) *J. Natl. Cancer Inst.* **77**, 1303–1308.
11. Bresalier, S., Raper, S. E., Hujanen, E. S. & Ken, Y. S. (1987) *Int. J. Cancer* **39**, 625–630.
12. Morikawa, K., Walker, S. M., Jessup, J. M. & Fidler, I. J. (1988) *Cancer Res.* **48**, 1943–1948.
13. Morikawa, K., Walker, S., Nakajima, M., Pathak, S., Jessup, J. M. & Fidler, I. J. (1988) *Cancer Res.* **48**, 6863–6871.
14. McLemore, T. L., Liu, M. C., Blacker, P. C., Gregg, M., Alley, M. C., Abbott, B. J., Shoemaker, R. H., Bohlman, M. E., Litterst, C. C., Hubbard, W. C., Brennan, R. H., McMahon, J. B., Fine, D. L., Eggleston, J. C., Mayo, J. G. & Boyd, M. R. (1987) *Cancer Res.* **47**, 5132–5140.
15. Vezeridis, M., Turner, M. D., Kajiji, S., Yankee, R. & Meitner, P. (1985) *Proc. Am. Assoc. Cancer Res.* **26**, 53.
16. Ahlering, T. E., Dubeau, L. & Jones, P. A. (1987) *Cancer Res.* **47**, 6660–6665.
17. Soloway, M. S., Nissenkorn, I. & McCallum, L. (1983) *Urology* **21**, 159–161.
18. Kozlowski, J., Fidler, I. J., Campbell, D., Xu, Z., Kaighn, M. E. & Hart, I. R. (1984) *Cancer Res.* **44**, 3522–3529.
19. Kozlowski, J., Hart, I., Fidler, I. J. & Hanna, N. (1984) *J. Natl. Cancer Inst.* **72**, 913–917.
20. Miller, F. & McInerney, D. (1988) *Cancer Res.* **48**, 3698–3701.
21. Basolo, F., Fontanini, G. & Squartini, F. (1988) *Cancer Res.* **48**, 3197–3202.
22. White, A. C., Levy, J. A. & McGrath, C. M. (1982) *Cancer Res.* **42**, 906–912.
23. Dinesman, A., Haughey, B., Gates, G. A., Aufdemorte, T. & Von Hoff, D. D. (1990) *Otolaryngol. Head Neck Surg.* **103**, 766–774.
24. Jessup, J. M., Giavazzi, R., Campbell, D., Cleary, K. R., Morikawa, K., Hostetter, R., Atkinson, E. N. & Fidler, I. J. (1989) *Cancer Res.* **49**, 6906–6910.
25. Hoffman, R. M. (1991) *Cancer Cells* **3**, 86–92.

Clinical & Experimental Metastasis **18**: 213–218. 2000.

Chronologically-specific metastatic targeting of human pancreatic tumors in orthotopic models

Michael Bouvet[1], Meng Yang[2], Stephanie Nardin[1], Xiaoen Wang[2], Ping Jiang[2], Eugene Baranov[2], A.R. Moossa[1] & Robert M. Hoffman[1,2]

[1]*Department of Surgery, University of California San Diego Medical Center, San Diego, California, USA;* [2]*AntiCancer, Inc., San Diego, California, USA*

Received 8 August 2000; accepted in revised form 29 September 2000

Key words: pancreatic cancer, metastasis, chronology, reporter gene, green fluorescence protein, fluorescence imaging, nude mice

Abstract

Pancreatic cancer is a highly metastatic disease that responds poorly to currently-available treatment. In order to better visualize and understand the chronology and specificity of metastatic targeting of pancreatic cancer, two human pancreatic cancer cell lines, expressing green fluorescent protein (GFP), were studied in orthotopic models. MIA-PaCa2-GFP and BxPC-3-GFP tumor fragments were transplanted by surgical orthotopic implantation (SOI) to the nude mouse pancreas for fluorescence visualization of the chronology of pancreatic tumor growth and metastatic targeting. BxPC-3-GFP tumors developed rapidly in the pancreas and spread regionally to the spleen and retroperitoneum as early as six weeks. Distant metastases in BxPC-3-GFP were rare. In contrast, MIA-PaCa-2-GFP grew more slowly in the pancreas but rapidly metastasized to distant sites including liver and portal lymph nodes. Regional metastases in MIA-PaCa-2-GFP were rare. These studies demonstrate that pancreatic cancers have highly specific and individual 'seed-soil' interactions governing the chronology and sites of metastatic targeting.

Abbreviations: SOI – surgical orthotopic implantation; GFP – green fluorescent protein

Introduction

A greater understanding of the metastatic process of pancreatic cancer is needed [1]. Transgenic rodent models of pancreatic cancer [2] as well as chemically induced pancreatic cancer in rodents have been useful to study this disease [3]. Metastases of human pancreatic cancer after s.c. transplantation in nude mice have only occasionally been reported, however [4, 5]. Vezeridis et al. [6] reported a metastatic model using splenic injection of a fast-growing variant of human pancreatic cancer. Although this was a valuable model for the study of certain steps of the metastatic process, it bypasses invasion from the primary tumor and in essence generates colonization rather than metastases.

It is important, however, to study clinically relevant metastases and their treatment. Tan and Chu [7], Marincola et al. [8, 9], and Bruns et al. [10] reported metastatic models of human pancreatic cancer using orthotopic implantation of tumor-cell suspensions, which resulted in invasive local tumor growth and subsequent metastases. Vezeridis et al. [11] used tumor tissue for orthotopic transplantation, resulting in extensive local growth and metastases to liver, lung, and lymph nodes. We have used histologically intact specimens of pancreatic cancer, including those directly removed from patients, for surgical orthotopic implantation (SOI) to nude mice to construct highly metastatic nude-mouse models of human pancreatic cancer [12–15]. The models using intact tissue for orthotopic implantation have been shown to have considerably higher metastatic rates than orthotopic models using cell suspensions [7–10].

The present report utilized nude mouse models of SOI human pancreatic tumors genetically engineered with green fluorescent protein (GFP) [8–9]. These models allow, for the first time, early visualization of the chronology of tumor growth, progression, and metastases of pancreatic tumors to specific target organs. Our hypothesis was that these models would demonstrate chronologically tumor-specific metastatic targeting. The results demonstrated that pancreatic tumors are highly specific with regard to metastatic sites and chronology of metastatic development.

Correspondence to: Robert M. Hoffman, AntiCancer, Inc., San Diego, CA 92111, USA. Tel: +1-858-654-2555; Fax: +1-858-268-4175; E-mail: all@anticancer.com

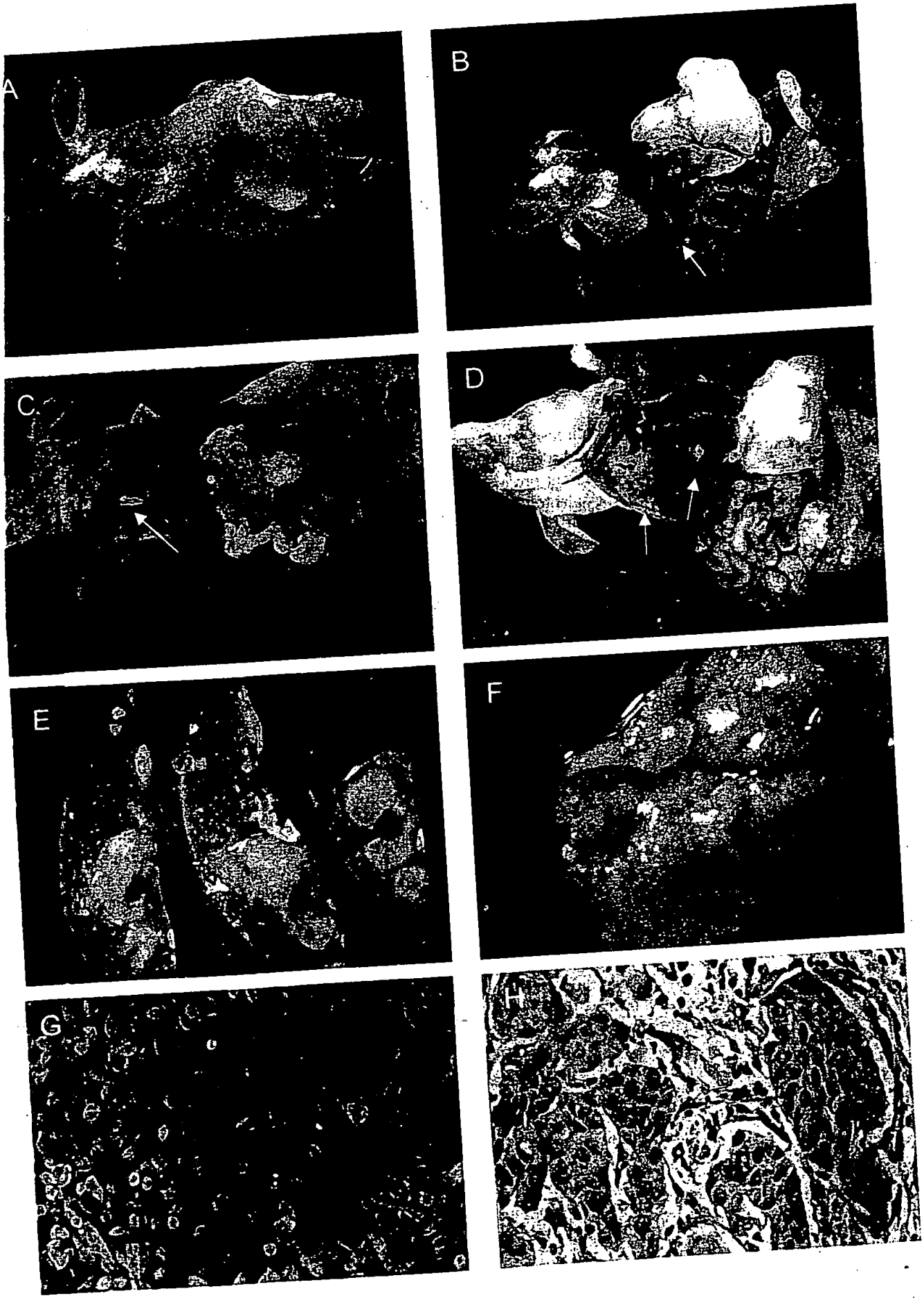
A
B
C
D
E
F
G
H

THIS PAGE BLANK (USP)

Figure 1. (A) The orthotopic BxPC-3-GFP pancreatic tumor is externally visualized with fluorescence through the skin of the nude mouse. (B) Laparotomy of the same mouse in (A) showing locally advanced BxPC-3-GFP tumor with portal lymph node metastases. This pattern of metastases was typical of BxPC-3-GFP. (C) Three 1-mm^3 fragments of s.c.-grown MIA-PaCa-2-GFP tumor were implanted to the pancreas of nude mice by SOI. The primary tumor formed in the pancreas at 12 weeks is visualized under bright-field microscopy. Numerous metastases and micrometastases, typical of MIA-PaCa-2-GFP, can be visualized by GFP under fluorescence microscopy in the stomach, spleen, periportal nodes (arrow), liver, and mediastinum (arrow). (D) MIA-PaCa-2-GFP tumor at week-10 post-SOI. Left arrow shows diaphragm metastases and right arrow shows liver metastases. (E) Bi-lobar high expressing MIA-PaCa-2 GFP liver metastases are noted under fluorescence microscopy. (F) MIA-PaCa-2 GFP-expressing lung metastases are noted. (G) Stable high-level expression GFP transductant *in vitro*. The human pancreatic cancer cell line MIA-PaCa-2 was transduced with the RetroXpress vector pLEIN that expresses enhanced GFP and the neomycin resistance gene on the same bicistronic message. The stable high expression clone was selected in 800 μg/ml of G418. (H) H&E section of MIA-PaCa-2-GFP tumor.

Materials and methods

Pancreatic cancer cell lines

The MIA-PaCa-2 and BxPC-3 human pancreatic cancer cell lines were obtained from the American Type Culture Collection (Rockville, Maryland). The cells were maintained in Dulbecco's Modified Eagle's Medium supplemented with 10% fetal calf serum, 2 mM glutamine, 100 μ/ml penicillin, 100 μg/ml of streptomycin, and 0.25 μg/ml of amphotericin B (Gibco-BRL, Life Technologies, Inc., Grand Island, New York). Both cell lines were incubated at 37 °C in a 5% CO_2 incubator.

GFP DNA expression vector

The RetroXpress vector pLEIN was purchased from Clontech Laboratories, Inc. (Palo Alto, California). The pLEIN vector expresses enhanced GFP and the neomycin resistance gene on the same bicistronic message, which contains an IRES site.

GFP-retrovirus vector production [20]

PT67, an NIH3T3-derived packaging cell line expressing the 10 A1 viral envelope, was purchased from Clontech Laboratories, Inc. PT67 cells were cultured in DMEM (Irvine Scientific, Santa Ana, California) supplemented with 10% heat-inactivated fetal bovine serum (Gemini Bioproducts, Calabases, California). For GFP-retrovirus production, packaging cells (PT67), at 70% confluence, were incubated with a precipitated mixture of DOTAP reagent (Boehringer Mannheim) and saturating amounts of pLEIN plasmid for 18 h. Fresh medium was replenished at this time. The cells were examined by fluorescence microscopy after 48 h. For selection of packaging cells producing high levels of GFP retrovirus, the cells were cultured in stepwise increasing amounts of 500–2000 μg/ml G418 (Life Technologies, Inc., Grand Island, New York) for 7 days.

GFP-retroviral transduction and selection of high GFP-expression MIA-PaCa-2 and BxPC-3 pancreatic cancer cells

For GFP gene transduction [16, 17], 20% confluent MIA-PaCa-2 or BxPC-3 cells were incubated with a 1:1 precipitated mixture of retroviral supernatants of the PT67 packaging cells and RPMI 1640 (Life Technologies, Inc.) for 72 h. Fresh medium was replenished at this time. MIA-PaCa-2 or BxPC-3 cells were harvested by trypsin/EDTA 72 h after infection and subcultured at a ratio of 1:15 into selective medium that contained 200 μg/ml of G418. The level of G418 was increased to 800 μg/ml stepwise. MIA-PaCa-2 and BxPC-3 clones expressing GFP (MIA-PaCa-2-GFP or BxPC-3-GFP) were isolated with cloning cylinders (Bel-Art Products, Pequannock, New Jersey) by trypsin/EDTA and were amplified and transferred by conventional culture methods. High GFP-expression clones were then isolated in the absence of G418 for more than 10 passages to select for stable expression of GFP.

Subcutaneous tumor growth

BALB/c nu/nu female mice, 6 weeks of age, were injected subcutaneously with a single dose of 5×10^6 MIA-PaCa-2-GFP or BxPC-3-GFP cells. Cells were first harvested by trypsinization and washed three times with cold serum-free medium and then injected in a total volume of 0.2 ml within 40 min of harvesting.

Surgical orthotopic implantation (SOI) [12–15]

Pancreatic tumors at the exponential growth phase, grown subcutaneously in nude mice, were resected aseptically. Necrotic tissues were cut away, and the remaining healthy tumor tissues were cut with scissors and minced into approximately 1 × 1 × 1 mm pieces in Hanks' balanced salt solution containing 100 units/ml penicillin and 100 μ/ml streptomycin. Each piece was weighed and adjusted with scissors to be 50 mg. Mice were anesthetized by isoflurane inhalation. The abdomen was sterilized with alcohol. An incision was then made through the left upper abdominal pararectal line and peritoneum. The pancreas was carefully exposed and three tumor pieces were transplanted on the middle of the pancreas with a 6-0 Dexon (Davis-Geck, Inc., Manati, Puerto-Rico) surgical suture. The pancreas was then returned into the peritoneal cavity, and the abdominal wall and the skin were closed with 6-0 Dexon sutures. Animals were kept in a sterile environment. All procedures of the operation described above were performed with a 7× microscope (Olympus). A total of 44 mice were used for the BxPC3-GFP model and 26 for the MIA-PaCa-2 model.

Fluorescence microscopy [20]

A Leica stereo microscope MZ 12 equipped with a mercury bulb as a light source was used for the imaging experiments. Selective excitation of GFP was produced through a D425/60 band-pass filter and a 470 DCXR dichroic mirror. Fluorescence was emitted through a GG475 long-pass

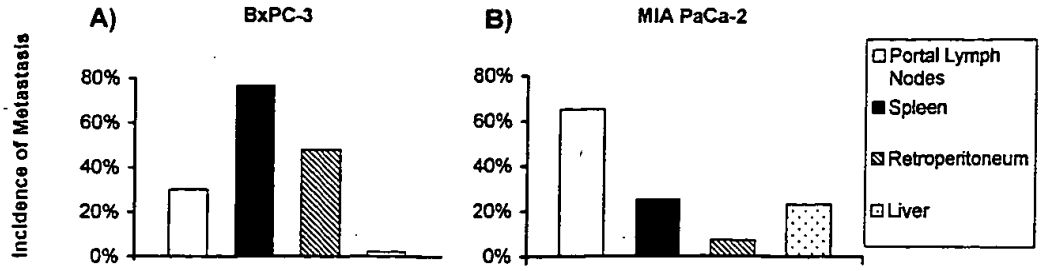

Figure 2. Site-specific metastases in human pancreatic cancer orthotopic models. A) BxPC-3-GFP. B) MIA-PaCa-2-GFP. Forty-four and twenty-six mice were used for the BxPC-3-GFP and MIA-PaCa-2 models, respectively. The y-axis represents cumulative percentage of mice with metastasis.

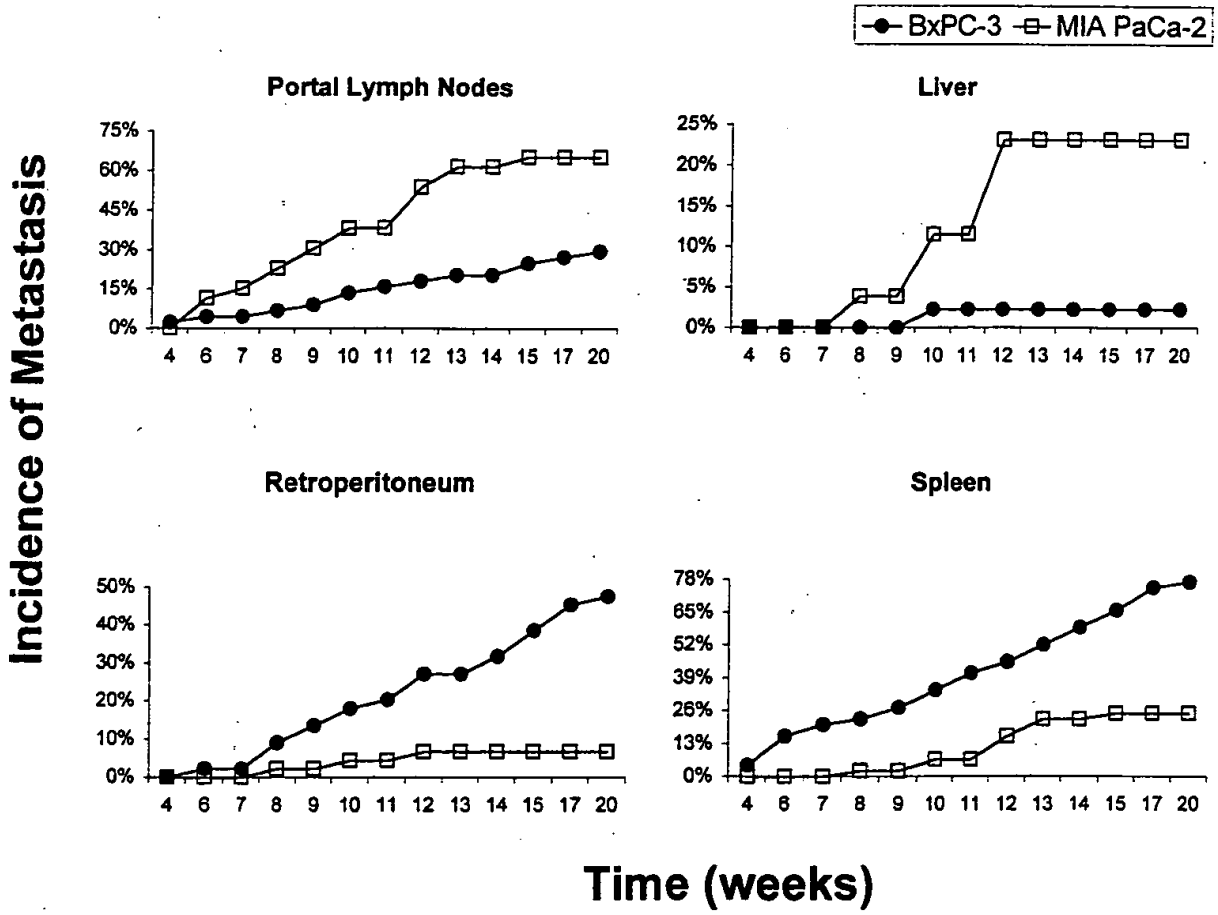

Figure 3. Chronology of site-specific metastasis. See Figure 2 for details of experimental conditions.

filter (Chroma Technology, Brattleboro, Vermont) and collected by a Hamamatsu Color Cooled CCD Video Camera HM C5810. High-resolution images were captured and processed with a Pro-Series Frame-Grabber and acquired by a Pentium-IV PC with Image Pro Plus 3.1 software (Media Cybernetics, Silver Spring, Maryland). Whole-body images were obtained by placing the mice in a fluorescent light box equipped with a fiberoptic light source of 490 nm (Lightools Research, Encinitas, CA) utilizing the CCD camera and filters mentioned above as previously described by Yang et al. [20].

Histological analysis

The primary orthotopic tumor was removed, weighed, and saved for histologic analysis carried out with standard hematoxylin and eosin (H&E) staining.

Analysis of metastasis

At indicated time points following SOI, mice were sacrificed and explored. The orthotopic tumor and all major organs were observed directly under fluorescence microscopy, images captured, and location and number of metastases were recorded for each mouse. At least one metastatic lesion per organ was needed to be present for an organ to be considered positive for metastasis. The sensitivity of the system was a single fluorescent tumor cell. The cumulative incidence

for each site of metastasis was determined by sacrificing approximately three mice per week.

Results and discussion

Isolation of stable high-level expression GFP transductants of MIA-PaCa-2 and BxPC-3 cells

The retroviral-vector transduced cells were able to grow *in vitro* at levels of G418 up to 800 μ/ml. The selected G418-resistant pancreatic cells had bright GFP fluorescence (Figure 1G). There was no difference in the cell proliferation rates of parental cells and the GFP transductants as determined by comparing their doubling times *in vitro* (data not shown).

Growth kinetics of primary pancreatic tumors

Both the MIA-PaCa-2-GFP and BxPC-3-GFP tumors grew extensively in the pancreas after orthotopic implantation. By 3–4 weeks after SOI, brightly fluorescent tumors were noted in the pancreata. MIA-PaCa-2-GFP tumors grew in a logarithmic manner, reaching a maximum weight of 3.8 grams by week-14 after SOI. BxPC-3-GFP tumors also grew logarithmically and reached a maximum weight of 10.4 grams by 15 weeks post-SOI. Both tumors showed pathologic features typical of human pancreatic adenocarcinoma on H&E staining (Figure 1H).

Tumor selective metastatic organ targeting

Figure 2 represents the incidence of metastasis in each model at week-20 post-SOI. The BxPC-3-GFP cell line produced locally-advanced, invasive tumors that metastasized regionally selectively to the spleen and the retroperitoneum with distant liver metastases very rare (Figure 2A). In contrast, metastases in the MIA-PaCa-2 model were selective to distant sites in the portal lymph nodes and liver with regional retroperitoneal lymph node metastasis very rare (Figure 2B).

Tumor selective metastatic chronology

Metastatic chronology markedly differed between the two pancreatic cancer models (Figure 3). With GFP expression, the metastatic targeting of each pancreatic tumor was readily detectable even early after transplantation (Figure 1). Rapid targeting of portal lymph nodes and liver was seen in MIA-PaCa-2 with metastases visible by 6 weeks and 8 weeks, respectively (Figure 3). At later time points, metastases were also seen in the lung (Figure 1F). In contrast, even after 20 weeks, only one mouse had retroperitoneal metastasis (Figure 3). In contrast, BxPC-3 preferentially targeted the retroperitoneum and spleen with metastasis visible by 8 and 6 weeks, respectively (Figure 3). Even at 20 weeks after SOI, only one animal with the BxPC-3 tumor had liver metastasis (Figure 3). Little data is available in the literature about the metastatic potential of the MIA-PaCa-2 and BxPC-3 cell lines [9]. Marincola previously observed liver metastasis following injection of MIA-PaCa-2 cell suspension into the pancreas of nude mice [9]. In our model, using the GFP and SOI techniques, numerous metastases at other sites in addition to the liver were visualized (Figures 1–3).

In the present study, we have utilized SOI and GFP in order to visualize the chronological specificity of pancreatic metastatic tageting for two human pancreatic cancer lines. We observed distinct chronological organ-specific metastasis for the two cancers. Both BxPC-3 and MIA-PaCa-2 have mutant p53 genes which therefore does not account for their distinct metastatic behavior [24]. BxPC-3 has wild type *ras* genes but MIA-PaCa-2 has a mutant k-*ras* [18]. Metastatic models such as described in the present report should be very useful to determine the role of such mutant oncogenes.

These two different metastatic models also provide new insights into clinical pancreatic cancer. For instance, approximately 25% of patients with pancreatic cancer present with locally-advanced unresectable tumors [19] similar to the metastatic pattern seen in the BxPC-3-GFP model. In contrast, 50% of patients have distant metastases to the liver and regional lymph nodes as seen in the MIA-PaCa-2-GFP model. Treatment strategies and prognosis differ for these two groups of patients and therefore clinically relevant models for these two major groups of pancreatic cancer patients such as we have described can be used to test new treatment modalities.

Acknowledgements

This study was supported in part by US National Cancer Institute Grant R44 CA 53963 and an American Cancer Society Institutional Research Grant and the Department of Health Services, California Cancer Research Program (97-12013).

References

1. Wanebo HJ and Vezeridis MP. Pancreatic carcinoma in perspecitve. A continuing challenge. Cancer 1996; 78 (Suppl.): 580–91.
2. Asa SL, Lee YC and Drucker DJ. Development of colonic and pancreatic endocrine tumours in mice expressing a glucagon-SV40 T antigen transgene. Virchows Arch 1996; 427: 595–606.
3. Zhou W, Povoski SP, Longnecker DS et al. Novel expression of gastrin (cholecystokinin-B) receptors in azaserine-induced rat pancreatic carcinoma: receptor determination and characterization. Cancer Res 1992; 52: 6905–11.
4. Kyriazis AP, Kyriazis AA, McCombs WB et al. Biological behavior of human malignant tumors grown in the nude mouse. Cancer Res 1981; 41: 3995–4000.
5. Kajii SM, Meitner, PA, Bogaars HA et al. Metastasis of human pancreatic adenocarcinoma (RWP-1) in nude mice. Br J Cancer 1982; 46: 970–5.
6. Vezeridis MP, Turner MD, Kajiji S et al. Metastasis of a human pancreatic cancer (HPC) to liver in nude mice. Proc Am Assoc Cancer Res 1985; 26: 53 (Abstr).
7. Tan MH and Chu TM. Characterization of the tumorigenic and metastatic properties of a human pancreatic tumor cell line (AsPC-1) implanted orthotopically into nude mice. Tumor Biol 1985: 6: 89–98.
8. Marincola F, Taylor-Edwards C, Drucker B et al. Orthotopic and heterotopic xenotransplantation of human pancreatic cancer in nude mice. Curr Surg 1987; 44: 294–7.
9. Marincola FM, Drucker BJ, Siao DY et al. The nude mouse as a model for the study of human pancreatic cancer. J Surg Res 1989: 47: 520–9.

10. Bruns CJ, Harbison MT, Kuniyasu H et al. *In vivo* selection and characterization of metastatic variants from human pancreatic adenocarcinoma by using orthotopic implantation in nude mice. Neoplasia 1999; 1: 50–62.
11. Vezeridis MP, Doremus CM, Tibbetts LM et al. Invasion and metastasis following orthotopic transplantation of human pancreatic cancer in the nude mouse. J Surg Oncol 1989; 40: 261–5.
12. Fu X, Guadagni F and Hoffman RM. A metastatic nude mouse model of human pancreatic cancer constructed orthotopically from histologically intact patient specimens. Proc Natl Acad Sci USA 1992; 89: 5645–49.
13. Furukawa T, Kubota T, Watanabe M et al. A novel 'patient-like' treatment model of human pancreatic cancer constructed using orthotopic transplantation of histologically-intact human tumor-tissue in nude mice. Cancer Res 1993; 53: 3070–2.
14. An Z, Wang X, Kubota T et al. A clinical nude mouse metastatic model for highly malignant human pancreatic cancer. Anticancer Res 1996; 16: 627–32.
15. Tomikawa M, Kubota T, Matsuzaki SW et al. Mitomycin C and cisplatin increase survival in a human pancreatic cancer metastatic model. Anticancer Res 1997; 17: 3623–6.
16. Hoffman RM. Orthotopic transplant mouse models with green fluorescent protein-expressing cancer cells to visualize metastasis and angiogenesis. Cancer Metastasis Rev 1999; 17: 271–7.
17. Hoffman RM. Green fluorescent protein to visualize cancer progression and metastasis. In Conn PM (ed): Methods in Enzymology, Green Fluorescent Protein, Vol. 302. San Diego: Academic Press 1999; 20–31.
18. Nielsen LL, Shi B, Hajian G et al. Combination therapy with the farnesyl protein transferase inhibitor SCH66336 and SCH58500 (p53 adenovirus) in preclinical cancer models. Cancer Res 1999; 59: 5896–901.
19. Evans DB, Abbruzzese JL, Rich TA. Cancer of the pancreas. In DeVita VT, Hellman S, Rosenberg SA (eds): Cancer, Principles & Practice of Oncology. Philadelphia: Lippincott 1997.
20. Yang M, Baranov E, Jiang P et al. Whole-body optical imaging of green fluorescent protein-expressing tumors and metastases. Proc Natl Acad Sci USA 2000; 97: 1206–11.

Proc. Natl. Acad. Sci. USA
Vol. 89, pp. 5645–5649, June 1992
Medical Sciences

14

A metastatic nude-mouse model of human pancreatic cancer constructed orthotopically with histologically intact patient specimens

XINYU FU*, FIORELLA GUADAGNI†, AND ROBERT M. HOFFMAN*‡

*AntiCancer, Inc., 5325 Metro Street, San Diego, CA 92110; †Regina Elena Cancer Institute, Viale Regina Elena, 291, Rome, Italy; and ‡Laboratory of Cancer Biology, University of California, San Diego, La Jolla, CA 92093-0609

Communicated by Sheldon Penman, March 2, 1992

ABSTRACT **Pancreatic cancer is one of the most intractable and least understood of all human cancers. Pancreatic cancer is the fourth-leading cause of cancer-related mortality in the United States with <2% of the patients surviving for 5 yr. In an effort to help develop more effective treatment modalities for pancreatic cancer and improve detection, we report an animal model for individual human pancreatic-cancer patients. The model involves orthotopic transplantation of histologically intact pancreatic-cancer specimens to the nude-mouse pancreas, which can result in models that resemble the clinical picture including (*i*) extensive local tumor growth, (*ii*) extension of the locally growing human pancreatic cancer to the nude-mouse stomach and duodenum, (*iii*) metastases of the human pancreatic tumor to the nude-mouse liver and regional lymph nodes, and (*iv*) distant metastases of the human pancreatic tumor to the nude-mouse adrenal gland, diaphragm, and mediastinal lymph nodes. In a series of five patient cases, a 100% take rate has been demonstrated, and of 17 mice transplanted, 15 supported tumor growth. Immunohistochemical analysis of the antigenic phenotype of the transplanted human pancreatic tumors showed a similar pattern of expression of two different human tumor-associated antigens, such as tumor-associated glycoprotein 72 and carcinoembryonic antigen in the transplanted tumors when compared with the original surgical biopsy, suggesting similarity between the two. This model should, therefore, prove valuable for treatment evaluation of individual cancer patients, as well as for evaluation of experimental treatment modalities for this disease.**

Cancer of the pancreas is one of the most intractable cancers and is the fourth-leading cause of cancer death in the United States (1–3). At surgery, most patients are found to have unresectable disease with no imminent effective treatment strategies; <2% of patients survive 5 yr (3). Despite the potential value of a relevant model for human pancreatic cancer, no animal model is available, to our knowledge, for the individual pancreatic-cancer patient.

Models based on athymic nude mice have been used for human cancer. However, metastatic rates from subcutaneous or intramuscular xenografts have been low or nonexistent, even from tumors that were highly metastatic in the patient from whom the tissues were derived (4–8).

Recent work from a number of laboratories has indicated that implanting human tumor cells orthotopically in the corresponding organ of nude mice resulted in much higher metastatic rates. Dissociated human colon cancer cells, when grown in culture and subsequently injected into the cecum of nude mice, produced tumors that eventually metastasized to the liver, showing that orthotopic implantation can enhance the metastatic capability of human tumor cells in nude mice (8–16). Similar results also have been achieved for orthotopic implantation of cell lines of human lung cancer (17), bladder cancer (18, 19), melanoma (20, 21), breast cancer (22–25), and head and neck cancer (26). Marincola and coworkers (27, 28), Pan and Chu (29), and Vezeridis *et al.* (30) have established orthotopically growing pancreatic tumors in nude mice, but these tumors were derived from cell lines.

Our approach is to avoid disruption of tumor integrity and to orthotopically implant histologically intact patient tumor tissue directly after surgery or biopsy. Such a model should better resemble the original properties of the human cancer and could be of great value in developing additional drugs and treatment strategies for cancer. Guided by this overall strategy, we have used nude mice to construct human colon-cancer models that directly use surgical specimens and can exhibit the variety of clinical behaviors seen in human subjects (31). These behaviors include (*i*) local growth, (*ii*) abdominal metastasis, (*iii*) general abdominal carcinomatosis with extensive peritoneal seeding, (*iv*) lymph-node metastasis, (*v*) liver metastasis, and (*vi*) colonic obstruction: a tumor-establishment rate of 13 cases in 20 attempts was found (31). We have constructed a similar set of models for human bladder cancer (32).

We report here the use of the orthotopic-transplant strategy of histologically intact patient specimens to develop a human pancreatic-cancer model with a 100% take rate and subsequent growth and metastatic behavior while retaining human tumor-associated antigens (TAAs), thereby resembling the clinical picture.

MATERIALS AND METHODS

Mice. Four-week-old outbred *nu/nu* mice of both sexes were used for tumor implantation. All animals were maintained in a sterile environment; cages, bedding, food, and water were all autoclaved. All animals were maintained on daily 12-hr light/12-hr dark cycle. Bethaprim pediatric suspension (containing sulfamethoxazole and trimethoprim) was added to the drinking water. Four- to-6-week-old outbred *nu/nu* mice of both sexes were used for the orthotopic-transplantation experiments.

Pancreatic-Cancer Specimens. Each pancreatic-cancer surgical specimen was cut into pieces of ≈1-mm^3 size. For each transplantation tumor, pieces were sampled from different regions of the specimen equally to take into account zonal heterogeneity in the tumor (31, 32). All cases analyzed in this report were adenocarcinomas.

Surgical Microprocedures. Nude mice were anesthetized with isoflurane (Forane) inhalation. A left lateral abdominal incision was made, the peritoneum was opened, and the part of the pancreas near the portal area of the spleen was well

The publication costs of this article were defrayed in part by page charge payment. This article must therefore be hereby marked "*advertisement*" in accordance with 18 U.S.C. §1734 solely to indicate this fact.

Abbreviations: CEA, carcinoembryonic antigen; mAb, monoclonal antibody; TAA, tumor-associated antigen; TAG-72, tumor-associated glycoprotein 72.

exposed. The pieces of 1-mm^3 tumor tissue were transplanted on the pancreas with 8-0 surgical sutures. The peritoneum and the skin were then closed in one layer with 7-0 surgical suture (31).

Monoclonal Antibodies (mAbs). The generation, characterization, and purification of murine mAbs CC49 and COL-1 to the human TAA tumor-associated glycoprotein 72 (TAG-72) and carcinoembryonic antigen (CEA), respectively, have been well described (33, 34). The murine IgG1, MOPC-21 (Litton Bionetics), was used as a negative control.

The detailed method for protein biotinylation has been described (35). Briefly, purified mAbs CC49 and COL-1 were dialyzed vs. 0.1 M sodium bicarbonate, pH 8.5; 150 μg of *N*-hydroxysuccinimidobiotin (bio-NHS, from Sigma), dissolved in dimethyl sulfoxide, was added per mg of protein and incubated at room temperature for 2 hr. The unincorporated bio-NHS was separated from the labeled antibody by gel filtration through Sephadex G-25 (10-ml column), and immunoreactivity of the mAbs was determined by ELISA by using cell extracts with known binding to these mAbs. MOPC-21 was biotinylated by using the same methods.

Immunohistochemical Methods. Expression of two human-TAAs TAG-72 and CEA was studied by using mAbs CC49 and COL-1, respectively. Tissues obtained from the mice and from human surgical biopsy were fixed in formalin and embedded in paraffin. Sections of 5 μm were assayed for TAG-72 and CEA expression by using a modification of described ABC immunohistochemical methods (36). Briefly, tissue sections were deparaffinized in xylene, rehydrated in graded ethanol, and treated for 20 min with 0.3% H_2O_2/methanol to block endogenous peroxidase. The sections were then incubated with 10% normal horse serum for 20 min and then incubated for 1 hr at room temperature with biotin-labeled mAbs CC49 and COL-1, as well as with control biotinylated IgG MOPC-21, at 40 μg/ml. After the phosphate-buffered saline (PBS) rinse, avidin dehydrogenase and biotinylated horseradish peroxidase H complex were added for 30 min at room temperature. The slides were then rinsed in PBS/0.06% diaminobenzidine (Sigma), and 0.01% H_2O_2 was added for 3–5 min to initiate the peroxidase reaction. PBS washes were then followed by counterstaining with hematoxylin (3 min).

RESULTS AND DISCUSSION

Five different cases of human pancreatic cancer were transplanted directly from surgery to the nude-mouse pancreas. Orthotopically growing tumors were established in all cases. Table 1 shows that not only were all cases established orthotopically in the nude mice, but of the total of 17 mice used, tumors were established in 15 mice. In addition, four out of five human cases demonstrated metastases. Nude-mouse models were constructed for pancreatic cancer that included (*i*) local growth, (*ii*) regional invasion of the stomach and duodenum, (*iii*) metastasis to regional lymph nodes, and (*iv*) distant metastasis to the liver, diaphragm, adrenal glands, mediastinal lymph nodes, and mesenteric lymph nodes.

Table 1. Human pancreatic cancer growing and metastasizing in nude mice after orthotopic transplantation of intact tissue

Case	Tumor growth	Local invasion	Metastasis	
			Lymph node*	Organ†
1957	+	+	+	+
2008	+	+	+	+
2020	+	+	+	+
2060	+	+	+	+
2090	+	+	−	−

*Lymph-node metastases include mediastinal lymph node, mesenteric lymph node, iliac lymph node, and inguinal lymph node metastasis.

†Organ metastases include liver, diaphragm, adrenal gland, stomach and duodenum, and abdominal-wall metastases.

In the clinical situation, the sites most frequently involved with pancreatic tumors include regional lymph nodes, liver, lung, peritoneum, duodenum, adrenal gland, stomach, gallbladder, spleen, kidney, intestine, and mediastinal lymph nodes (3). Of these 12 sites, our relatively small sample of cases in nude mice involved 8 of these sites, resembling the clinical picture of pancreatic-cancer spread in the nude mice after orthotopic transplantation of intact tissue.

Local Growth. Extensive local growth was seen in all five cases transplanted. The range in local tumor size was large, even for a given case. For example, in tumor 1957, tumor size ranged from 2 × 2 to 20 × 30 mm >200 days after transplantation (Fig. 1*A*). For case 2008, local growth ranged from 2.5 × 3.9 to 20 × 30 mm >174 days after transplantation.

Regional Invasion. In case 2020, where local tumor growth ranged from 6.3 × 5 to 16 × 15 mm, extensive invasion of the stomach and duodenum occurred in one out of three mice. In case 2008, regional invasion of the stomach and duodenum was also observed (Fig. 1*D*).

Distant Metastasis to Liver. Metastases to the liver surface were seen in case 2020 (Fig. 1*B*).

Very Distant Metastases. Case number 2020 involved metastasis to mesenteric lymph nodes, and case number 2008 involved distant metastases to the diaphragm, adrenal glands (Figs. 1 *C*, *F*, and *G*), mesenteric lymph nodes, and mediastinal lymph nodes (Fig. 1*E*), and iliac lymph nodes (Fig. 1*C*). It should be emphasized that metastasis to distant sites such as mediastinal lymph nodes clearly demonstrates that actual metastasis can occur in the model, as opposed to just extension or seeding. The metastatic pattern seen in the model thus resembles, to a much greater degree, the clinical picture than subcutaneous transplant models, in which metastasis rarely occurs.

Maintenance of Expression of TAAs TAG-72 and CEA After Orthotopic Transplantation. Human pancreatic carcinoma cells express a variety of human TAAs including TAG-72, CA 19-9, DU-PAN-2, and CEA (37, 38). Numerous biochemical and immunohistochemical studies on human carcinoma biopsies or surgical samples have characterized the tissue distribution of these antigens and their biochemical characteristics (37, 39, 43). These human TAAs (i.e., CEA) are normally not expressed in rodent tumors (44). However, efforts have been made to transfect human CEA in murine carcinoma (45, 46). The expression of two different TAAs, TAG-72 and CEA, in the human pancreatic-tumor tissue specimens before and after orthotopic transplantation, growth and metastasis is similar, further suggesting a resemblance of clinical behavior of the human pancreatic cancer in the nude-mouse model described here.

Serial sections from formalin-fixed, paraffin-embedded human pancreatic adenocarcinomas either before or after orthotopical transplantation in the mouse model were treated with mAbs CC49 and COL-1 by using the ABC immunoperoxidase method to determine whether the expression of TAG-72 and CEA, respectively, was maintained after orthotopic transplantation of the human pancreatic tumor to the pancreas of the nude mice. Fig. 2 illustrates the immunohistochemical reactivity of mAbs CC49 with tissue sections of two different cases (2008 and 1957). Fig. 2*A* shows the mAb CC49 reactivity with the pretransplantation human post-surgical specimens of case 2008, and Fig. 2 *B* and *C* show the CC49 reactivity with two lymph-node metastases found in the nude mouse itself after orthotopic transplantation. Note the similarity of expression in the patient and in the metastases formed in the mouse after orthotopic transplantation of the specimens.

Fig. 2*D* represents the reactivity of mAb CC49 with the locally growing tumor in the nude mouse of case 1957. Fig.

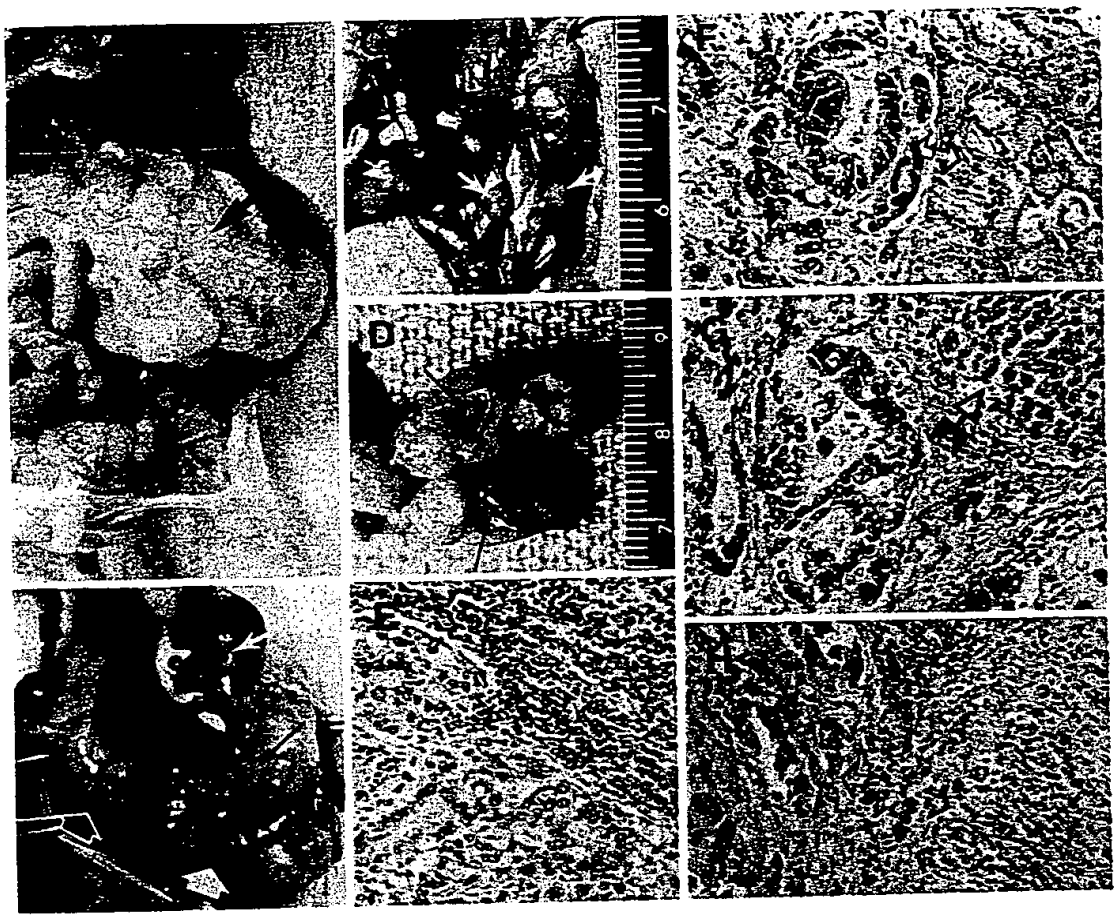

FIG. 1. (*A*) Nude mouse bearing human pancreatic cancer. Arrow indicates extensive tumor growth on nude-mouse pancreas. (*B*) Human pancreatic cancer growing in nude-mouse orthotopically (wide white arrow) and metastasized to the liver (small white arrow). Black arrow indicates that tumor invaded the stomach. White hollow arrow indicates nude-mouse duodenum. (*C*) Human pancreatic cancer metastasis to nude-mouse iliac lymph nodes (white arrows) and to the nude-mouse adrenal gland (blue curved arrow). (*D*) Section of the nude-mouse stomach invaded by human pancreatic cancer grown on nude-mouse pancreas. Arrows indicate the stomach lumen of nude-mouse. Note the stomach wall is thickened as a result of tumor invasion. (*E*) Histopathology of nude-mouse mediastinal lymph-node metastases after orthotopic transplantation of human pancreatic cancer. (×115.) (*F*) Histopathology of human pancreatic-cancer metastasis to the nude-mouse adrenal gland. Arrow pointing left indicates tumor growth. Arrow pointing right indicates nude-mouse renal tubules. (×115.) (*G*) Histopathology of human pancreatic-cancer metastasis to the nude-mouse adrenal gland after orthotopic transplantation of human pancreatic cancer. Arrow indicates nude-mouse adrenal gland. (×115.) (*H*) Histopathology of human pancreatic-cancer invasion of nude-mouse duodenum. Arrow pointing left indicates tumor invasion; arrow pointing right indicates normal mucosa. (×115.)

2 *E* and *F* represent reactivity of CC49 with lymph-node metastases in the nude mouse.

As can be seen from these figures, the expression of human TAA TAG-72 is well maintained in the locally growing transplanted tumor and in the metastatic lymph nodes, further suggesting that the human pancreatic carcinomas growing and metastasizing in the nude mice resemble the original tumors removed from the patient. Similar results were seen for the human-TAA CEA (data not shown). Our findings indicate that this mouse model maintains the native structure of the human tumor and its original antigenic phenotype, further suggesting that this model is, indeed, resembling the natural biological behavior of the human tumor.

Significance of the Findings. In this report we demonstrate an animal model for the pancreatic-cancer patient, in that histologically intact pancreatic-cancer specimens can be taken directly from surgery and transplanted to the nude-mouse pancreas with resulting primary growth, extension, and metastases. As mentioned above, of the 12 sites most frequently involved with pancreatic-cancer metastases clinically, 8 are represented in our model developed from only five cases. Thus, the models resemble the clinical picture. Because distant sites, such as the nude-mouse mediastinal lymph nodes, can be involved by the human pancreatic tumors, it is strongly indicated that such metastases are specific and not from seeding.

Although Marincola and coworkers (27, 28), Pan and Chu (29), and Vezerides *et al.* (30) have established orthotopically growing pancreatic tumors in the nude-mouse pancreas, they all used human pancreatic-cancer cell lines and not patient specimens. In this study we report the orthotopic transplantation of intact human pancreatic-carcinoma biopsies, which now offers the possibility of evaluating treatment modalities *in vivo*, such as drug responses for individual cancer patients and prediction of their clinical course.

Although the use of nude mice for modeling human pancreatic tumors will differ somewhat from the patient in a number of areas—in particular, the immunological environment—it should be noted that we have successfully applied the orthotopic-transplant method described here to severe-combined immunodeficient (SCID) mice (data not shown), in which others have shown that human T cells and B cells can be engrafted (47). Orthotopically engrafting both the histologically intact tumor and immune elements from the same patient into SCID mice would further imitate the clinical situation.

Significance of the Approach. The key aspects of the models are the orthotopic transplantation of histologically intact

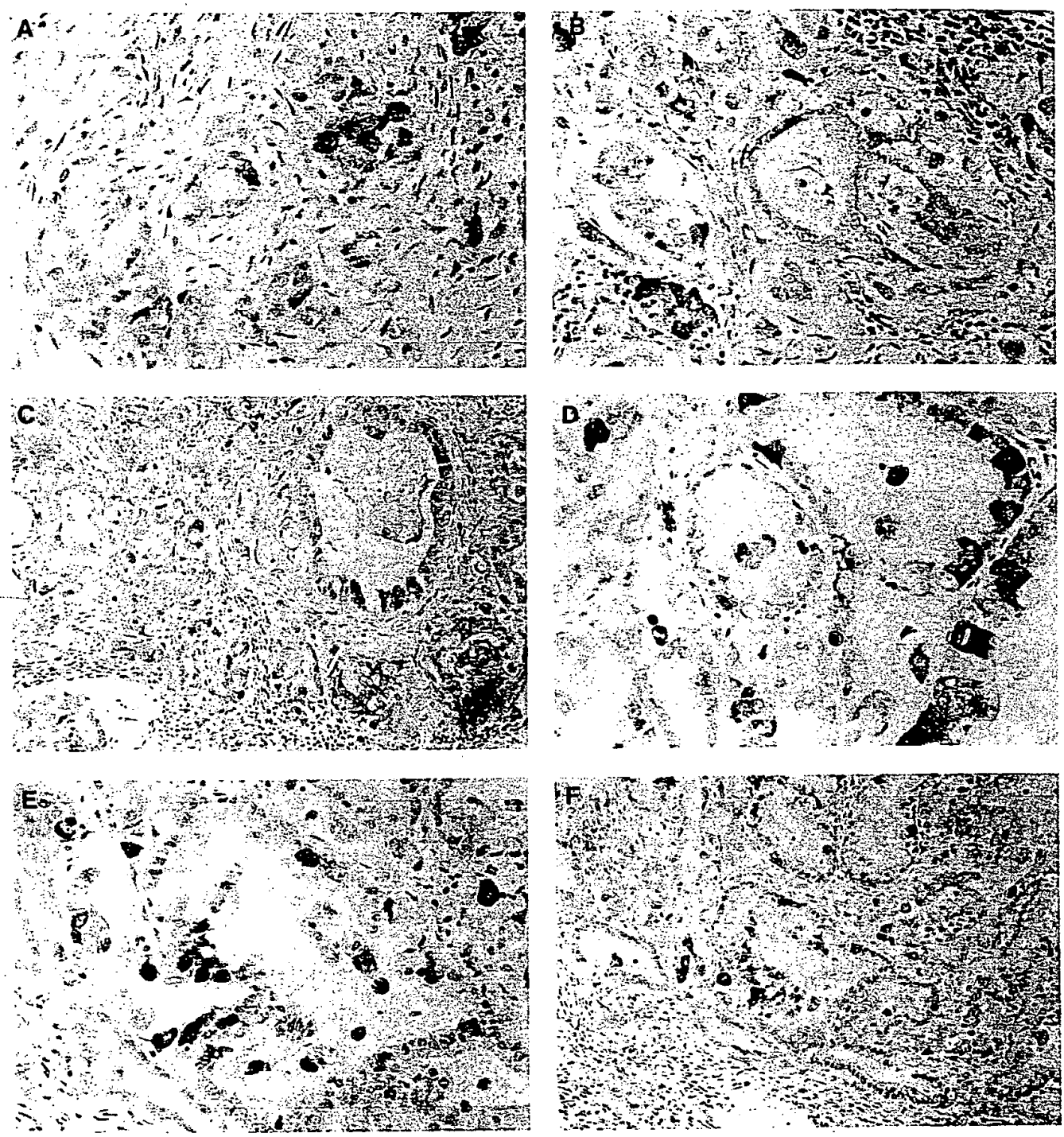

FIG. 2. Immunoperoxidase staining of human pancreatic adenocarcinoma 2008. Pretransplanted tumor (*A*) and mesenteric lymph-node metastases from the nude mouse found after orthotopic transplantation of the human pancreatic tumor (*B* and *C*), stained with mAb CC49. Immunoperoxidase staining of human pancreatic adenocarcinoma 1957, locally growing in nude mouse after orthotopic transplantation (*D*) and lymph-node metastases in the mouse found after orthotopic transplantation of the human pancreatic tumor (*E* and *F*), stained with mAb CC49.

patient tissue to the nude mice, as opposed to the use of tumor cell lines, which may greatly deviate from the original tumor. In our previous study of bladder tumors, orthotopic transplantation of intact tissue to nude mice (32) led to much more extensive metastasis than orthotopic injection of disaggregated cells (48). We also noted that the orthotopically growing and metastasizing human tumors in the nude mice can be passaged to other nude mice and maintain their characteristics (data not shown). This procedure, thus, suggests the creation of a library of specific types and subtypes, according to stage, grade, and drug-response spectrum, of patient tumors that can be indefinitely propagated and cataloged for use in research and treatment of human cancer. Such models should significantly enhance our understanding of human cancer and its treatment because the transplantation of a patient's intact tissue orthotopically potentially allows almost every patient to have his or her own tumor modeled in a system similar to that described here.

This paper is dedicated to Professor Konrad Bloch on his 80th birthday. We are grateful to Polly Jayne Pomeroy for word processing. This work was supported by National Cancer Institute Small

Business Innovation Research Grant 43 CA53963 and partially supported by the Consiglio Nazionale delle Ricerce (Italy).

1. Malagelada, J.-R. (1979) *Mayo Clin. Proc.* **54**, 459–467.
2. Livstone, E. M. & Spiro, H. M. (1984) *World J. Surg.* **8**, 803–807.
3. DeVita, V., Hellman, S. & Rosenberg, S. (1982) *Cancer, Principles and Practice of Oncology* (Lippincott, Philadelphia).
4. Sordat, B., Fritsche, R., Mach, J. P., Carrel, S., Ozzello, L. & Cerotini, J. C. (1973) in *Proceedings of the First International Workshop on Nude Mice*, eds. Rygaard, J. & Povlsen, C. O. (Fischer, Stuttgart, F.R.G.), pp. 269–277.
5. Povlsen, C. O. & Rygaard, J. (1976) in *In Vitro Methods of Cell Mediated in Tumor Immunity*, eds. Bloom, B. B. & David, J. R. (Academic, New York), pp. 701–711.
6. Kyriazis, A. P., Dipersio, L., Michael, G. J., Pesce, A. J. & Stinnett, J. D. (1978) *Cancer Res.* **38**, 3186–3190.
7. Fidler, I. J. (1986) *Cancer Metastasis Rev.* **5**, 29–49.
8. Fidler, I. J. (1990) *Cancer Res.* **50**, 6130–6138.
9. Naito, S., Giavazzi, R., Walker, S. M., Itoh, K., Mayo, J. & Fidler, I. J. (1987) *Clin. Exp. Metastasis* **5**, 135–146.
10. Naito, S., von Eschenback, A. C. & Fidler, I. J. (1987) *J. Natl. Cancer Inst.* **78**, 377–385.
11. Naito, S., von Eschenback, A. C., Giavazzi, R. & Fidler, I. J. (1986) *Cancer Res.* **46**, 4109–4115.
12. Bodgen, A. E. & Von Hoff, D. D. (1984) *Cancer Res.* **44**, 1087–1090.
13. Giavazzi, R., Jessup, J. M., Campbell, D. E., Walker, S. M. & Fidler, I. J. (1986) *J. Natl. Cancer Inst.* **77**, 1303–1308.
14. Bresalier, S., Raper, S. E., Hujanen, E. S. & Kim, Y. S. (1987) *Int. J. Cancer* **39**, 625–630.
15. Morikawa, K., Walker, S. M., Jessup, J. M. & Fidler, I. J. (1988) *Cancer Res.* **48**, 1943–1948.
16. Morikawa, K., Walker, S., Nakajima, M., Pathak, S., Jessup, J. M. & Fidler, I. J. (1988) *Cancer Res.* **48**, 6863–6871.
17. McLemore, T. L., Liu, M. C., Blacker, P. C., Gregg, M., Alley, M. C., Abbott, B. J., Shoemaker, R. H., Bohlman, M. E., Litterst, C. C., Hubbard, W. C., Brennan, R. H., McMahon, J. B., Fine, D. L., Eggleston, J. C., Mayo, J. G. & Boyd, M. R. (1987) *Cancer Res.* **47**, 5132–5140.
18. Ahlering, T. E., Dubeau, L. & Jones, P. A. (1987) *Cancer Res.* **47**, 6660–6665.
19. Soloway, M. S., Nissenkorn, I. & McCallum, L. (1983) *Urology* **21**, 159–161.
20. Kozlowski, J., Fidler, I. J., Campbell, D., Xu, Z., Kaighn, M. E. & Hart, I. R. (1984) *Cancer Res.* **44**, 3522–3529.
21. Kozlowski, J., Hart, I., Fidler, I. J. & Hanna, N. (1984) *J. Natl. Cancer Res.* **72**, 913–917.
22. Miller, F. & McInerney, D. (1988) *Cancer Res.* **48**, 3698–3701.
23. Basolo, F., Fontanini, G. & Squartini, F. (1988) *Cancer Res.* **48**, 3197–3202.
24. White, A. C., Levy, J. A. & McGrath, C. M. (1982) *Cancer Res.* **42**, 906–912.
25. Price, J. E., Polyzos, A., Zhang, R. D. & Daniels, L. M. (1990) *Cancer Res.* **50**, 717–721.
26. Dinesman, A., Haughey, B., Gates, G. A., Aufdemorte, T. & Von Hoff, D. D. (1990) *Otolaryngol. Head Neck Surg.* **103**, 766–774.
27. Marincola, F., Taylor-Edwards, C., Drucker, B. & Holder, W. (1987) *Curr. Surg.* **44**, 294–297.
28. Marincola, F., Drucker, B. J., Siao, B., Hough, K. & Holder, W. D. (1989) *J. Surg. Res.* **47**, 520–529.
29. Pan, M. & Chu, T. (1985) *Tumour Biol.* **6**, 89–98.
30. Vezeridis, M., Doremus, C., Tibbetts, L., Tzanakakis, G. & Jackson, B. (1989) *J. Surg. Oncol.* **40**, 261–265.
31. Fu, X., Besterman, J. M., Monosov, A. & Hoffman, R. M. (1991) *Proc. Natl. Acad. Sci. USA* **88**, 9345–9349.
32. Fu, X., Theodorescu, D., Kerbel, R. S., Monosov, A. & Hoffman, R. M. (1991) *Int. J. Cancer* **49**, 938–939.
33. Muraro, R., Kuroki, M., Wunderlich, D., Poole, D. J., Colcher, D., Thor, A., Greiner, J. W., Simpson, J. F., Molinolo, A., Noguchi, P. & Schlom, J. (1988) *Cancer Res.* **48**, 4588–4596.
34. Muraro, R., Wunderlich, D., Thor, A., Lundy, J., Noguchi, P., Cunningham, R. & Schlom, J. (1985) *Cancer Res.* **45**, 5769–5780.
35. Segal, D. M., Titus, J. A. & Stephany, A. D. (1987) *Methods Enzymol.* **150**, 478–492.
36. Hsu, S. M., Raine, L. & Fanger, H. (1981) *J. Histochem. Cytochem.* **29**, 577–580.
37. Takasaki, H., Tempero, M. A., Uchida, E., Büchler, M., Ness, M. J., Burnett, D. A., Metzgar, R. S., Colcher, D., Schlom, J. & Pour, P. M. (1988) *Int. J. Cancer* **42**, 681–686.
38. Guadagni, F., Schlom, J., Johnston, W. W., Szpak, C. A., Goldstein, D., Smalley, R., Simpson, J. F., Borden, E. C., Pestka, S. & Greiner, J. W. (1989) *J. Natl. Cancer Inst.* **81**, 502–512.
39. Thor, A., Ohuchi, N., Spzak, C. A., Johnston, W. W. & Schlom, J. (1986) *Cancer Res.* **46**, 3118–3122.
40. Thor, A., Gorstein, F., Ohuchi, N., Szpak, C. A., Johnston, W. W. & Schlom, J. (1986) *J. Natl. Cancer Inst.* **76**, 995–1006.
41. Johnson, V. G., Schlom, J., Paterson, A. J., Bennett, J., Magnani, J. L. & Colcher, D. (1986) *Cancer Res.* **46**, 850–857.
42. Sheer, D. G., Schlom, J. & Cooper, H. (1988) *Cancer Res.* **48**, 6811–6818.
43. Kuroki, M., Greiner, J. W., Simpson, J. F., Primus, J., Guadagni, F. & Schlom, J. (1989) *Int. J. Cancer* **44**, 208–218.
44. Beachemin, N., Turbide, C., Afar, D., Bell, J., Raymond, M., Stanners, C. & Fuks, A. (1989) *Cancer Res.* **49**, 2017–2021.
45. Eglitis, M. A., Kanjoff, P., Gilboa, E. & Anderson, W. F. (1985) *Science* **230**, 1395–1398.
46. Robbins, P. F., Kantor, J., Salgaller, M., Hand, P. H., Fernsten, P. D. & Schlom, J. (1991) *Cancer Res.* **51**, 3657–3662.
47. McCune, J. M., Namikawa, R., Kaneshima, H., Shults, L. D., Lieberman, M. & Weissman, I. L. (1988) *Science* **241**, 1632–1639.
48. Theodorescu, D., Cornil, I., Fernandez, B. & Kerbel, R. (1990) *Proc. Natl. Acad. Sci. USA* **87**, 9047–9051.

THIS PAGE BLANK (US

ANTICANCER RESEARCH *13*: 287-292 (1993)

15

Immunochemotherapy Prevents Human Colon Cancer Metastasis after Orthotopic Onplantation of Histologically-intact Tumor Tissue in Nude Mice

TOSHIHARU FURUKAWA[1], TETSURO KUBOTA[1], MASAHIKO WATANABE[1], TSONG-HONG KUO[1], SUGURU KASE[1], YOSHIRO SAIKAWA[1], HIROKAZU TANINO[1], TATSUO TERAMOTO[1], KYUYA ISHIBIKI[1], MASAKI KITAJIMA[1] and ROBERT M. HOFFMAN[2,3]

[1]*The Department of Surgery, School of Medicine, Keio University, 35 Shinanomachi, Shinjuku-ku, Tokyo 160, Japan;* [2]*Laboratory of Cancer Biology, Department of Pediatrics, 0609F, University of California, San Diego, School of Medicine, La Jolla, California 92110,* [3]*AntiCancer Inc., 5325 Metro Street, San Diego, California 92110, U.S.A.*

Abstract. *A metastatic model of human colon cancer has been previously established using orthotopic onplantation of histologically intact in tissue nude mice. In this study, effects of immunochemotherapy using OK-432, 5-fluorouracil (5-FU) and mitomycin C (MMC) on Col-2-JCK, a human colon cancer xenograft, were evaluated using this model. When 5-FU and MMC were administered without OK-432, liver metastases were not reduced even at maximum tolerated doses of both drugs, although cecal tumor growh was significantly reduced. On the other hand, when combined with OK-432, both 5-FU and MMC reduced liver metastases with synergistic reduction of cecal tumor growth, demonstrating the potential of combining immunotherapy with chemotherapy against metastases.*

Although a number of chemotherapeutic regimens have been studied against liver metastases of colon cancers, most of them have demonstrated limited efficacy (1, 2). Moreover, even in the chemoresponsive cases, such effects are mostly partial and temporary, failing to improve patients prognosis (1-3). Therefore, it is critical to develop new therapeutics against liver metastases of colon cancer. However, the lack of relevant animal models has impeded us in the development of such effective strategies for the prevention or treatment of liver metastases of human colon cancer.

Various types of human cancers have been grown in nude mice subcutaneously where they resemble the original tumors morphologically and biochemically. However, metastasis rarely occurred from subcutaneously-growing tumors in nude mice even if the xenografted tumors were derived from patients with extensice metastasis (4). Recently, we have established a metastatic model of human colon cancer (5-7), bladder cancer (8. 9), pancreatic cancer (10), stomach cancer (11) and lung cancer (12) using orthotopic onplantation of histologically-intact cancer-tissue in nude mice. The tumors in these models grow locally, extend, and metastasize in patterns closely resembling the clinical situation. In this study, we utilized this model to study the efficacy of experimental immunochemotherapy against metastatic human colon cancer.

Correspondence to: Tetsuro Kubota, M.D. Department of Surgery, School of Medicine, Keio University, 35 Shinanomachi, Shinjuku-Ku, Tokyo 160, Japan. FAX: 81-33-355-4704.

Key Words: Colon cancer, metastasis, immunotherapy, orthotopic onplantation, nude mice.

Materials and Methods

Mice. Male Balb/c nu/nu mice, which originated from the Central Institute for Experimental Animals, Kawasaki, Japan, were obtained from CLEA Japan Inc., Tokyo, Japan. Animals which were 6 weeks old and weighed 20-22 g were used.

Drugs. Five-fluorouracil (5-FU) and mitomycin C (MMC) were purchased from Kyowa Hakko Kogyo, Co. Ltd., Tokyo. OK-432, a Streptococcus preparation was purchased from Chugai Seiyaku, Co. Ltd., Tokyo.

Human colon cancer xenograft. Col-2-JCK, a poorly differentiated human colon adenocarcinoma xenograft established in Tokai University, Atsugi, Japan, was provided from the Central Institute for Experimental Animals and maintained by serial transplantation into nude mice at the Keio University School of Medicine.

Orthotopic onplantation of hitologically-intact tissue. Tumor tissues were onplanted on the cecal wall of nude mice as reported previously (5-7). Tumors growing subcutaneously in the exponential growth phase in nude mice were resected aseptically, necrotic tissues were cut away and the remaining healthy tumor tissues were scissor-minced into pieces about 3 mm in diameter in Hank's balanced salt solution. Each piece of tumor was weighed on a Mettler AM 100 balance (Mettler Toledo Ag, Switzerland), and adjusted to be 50 mg with scissors. Mice were anesthetized with a 2.5% solution of a mixture of 2,2,2-tribromoethanol and tertamylalcohol (1: 1), and an incision was made through the left lower abdominal pararectal line and peritoneum. The cecal wall was carefully exposed and a part of the serosal membrane, about 2 mm in diameter, was mechanically injured using a scissors. One of the tumor pieces of 50 mg was then fixed on each injured site of the serosal surface with a 6-0 Dexon (Davis-Geck Inc., Manati, PR) transmural suture. The cecum was then returned into the peritoneal cavity, and the abdominal wall and the skin were closed with 6-0 Dexon sutures. Animals were kept in a sterile environment.

Experimental immunochemotherapy. Seven days after onplantation (day

0250-7005/93 $2.00+.40

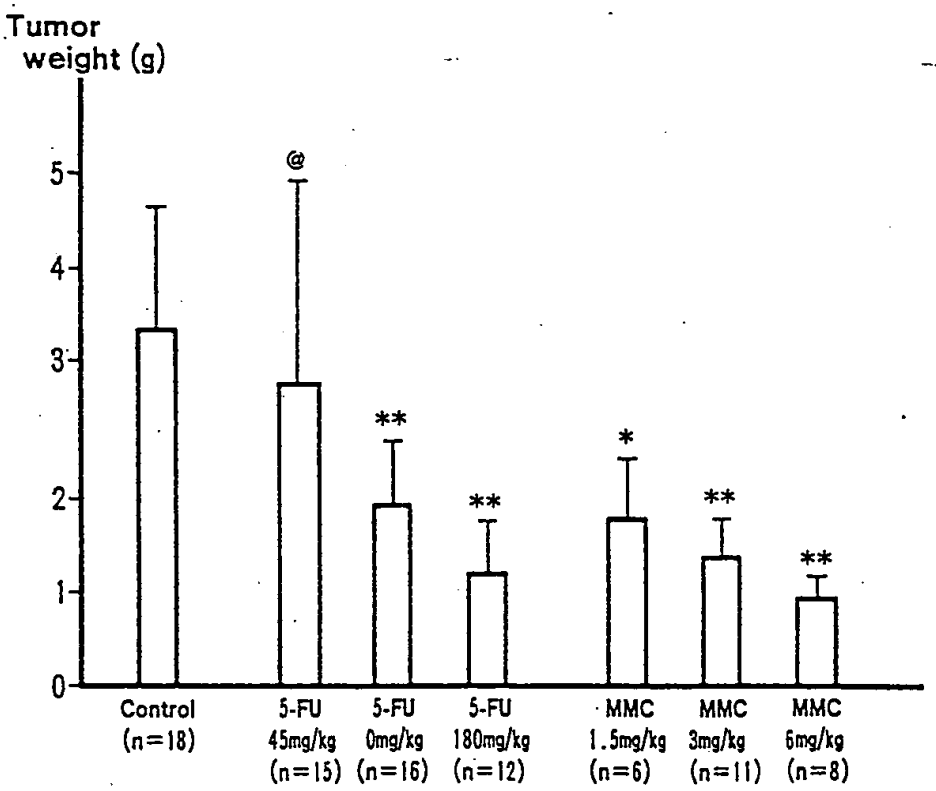

Figure 1. *Cecal tumor weight of the control and the treated mice with each dose of 5-FU or MMC. Mice were implanted with 50 mg of the Col-2-JCK tumor on day 0, treated with each dose of 5-FU or MMC indicated on day 7 and sacrificed on day 28. Cecal tumors were removed and weighed. n, number of mice evaluable, superscript not significant, * $p<0.05$, ** $p<0.0001$ between control by Student's t-test.*

7), mice were randomized into control and treated groups, and 5-FU and MMC were administered. Drugs were dissolved in 0.2 ml of physiological saline solution and administered intraperitoneally (ip) as boluses. The doses of the drugs used were 180, 90 and 45 mg/kg for 5-FU and 6, 3 and 1.5 mg/kg for MMC, which were equivalent to maximum tolerated doses (MTDs), half MTDs and quarter MTDs, respectively, as determined in our previous studies (14). OK-432 was also dissolved in 0.2 ml of physiological saline solution and was given subcutaneously (sc) as 3 injections with a one day interval on days 5, 7 and 9 at 0.5 KE per mouse. Mice were observed every day and sacrificed on day 28. The tumor on the cecal wall and the liver were removed from each mouse, weighed and processed for routine histological examination after careful macroscopic examination.

Results

Figure 1 and Table I show anticancer effects of 5-FU and MMC on cecal tumor growth and liver metastases of Col-2-JCK. As shown in Figure 1, cecal tumor growth was inhibited in a dose-dependent manner by both drugs, with a statistically significant difference at half and full MTDs. However, as shown in Table I, the frequency of mice with liver metastases was not significantly reduced even in the mice given MTDs. Only the number of metastatic nodules in the liver was reduced in the mice treated at MTDs (Table I). Although viable cancer cells were rare in histological preparations of the cecal tumors of the mice treated with MTDs of 5-FU, liver metastases in those mice maintained intact cancerous structures as observed histologically (Figure 2). Similar effects were seen with MMC (data not shown). On the other hand, OK-432 alone and particularly in combination with half MTDs of 5-FU or MMC was effective in preventing formation of liver metastases of Col-2-JCK. As shown in Figure 3, OK-432 alone did not reduce cecal tumor growth to any significant degree, while a highly significant reduction was observed when it was combined with half MTDs of 5-FU or MMC. Furthermore, as shown in Table II, OK-432 alone reduced only the number of metastatic nodules in the liver, with a limited reduction in the frequency of mice having liver metastases, which were, however, significantly reduced when OK-432 was combined with half MTDs of either 5-FU or MMC (Table II).

Discussion

The lack of relevant animal models to study the metastatic behavior of human colon cancer has impeded us in the development of effective treatment of this cancer. Recently, we have developed a new metastatic model of human colon cancer using orthotopic onplantation of histologically-intact cancer-tissue in nude mice (5-7) which allowed a significantly higher growth rate of local tumors and frequency of subse-

Table I. *Anticancer effects of 5-FU and MMC against Col-2-JCK.*

Treatment		T/C value of cecal tumor (%)	Liver metastases	
			Mice with metastases	Number of nodules
	Control		12/18[b]	6.72 (7.59)[c]
5-FU	45 mg/kg	76.3[a]	8/15@	4.07 (4.63) $
	90 mg/kg	54.0	10/16@	4.25 (4.25) $
	180 mg/kg	33.1	6/12@	1.08 (1.80) *
MMC	1.5 mg/kg	49.9	3/6 @	3.83 (4.22) $
	3 mg/kg	38.2	5/11@	2.82 (3.21) $
	6 mg/kg	26.0	3/8 @	1.38 (1.89) *

Each dose of 5-FU or MMC was administered as ip bolus on day 7 after cecal implantation.
a. Data are calculated from the data shown in Figure 1 as follows: (mean actual cecal tumor weight in the treated mice/mean actual cecal tumor weight in the control mice) × 100.
b. Data are shown as number of mice in which liver metastases were observed/number of mice evaluable.
c. Data are shown as mean (standard deviation) of number of liver metastatic nodules observed in the evaluable mice.
@ not significant between control by chi-squared test. $ not significant. * $p<0.01$ between control by Student's *t*-test.

Table II. *Anticancer effects of OK-432 alone and in combination with 5-FU or MMC against Col-2-JCK.*

Treatment	T/C value of cecal tumor (%)	Liver metastases	
		Mice with metastases	Number of nodules
Control		12/18[b]	6.72 (7.59)[c]
OK-432 alone	74.9[a]	3/8@	1.25 (1.64)*
OK-432 +5-FU 90 mg/kg	22.0	1/8 +	0.25 (0.66)*
OK-432 + MMC 3 mg/kg	10.9	0/8**	0 (ND)

OK-432 was administered sc on days 5, 7 and 9 at a dose of 0.5 KE/mouse after the cecal implantation. 5-FU or MMC was administered as ip bolus on day 7.
a. Data are calculated from the data shown in Figure 3 as follows: (mean actual cecal tumor weight in the treated mice/mean actual cecal tumor weight in the control mice) × 100.
b. Data are shown as number of mice in which liver metastases were observed/number of mice evaluable.
c. Data are shown as mean (standard deviation) of number of liver metastatic nodules in the evaluable mice.
@ not significant. + $p<0.05$, * * $p<0.01$ between control by chi-squared test. * $p<0.05$ between control by Student's *t*-test.

quent metastases in comparison with cecal implantation of cell suspensions (5). In this study, we utilized this model to evaluate the effects of immunochemotherapy using OK-432, 5-FU and MMC against liver metastases of human colon cancer.

Although 5-FU and MMC have been the most frequently used drugs in the treatment of colon cancer, clinical response rates of both drugs have been limited with a range of 10-25% (13). On the other hand, in the experimental chemotherapy of subcutaneously growing human colon cancer xenografts in nude mice, the efficacy rates of both drugs have been overestimated (14, 15, 16). In this study, the antitumor effects of both drugs were significant on cecal tumor growth, but not on the formation of liver metastases even at MTDs. Therefore, the results observed in experimental chemotherapy using the metastatic model described in this report seemed to reflect clinical chemotherapeutic efficacy more closely than the results observed using subcutaneous implantation. Since nude mice lack functional T-lymphocytes, the main immune defense against human cancer xenografts is thought to be natural killer (NK) cell activity which may be above normal in nude mice (17). The treatment failure against liver metastases observed in this study possibly resulted in part from the reduced NK cell activity observed due to 5-FU and MMC chemotherapy (Furukawa T, unpublished observations), as well as due to the intrinsic resistance of the

Figure 2

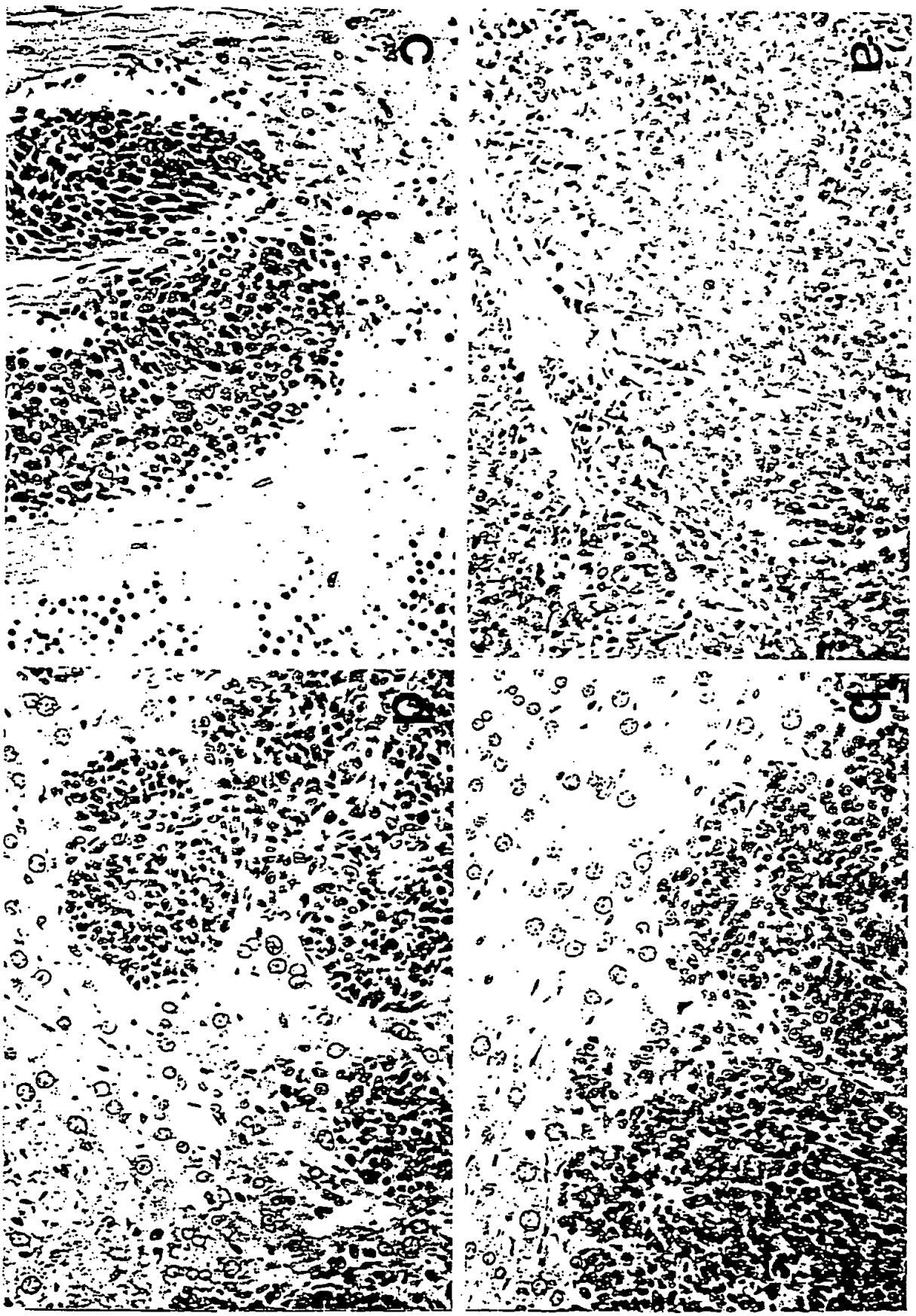

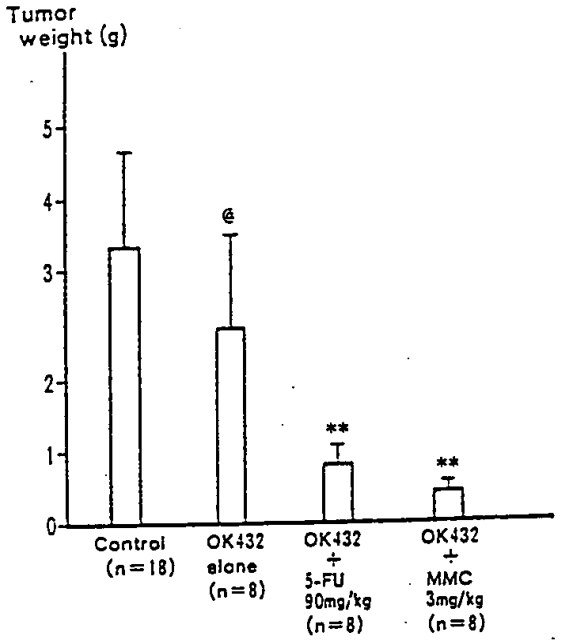

Figure 3. *Cecal tumor weight of the control and the treated mice with OK-432 alone and in combination with half MTD of 5-FU or MMC. Mice were implanted with 50 mg of the Col-2-JCK tumor on day 0, treated with 0.5 KEImouse of K-432 on days 5, 7 and 9 and 90 mg/kg of 5-FU or 3 mg/kg of MMC on day 7, and sacrificed on day 28. Cecal tumors were removed and weighed n, number of mice evaluable. @ not significant, ** $p<0.0001$ between control by Student's t-test.*

metastases themselves. As shown in Figure 2, liver metastases were resistant to chemotherapy even if the cecal tumor was considerably more sensitive. On the other hand, when combined with OK-432, both 5-FU and MMC at half MTDs reduced liver metastases as well as cecal tumor growth.

Since the antitumor effects of OK-432 in nude mice might be mainly mediated by activation of NK cells, the results in this study seemed to suggest the importance of the host immune mechanism in the treatment of human colon cancer with chemotherapeutic drugs, in particular, against liver metastaces. It should be noted, however, that the human immune system is very different than that of the nude mouse and that other immunopotentiators may be more effective in humans. Interleukin-2 stimulation of human T-killer cells has shown some efficacy in patients (18), for example. The ability to construct orthotopic-onplant metastatic models of human colon cancer has been extended to severe combined immunodeficient mice (7), where it is also possible to engraft actual human T-and B-immune elements (19) which should enable even more clinically-relevant immunochemotherapeutic experiments to be carried out.

Figure 2. *Histological view of the COL-2-JCK tumor in a control mouse and a mouse treated with 5-FU at 180 mg/kg. Cecal tumors and liver metastases were processed for routine histological examination and stained using hematoxylin and eosin (x200). Cecal tumor (A) and liver metastases (B) in a control mouse; cecal tumor (C) and liver metastases (D) in a treated mouse. The number of viable cancer cells is greatly reduced in the cecal tumor of the treated mouse, demonstrating a significant effect of the chemotherapy (compare A and C). Cancer cells are viable in both of the liver metastases, demonstrating ineffectiveness of the chemotherapy (compare B and D).*

References

1 Cohen AM, Schaeffer N and Higgins J: Treatment of metastatic colorectal cancer with hepatic artery combination chemotherapy. Cancer *57*: 1115-1117, 1986.

2 Ekberg H, Tranberg KG, Lundstedt C *et al*: determinants of survival after intraarterial infusion of 5-fluorouracil for liver metastases from colorectal cancer: a multivariate analysis. J Surg Oncol *31*: 246-254, 1986.

3 Welch JP and Donaldson GA: Detection and treatment of recurrent cancer of the colon and rectum. Am J Surg *135*: 505-511, 1978.

4 Fidler IJ: Critical factors in the biology of human cancer metastasis: twenty-eighth G. H. A. Clowes memorial award lecture. Cancer Res *50*: 6130-6138, 1990.

5 Furukawa T, Kubota T, Watanabe M *et al*: A metastatic model of human colon cancer constructed using cecal implantation of cancer-tissue in nude mice. Surg Today, in Press.

6 Fu X, Besterman JM, Monosov A *et al*: Models of human metastatic colon cancer in nude mice orthotopically constructed by using hitologically intact patient specimens. Proc Natl Acad Sci USA *88*: 9345-9349, 1991.

7 Fu X, Herrera H, Kubota T *et al*: Extensive liver metastases from human colon cancer in nude and scid mice after orthotopic onplantation of histologically-intact human colon carcinoma tissue. Anticancer Res. 12: 1395-1398, 1992.

8 Fu X, Theodorescu D, Kerbel RS *et al*: Extensive multiorgan metastasis following orthotopic onplantation of histologically-intact human bladder carcinoma tissue in nude mice. Int J Cancer *49*: 938-939, 1991.

9 Fu X and Hoffman RM: Human RT-4 bladder carcinoma is highly metastatic in nude mice and comparable to *ras* H transformed RT-4 when orthotopically onplanted as histologically intact tissue. Int J Cancer. 51: 989-991, 1992.

10 Fu X, Guadagni F and Hoffman RM: A metastatic nude-mouse model of human pancreatic cancer constructed orthotopically from histologically-intact patient specimen. Proc Natl Acad Sci USA 89: 5645-5649, 1992.

11 Furukawa T, Fu X, Kubota etal: Nude mouse metastatic models of human stomach cancers constructed using orthotopic implantation of histologically-intact tissue. Cancer Research, in Press.

12 Wang X, Fu X, and Hoffman RM: A new patient-like metastatic model of human lung cancer constructed orthotopically with intact tissue via thoracotomy in immunodeficient mice. Int J Cancer 51:992-995, 1992.

13 Carter SK and Friedman M: Integration of chemotherapy into combined modality treatment of solid tumors. II. Large bowel carcinoma. Cancer Treat Rev *1*: 111-120, 1974.

14 Kubota T, Ishibiki K and Abe O: The clinical usefulness of human xenografts in nude mice. *In*: Hall TC (ed), Prediction of Response to Cancer Therapy. New York, NY, Alan R Liss, 1988, pp 213-225.

15 Inaba M, Kobayashi T, Tashiro T and Sakurai Y: Pharmacokinetic approach to rational therapeutic doeses for human tumor-bearing nude mice. Jpn J Cancer Res (Gann) *79*: 509-516 1988.

16 Kase S, Kubota T, Furukawa T *et al*: Establishment of transplantable human colon cancer cell lines, chemosensitivity of colon carcinomas and the serially transplantable strains with MTT assay. Jpn J Cancer Chemother *18*: 2247-2253, 1991. (In Japanese with English abstact).

17 Kindred B: Nude mice in immunology. Prog. Allergy *26*: 137-238, 1979.

18 Elias EG: Is there an established role for immunotherapy for any of our surgical cancers? J Surg Oncol *48*: 149-152, 1991.

19 Simpson E, Farrant J, Chandler P: Phenotypic and functional studies of human peripheral blood lymphocytes engrafted in scid mice. Immunol Rev *124*: 97-111, 1991.

Received October 27, 1992
Accepted January 15, 1993

Clinical & Experimental Metastasis 18: 379–384, 2001.

Antimetastatic efficacy of adjuvant gemcitabine in a pancreatic cancer orthotopic model

Natalie C. Lee[1,3], Michael Bouvet[2], Stephanie Nardin[2], Ping Jiang[1], Eugene Baranov[1], Babak Rashidi[1], Meng Yang[1], Xiaoen Wang[1], A.R. Moossa[2] & Robert M. Hoffman[1,2]

[1]*AntiCancer, Inc., San Diego, California, USA;* [2]*Department of Surgery, University of California San Diego Medical Center, San Diego, California, USA;* [3]*Department of Surgery, University of California San Francisco Medical Center, San Francisco, California, USA*

Received 11 December 2000; accepted in revised form 30 January 2001

Key words: adjuvant therapy, gemcitabine, green fluorescent protein, metastasis, nude mice, pancreatectomy, pancreatic cancer, surgical orthotopic implantation

Abstract

Gemcitabine is a promising new agent that has been recently studied for palliation of advanced (stage IV) unresectable pancreatic cancer. We hypothesized that adjuvant gemcitabine would reduce recurrence and metastases following surgical resection of pancreatic cancer. To test this hypothesis, we evaluated gemcitabine on a green fluorescent protein (GFP) transductant of the human pancreatic cancer cell line BxPC-3 (BxPC-3-GFP) using surgical orthotopic implantation (SOI) in nude mice. GFP enabled high resolution fluorescent visualization of primary and metastatic growth. Five weeks after SOI, the mice were randomized into three groups: Group I received exploratory laparotomy only. Group II underwent surgical resection of the pancreatic tumor without further treatment. Group III underwent tumor resection followed by adjuvant treatment with gemcitabine, 100 mg/kg every three days for a total of four doses, starting two days after resection. The mice were sacrificed at thirteen weeks following implantation and the presence and location of recurrent tumor was recorded. Gemcitabine reduced the recurrence rate to 28.6% compared to 70.6% with resection only ($P = 0.02$) and reduced metastatic events 58% in the adjuvant group compared to resection only. This study, demonstrating that gemcitabine is effective as adjuvant chemotherapy post-pancreatectomy, suggests this new indication of the drug clinically.

Abbreviations: SOI – surgical orthotopic implantation; GFP – green fluorescent protein, 5-FU – 5-fluorouracil

Introduction

Pancreatic cancer is the fourth most common cause of cancer death in the United States, and the second most common cause of death from GI-related neoplasms [1]. The prognosis for this disease has remained dismal, even after curative attempts with surgical resection. Previously, 5-fluorouracil (5-FU) was the most widely used and studied chemotherapeutic agent for pancreatic cancer. Recently, gemcitabine has been shown to be more effective than 5-FU in alleviating disease-related symptoms and increasing survival in patients with advanced (stage IV) unresectable pancreatic cancer [2].

Surgical resection of pancreatic cancer remains the only curative option for this disease, but survival remains poor, even after pancreatectomy [3]. Most patients develop locoregional recurrences as well as hepatic and distant metastases after curative resection. To improve the low rate of cure of pancreatic cancer, several studies have been done on adjuvant and neoadjuvant chemotherapy and radiation. Most studies with adjuvant chemotherapy, however, have been performed using 5-fluorouracil. The Gastrointestinal Tumor Study Group demonstrated that adjuvant chemoradiation using 5-FU conferred a survival advantage (median survival of 20 months) versus 11 months with surgery alone [4]. Another study of adjuvant 5-FU post-pancreaticoduodenectomy showed an increased median survival of 19.5 months with adjuvant 5-FU compared to 13.5 months with no postoperative therapy [5]. However, other studies have shown little to no benefit of adjuvant chemotherapy with 5-FU alone, with a response rate of 10% or less.

Given the results of the recent trials showing enhanced efficacy of gemcitabine over 5-FU for palliative chemotherapy, we studied the use of adjuvant chemotherapy with gemcitabine in the setting of surgically resectable pancreatic cancer.

This study evaluated the efficacy of adjuvant gemcitabine using a clinically relevant mouse model developed from surgical orthotopic implantation (SOI) of human pancreatic adenocarcinoma [6–9]. This study utilized the BxPC-3 pancreatic tumor cell line transduced with green fluorescent

Correspondence to: Robert M. Hoffman, AntiCancer, Inc., San Diego, CA 92111, USA. Tel: +1-858-654-2555; Fax: +1-858-268-4175; E-mail: all@anticancer.com

protein (GFP) [10–17]. GFP expression allows for visualization and imaging of tumor growth and metastasis, an important factor for the understanding and treatment of the metastatic process.

Materials and methods

Pancreatic cancer cells

The BxPC-3 human pancreatic cancer cell line was obtained from the American Type Culture Collection (Rockville, Maryland). The cells were maintained in Dulbecco's Modified Eagle's Medium (DMEM) supplemented with 10% fetal calf serum, 2 mM glutamine, 100 U/ml penicillin, 100 μg/ml of streptomycin, and 0.25 μg/ml of amphotericin B (Gibco-BRL, Life Technologies, Inc., Grand Island, New York). Cells were incubated at 37 °C in a 5% CO_2 incubator.

GFP transduction [18]

The RetroXpress vector pLEIN was purchased from Clontech Laboratories, Inc. (Palo Alto, California). The pLEIN vector expresses enhanced GFP and the neomycin resistance gene on the same bicistronic message, which contains an IRES site. pLEIN was produced in PT67 packaging cells. BxPC-3 cells were transduced with supernatants of the pLEIN-producing PT67 cells. Stable high-expression GFP transductants were selected in neomycin as previously described [18].

Surgical Orthotopic Implantation (SOI) [6–9]

Pancreatic tumors at the exponential growth phase, grown subcutaneously in nude mice, were resected aseptically and cut with scissors and minced into approximately 3 × 3 × 3 mm pieces as previously described [6–9]. Mice were anesthetized by isoflurane inhalation (Fort Dodge Animal Health, Fort Dodge, Iowa). The abdomen was sterilized with alcohol. A subcostal incision was then made through the left upper abdominal pararectal line and peritoneum. The pancreas was carefully exposed and three tumor pieces were transplanted on the middle of the pancreas with an 8-0 silk surgical suture (Ethicon Inc., Somerville, New Jersey). The pancreas was then returned into the peritoneal cavity, and the abdominal wall and the skin were closed with 6-0 silk suture. Animals were kept in a sterile environment. All procedures of the operation described above were performed with a ×7 microscope (Olympus).

At 5 weeks after orthotopic implantation, mice were randomized into 3 different groups of 18 mice each for treatment purposes (Figure 1). Group I underwent exploratory laparotomy only, without resection of the pancreatic tumor. Group II animals underwent resection of the pancreatic tumor via the same subcostal incision used for original implantation. Group III underwent resection as described above and postoperative adjuvant treatment with gemcitabine.

Resection of primary tumor

Tumor was removed by sharp dissection with scissors. Hemostasis was obtained with 8-0 silk sutures. The skin was closed with 6-0 silk sutures.

Fluorescence microscopy and image analysis (18)

A Leica stereo microscope MZ 12 equipped with a mercury bulb as a light source was used for the imaging experiments. Selective excitation of GFP was produced through a D425/60 band-pass filter and a 470 DCXR dichroic mirror. Fluorescence was emitted through a GG475 long-pass filter (Chroma Technology, Brattleboro, Vermont) and collected by a Hamamatsu Color Cooled CCD Video Camera HM C5810. High-resolution images were captured and processed with a Pro-Series Frame-Grabber and acquired by a Pentium-IV PC with Image Pro Plus 3.1 software (Media Cybernetics, Silver Spring, Maryland).

Gemcitabine treatment

Gemcitabine (Eli Lilly, Indianapolis, Indiana) was reconstituted in saline to a concentration of 5.2 mg/ml and administered intraperitoneally at a dose of 100 mg/kg/dose [2]. The first dose was given to Group III animals two days after resection. The dose was repeated every 3 days for a total of 4 doses. There was no apparent toxicity for this dose regimen as evidenced by mouse survival and body weight (data not shown).

Analysis of metastasis

At 13 weeks following SOI, mice were sacrificed and explored. Any recurrent tumor and all major organs were observed directly under fluorescence microscopy with images captured as described above. Weight of recurrent tumor and location of metastases were recorded for each mouse. The average number of metastatic events per mouse was calculated by dividing the total number of metastatic events per group by the number of mice per group.

Histological analysis

Recurrent tumor was removed, weighed, and saved for histologic analysis carried out with standard hematoxylin and eosin (H&E) staining.

Statistical analysis

The chi-squared test was used to measure differences between recurrence rates among the treatment groups (Microsoft Excel, Redmond, Washington). The t-test was used to measure differences in average tumor weight among the various groups (Microsoft Excel, Redmond, Washington). A $P \leq 0.05$ was considered to be statistically significant.

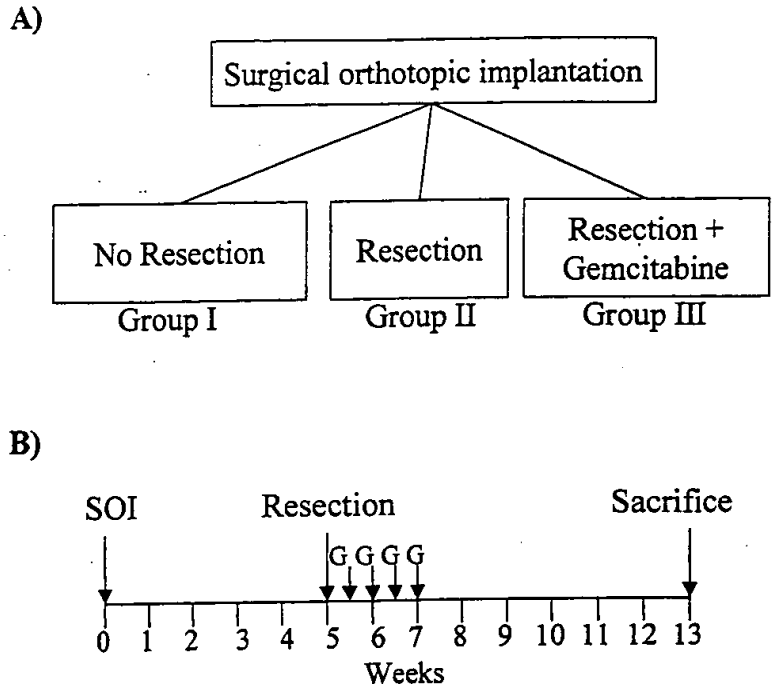

Figure 1. At 5 weeks following surgical orthotopic implantation, mice were randomly divided into three treatment groups. Group I underwent exploratory laparotomy without resection. Group II underwent surgical resection of the tumor. Group III underwent resection and received postoperative gemcitabine. B) Exploratory laparotomy (Group I) and resections (Groups II and III) were performed at 5 weeks after implantation. Group III received gemcitabine starting two days post-resection, with 100 mg/kg/dose q3d for a total of 4 doses. The mice were sacrificed at 13 weeks after implantation, and the presence of recurrent tumor and location of metastases were recorded.

Results and discussion

Tumor recurrence

The recurrence rate following resection alone (Group II) was 70.6%, whereas in the resection plus gemcitabine group (Group III), the recurrence rate was reduced to 28.6% (Figure 2). This 42% reduction in recurrence rate was statistically significant ($P = 0.02$, chi-squared test). The mean primary tumor weight was significantly higher for Group I (3492.3 mg) compared to Group II (1403.6 mg) ($P = 0.002$, t-test) and Group III (1829.2 mg) ($P = 0.02$, t-test). The difference in mean primary tumor weight between Group II and Group III was not statistically significant ($P = 0.36$, t-test).

Metastatic patterns

Figure 3 documents the location of metastases for each treatment group. In Group I, large tumors were noted in the pancreas as well as local and distant sites including spleen, retroperitoneum, portal nodes, diaphragm, small intestine, colon, liver, kidney, mediastinum, and lungs. In Group II, recurrences were also seen in the bed of the resected pancreas and in distant sites, including spleen, retroperitoneum, portal lymph nodes, diaphragm, small intestine, colon, mediastinum, and lungs. There was an average of 2.4 metastatic events per mouse. However, in Group III, significantly fewer metastases occurred, an average of 1 per mouse, ($P = 0.02$, chi-squared test), and there were no distant metastases to sites such as liver, kidney, mediastinum, and lungs. Recurrences in this group were limited to locoregional areas such as the spleen, retroperitoneum, portal lymph nodes, diaphragm, and bowel. The primary BxPC-3 tumor as well as the metastases were visualized using GFP (Figures 4A–C). Tumors were confirmed to be ductal adenocarcinoma by standard microscopy H&E stained sections (Figure 4D).

Bruns et al. recently described limited effects of gemcitabine in an orthotopic model of human pancreatic cancer in nude mice implanted with tumor cell suspensions [19, 20]. In these experiments, mice were treated with either gemcitabine or gemcitabine with an EGF-receptor inhibitor [19, 20]. In the present study, with the use of SOI to enhance metastasis and the addition of GFP as an aid to visualize metastasis of pancreatic cancer, we have made a significantly advanced metastatic model. For example, in the present study, metastases were visualized in the spleen, retroperitoneum, portal lymph nodes, diaphragm, small intestine, colon, liver, kidney, mediastinum, and lungs as opposed to only the liver and lymph nodes in the Bruns et al. studies [19, 20].

The present study has demonstrated adjuvant therapy with gemcitabine, in contrast to standard therapy with resection alone, reduced both the incidence and the rate of metastatic spread. Gemcitabine reduced the number of mice with recurrent tumor by 42% and reduced the metastatic rate by 58% per mouse compared to resection alone. Since surgical resection in humans still carries a high risk of recurrence, adding gemcitabine should allow for a higher rate of cure. The metastases in the mice treated with gemcitabine tended to occur locally in the retroperitoneum, spleen and diaphragm as opposed to extensive distant metastases in the untreated mice. This indicates that adjuvant gemcitabine

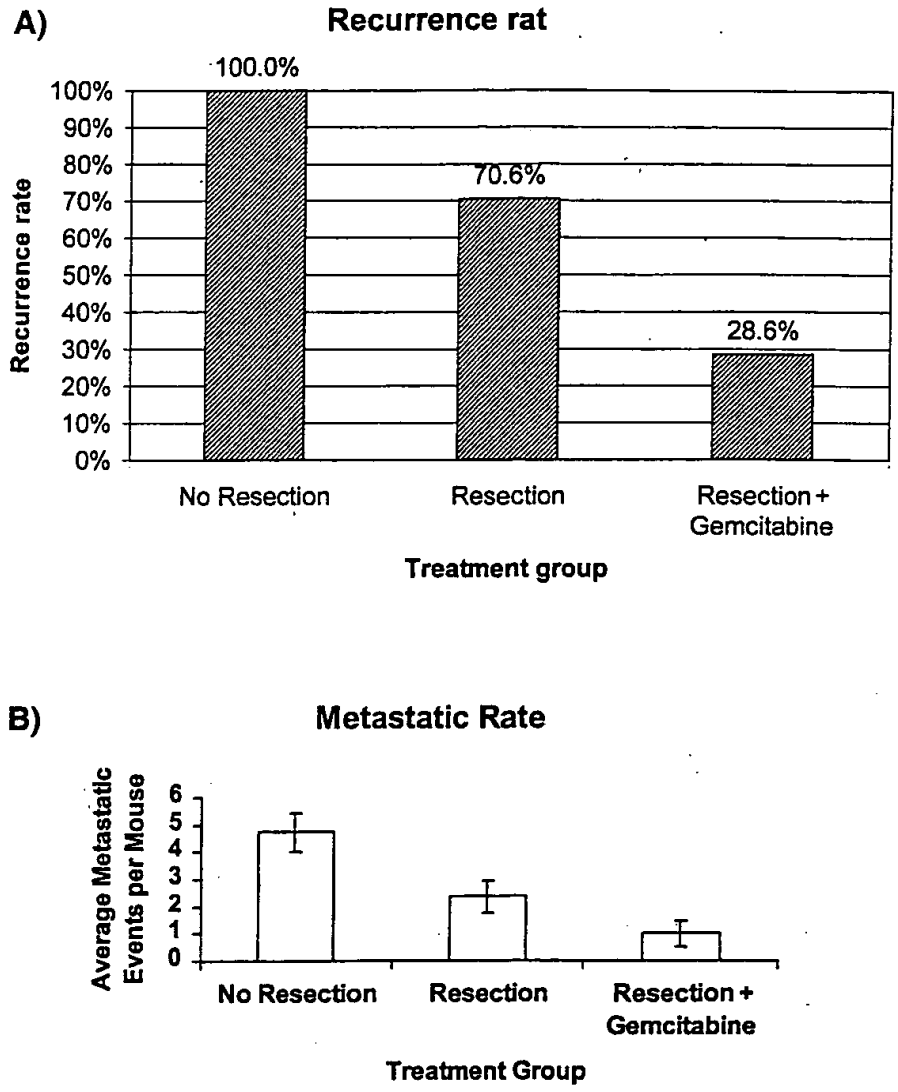

Figure 2. A) Percentage of mice in each group with recurrent tumor. All mice in the exploratory laparotomy group had tumor, whereas 70.6% of the resection group and 28.6% of the resection + gemcitabine group had tumor. B) Average metastatic events per mouse. The addition of gemcitabine reduced metastatic events by 58%.

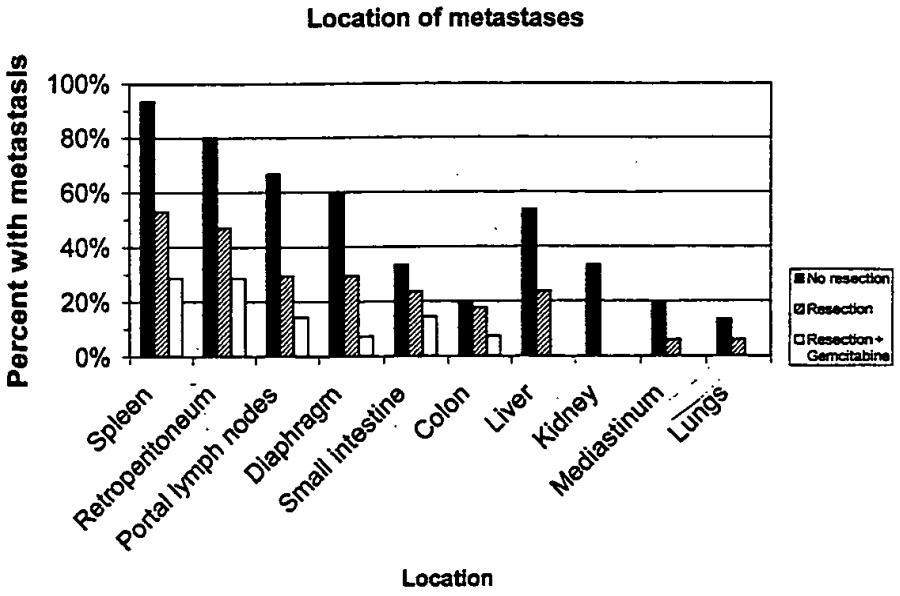

Figure 3. Location of metastases. Percentage of mice in each treatment group with recurrence in the specified location.

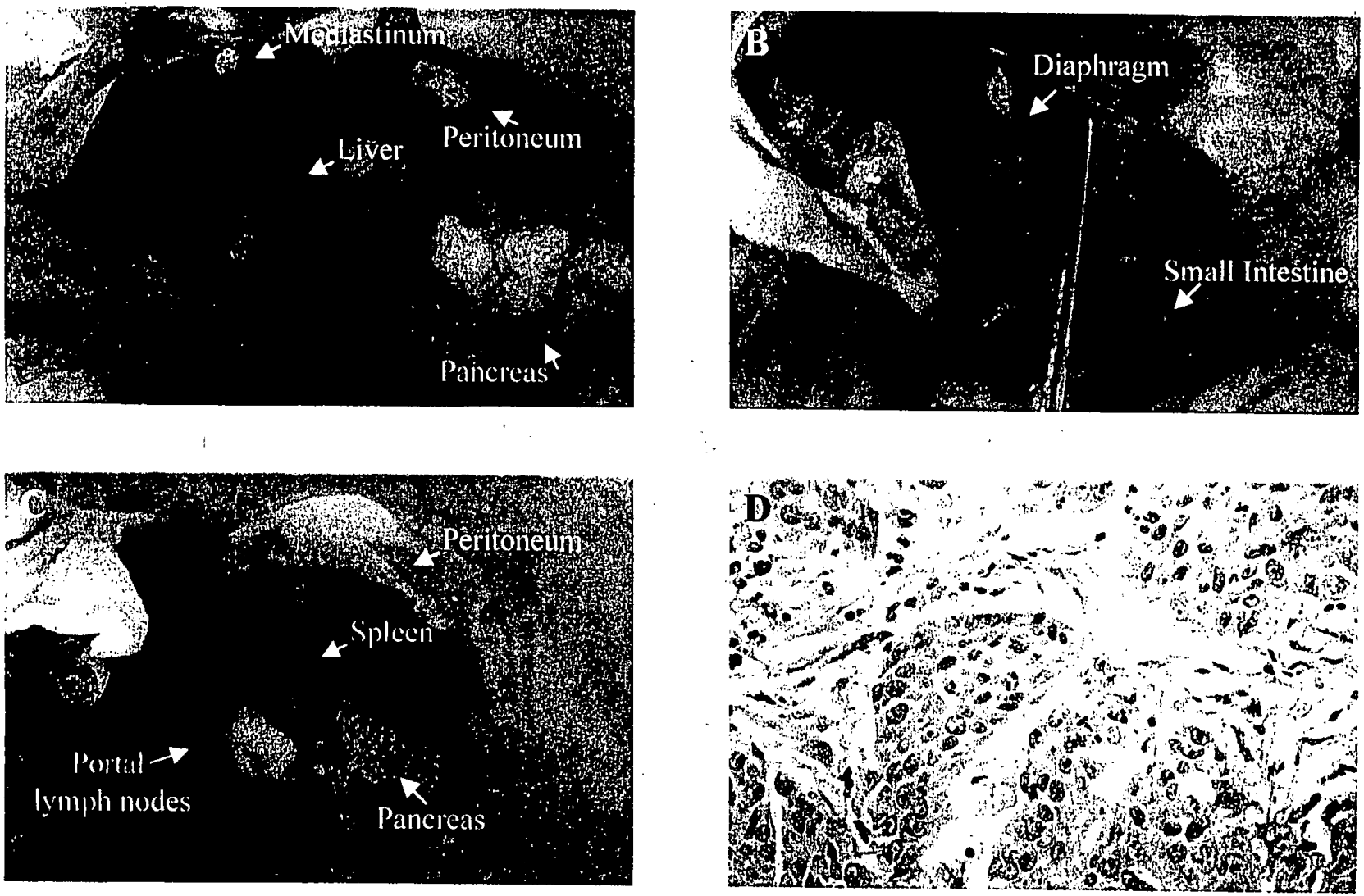

Figure 4. (A–C) Visualization of extensive metastases in three mice from Group I, including metastases to spleen, retroperitoneum, diaphragm, portal lymph nodes, small intestine, liver, and mediastinum. (D) H&E stain of the BxPC-3-GFP pancreatic adenocarcinoma.

acts to slow the rate of metastatic spread as well as reduce recurrence at the primary site, which could correlate to a prolonged disease-free survival in humans as compared to standard gemcitabine therapy [19, 20]. Furthermore, to our knowledge, our study is the first to combine gemcitabine with surgical resection of pancreatic cancer in an orthotopic model. The results of this study suggest clinical feasibility of combining surgical resection of pancreatic cancer with adjuvant gemcitabine therapy.

Acknowledgements

This study was supported in part by an American Cancer Society Institutional Research Grant and the Department of Health Services, California Cancer Research Program (97-12013).

References

1. Greenlee RT, Murray T, Bolden S et al. Cancer Statistics, 2000. CA Cancer J Clin 2000; 50: 7–33.
2. Burris HA, Moore MJ, Andersen J et al. Improvements in survival and clinical benefit with gemcitabine as first-line therapy for patients with advanced pancreas cancer: a randomized trial. J Clin Oncol 1997; 15: 2403–13.
3. Bouvet M, Gamagami RA, Gilpin EA et al. Factors influencing survival after resection for periampullary neoplasms. Am J Surg 2000; 180: 13–7.
4. Gastrointestinal Tumor Study Group. Further evidence of effective adjuvant combined radiation and chemotherapy following curative resection of pancreatic cancer. Cancer 1987; 59: 2006–10.
5. Yeo CJ, Abrams RA, Grochow LB et al. Pancreaticoduodenectomy for pancreatic adenocarcinoma: postoperative adjuvant chemoradiation improves survival. Ann Surg 1997; 225: 621–33.
6. Fu X, Guadagni F, Hoffman RM. A metastatic nude-mouse model of human pancreatic cancer constructed orthotopically from histologically-intact patient specimens. Proc Natl Acad Sci USA 1992; 89: 5645–49.
7. Furukawa T, Kubota T, Watanabe M et al. A novel 'patient-like' treatment model of human pancreatic cancer constructed using orthotopic transplantation of histologically-intact human tumor-tissue in nude mice. Cancer Res 1993; 53: 3070–2.
8. An Z, Wang X, Kubota T et al. A clinical nude mouse metastatic model for highly malignant human pancreatic cancer. Anticancer Res 1996; 16: 627–32.
9. Tomikawa M, Kubota T, Matsuzaki SW et al. Mitomycin C and cisplatin increase survival in a human pancreatic cancer metastatic model. Anticancer Res 1997; 17: 3623–5.
10. Chishima T, Miyagi Y, Wang X et al. Cancer invasion and micrometastasis visualized in live tissue by green fluorescent protein expression. Cancer Res 1997; 57: 2042–7.
11. Chishima T, Miyagi Y, Wang X et al. Metastatic patterns of lung cancer visualized live and in process by green fluorescent protein expression. Clin Exp Metastasis 1997; 15: 547–52.
12. Chishima T, Miyagi Y, Wang X et al. Visualization of the metastatic process by green fluorescent protein expression. Anticancer Res 1997; 17: 2377–84.
13. Chishima T, Miyagi Y, Li L et al. Use of histoculture and green fluorescent protein to visualize tumor-cell host-tissue interaction. In Vitro Cell Dev Biol Anim 1997; 33: 745–7.
14. Chishima T, Yang M, Miyagi Y et al. Governing step of metastasis visualized *in vitro*. Proc Natl Acad Sci USA 1997; 94: 11573–6.
15. Yang M, Hasegawa S, Jiang P et al. Widespread skeletal metastatic potential of human lung cancer revealed by green fluorescent protein expression. Cancer Res 1998; 58: 4217–21.
16. Yang M, Jiang P, Sun FX et al. A fluorescent orthotopic bone metastasis model of human prostate cancer. Cancer Res 1999; 59: 781–6.
17. Yang M, Jiang P, An Z et al. Genetically fluorescent melanoma bone and organ metastasis models. Clin Cancer Res 1999; 5: 3549–59.
18. Yang M, Baranov E, Jiang P et al. Whole-body optical imaging of green fluorescent protein-expressing tumors and metastases. Proc Natl Acad Sci USA 2000: 97: 1206–11.
19. Bruns CJ, Solorzano CC, Harbison MT et al. Blockade of the epidermal growth factor receptor signaling by a novel tyrosine kinase inhibitor leads to apoptosis of endothelial cells and therapy of human pancreatic carcinoma. Cancer Res 2000; 60: 2926–35.
20. Bruns CJ, Harbison MT, Davis DW et al. Epidermal growth factor receptor blockade with C225 plus gemcitabine results in regression of human pancreatic carcinoma growing orthotopically in nude mice by antiangiogenic mechanisms. Clin. Cancer Res 2000; 6: 1936–48.

ANTICANCER RESEARCH *16:* 627-632 (1996)

A Clinical Nude Mouse Metastatic Model for Highly Malignant Human Pancreatic Cancer

ZILI AN[1], XIAOEN WANG[1], TETSURO KUBOTA[2], A. R. MOOSSA[3] and ROBERT M. HOFFMAN[1,3]

[1]*AntiCancer Inc., 7917 Ostrow Street, SanDiego, CA 92111, U.S.A.;*
[2]*Department of Surgery, School of Medicine, Keio University, 35 Shinanomachi, Shinjuku-ku, Tokyo 160, Japan;*
[3]*Laboratory of Surgical Oncology, Department of Surgery, School of Medicine, University of California, San Diego, CA, U.S.A.*

Abstract. *Pancreatic cancer is a highly aggressive and treatment-refractory cancer. A clinically-relevant animal model is necessary to develop therapy for metastatic pancreatic cancer. In this study we evaluated the efficacy of mitomycin C (MMC) and 5-FU against the human pancreatic adenocarcinoma cell line PAN-12 in an orthotopic human metastatic pancreatic cancer nude mice model. The model is constructed by surgical orthotopic implantation (SOI) of histologically intact tumor tissue in the tail portion of the pancreas near the spleen. PAN-12 grew very aggressively in the control group of nude mice with extensive local invasion and distant metastasis to various organs with a propensity for the lung but to other organs as well, including the liver, kidney and regional and distant lymph nodes. In a striking effect none of the mice in the MMC-treated group developed tumor. Although mice in the 5-FU treated group survived statistically significantly longer than those in the untreated control, the overall incidence of metastasis in these mice was equivalent to those in the control. However no liver or kidney metastases were found in the 5-FU treated animals perhaps accounting in part for their longer survival. This "clinical" nude mouse model of highly metastatic pancreatic cancer can now be used to discover new effective agents for this disease.*

Pancreatic cancer is one of the most aggressive and treatment-refractory malignancies in humans. The five year survival rate is not more than 5% (1). In patients with locally unresectable advanced tumor, especially in those complicated with distant metastasis, the median survival time is as short as 3 to 6 months (2). To date no effective treatment is available for this deadly disease. Clinical trials dealing with patients have many limitations. It would be advantageous to have a reliable animal model to predict effective therapy in humans. However, previous rodent models did not demonstrate the metastatic property of malignant human diseases and therefore have doubtful clinical value. Recent work from a number of laboratories has indicated that implanting human tumor cells orthotopically in the corresponding organ of nude mice resulted in much higher metastatic rates. Vezeridis *et al* (9) established orthotopically growing pancreatic tumors by orthotopic transplantation of tumor line xenografts, which metastasized to regional lymph nodes, the liver and the lungs of the animals.

Recently we developed a new patient-like model of pancreatic cancer by surgical orthotopic implantation (SOI) using histologically intact patient tumor tissue (3). This nude mouse model, termed MetaMouse together with other orthotopic transplant models developed by us, demonstrate invasive local growth and greater metastatic potential than other models (4, 10, 11, 12, 13, 14, 15, 16, 17, 18) and are able to act as a clinical profile for cancer patients in assessing new treatment options.

In this study, we further developed with SOI a "clinical" nude-mouse model of a highly metastatic human pancreatic tumor line PAN- 12, against which the efficacy of mitomycin C (MMC) and 5-FU were evaluated as model drugs.

Materials and Methods

Mice. Male BALB/c nu/nu mice (Charles River Laboratory, Wilminton, MA), aged 4-5 weeks weighing 20-25 grams, were used in the study. They were kept in specific pathogen-free conditions. The animal diets were obtained from Harlan Teklad (Madison, WI). HCl (0.15%) was added to the drinking water.

Drugs. MMC and 5-FU were purchased from the Sigma Chemical Company (St. Louis, MO).

Correspondence to: Dr. Robert M. Hoffman, 7917 Ostrow St., San Diego, CA 92111, Tel: 619-654-2555, Fax: 619-268-4175.

Key Words: Metastatic model, nude mouse, human pancreatic cancer.

0250-7005/96 $2.00+.40

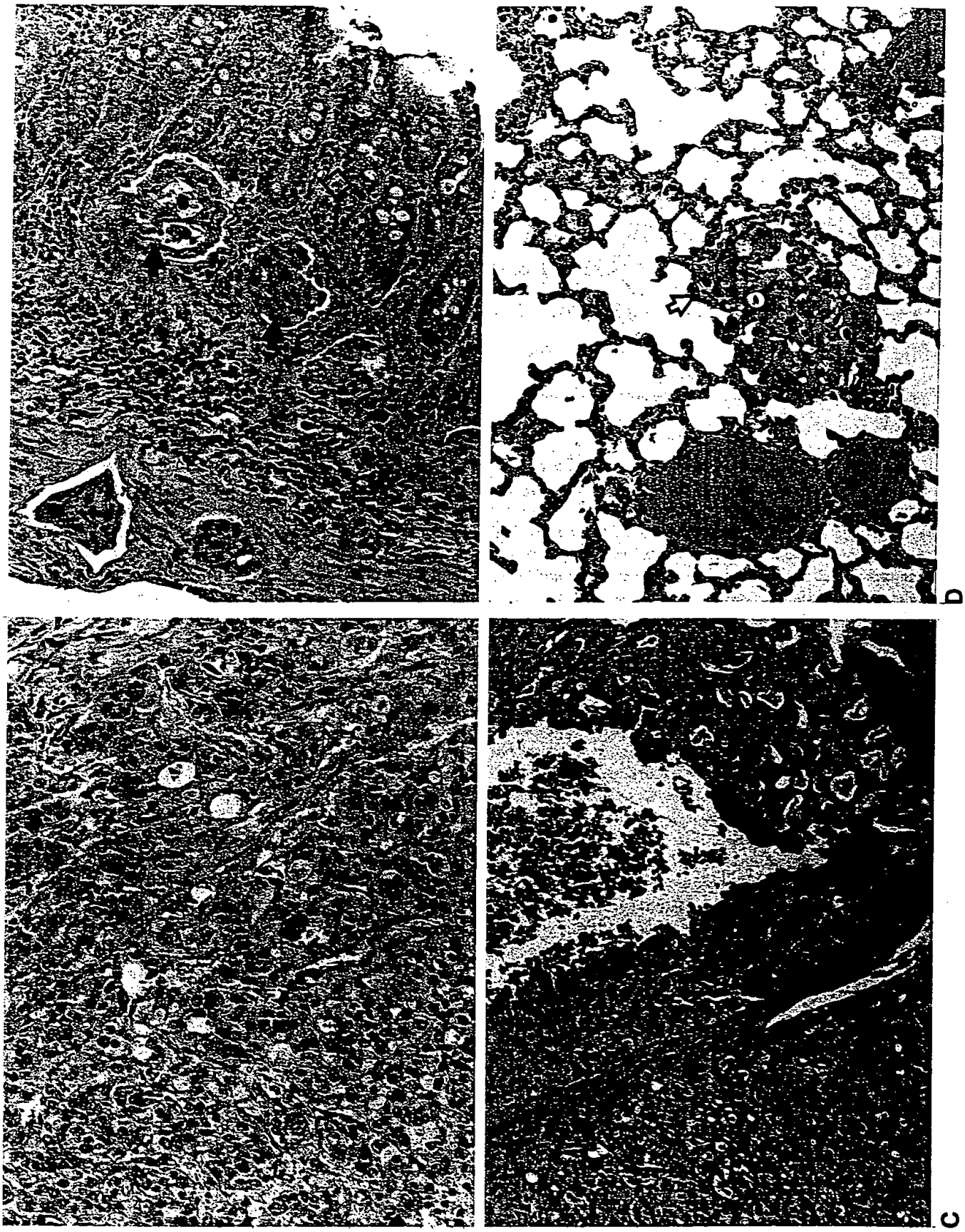
B
D
A
C

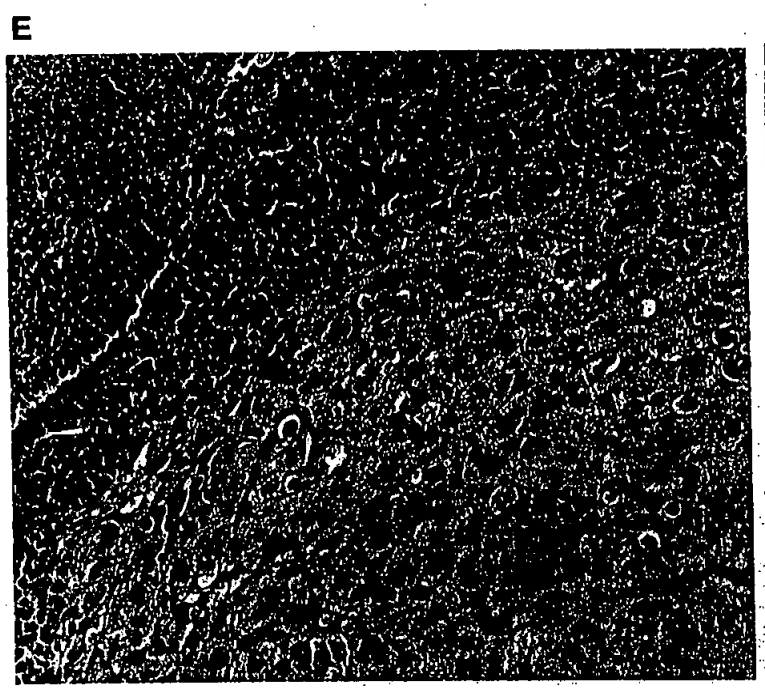

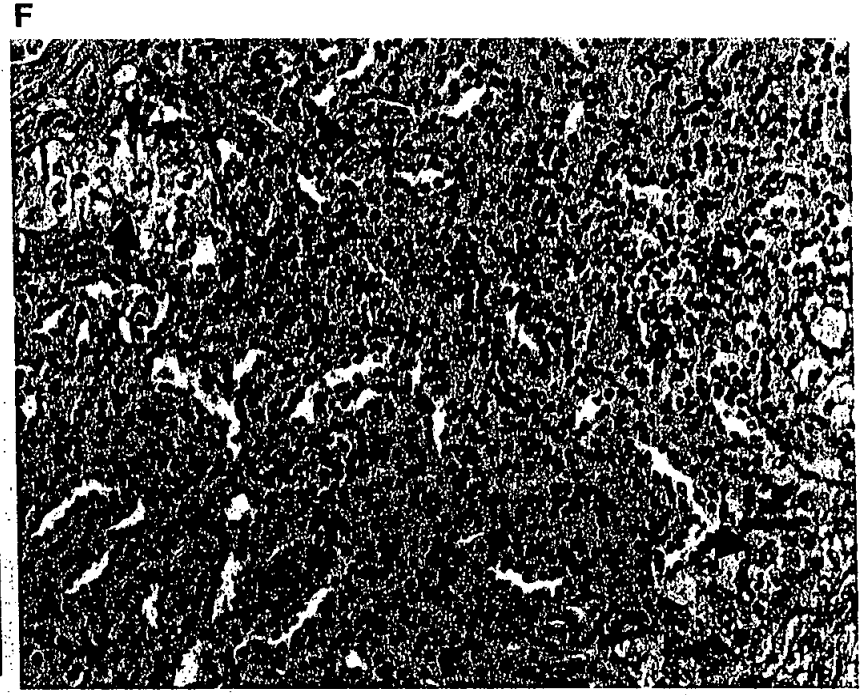

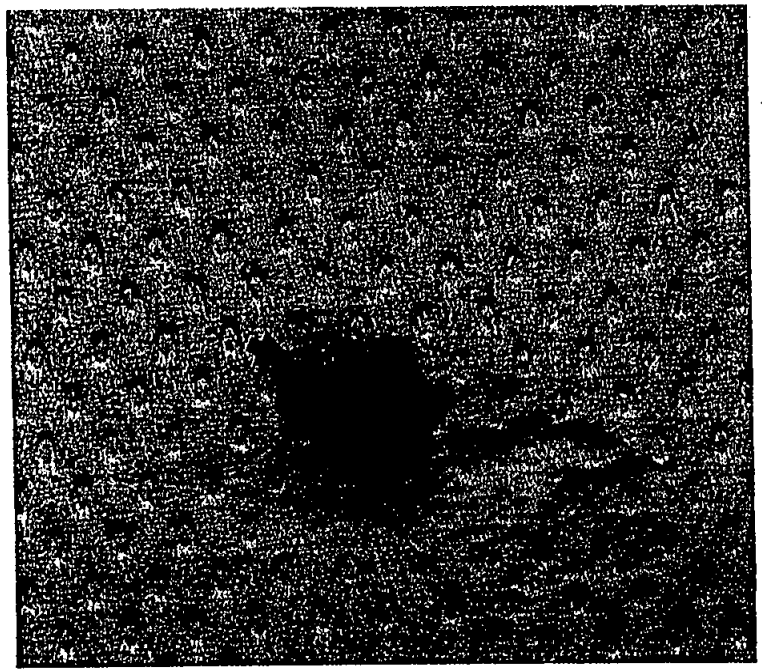

Figure 1. *Gross and microscopic views of primary and metastatic tumor of human pancreatic cancer PAN-12 in the untreated control and 5-FU-treated groups. Human pancreatic cancer cell line PAN-12 was orthotopically transplanted in the pancreas of the nude mice. 5-FU was administered intravenously through tail vein injection three times per week with a one-week rest between treatment cycles for a total of 8 cycles. A. Microscopic view of primary tumor by hematoxylin and eosin staining. B. Local invasive growth to mucous layer of the small intestine (hollow diamond: mucous layer of small intestine; black arrow: tumor nest) C. Local invasive growth to left adrenal gland (hollow diamond: tumor; solid diamond: adrenal gland; arrow: invasion of tumor) D. Lung metastasis (hollow arrow). E. Lymph node metastasis arrow). F. Kidney metastasis (black arrows). G. Gross picture of kidney metastasis (arrow).*

Table I. *Antitumor activity of MMC and 5-FU against PAN-12 in an orthotopic nude mice model constructed by surgical orthotopic implantation (SOI) of histologically intact tumor tissue.*

Treatment	Survival time[a] (Mean±SD) (days)	Tumor weight[b] (Mean±SD) (g)	Metastasis[c] rate
Control	73.73 ± 21.08	1.99 ± 0.99	10/15
5-FU	104.13 ± 28.00	2.16 ± 1.34	10/15
MMC	127.93 ± 29.91	No tumor growth	0/15

PAN-12 was transplanted into nude mice on day 0. Two mg/kg of MMC and 7.5 mg/kg of 5-FU were administered intravenously through tail vein injection three times a week with a one-week period rest between treatment cycles for a total of 8 cycles. When the last mouse in the 5-FU group died, the mice that were still alive in the MMC group were sacrificed after absence of tumor growth was confirmed by laparotomy exploration.

[a] $P<0.01$ when MMC and 5-FU were compared with control; $P<0.05$ when statistical comparison was performed between the MMC and 5-FU groups.
[b] $P>0.05$ between control and 5-FU.
[c] See Table II for details about sites of metastasis.

Human pancreatic cancer xenograft. Human pancreatic carcinoma cell line PAN-12 was from Keio University, Tokyo. PAN-12 was maintained by s.c. transplantation in nude mice.

Surgical orthotopic implantation (SOI) of histologically intact tissue. Pancreatic tumor tissues were transplanted orthotopically in nude mice using the methods developed by us previously (3). Subcutaneous tumors in the exponential growth phase in nude mice were resected aseptically. Necrotic tissues were then cut away. The remaining healthy tumor tissues were cut into approximately 1 × 1 × 1 mm pieces in RPMI 1640 culture medium containing fetal bovine serum and antibiotics (100 units/ml of penicillin and 100 µlg/ml of streptomycin).

Mice were anesthetized by isoflurane inhalation and put in a supine position. An incision was made through the left upper abdominal pararectal line and the peritoneum. A retractor was used to expose the pancreas. Approximately 10 pieces of tumor tissue were then transplanted on the tail of the pancreas near the spleen using 8-0 nylon sutures (Look Incorporated, Norwell, MA). The abdominal wall and skin were closed with 6-0 silk sutures (Look Incorporated, Norwell, MA).

Experimental chemotherapy. One week after surgical orthotopic implantation (SOI), mice were randomly assigned into 3 groups (control, 5-FU-treated, and MMC-treated) with 15 mice in each group. The doses of MMC and 5-FU used were 2 mg/kg and 7.5 mg/kg, respectively. The drugs were dissolved in physiological saline and administered i.v. by tail vein injection on a schedule of 3 times a week followed by a one-week period of rest for a total of 8 weeks. Dead mice were immediately immersed in formalin for subsequent autopsy, at which time they were carefully examined for local tumor growth and distant metastasis. Histological study was performed by standard hematoxylin and eosin staining. Survival time, primary tumor size and weight data were collected at the end of the study.

Results and Discussion

Orthotopic implantation of intact PAN-12 tumor tissue into nude mice resulted in local invasive growth and a very high incidence of metastasis to various organs including the lungs, the liver and the kidneys, as well as regional and distant lymph nodes in the control as well as 5-FU-treated mice (Figure 1) (Table II). PAN-12 demonstrated a propensity for lung metastasis as seen in 8/15 control animals and in 7/15 5-FU-treated animals. In striking contrast none of the MMC-treated mice had even primary tumor growth.

Table II. *Sites of metastasis of PAN-12 in control and treated groups in the SOI model.*

Treatment	Metastatic sites			
	Lung	Liver	Kidney	Lymph node*
Control	8/15	1/15	1/15	7/15
5-FU	7/15	-	-	8/15
MMC	-	-	-	-

*Metastatic lymph nodes include those in the abdomen, mediastinum and lung hilus.

Table I shows the efficacy of MMC and 5-FU against Panc-12 after surgical orthotopic implantation (SOI) in nude mice. At the time when the last mouse died in the 5-FU-treated group (at this time no mice were surviving in the control group), eight mice were still alive in the MMC-treated group. They were sacrificed on the same day after the absence of tumor growth was confirmed by laparotomy. Therefore the maximum survival time of these animals was at the time the last mouse in the 5-FU-treated group died. Even so, statistical differences in survival still existed between the MMC-treated group and the other two groups (control and 5-FU-treated). In this study 5-FU showed some degree of antitumor activity by prolonged survival with statistical difference when compared with the control. However no statistical differences were observed in primary tumor size and weight nor the metastasis rate as determined at autopsy at the end of the study.

The fact that the orthotopic model developed by SOI allows much more invasive local tumor growth and the fact that metastasis can occur and to relevant targets provide significantly more options for evaluating potential new therapeutics for pancreatic cancer. The model should, therefore, bring experimental therapeutics for pancreatic cancer closer to clinical practice. In an unsuccessful phase III clinical trial of chemotherapy for advanced pancreatic cancer based on a nude mouse s.c. xenograft model study, Kelsen *et al* (5) concluded that use of s.c. xenograft model as a basis for clinical trial of pancreatic cancer was an "unconfirmed approach". Unlike the s.c. xenograft model, this novel orthotopic model constructed by SOI with histologically intact tumor tissue demonstrates broad resemblances to clinical patients with regard to local invasive growth and distant metastasis through lymphatic and blood vessels. This model of pancreatic cancer is particularly interesting since the main

metastatic organ is the lung. Further studies will compare the characteristics of PAN-12, including molecular markers of the pancreatic tumors for which the liver is the main metastatic organ. Moreover, experimental therapy can be initiated at any time point during tumor development in the model so as to provide informative data for clinical trials for cancer patients in various stages.

As an antitumor antibiotic, mitomycin C has been investigated for more than 30 years (6). However, its therapeutic effects on pancreatic cancer still need further experimentation. In the present study the pancreatic cell line PAN-12 was completely suppressed by MMC resulting in no orthotopic tumor growth or metastasis in nude mice. The results were better than those of a previous study by Furukawa *et al* (7), in which both MMC and 5-FU were administered intraperitoneally as boluses at maximum tolerated doses in nude mice with an orthotopically-transplanted human pancreatic tumor line. In the present study MMC was given intravenously with a repeated schedule of three times per week. We designed a one-week rest period after the treatment week and this effectively saved the tail vein from the strong irritation by MMC for further treatment. We also believe that the one-week rest period had a rescue effect in reducing the toxicity of MMC in long-term treatment. Therefore it is suggested that different dosing schedules may give rise to different antitumor effects for pancreatic cancer.

In this study 5-FU demonstrated lower antitumor efficacy than MMC as determined by increased survival time. However, the high metastasis rate as determined at autopsy with no difference from the control suggested very limited antimetastatic efficacy of 5-FU. Perhaps the increased survival seen in the 5-FU treated mice was due to suppressed primary tumor growth, possibly with some qualitative differences in the metastatic pattern having some effects (Table II).

Seven out of 15 mice in the MMC-treated group succumbed before the last mouse in the 5-FUtreated group died. The only possible cause seems to be the toxicity of MMC, which is mainly thrombocytopenia and leukocytopenia (6). Pale skin color was observed in the MMC-treated group throughout the experiment.

Susceptibility to antitumor drugs has been assumed to correlate with the degree of differentiation of pancreatic cancer (8). The cell line used in this study is a poorly-differentiated adenocarcinoma, which may be very susceptible to chemotherapeutic agents. The present study illustrates the superiority of MMC over 5-FU in the treatment of PAN-12 in the nude mice model. Since the median survival for combination therapy is no better than that attained with single-agent therapy in patients (2), the results from this study should be very encouraging. Screening agents against primary and metastatic tumor growth in this clinical model of human pancreatic cancer in nude mice should enhance clinical development of effective therapy for pancreatic cancer.

References

1 Brennan M, Kinsella T and Friedman M: Cancer of the pancreas. *In:* Devita V, Hellman S and Rosenberg, S, eds. Cancer Principles and Practice of Oncology, ed. 3. Philadelphia: JB Lippincott Co., 1989; 800-835.

2 Arbudk SG: Chemotherapy for pancreatic cancer. Baillieres Clinical Gastroenterology *4*(4): 935-968, 1990.

3 Fu X, Guadagni F and Hoffman RM: A metastatic nude-mouse model of human pancreatic cancer constructed orthotopically from histologically-intact patient specimens. Proc Natl Acad Sci USA *89:* 5645-5649, 1992.

4 Hoffman RM: Patient-like models of cancer in mice: A review and critique of their development. Current Perspectives on Molecular and Cellular Oncology *1*(B): 311-329, 1992.

5 Kelsen D and Rosenbluth R *et al:* A phase III comparison trial of streptozotocin, mitomycin and 5FU with cisplatin, cytosine arabinoside, and caffeine in patients with advanced pancreatic carcinoma. Cancer *68:* 965-969, 1991.

6 Verweij J and Pinedo HM: Mitomycin C: mechanism of action, usefulness and limitations. Anti-Cancer Drugs *1*(1): 5-13, 1990.

7 Furukawa T, Kubota T, Watanabe M, Kitajima M and Hoffman RM: A novel "patient-like" treatment model of human pancreatic cancer constructed using orthotopic transplantation of histologically intact human tissue in nude mice. Cancer Res *53:* 3070-3072, 1993.

8 Chang BK, and Grefory JA: Comparison of the cellular pharmacology of doxorubicin in resistant and sensitive models of pancreatic cancer. Cancer Chemother Pharmacol *14:* 132-134, 1985.

9 Vezeridis MP, Doremus CM, Tibbetts LM, Tzanakakis G and Jackson BT: Invasion and metastasis following orthotopic transplantation of human pancreatic cancer in the nude mice. J Surg Oncol *40:* 261-265, 1989.

10 Hoffman RM: Orthotopic is orthodox: Why are orthotopic-transplant metastatic models different from all other models? J Cell Biochem *56:* 1-4, 1994.

11 Fu X, Besterman JM, Monosov A and Hoffman RM: Models of human metastatic colon cancer in nude mice orthotopically constructed by using histologically-intact patient specimens. Proc Natl Acad Sci USA *88:* 9345-9349, 1991.

12 Fu X and Hoffman RM: Human ovarian carcinoma metastatic models constructed in nude mice by orhtotopic transplantation of histologically-intact patient specimens. Anticancer Res *13:* 283-286, 1993.

13 Fu X, Le P and Hoffman RM: A metastatic orthotopic transplant nude-mouse model of human breast cancer. Anticancer Res *13:* 901-904, 1993.

14 Wang X, Fu X and Hoffman RM: A new patient-like metastatic model of human small-cell lung cancer constructed orthotopically with intact tissue via thoracotomy in immunodeficient mice. Anticancer Res *12:* 1403-1406, 1994.

15 Astoul P, Colt HG, Wang X and Hoffman RM: A "patient-like" nude mouse model of parietal human lung adenocarcinoma. Anticancer Res *14:* 85-91, 1994.

16 Wang X, Fu X and Hoffman RM: A patient-like metastasizing model of human lung adenocarcinoma constructed via thoracotomy in nude mice. Anticancer Res *12:* 1399-1401, 1992.

17 Fu X, Theodorescu D, Kerbel RS and Hoffman RM: Extensive multi-organ metastasis following orthotopic onplantation of histologically-intact human bladder carcinoma tissue in nude mice. Int J Cancer *49:* 938-939, 1991.

18 Astoul P, Colt HG, Wang X, Boutin C and Hoffman RM: A "patient-like" nude-mouce model of advanced human pleural cancer. J Cellular Blochem *56:* 9-15, 1994.

Received October 10, 1995
Accepted December 1, 1995

THIS PAGE BLANK (USP

ANTICANCER RESEARCH *17*: 3623-3626 (1997)

18

Mitomycin C and Cisplatin Increase Survival in a Human Pancreatic Cancer Metastatic Model

MORIAKI TOMIKAWA[1], TETSURO KUBOTA[1], SHINJIRO WILSON MATSUZAKI[1], SHIN TAKAHASI[1], MASAKI KITAJIMA[1], A.R. MOOSA[3] and ROBERT M. HOFFMAN[2,3]

[1]*Department of Surgery, School of Medicine, Keio University, 35 Shinanomachi, Shinjuku-ku, Tokyo 160, Japan;*
[2]*AntiCancer Inc., 7917 Ostrow Street, San Diego, CA 92111, U.S.A.;*
[3]*Department of Surgery, University of California School of Medicine, 200 W. Arbor Dr., San Diego, CA 92103-8220, U.S.A.*

Abstract. *Pancreatic cancer is one of the most intractable of all human cancers. We have previously developed a patient-like model of human pancreatic cancer by surgical orthotopic implantation (SOI). After SOI of the human tumor xenograft PAN-12-JCK into the tail of the nude mouse pancreas, mitomycin C (MMC) and cisplatin (DDP) were administered intraperitoneally at a dose of 4 and 6 mg/kg, respectively, on day-7. The mice were observed for 95 days. There was a statistically significant increase in disease-free and overall survival rates in the MMC - and MMC + DDP-treated groups. Local tumor growth was eliminated only in the group treated with MMC + DDP. Hepatic metastasis and peritoneal disseminations were completely inhibited by MMC but not DDP. This study demonstrates the usefulness of the SOI model of pancreatic cancer to study the differential efficacy of agents affecting primary tumor growth metastasis and survival, thus presenting an opportunity for the discovery of new agents for this highly resistant cancer.*

Pancreatic cancer is one of the most intractable of human cancers. The five-year-survival rate after radical surgery is approximately 15% (1). We have previously developed patientlike models of all the major human tumors (10) including human pancreatic cancer by surgical orthotopic implantation (SOI) of histologically intact human tumor tissues in nude mice (2,3,7). The SOI pancratic models replicate the clinical behavior of pancreatic cancer including local gtrowth and regional and distant metastasis (2,3,7). We have reported earlier that mitomycin C, but not 5-FU, was active against a SOI model of the human pancreatic cancer xenograft PAN-12-JCK in nude mice (7). In the present study, we report the differential antitumor, antimetastatic, and survival efficacy of mitomycin C and cisplatin alone and in combination in nude mice transplanted with PAN-12-JCK using SOI.

Correspondence to: Robert M. Hoffman, Ph.D., AntiCancer, Inc., 7917 Ostrow Street, San Diego, CA 92111, USA. TEL: 619-654-2555, FAX: 619-268-4175, E-mail: antica@ix.netcom.com

Key Words: Pancreatic cancer, surgical implantation, metastatic model, nude mice, combination chemotherapy.

Materials and Methods

Mice. Male BALB/c nu/nu mice were obtained from CLEA Japan, Inc. (Tokyo, Japan). Six to 8-week-old mice were used.

Drugs. Mitomycin C (MMC) and cisplatin (DDP) were purchased from Kyowa Hakko Kogyo Co., Ltd. (Tokyo, Japan), and Bristol-Myers Squibb K.K. (Tokyo, Japan), respectively.

Human pancreas cancer xenograft. PAN-12-JCK, a human pancreatic carcinoma xenograft, was provided by Dr. Y. Ohnishi of the Central Institute for Experimental Animals (Kawasaki, Japan). The tumor was maintained by serial subcutaneous transplantation into nude mice at Keio University School of Medicine.

Surgical orthotopic implantation (SOI) of histologically intact tumor tissue. Pancreatic tumor tissues were transplanted orthotopically in nude mice using the method of Fu *et al* (2) and Furukawa *et al* (3) with some modifications. Tumors growing exponentially in the subcutaneous space were resected aseptically from the nude mice. Necrotic tissues were cut away and the remaining healthy tumor tissues were cut with a scissors and were minced into approximately 3 × 3 × 3 mm pieces in Hanks' balanced salt solution (HBSS) containing 100 units/ml penicillin and 100 μg/ml streptomycin. Each piece was weighed and adjusted with scissors to a final weight of 50 mg.

Mice were anesthetized by intraperitoneal (ip) administration of a 2.5% solution of a mixture (0.3 ml/mouse) of 2,2,2-tribromoethanol (Aldrich Chemical Company, Inc., Milwaukee, WI) and tert-amyl alcohol (Wako Pure Chemical Industries, Ltd., Osaka, Japan) (1:1). An incision was then made through the upper left abdominal pararectal line and peritoneum. The pancreas was carefully exposed and a tumor piece was transplanted on the tail of the pancreas close to the portal area of the spleen with a 6-0 TI-CRON (Davis-Geck) surgical suture. The pancreas was then returned into the peritoneal cavity, and the abdominal wall and the skin were closed with a 5-0 Dexon (Davis-Geck, Inc., Manati, Puerto Rico) surgical suture. Animals were kept in a sterile environment.

Experimental chemotherapy. On day 7 after orthotopic transplantation, mice were randomized into control and treated groups. MMC and/or DDP, dissolved in 0.2 ml of physiological saline solution, were administered ip as a bolus. The doses of the drugs used were 4 mg/kg for

0250-7005/97 $2.00+.40

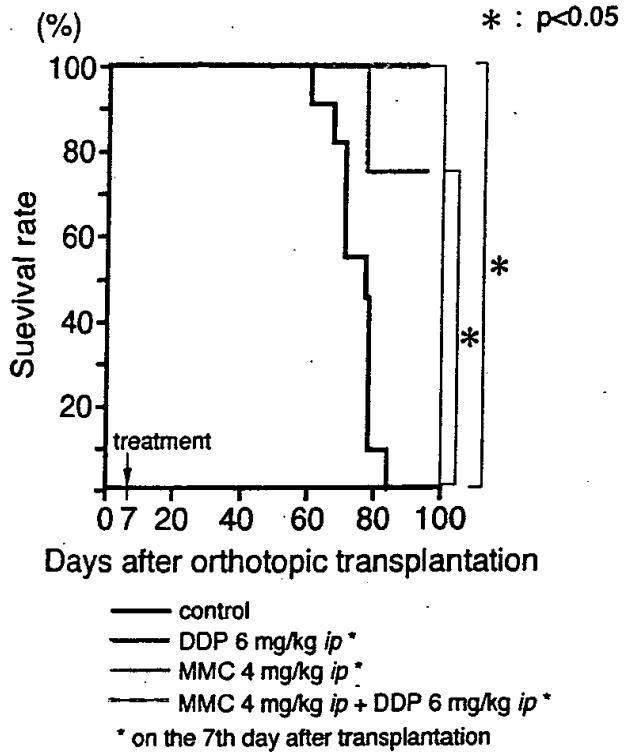

Figure 1. *Survival rate of the nude mice bearing a human pancreatic carcinoma xenograft, PAN-12-JCK and treated with cisplatin and/or mitomycin C. A human pancreatic carcinoma xenograft, PAN-12-JCK was surgically orthotopically implanted into the tail of the pancreas of nude mice on Day-0. Six mg of cisplatin (DDP) and/or 4 mg of mitomycin C (MMC) per kg were administered intraperitoneally on day-7. There were statistically significant differences between the survival periods of control and DDP-alone treated animals at p<0.05; and between the control and MMC-alone or the MMC + DDP combination treated animals, respectively at p<0.05.*

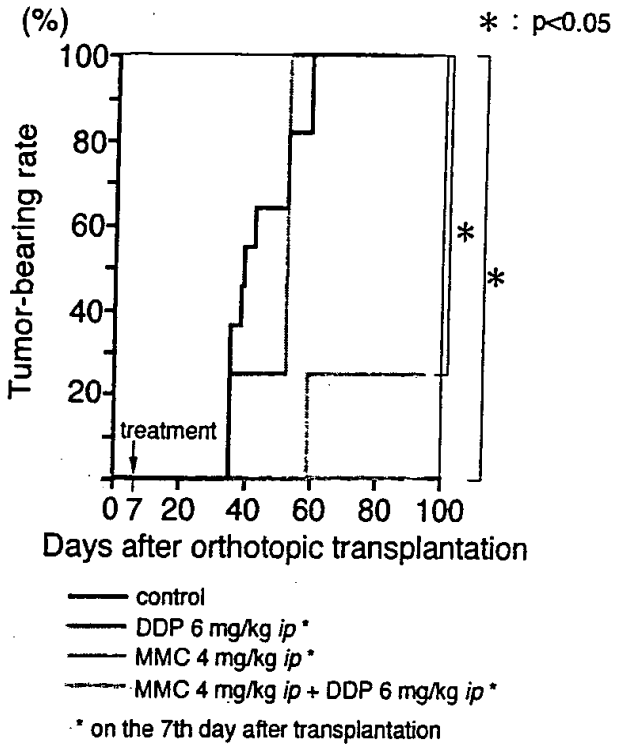

Figure 2. *Cumulative incidence of tumor-bearing mice. The mice were palpated two times per week, and the incidence of intraabdominal tumor was assessed. There were statistically significant differences between control or DDP-alone group and the MMC-alone group at p<0.05. This statistical difference was also observed between the control or DDP-alone group and the MMC + DDP combination group at p<0.05.*

MMC and/or 6 mg/kg for DDP. These doses were determined as 2/3 maximum tolerated doses (MTD) in nude mice in our previous studies (5,6). On the 95th day after orthotopic transplantation, any mice still alive wae sacrificed and the tumors growing in the peritoneal cavity and the liver were removed from each mouse, and then examined histologically after careful macroscopic examination.

The first experiment consisted of control, MMC-alone and the combination of MMC + DDP. The second experiment consisted of control, DDP-alone, and the combination of MMC + DDP.

Statistical analysis. The survival rate of tumor-bearing mice was analyzed by the generalized Wilcoxon test. The incidence of local tumor growth and metastasis was analyzed by the chi-squared test.

Results and Discussion

All the control mice died within 83 days after tumor inoculation. One of five DDP-treated mice died 77 days after tumor inoculation. All the mice survived until day-100 after tumor inoculation if they were treated with MMC alone or MMC + DDP in combination. There was a statistically significant difference between the survival periods of control and DDP alone at $p<0.05$. There was also a statistically significant difference between the survival of the control and MMC-alone or MMC + DDP in combination groups, respectively, at $p<0.05$ (Figure 1).

The incidence of tumor-bearing mice increased with time in the control and DDP-alone group with all mice having tumor growth by 45 days after tumor inoculation. On the other hand, no tumor was observed in the mice treated with MMC and DDP in combination, while one of four mice treated with MMC alone developed a primary tumor. There were statistically significant differences between the control or DDP-alone group and the MMC-alone group at $p<0.05$. A statistically significant difference was also observed between the control or DDP-alone group and the MMC + DDP combination at $p<0.05$. Thus, MMC treatment resulted in prolonged disease-free and overall survival extending our previous studies on MMC in the SOI pancreatic tumor model (7).

At the end of experiments, all the mice were sacrificed and the presence of tumor was confirmed (Table I). All the mice had tumors growing on the implanted site in the control and DDP-alone groups. No tumors were found in the MMC +

Table I. *Efficacy of Mitomycin C and Cisplatin on orthotopically implanted human pancreatic cancer xenograft, PAN-12-JCK.*

	Survival[a)]	Period[b)]	Local[c)]	Liver mets[d)]	Periton. mets[e)]
Experiment 1					
Control	3/5	78-84	3/3*	1/3	2/3
MMC	4/4	95	1/4	0/4	0/4
MMC + DDP	4/4	95	0/4	0/4	0/4
Experiment 2					
Control	3/6	60-77	3/3**	1/3	1/3
DDP	4/5	77-95	4|4	2|4	0/4
MMC + DDP	4/4	95	0/4	0/4	0/4

a) Surviving mice/experimental mice.
b) Survival period after the treatment.
c) Number of mice with local tumors/number of mice explored.
d) Number of mice with hepatic metastasis/number of mice explored.
e) Number of mice with peritoneal dissemination/number of mice explored.

* $p<0.05$ to MMC-alone and MMC + DDP by chi-squared test.
** $p<0.05$ to MMC + DDP by chi-squared test.

DDP group and only one of four mice developed intra-abdominal tumor in the group treated with MMC alone. These results were consistent with the survival of the mice.

Hepatic metastasis was observed in 2 of 6 control mice and 2 of 4 mice treated with DDP alone. No MMC-treated mice had hepatic metastasis. Three of six control mice developed peritoneal dissemination, while peritoneal dissemination was completely prevented by DDP alone, MMC alone, and MMC + DDP in combination. All the untreated mice developed tumors in the pancreas as well as hepatic metastasis and peritoneal dissemination.

The clinical efficacy rates of MMC and DDP are reported to be 27% (8) and 0% (9), respectively, against human pancreatic cancer, although synergism was not clinically evaluated. The mechanism of the combination of MMC and DDP is not understood, although we have previously reported that this combination was effective against human gastric carcinoma *in vitro* (4) and *in vivo* (5). MMC reduced the concentration of glutathione which can cause DDP resistance (5). The combined antitumor activity of MMC and DDP might also be due to independent antitumor activity of both the drugs against human pancreatic cancer.

In conclusion, the present study has demonstrated that the SOI metastatic model of pancreatic cancer can differentially evaluate the efficacy of agents on primary tumor growth, tumor dissemination, metastasis, disease-free survival and survival. Thus, the SOI model of pancreatic cancer accurately represents the patient and offers the opportunity for effective drug discovery for this currently devastating disease.

References

1 Takahashi S, Ogata Y and Tsuzuki T: Combined resection of the pancreas and portal vein for pancreatic cancer. Br J Surg *81:* 1190-1193, 1994.
2 Fu X, Guadagni F and Hoffman RM: A metastatic nude mouse model of human pancreatic cancer constructed orthotopically from histologically intact patient specimens. Proc Natl Acad Sci USA *89:* 5645-5649, 1992.
3 Furukawa T, Kubota T, Watanabe M, Kitajima M, and Hoffman RM: A novel "patient-like" treatment model of human pancreatic cancer constructed using orthotopic transplantation of histologically intact human tumor tissue in nude mice. Cancer Res *53:* 3070-3072, 1993.
4 Saikawa Y, Kubota T, Kuo T, Kase S, Furukawa T, Tanino H, Ishibiki K and Kitajima M: Synergistic antitumor activity of mitomycin C and cisplatin against gastric cancer cells *in vitro*. J Surg Oncol *54:* 98-102, 1993.
5 Saikawa Y, Kubota T, Kuo T, Furukawa T, Kase S, Tanino H, Isobe Y, Watanabe M, Ishibiki K, Arimori M and Kitajima M: Synergistic antitumor activity of combination chemotherapy with mitomycin C and cisplatin against human gastric cancer xenografts in nude mice. J Surg Oncol *56:* 242-245, 1994.
6 Kubota T, Ishibiki K and Abe O: Clinical usefillness of human xenografts in nude mice. Prog Clin Biol Res *276:* 213-225, 1988.
7 An Z, Wang X, Kubota T, Moossa AR, Hoffman RM: A clinical nude mouse metastatic model for highly malignant human pancreatic cancer. Anticancer Res *16:* 627-632, 1996.
8 Carter SK: The integration of chemotherapy into a combined modality approach for cancer treatment. Cancer Treat Rev *2:* 193-214, 1975.
9 Kelsen D: The use of chemotherapy in the treatment of advanced gastric and pancreas cancer. Semen Oncol *21(suppl. 7):* 58-66, 1994.
10 Hoffman RM: Fertile seed and rich soil: The development of clinically relevant models of human cancer by surgical orthotopic implantation of intact tissue. *In:* Teicher B, ed. Anticancer Drug Development Guide: Preclinical Screening, Clinical Trials, and Approval. Totowa, NJ: Humana Press Inc, 127-144, 1997.

Received May 5, 1997
Accepted June 9, 1997

THIS PAGE BLANK

March 1, 2002
Volume 62
Number 5
Pages 1235–1581

Cancer Research

Functions of Mutant Human Androgen Receptors

HER-2/neu in BRCA1-Associated Breast Cancer

Intravital GFP-Imaging of Liver Micrometastasis

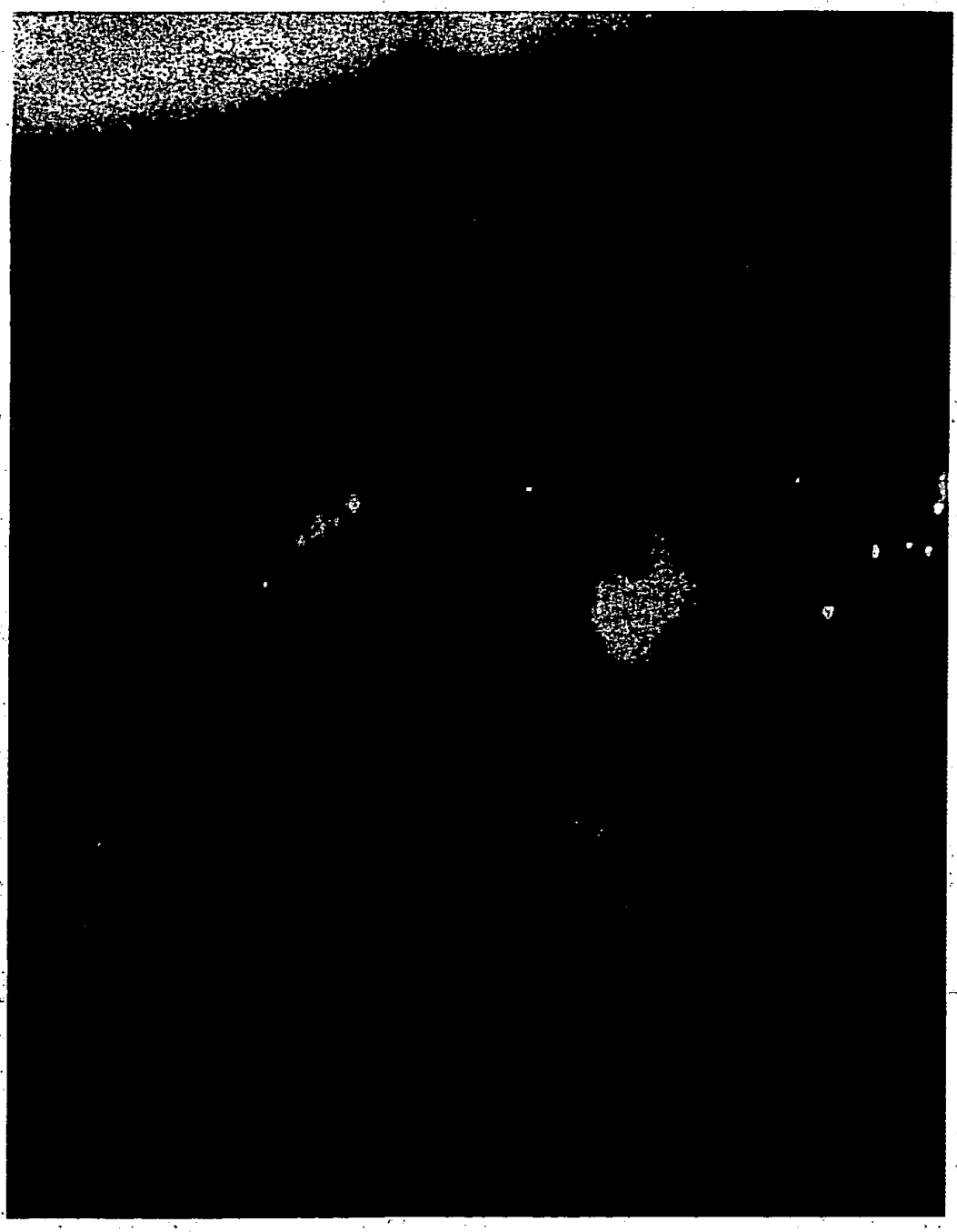

AACR American Association for Cancer Research

March 1, 2002
Volume 62
Number 5
Pages 1235–1581

Cancer Research

20

Functions of Mutant Human Androgen Receptors

HER-2/neu in BRCA1-Associated Breast Cancer

Intravital GFP-Imaging of Liver Micrometastasis

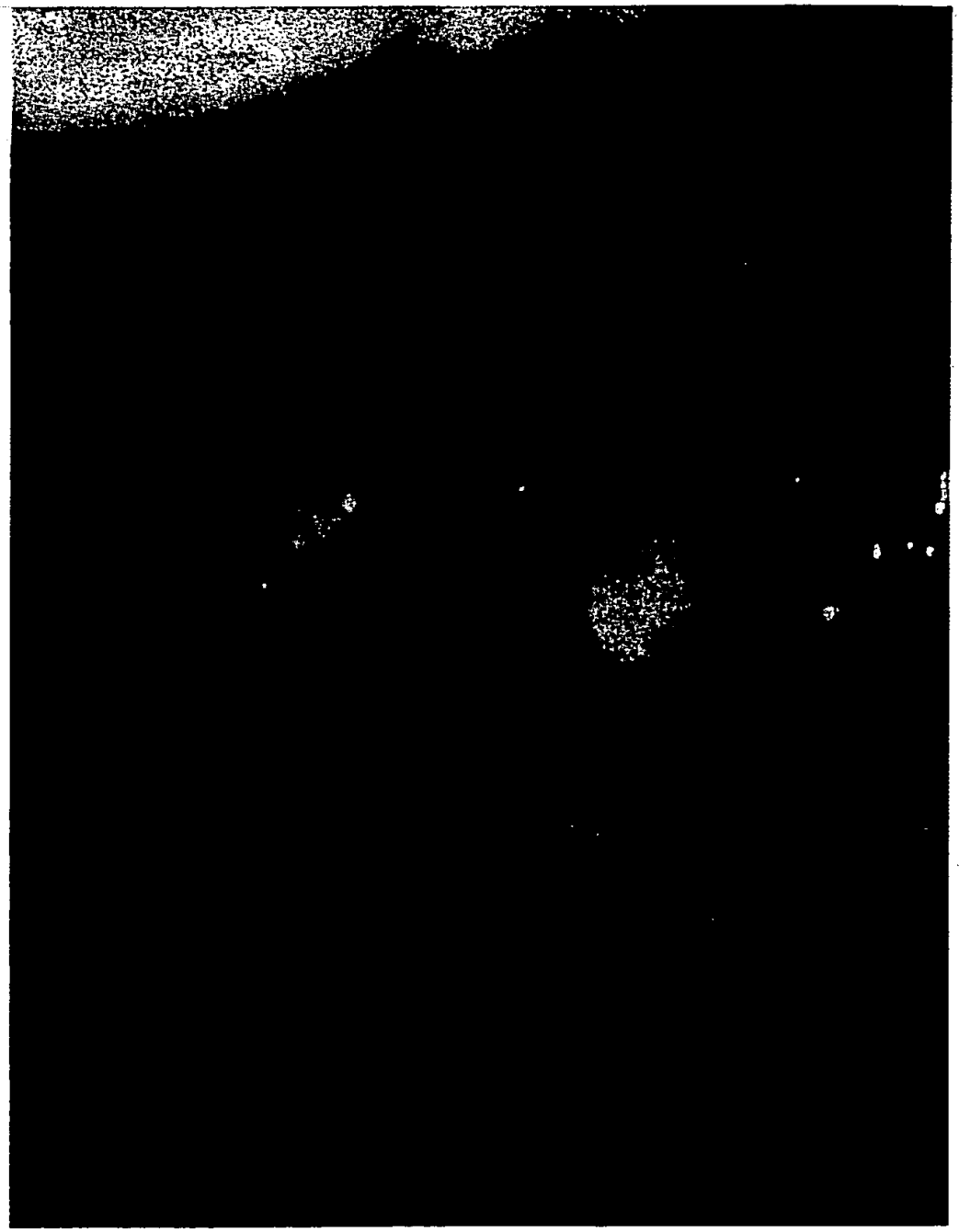

www.aacrjournals.org

AACR American Association for Cancer Research

[CANCER RESEARCH 62, 1534–1540, March 1, 2002]

Real-Time Optical Imaging of Primary Tumor Growth and Multiple Metastatic Events in a Pancreatic Cancer Orthotopic Model[1]

Michael Bouvet, Jinwei Wang, Stephanie R. Nardin, Rounak Nassirpour, Meng Yang, Eugene Baranov, Ping Jiang, A. R. Moossa, and Robert M. Hoffman[2]

Department of Surgery, University of California San Diego, San Diego, California 92161 [M. B., S. R. N., R. N., A. R. M., R. M. H.], and AntiCancer, Inc., San Diego, California 92111 [J. W., M. Y., E. B., P. J., R. M. H.]

ABSTRACT

We report here whole-body optical imaging, in real time, of genetically fluorescent pancreatic tumors growing and metastasizing to multiple sites in live mice. The whole-body optical imaging system is external and noninvasive. Human pancreatic tumor cell lines, BxPC-3 and MiaPaCa-2, were engineered to stably express high-levels of the *Aequorea victoria* green fluorescent protein (GFP). The GFP-expressing pancreatic tumor cell lines were surgically orthotopically implanted as tissue fragments in the body of the pancreas of nude mice. Whole-body optical images visualized real-time primary tumor growth and formation of metastatic lesions that developed in the spleen, bowel, portal lymph nodes, omentum, and liver. Intravital images in the opened animal confirmed the identity of whole-body images. The whole-body images were used for real-time, quantitative measurement of tumor growth in each of these organs. Intravital imaging was used for quantification of growth of micrometastasis on the liver and stomach. Whole-body imaging was carried out with either a *trans*-illuminated epi-fluorescence microscope or a fluorescence light box, both with a thermoelectrically cooled color CCD camera. The simple, noninvasive, and highly selective imaging made possible by the strong GFP fluorescence allowed detailed simultaneous quantitative imaging of tumor growth and multiple metastasis formation of pancreatic cancer. The GFP imaging affords unprecedented continuous visual monitoring of malignant growth and spread within intact animals without the need for anesthesia, substrate injection, contrast agents, or restraint of animals required by other imaging methods. The GFP imaging technology presented in this report will facilitate studies of modulators of pancreatic cancer growth, including inhibition by potential chemotherapeutic agents.

INTRODUCTION

Pancreatic cancer is often a fatal disease with 5-year survival rates of only 1–4% (1). Reasons for low survival in this disease include aggressive tumor biology, high metastatic potential, and late presentation at the time of diagnosis (2). Clearly, new treatment modalities for this disease need to be explored if progress is to be made. To this end, we and others have developed orthotopic models of human pancreatic cancer in the nude mouse that simulate tumor growth, progression, and metastasis and allow for testing of novel treatment strategies (3–9).

Recently, we have improved these models by transforming the tumors with the *GFP*[3] gene of the jellyfish *Aequorea victoria* to enable better detection of primary tumor growth and metastasis (10). Tracking of pancreatic cancer cells that stably express GFP *in vivo* is far more sensitive and rapid than the traditional cumbersome procedures of histopathological examination or immunohistochemistry. In other orthotopic GFP models such as lung cancer, prostate cancer, and melanoma, GFP labeling markedly improves the ability to visualize metastases in fresh tissue (11–13).

A major advantage of GFP-expressing tumor cells is that imaging requires no preparative procedures, contrast agents, substrates, anesthesia, or light-tight boxes as do other imaging techniques (14). GFP imaging is thus uniquely suited for whole-body imaging of tumor growth and metastases in live animals (15–17). In the current study using stable, high GFP-expression pancreatic tumor cells (10), we demonstrate external, noninvasive, simultaneous real-time, whole-body as well as intravital fluorescence imaging of orthotopic pancreatic tumor growth and multiple metastasis in mouse models.

MATERIALS AND METHODS

Pancreatic Cancer Cell Lines. The BxPC-3 and MIA-PaCa-2 human pancreatic cancer cell lines were obtained from the American Type Culture Collection (Rockville, MD). The cells were maintained in DMEM supplemented with 10% FCS, 2 mM glutamine, 100 units/ml penicillin, 100 μg/ml of streptomycin, and 0.25 μg/ml of amphotericin B (Gibco-BRL, Life Technologies, Inc., Grand Island, NY). Both cell lines were incubated at 37°C in 5% CO_2.

GFP-Retroviral Transduction and Selection of High GFP-Expression MIA-PaCa-2 and BxPC-3 Pancreatic Cancer Cells. For *GFP* gene transduction, 20% confluent MIA-PaCa-2 or BxPC-3 cells were incubated with a 1:1 precipitated mixture of retroviral supernatants of the PT67 packaging cells and RPMI 1640 (Gibco-BRL, Life Technologies, Inc.) for 72 h. Fresh medium was replenished at this time. MIA-PaCa-2 or BxPC-3 cells were harvested by trypsin/EDTA 72 h after infection with the GFP retroviral supernatants and subcultured at a ratio of 1:15 into selective medium that contained 200 μg/ml of G418. The level of G418 was increased to 800 μg/ml stepwise. MIA-PaCa-2 and BxPC-3 clones expressing GFP (MIA-PaCa-2-GFP or BxPC-3-GFP) were isolated with cloning cylinders (Bel-Art Products, Pequannock, NJ) by trypsin/EDTA and were amplified and transferred by conventional culture methods. High GFP-expression clones were then isolated in the absence of G418 for >10 passages to select for stable expression of GFP.

Animals. Nude *nu/nu* mice were maintained in a barrier facility on HEPA-filtered racks. The animals were fed with autoclaved laboratory rodent diet (Teckland LM-485; Western Research Products, Orange, CA). All animal studies were conducted in accordance with the principles and procedures outlined in the NIH Guide for the Care and Use of Animals under assurance number A3873-1.

SOI. Pancreatic tumors, grown s.c. in nude mice, were harvested at the exponential growth phase and resected under aseptic conditions. Necrotic tissues were cut away, and the remaining healthy tumor tissues were cut with scissors and minced into approximately 3 × 3 × 3-mm pieces in HBSS containing 100 units/ml penicillin and 100 μg/ml streptomycin. Each piece was weighed and adjusted with scissors to be 50 mg. For orthotopic surgery, mice were anesthetized by injection of 0.02 ml of solution of 50% ketamine, 38% xylazine, and 12% acepromazine maleate. The abdomen was sterilized with alcohol. An incision was then made through the left upper abdominal pararectal line and peritoneum. The pancreas was carefully exposed, and three tumor pieces were transplanted on the middle of the pancreas with a 6-0 Dexon (Davis-Geck, Inc., Manati, Puerto-Rico) surgical suture. The pancreas was then returned to the peritoneal cavity, the abdominal wall, and the skin was closed with 6-0 Dexon sutures. Animals were kept in a sterile environment. All procedures of the operation described above were performed with a 7 × microscope (Olympus).

Received 10/31/01; accepted 1/4/02.

The costs of publication of this article were defrayed in part by the payment of page charges. This article must therefore be hereby marked *advertisement* in accordance with 18 U.S.C. Section 1734 solely to indicate this fact.

[1] Supported in part by National Cancer Institute Grant I R43 89779-01, the Department of Health Services, California Cancer Research Program 97-12013, and the UCSD Specialized Cancer Center support National Cancer Institute Grant P30 CA23100-18S1.

[2] To whom requests for reprints should be addressed, at AntiCancer, Inc., San Diego, CA 92111. Phone: (858) 654-2555; Fax: (858) 268-4175; E-mail: all@anticancer.com.

[3] The abbreviations used are: GFP, green fluorescent protein; SOI, surgical orthotopic implantation.

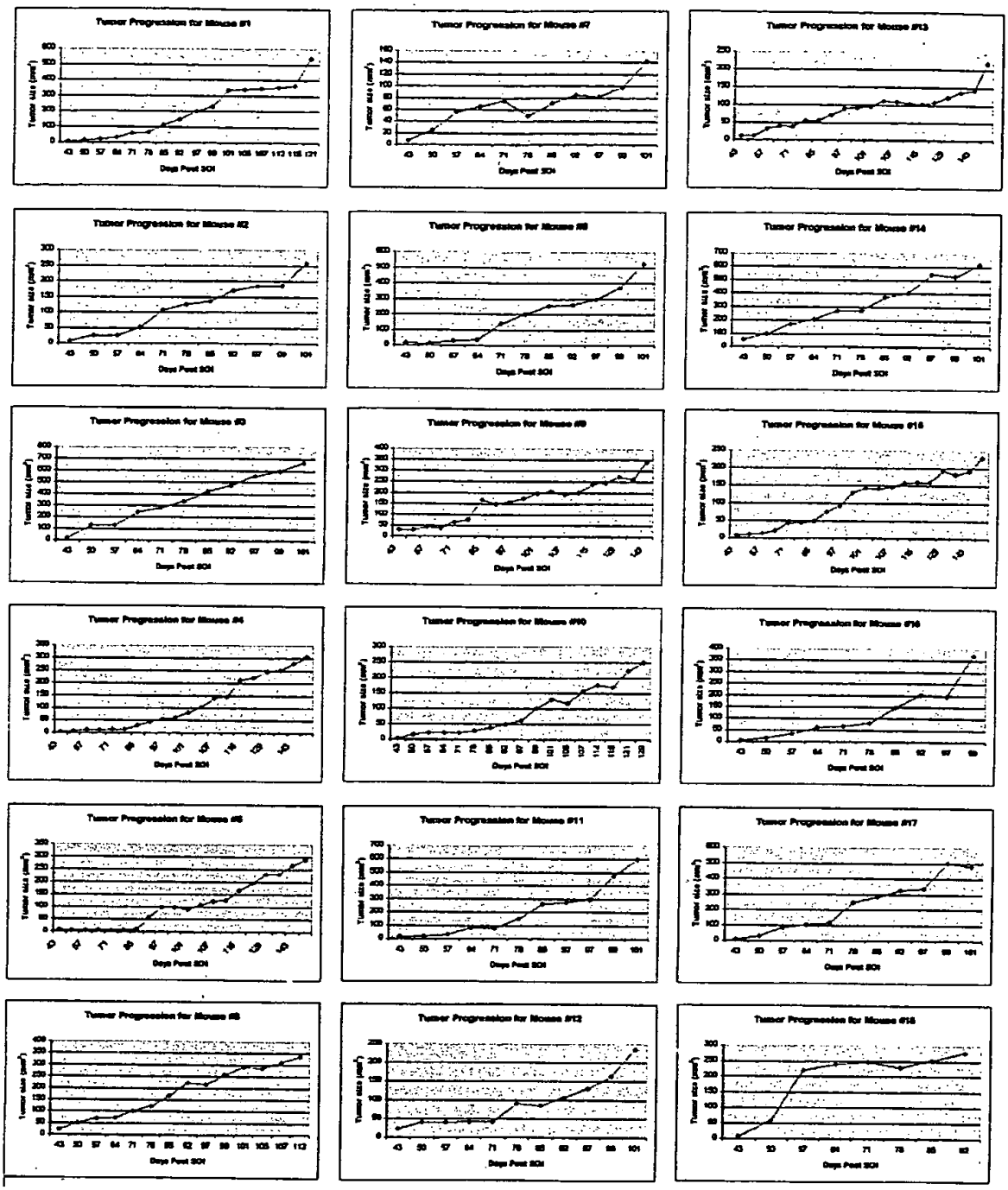

Fig. 1. Whole-body optical imaging of primary tumor growth in 18 orthotopically implanted pancreatic tumor-bearing mice. Consecutive external whole-body images of internally-growing BxPC-3 GFP tumors are demonstrated for 18 orthotopic mice. Although there were slight variations in tumor growth, a consistent increase in size was documented for each mouse by whole-body imaging without the need for laparotomy or any invasive procedure. See "Materials and Methods" for the GFP imaging procedure.

Portal Vein Injection. Six-week-old female B57Cl/6 mice were injected with 10^6 MiaPaCa-2-GFP cells in the portal vein. Cells were harvested by trypsinization and washed three times with cold serum-free medium and then injected in a total volume of 0.2 ml by using a 1-ml 27-gauge, latex-free syringe (Becton Dickinson, Franklin Lakes, NJ) within 30 min of harvesting.

Imaging. A Leica fluorescence stereo microscope model LZ12 (Leica Microsystems, Inc., Bannockburn, IL) equipped with a mercury 50W lamp power supply was used. Selective excitation of GFP was produced through a D425/60 band-pass filter and 470 DCXR dichroic mirror. Emitted fluorescence was collected through a long-pass filter GG475 (Chroma Technology, Brattleboro, VT) on a Hamamatsu C5810 3-chip cooled color CCD camera (Hamamatsu Photonics Systems, Bridgewater, NJ). Periodically, the tumor-bearing mice were also examined in a fluorescence light box illuminated by fiberoptic lighting at 440/20 nm with images collected with the Hamamatsu camera described above (Lightools Research, Inc., Encinitas, CA). High resolution images of 1024 × 724 pixels were captured directly on an IBM PC or continuously through video output on a high-resolution Sony VCR model SLV-R1000 (Sony Corp., Tokyo Japan). Images were processed for contrast and brightness and analyzed with the use of Image Pro Plus 4.0 software (Media Cybernetics, Silver Springs, MD).

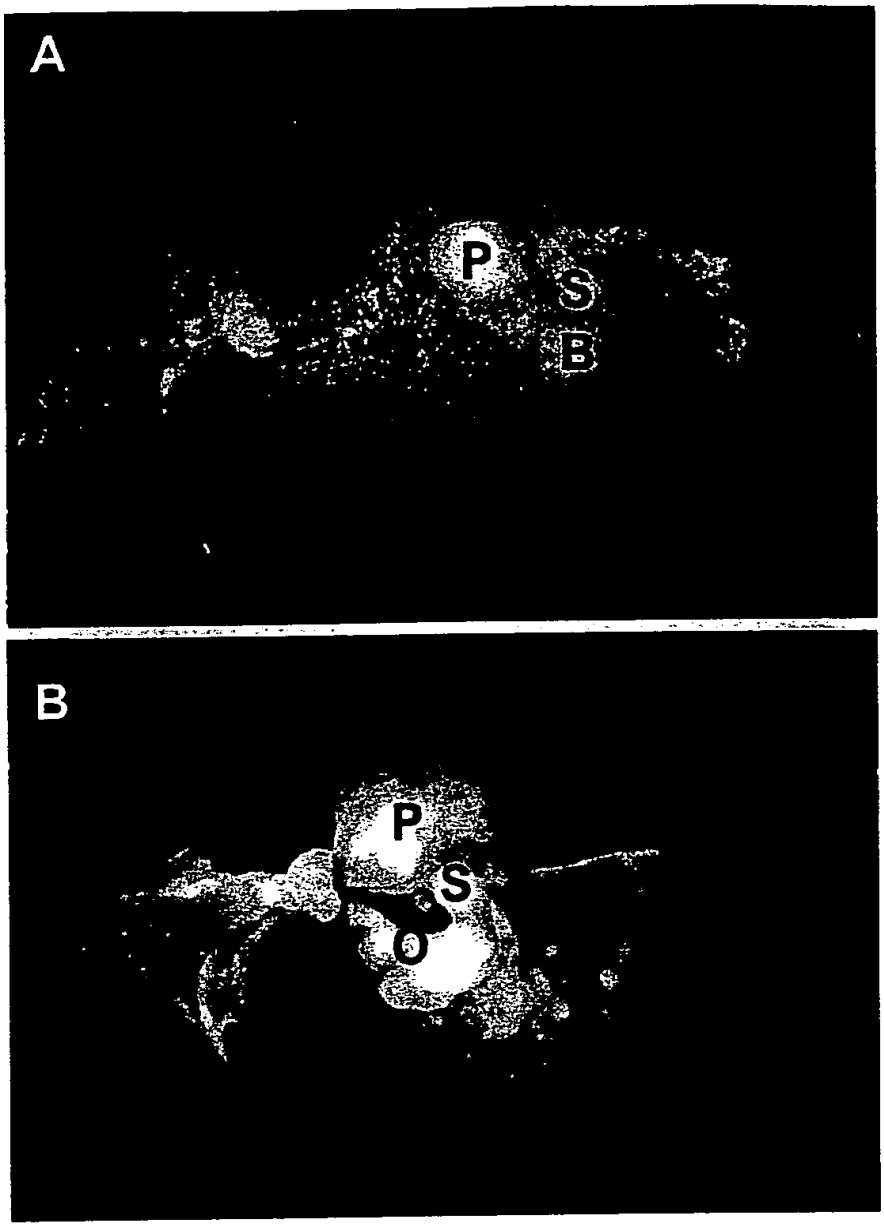

Fig. 2. External whole-body images of the BxPC-3-GFP primary tumor compared with internal images. See "Materials and Methods" for imaging equipment and procedures. *A*, fluorescent images of the primary pancreatic tumor (*P*), omental (*O*), bowel (*B*), and spleen. (*S*) metastases. *B*, an image of the same mouse after laparotomy internally localized the external images of metastatic tumors.

The image detection sensitivity and resolution as a function of tumor size and depth of this technology have been described previously (18).

RESULTS

Isolation of Stable, High-Level Expression GFP Transductants of BxPC-3-GFP and MiaPaCa-2-GFP Cells. GFP- and neomycin-transduced BxPC-3 and MiaPaCa-2 cells were selected previously in multiple steps for growth in levels of Geneticin (G418) up to 800 μg/ml and for high GFP expression (10). The selected BxPC-3-GFP and MiaPaCa-2-GFP cells have a strikingly bright GFP fluorescence that remains stable in the absence of selective agents after numerous passages (10).

Whole-Body Optical Imaging of Primary Tumor Growth in Orthotopically-Implanted Pancreatic Tumor-bearing Mice. Consecutive external whole-body images of internally growing BxPC-3-GFP primary tumors are demonstrated for 18 mice (Fig. 1). Although there were slight variations in the rate of tumor growth, a consistent increase in size over ~100 days was documented for each mouse by whole-body imaging without the need for laparotomy or any invasive procedure.

Comparison of External Whole-Body and Direct Intravital Images of the BxPC-3-GFP Primary Tumor and Multiple Metastases. The primary pancreatic tumor as well as spleen, omental, and bowel metastases were simultaneously visualized by whole-body imaging through the skin of the nude mouse with GFP (Fig. 2*A*). An image of an opened mouse internally localizes the external images of primary and metastatic tumors (Fig. 2*B*).

Real-Time Simultaneous Whole-Body Imaging of BxPC-3-GFP Tumor and Multiple Metastatic Growths. Consecutive whole-body simultaneous images of the primary BxPC-3-GFP pancreatic tumor, spleen, bowel, and omentum metastases are shown in Fig. 3*A*. These images were simultaneously obtained in a single animal on

THIS PAGE BLANK (USPTO)

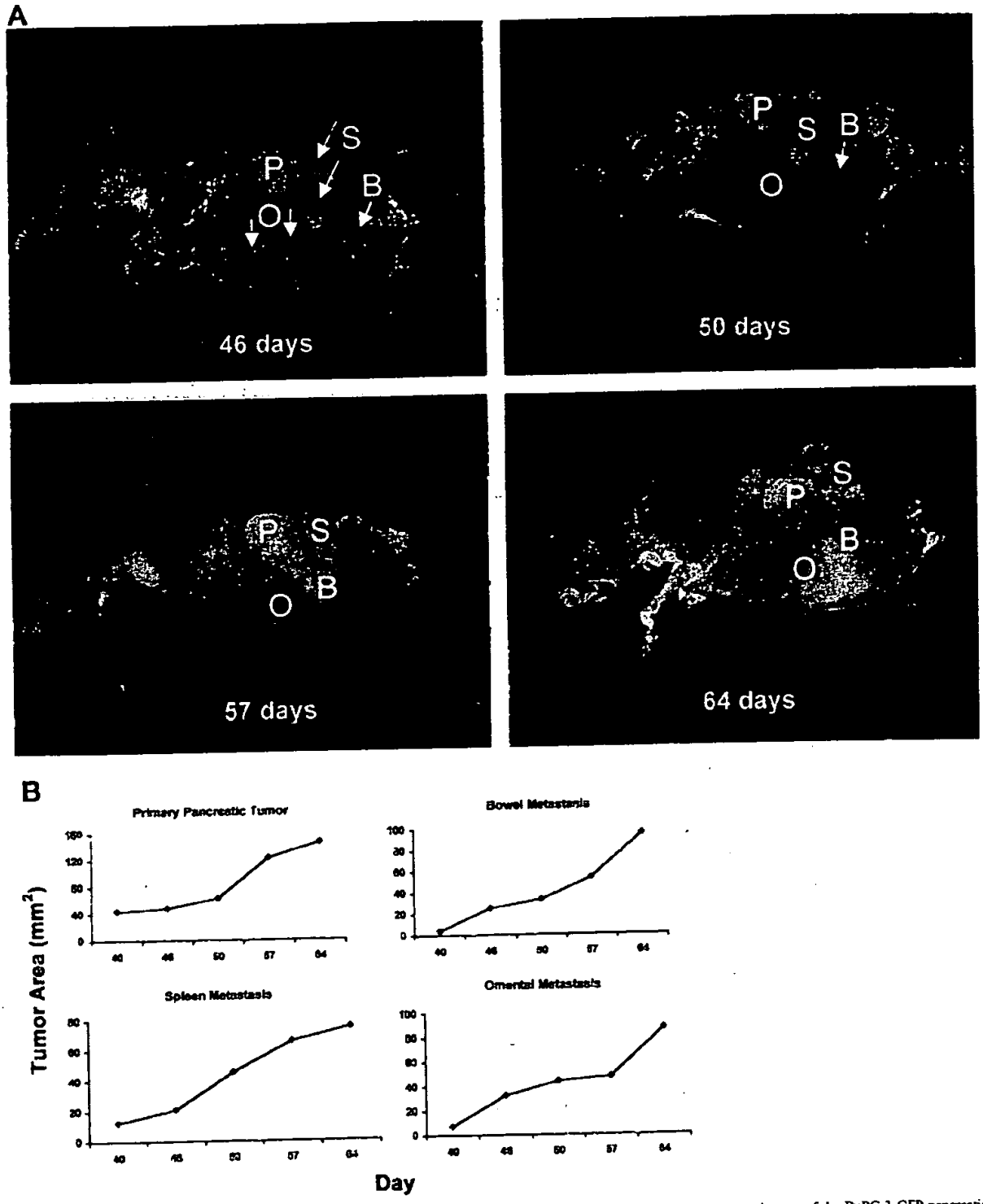

Fig. 3. *A*, consecutive external whole-body images of internally-growing BxPC-3-GFP tumors. A series of external fluorescence images of the BxPC-3-GFP pancreatic tumor in a single animal was obtained from days 46 to 64 after SOI of BxPC-3-GFP in a nude mouse. *B*, growth curves for primary pancreatic tumor (*P*), splenic metastasis (*S*), omental metastases (*O*), and bowel metastasis (*B*) as determined by whole-body imaging.

days 46, 50, 57, and 64 after SOI. In each of the sites, tumor growth and progression were quantified with image analysis. Growth curves (Fig. 3*B*) for the primary tumor and metastases at each of the above sites were constructed from the whole-body images. Thus, simultaneous metastases can be quantitated with whole-body imaging.

Comparison of Whole-Body and Intravital Images of Experimental Liver Metastasis of MiaPaCa-2-GFP. Metastatic lesions of MiaPaCa-2-GFP in the nude mouse liver were formed after portal vein injection. A clear external whole-body image of multiple metastatic lesions in the liver could be visualized through the

THIS PAGE BLANK (USPTO)

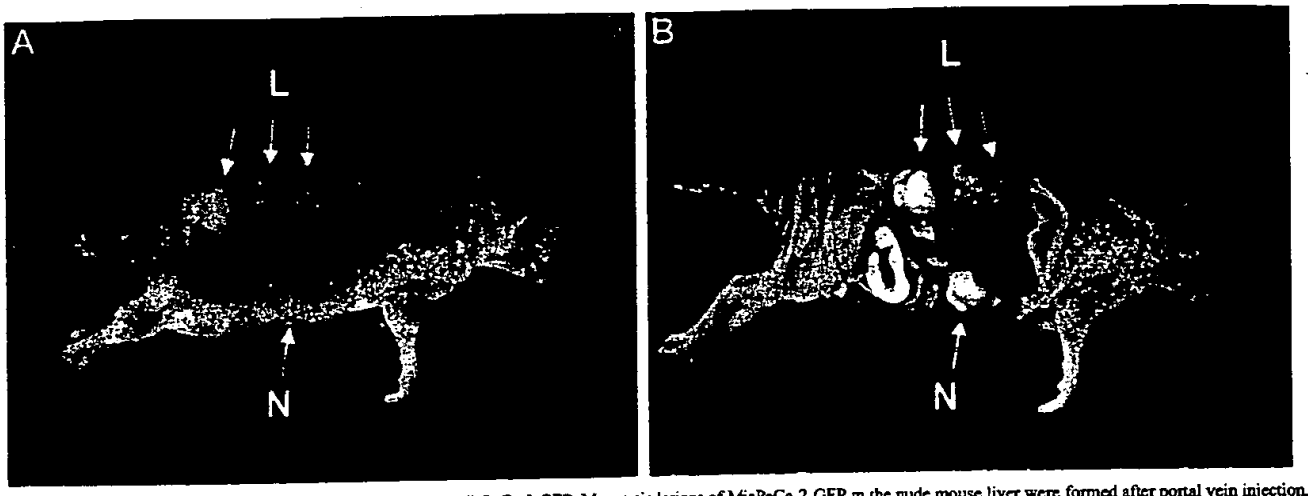

Fig. 4. *A*, external images of whole-body liver metastasis of MiaPaCa-2-GFP. Metastatic lesions of MiaPaCa-2-GFP in the nude mouse liver were formed after portal vein injection. A clear whole-body image of multiple metastatic lesions in the liver could be seen through the abdominal wall of the intact mouse. *B*, the whole-body image was comparable with the intravital image acquired from the exposed liver. *L*, liver metastases; *N*, nodal metastases.

abdominal wall of the intact mouse (Fig. 4*A*). Tumors were visualized throughout the multiple lobes of the liver. The whole-body image was comparable with the intravital image acquired from the exposed liver (Fig. 4*B*).

Sequential Intravital Images of Omental Micrometastasis of BxPC-3-GFP. A series of internal intravital fluorescence images of an omental micrometastasis from a BxPC-3-GFP pancreatic tumor in a single animal was obtained from days 36 to 70 after SOI of

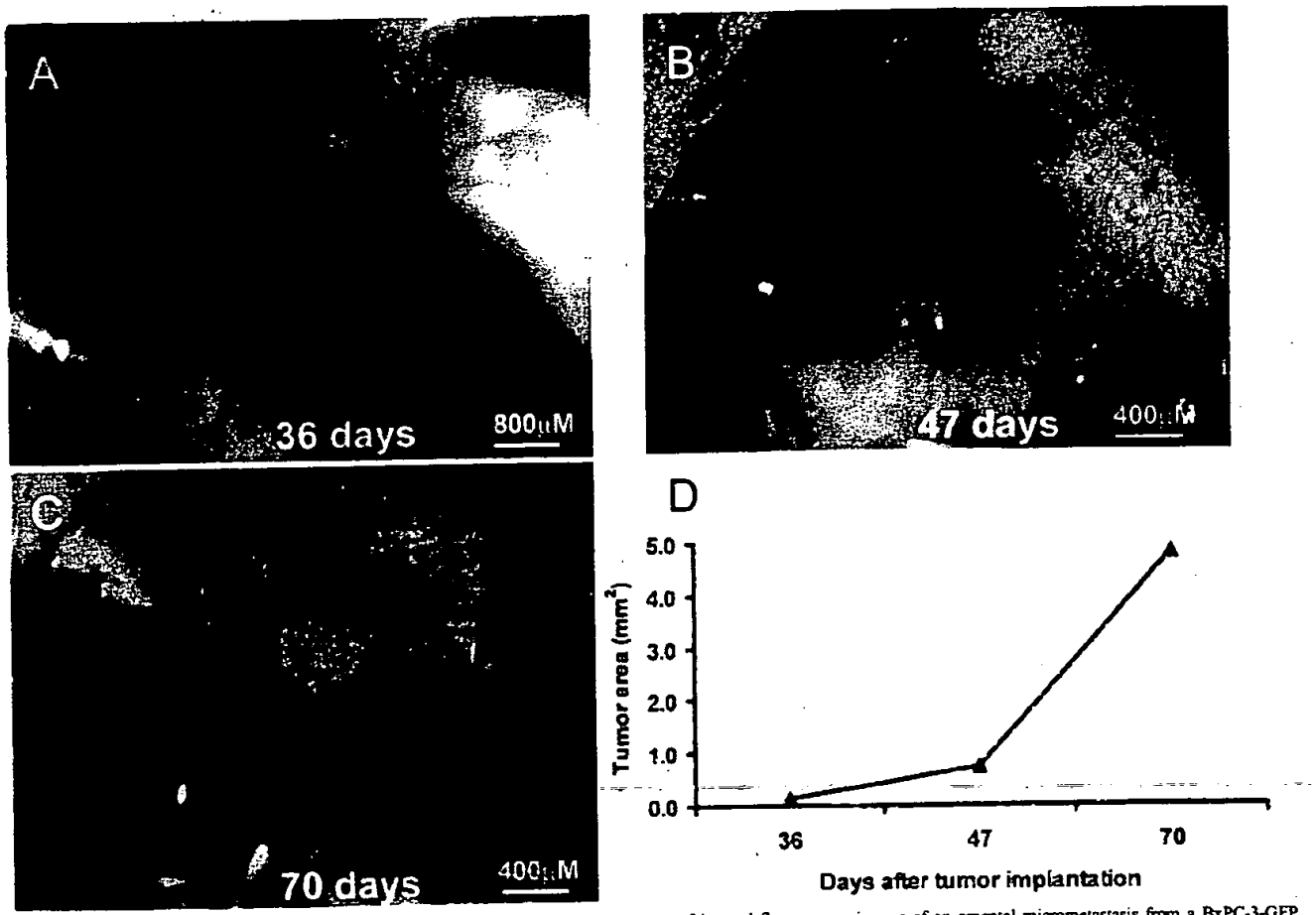

Fig. 5. Sequential intravital images of omental micrometastasis of BxPC-3-GFP. A series of internal fluorescence images of an omental micrometastasis from a BxPC-3-GFP pancreatic tumor in a single animal was obtained from days 36 to 70 after SOI of BxPC-3-GFP in a nude mouse during a laparotomy procedure (*A–C*). See "Materials and Methods" for details. As determined by internal imaging, the size of the metastatic lesion grew progressively with time (*D*). The area of the external image was 0.12 mm^2 at day 36, 0.74 mm^2 at day 47, and 4.8 mm^2 at day 70.

THIS PAGE BLANK (USP

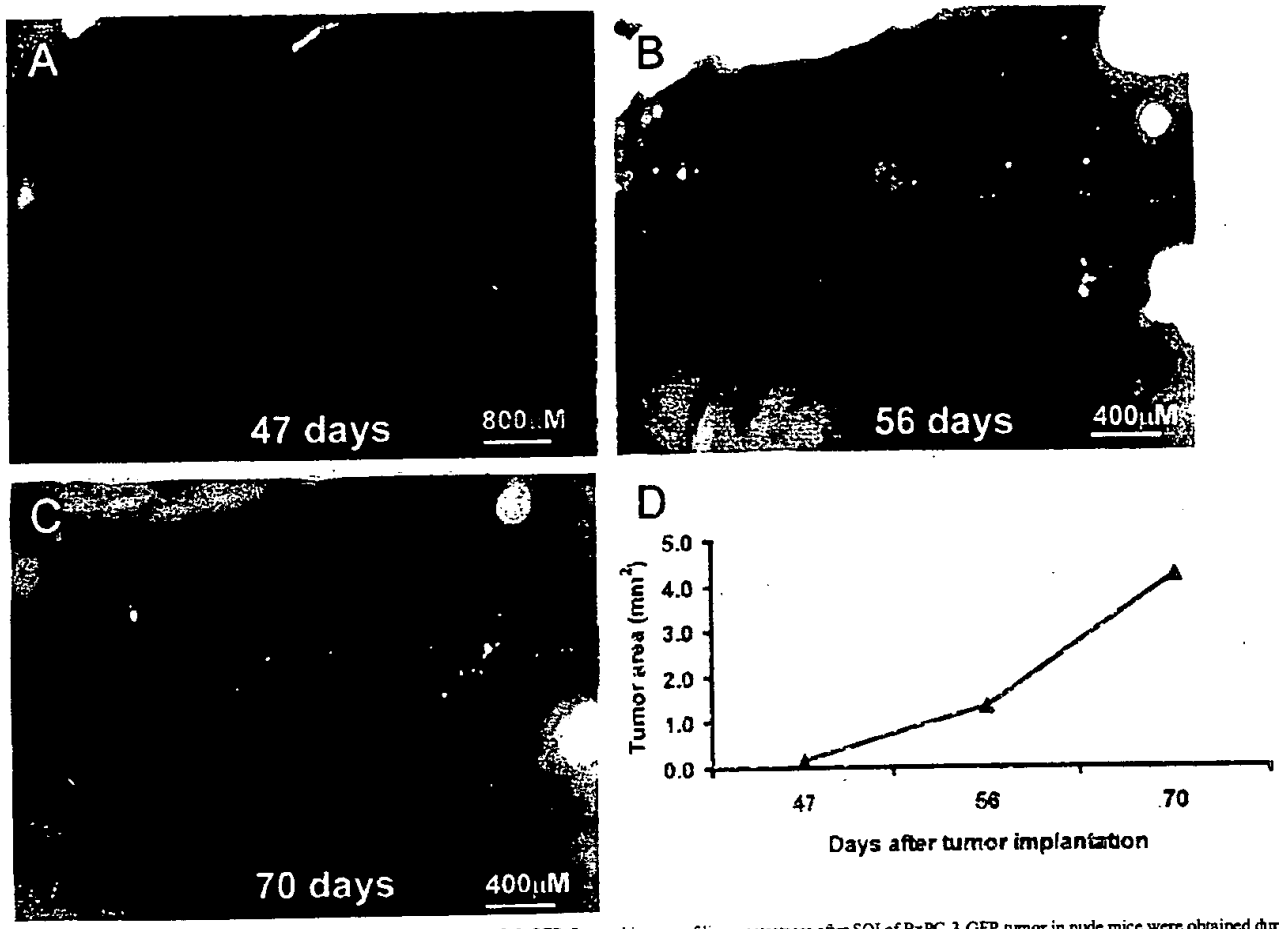

Fig. 6. Sequential intravital images of liver micrometastasis of BxPC-3-GFP. Internal images of liver metastases after SOI of BxPC-3-GFP tumor in nude mice were obtained during a laparotomy procedure (*A–C*). See "Materials and Methods." The area of the metastatic lesion was 0.14 mm^2 at day 47, 1.33 mm^2 at day 56, and 4.22 mm^2 at day 70 (*D*).

BxPC-3-GFP in a nude mouse. The images were acquired during a laparotomy procedure. As determined by intravital imaging, the size of the metastatic lesion grew progressively with time (Fig. 5). The area of the external image was 0.12 mm^2 at day 36, 0.74 mm^2 at day 47, and 4.8 mm^2 at day 70.

Sequential Intravital Images of Liver Micrometastasis of BxPC-3-GFP. Fig. 6 show a series of intravital fluorescence images of liver micrometastases after SOI of BxPC-3-GFP in nude mice. The area of the metastatic lesion was 0.14 mm^2 at day 47, 1.33 mm^2 at day 56, and 4.22 mm^2 at day 70.

DISCUSSION

In this report, we demonstrate an orthotopic model of metastatic pancreatic cancer where primary and site-specific metastatic growth can be readily imaged by GFP fluorescence in real time. The whole-body imaging of primary pancreatic tumors (Fig. 1) correlated with the more established method of tumor weight measurement. The whole-body images correlate with direct intravital images (Figs. 2 and 4). The whole-body imaging data can be quantitated (Fig. 3), thereby eliminating cumbersome, tedious dissection of the primary tumor and its metastases. Most importantly, primary and site-specific metastatic tumor growth can be simultaneously visualized and quantified in real time in the same mouse by whole-body imaging. GFP-expressing pancreatic tumors enabled the intravital imaging of micrometastasis, which were followed over time in the liver and spleen by rapid laparotomy and image acquisition. This could be repeated for at least three time points (Figs. 5 and 6).

The GFP-based fluorescence optical tumor imaging system presents many powerful and unique features. GFP expression in the tumor cells is stable over indefinite time periods, allowing the quantitative imaging of tumor growth and metastasis formation. Only the tumors and metastases contain the heritable *GFP* gene and are therefore selectively imaged with very high intrinsic contrast to other tissues. The very bright GFP fluorescence enables internal tumors and metastases to be externally observed in critical organs, such as the pancreas, spleen, and liver. No contrast agents, substrates, radioactive materials, other compounds, anesthesia, or treatment need be administered to the animals; only blue light illumination is necessary.

The GFP-expressing pancreatic tumor model should be useful for the evaluation of novel treatment strategies for pancreatic cancer including neoadjuvant chemotherapy or gene therapy (19, 20). Such strategies are needed to combat this highly lethal tumor that is seldom curable. In addition, early detection of pancreatic cancer can be evaluated in this model by the measurement of serum tumor markers (21). Finally, a greater understanding of the aggressive growth and metastatic potential of pancreatic cancer will be facilitated by the use of GFP-expressing tumor cells.

REFERENCES

1. Bouvet, M., Gamagami, R. A., Gilpin, E. A., Romeo, O., Sasson, A., Easter, D. W., and Moossa, A. R. Factors influencing survival after resection for periampullary neoplasms. Am. J. Surg., *180:* 13–17, 2000.
2. Bouvet, M., Binmoeller, K. F., and Moossa, A. R. Diagnosis of adenocarcinoma of the pancreas. *In:* J. L. Cameron (ed.) American Cancer Society Atlas of Clinical Oncology, pp. 67–86: Pancreatic Cancer. Hamilton, Ontario, Canada: BC Decker, 2001.

3. Marincola, F. M., Drucker, B. J., Siao, D. Y., Hough, K. L., and Holder, W. D., Jr. The nude mouse as a model for the study of human pancreatic cancer. J. Surg. Res., *47:* 520–529, 1989.
4. Bruns, C. J., Harbison, M. T., Kuniyasu, H., Eue, I., and Fidler, I. J. *In vivo* selection and characterization of metastatic variants from human pancreatic adenocarcinoma by using orthotopic implantation in nude mice. Neoplasia, *1:* 50–62, 1999.
5. Vezeridis, M. P., Doremus, C. M., Tibbetts, L. M., Tzanakakis, G., and Jackson, B. T. Invasion and metastasis following orthotopic transplantation of human pancreatic cancer in the nude mouse. J. Surg. Oncol., *40:* 261–265, 1989.
6. Fu, X., Guadagni, F., and Hoffman, R. M. A metastatic nude-mouse model of human pancreatic cancer constructed orthotopically with histologically intact patient specimens. Proc. Natl. Acad. Sci. USA, *89:* 5645–5649, 1992.
7. An, Z., Wang, X., Kubota, T., Moossa, A. R., and Hoffman, R. M. A clinical nude mouse metastatic model for highly malignant human pancreatic cancer. Anticancer Res., *16:* 627–631, 1996.
8. Furukawa, T., Kubota, T., Watanabe, M., Kitajima, M., and Hoffman, R. M. A novel patient-like treatment model of human pancreatic cancer constructed using orthotopic transplantation of histologically intact human tumor tissue in nude mice. Cancer Res., *53:* 3070–3072, 1993.
9. Tomikawa, M., Kubota, T., Matsuzaki, S. W., Takahasi, S., Kitajima, M., Moossa, A. R., and Hoffman, R. M. Mitomycin C and cisplatin increase survival in a human pancreatic cancer metastatic model. Anticancer Res., *17:* 3623–3625, 1997.
10. Bouvet, M., Yang, M., Nardin, S., Wang, X., Jiang, P., Baranov, E., Moossa, A., and Hoffman, R. Chronologically-specific metastatic targeting of human pancreatic tumors in orthotopic models. Clin. Exp. Metastasis, *18:* 213–218, 2000.
11. Yang, M., Jiang, P., An, Z., Baranov, E., Li, L., Hasegawa, S., Al-Tuwaijri, M., Chishima, T., Shimada, H., Moossa, A. R., and Hoffman, R. M. Genetically fluorescent melanoma bone and organ metastasis models. Clin. Cancer Res., *5:* 3549–3559, 1999.
12. Yang, M., Jiang, P., Sun, F. X., Hasegawa, S., Baranov, E., Chishima, T., Shimada, H., Moossa, A. R., and Hoffman, R. M. A fluorescent orthotopic bone metastasis model of human prostate cancer. Cancer Res., *59:* 781–786, 1999.
13. Chishima, T., Miyagi, Y., Wang, X., Baranov, E., Tan, Y., Shimada, H., Moossa, A. R., and Hoffman, R. M. Metastatic patterns of lung cancer visualized live and in process by green fluorescence protein expression. Clin. Exp. Metastasis, *15:* 547–552, 1997.
14. Budinger, T. F., Benaron, D. A., and Koretsky, A. P. Imaging transgenic animals. Annu. Rev. Biomed. Eng., *01:* 611–648, 1999.
15. Flotte, T. R., Beck, S. E., Chesnut, K., Potter, M., Poirier, A., and Zoloukhin, S. A fluorescence video-endoscopy technique for detection of gene transfer and expression. Gene Ther., *5:* 166–173, 1998.
16. Fu, X. Y., Besterman, J. M., Monosov, A., and Hoffman, R. M. Models of human metastatic colon cancer in nude mice orthotopically constructed by using histologically intact patient specimens. Proc. Natl. Acad. Sci. USA, *88:* 9345–9349, 1991.
17. Sun, F. X., Sasson, A. R., Jiang, P., An, Z., Gamagami, R., Li, L., Moossa, A. R., and Hoffman, R. M. An ultra-metastatic model of human colon cancer in nude mice. Clin. Exp. Metastasis, *17:* 41–48, 1999.
18. Yang, M., Baranov, E., Jiang, P., Sun, F-X., Li, X-M., Li, L., Hasegawa, S., Bouvet, M., Al-Tuwaijri, M., Chishima, T., Shimada, H., Moossa, A. R., Penman, S., and Hoffman, R. M. Whole-body optical imaging of green fluorescent protein-expressing tumors and metastases. Proc. Natl. Acad. Sci. USA, *97:* 1206–1211, 2000.
19. Bouvet, M., Bold, R. J., Lee, J., Evans, D. B., Abbruzzese, J. L., Chiao, P. J., McConkey, D. J., Chandra, J., Chada, S., Fang, B., and Roth, J. A. Adenovirus-mediated wild-type *p53* tumor suppressor gene therapy induces apoptosis and suppresses growth of human pancreatic cancer. Ann. Surg. Oncol., *5:* 681–688, 1998.
20. Lee, N.C., Bouvet, M., Nardin, S., Jiang, P., Baranov, E., Rashidi, B., Yang, M., Wang, X., Moossa, A. R., and Hoffman, R. M. Antimetastatic efficacy of adjuvant gemcitabine in a cancer pancreatic cancer orthotopic model. Clin. Exp. Metastasis, *18:* 379–384, 2000.
21. Bouvet, M., Nardin, S. R., Burton, D. W., Lee, N. C., Yang, M., Wang, X., Baranov, E., Behling, C., Moossa, A. R., Hoffman, R. M., and Deftos, L. J. Parathyroid hormone-related protein acts as a tumor marker in an orthotopic model of pancreatic adenocarcinoma. Pancreas, in press, 2002.

THIS PAGE BLANK (US

Int. J. Cancer: 49, 938–939 (1991)

Publication of the International Union Against Cancer
Publication de l'Union Internationale Contre le Cancer

LETTER TO THE EDITOR

Dear Sir,

Extensive multi-organ metastasis following orthotopic onplantation of histologically-intact human bladder carcinoma tissue in nude mice

Human transitional-cell bladder carcinoma can vary from low invasive potential to high metastatic activity. Until recently, there were no appropriate models to study the potential for metastasis and mechanisms involved in bladder carcinoma. A possible solution to these problems has emerged with the implementation of so-called "orthotopic" transplantation techniques (Fidler, 1990). Ibrahiem et al. (1983) and Ahlering et al. (1987) found that orthotopic implantation of a bladder tumor-cell suspension into the rat bladder produced some tumor metastasis, whereas subcutaneous implantation did not. These results indicated that the orthotopic site of injection enabled the transitional-cell carcinoma cells to express part of their invasive potential.

Theodorescu et al. (1990) observed that the RT-4 human bladder carcinoma line is not invasive in nude mice, even after orthotopic injection. However, when a mutated human H-ras gene was transfected into RT-4 so that over-expression of the gene occurred in selected cell lines such as RT-4-mr-10 (RT-10), the selected cell line was able to locally invade the bladder after transurethral orthotopic inoculation of disaggregated cells. With regard to the orthotopically-implanted RT-10 in the nude mouse, broad areas of invasion of transitional-cell carcinoma deep into the muscularis propria of the bladder occurred which in some instances extended into the surrounding adipose tissue and vascular spaces. However, no contiguous or metastatic spread of RT-10 was found in other organs. The parental cell lines and the ras-transfectants all produced tumors when inoculated s.c. However, the tumors grew in the s.c. site as pseudo-encapsulated masses with no evidence of tissue invasion at the s.c. site.

We have developed an intact-tissue onplant method of orthotopic transplantation of human tumors in nude mice (Fu et al., 1991). This method, first developed with colon cancer, allows patient tissue to be directly onplanted on the scraped serosa of colon or cecum, with resulting facilitation of local growth, extensive regional metastases, lymph-node involvement and liver metastases (Fu et al., 1991). In the present study, the onplant method was carried out using subcutaneously-grown tissue of RT-10 as a tissue source. The RT-10 xenograft was grown s.c. in a 4-week-old outbred female nude mice, removed and cut into 2-mm^3 pieces. Nine nude mice were anesthetized with isofluorene inhalation. The lower abdomen of the nude mouse was sterilized with iodine and alcohol swabs, then a small midline incision was made and the urinary bladder exposed. The surgical adhesive 2-cyanoacrylic acid ester was applied on one side of the 2-mm^3 tumor xenograft tissue and the piece of tumor was subsequently glued on top of the urinary bladder. The abdominal incision was closed with 7-0 silk surgical sutures in one layer and the animals were then kept in a sterile environment. For s.c. implantation, 4 nude mice were anesthetized with isoflurane inhalation. One side of the flank was sterilized with iodine and alcohol swabs and, after a small incision was made, a 2-mm^3 piece of RT-10 xenograft tissue was implanted s.c. The wound was then closed with 7-0 silk surgical sutures and the animals were kept in a sterile environment. When the mice were moribund or dead, full autopsies were performed. At autopsy all major organs were grossly examined. Each organ was then fixed in 10% formalin, dehydrated, embedded in paraffin, sectioned and stained with hematoxylin and eosin.

The results described below indicate extensive local growth and invasion of the bladder, with metastases occurring in the regional and distant lymph nodes, liver, pancreas, spleen, and tissue adjacent to the adrenal gland and ureter, as well as the lungs, after orthotopic onplantation of histologically-intact RT-10 bladder carcinoma (Table I, Fig. 1). These results contrast with those seen when disaggregated RT-10 cells are injected transurethrally, in which case no metastases are formed (Theodorescu et al., 1990). They also contrast with results seen when RT-10 was implanted s.c., only encapsulated tumors being formed in this case. Therefore, it appears that the orthotopic onplant method using histologically-intact tissue makes for very extensive metastatic capability, possibly as a result of the maintenance of the native tissue architecture of the tumor and site of onplantation.

For bladder tumors and possibly others, it may be crucial for the tissue to remain histologically intact in the orthotopic xenografting process in order that the metastatic potential be fully expressed. Thus, it is quite possible that native cell-cell interactions are necessary for the full expression of metastatic potential in these tumors. The orthotopic onplant model described

TABLE I – ORTHOTOPIC ONPLANTATION OF HISTOLOGICALLY-INTACT HUMAN BLADDER CARCINOMA RT-4-mr-10 TISSUE *VS.* ORTHOTOPIC INJECTION OF DISAGGREGATED RT-4-mr-10 CELLS *VS.* SUBCUTANEOUS GROWTH

Implantation strategy	Mouse number	Primary tumor growth	Local invasion	LN metastasis[1]	Organ metastasis[2]
Orthotopic onplantation of intact tissue	Total of 9	9/9	9/9	8/9	7/9
Orthotopic injection of disaggregated cells[3]	Total of 20	8/20	8/20	0/20	0/20
Subcutaneous implantation in flank	Total of 4	3/4	0/4	0/4	0/4

See text for experimental details.
[1]Lymph nodes include iliac, inguinal and axillary.–[2]Organs involved include liver, lung, pancreas spleen, diaphragm, adjacent tissue of adrenal gland and ureter.–[3]From Theodorescu *et al.* (1990).

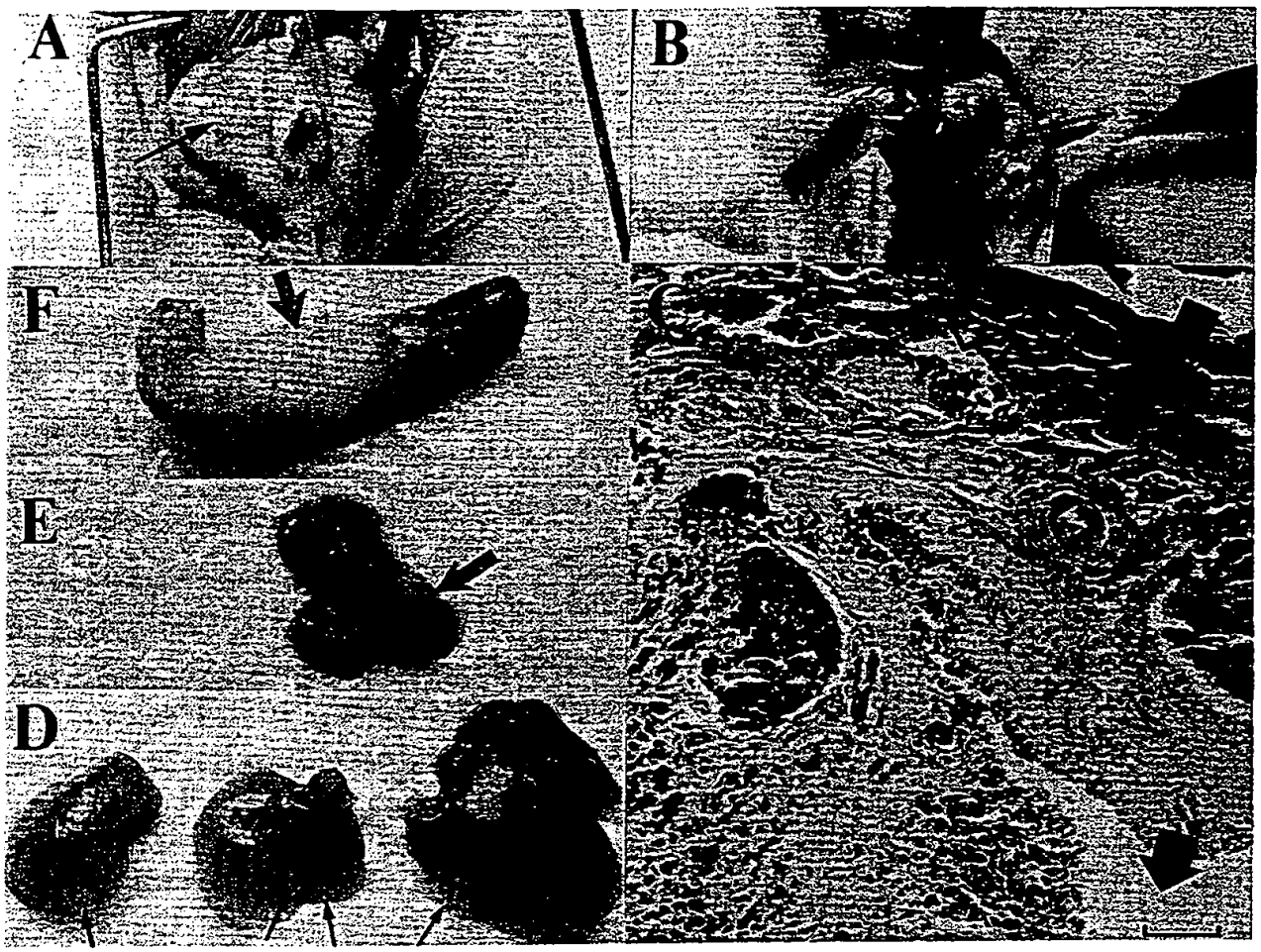

FIGURE 1 – Orthotopic growth and distant metastases of orthotopically-onplanted histologically-intact human bladder carcinoma in nude mice. Tumor was onplanted as described in the text. *(a)* Local growth of onplanted bladder tumor measuring 18 × 22 mm (black arrow). Original mouse bladder marked by blue arrow. *(b)* Metastatic spread of bladder tumor to the axillary lymph nodes (blue arrows). *(c)* Pathohistology of tumor invading nude mouse bladder. Blue arrow indicates the bladder wall. Black arrow indicates the remaining lumen of the bladder. Tumor invaded the majority of the bladder (the area below the hollow arrows). Bar = 14 μm. *(d)* Bladder tumor metastasized to the liver (arrows indicate the tumor deposits). *(e)* Bladder tumor metastasized to the pancreas. Arrow indicates the tumor mass. *(f)* Bladder tumor metastasized to the spleen. Arrow indicates the tumor mass. Pathohistology of all metastases is similar to that of primary tumor shown in *(c)*.

here seems very realistic for metastatic bladder cancer in that, in the clinical situation, the tumor can invade the serosa transmurally and metastasize distantly, growing out from the serosa as in the model described here.

Yours sincerely,

Xinyu FU, Dan THEODORESCU, Robert S. KERBEL and Robert M. HOFFMAN

AntiCancer, Inc., 5325 Metro Street, San Diego, CA 92110; Sunnybrook Health Science Centre, Reichmann Research Building, 2075 Bayview Ave., S-218 Toronto, Ontario M4N 3M5, Canada; Laboratory of Cancer Biology, Department of Pediatrics, 0609F, University of California, San Diego, La Jolla, CA 92093-0609, USA.

April 30, 1991.

REFERENCES

AHLERING, T., DUBEAU, L. and JONES, P.A., A new *in vivo* model to study invasion and metastasis of human bladder carcinoma. *Cancer Res.*, **47**, 6660–6665 (1987).

FIDLER, I.J., Critical factors in the biology of human cancer metastasis: twenty-eighth G.H.A. Clowes Memorial Award Lecture. *Cancer Res.*, **50**, 6130–6138 (1990).

FU, X., BESTERMAN, J.M., MONOSOV, A. and HOFFMAN, R.M., Models of human metastatic colon cancer in nude mice orthotopically constructed by using histologically-intact patient specimens. *Proc. nat. Acad. Sci. (Wash.)*, **88**, 9345–9349 (1991).

IBRAHIEM, EL H.I., I., NIGAM, V.N., BRAILOVSKY, C.A., MADARNAS, P. and ELHILALI, M., Orthotopic implantation of primary *N*-[4-(5-Nitro-2-furyl)-2-thiazolyl]formamide-induced bladder cancer in bladder submucosa: an animal model for bladder cancer study. *Cancer Res.*, **43**, 617–622 (1983).

THEODORESCU, D., CORNIL, I., FERNANDEZ, B. and KERBEL, R.S., Overexpression of normal and mutated forms of *Hras* induces orthotopic bladder invasion in a human transitional cell carcinoma. *Proc. nat. Acad. Sci. (Wash.)*, **87**, 9047–9051, (1990).

COMPARISON OF OTTO AND ANTICANCER MODELS WITH CLINICAL PATTERN OF METASTASIS

Tumor Type	Cell Line	Otto (1)	AntiCancer MetaMouse	Clinical Pattern of Metastasis
Renal cell carcinoma	RCC 7 RCC 9 RCC 14	No metastasis.		Lung, lymph nodes, liver,and brain (3, Chapter 1057).
	SN12C		Lung, lymph nodes, liver.	

REFERENCES:

1. Otto, U., Huland, H., Baisch, H., and Kloppel, G. Transplantation of human renal cell carcinoma into NMRI nu/nu mice. III. Effect of irradiation on tumor acceptance and tumor growth. J. Urol. 134, 170-174, 1985.

2. An, Z., Jiang, P., Wang, X., Moossa, A.R., and Joffman, R.M. Development of a high metastatic orthotopic model of human renal cell carcinoma in nude mice: benefits of fragment implantation compared to cell-suspension injection. Clinical & Experimental Metastasis 17, 265-270, 1999.

3. Holland, James E., and Frei, Emil III (eds.), Cancer Medicine, 5th Edition. Hamilton, Ontario, Canada: B.C. Decker, Inc., 2000.

Exhibit 3 RMH

THIS PAGE BLANK

Clinical & Experimental Metastasis 17: 265–270, 1999.

2

Development of a high metastatic orthotopic model of human renal cell carcinoma in nude mice: benefits of fragment implantation compared to cell-suspension injection

Zili An[1], Ping Jiang[1], Xiaoen Wang[1], A.R. Moossa[2] & Robert M. Hoffman[1,2]
[1]*AntiCancer, Inc., 7917 Ostrow St., San Diego, CA 92111, USA;* [2]*Department of Surgery, University of California, 200 W. Arbor Dr., San Diego, CA 92103-8220, USA*

Received 15 February 1999; accepted in revised form 25 March 1999

Key words: angiogenesis, metastasis, orthotopic fragment transplant, renal cancer

Abstract

In this study we compared the metastatic rate of human renal cell carcinoma SN12C in two orthotopic nude mouse models: surgical orthotopic implantation (SOI) of histologically intact tumor tissue and cellular orthotopic injection (COI) of cell suspensions in the kidney. The primary tumors resulting from SOI were larger and much more locally invasive than primary tumors resulting from COI. SOI generated higher metastatic expression than COI. The differences in metastatic rates in the involved organs (lung, liver, and mediastinal lymph nodes) were 2–3 fold higher in SOI compared to COI ($P < 0.05$). Median survival time in the SOI model was 40 days, which was significantly shorter than that of COI (68 days) ($P < 0.001$). Histological observation of the primary tumors from the SOI model demonstrated a much richer vascular network than the COI model. Lymph node and lung metastases were larger and more cellular in the SOI model compared to COI. We conclude that the tissue architecture of the implanted tumor tissue in the SOI model plays an important role in the initiation of primary tumor growth, invasion, and distant metastasis. This study directly demonstrates that the implantation of histologically intact tumor tissue orthotopically allows accurate expression of the clinical features of human renal cancer in nude mice. This model should be of value in cancer research and antimetastatic drug discovery for renal cancer, a currently very poorly responding malignancy.

Introduction

Human renal cell carcinoma, although a relatively uncommon type of cancer, has a very poor prognosis due to the lack of effective therapy. The prognosis of patients with renal cancer is determined mainly by the extent of metastasis, primarily in the lung [1].

The search for new anticancer agents and treatment modalities has been impeded by the limited availability of a clinically accurate mouse model, especially a highly metastatic model. Currently orthotopic implantation of human cancer into nude mice has already gained wide acceptance as the optimal method of creating more reliable models to study human cancer growth and progression *in vivo*, especially metastasis. Orthotopic implantation, as opposed to heterotopic implantation, allows more accurate expression of the biological nature of the original human tumor, including growth rate, morphology and metastasis [2–4].

Several laboratories have established metastatic nude mice models of human renal cell carcinoma by injecting tumor cell suspensions into the renal subcapsule of the nude mice [1, 5–8]. Cell leakage can cause experimental variability in this technique [6, 26]. In addition, mechanical and/or enzyme processing of tumor cells disrupts inter-cell communication and the natural tumor-stromal structure. Thus, cell suspensions do not have the native three-dimensional tissue architecture, which seems important for the full expression of their spontaneous metastatic potential as seen in direct comparisons of orthotopic implantation of cell suspensions and intact tissue [18, 20].

Over the past eight years in our laboratory, we have established novel methods of surgical orthotopic implantation (SOI) of histologically intact human tumor tissue of various types in nude mice [9–14, 17–20]. The SOI models demonstrated extensive metastatic potential. In this study we applied the principle of SOI to human renal cell carcinoma. A head-to-head comparison of tumor growth, invasion, metastasis, and survival was made between the SOI model and the cellular orthotopic injection (COI) of cell suspensions. The results demonstrate that the intact tumor tissue implantation is significantly advantageous over cell suspension injection for expression of malignancy, metastasis, and shortened survival.

Correspondence to: Robert M. Hoffman, AntiCancer, Inc., 7917 Ostrow St., San Diego, CA 92111, USA. Tel: +1-619-654-2555; Fax: +1-629-268-4175; E-mail: all@anticancer.com

Materials and methods

Animals

Athymic nu/nu Balb/c mice (Charles River Laboratories, Wilmington, MA), 4–5 weeks old, were used in the study. They were maintained in a specific pathogen-free environment in compliance with USPHS guidelines governing the care and maintenance of experimental animals. All animal studies were conducted in accordance with the principles and procedures outlined in the National Institutes of Health Guide for the Care and Use of Laboratory Animals under assurance number A3873-1. Mice were fed with autoclaved laboratory rodent diet (Tecklad LM-485, Western Research Products, Orange, CA).

Cell and cell culture conditions

Human renal cell carcinoma cell line SN12C was first established in culture from a primary renal cell carcinoma from a 43-year-old man [4]. The cells used in this study were from cryopreserved vials. Prior to implantation, frozen cells were thawed and passed twice in RPMI 1640 culture medium (Bio-Whittaker, Walkersville, MD) supplemented with 10% fetal bovine serum, nonessential amino acids, L-glutamine, sodium pyruvate, sodium bicarbonate, glucose, and two-fold vitamin solution (GIBCO BRL, Grand Island, NY). 100 μ/ml of penicillin and 100 ug/ml streptomycin were added in the culture medium. The cells were cultured in a humidified atmosphere containing 5% CO_2 and 95% air. All cells were examined and found to be free of *Mycoplasma* and viruses prior to use (Microbiological Associates, Bethesda, MD).

Cells for implantation were harvested from subconfluent cultures with a solution of 0.25% trypsin and 0.02% EDTA, collected and washed twice in Hanks balanced salt solution (HBSS) and resuspended in HBSS to give the appropriate volume for orthotopic and subcutaneous injection. Only single-cell suspensions with viability of more than 90% as assessed by trypan blue dye exclusion were used for injection.

Renal subcapsule cellular orthotopic injection (COI) of cell suspensions

Mice were anesthetized with isoflurane (Ohameda Caribe Inc., Guayama, PR). A small incision was made along the left flank of the mouse. The kidney was exposed with a small retractor. A 27-gauge needle was used for the tumor cell injection. The needle was inserted into the lower pole of the kidney and advanced until its point reached just below the renal subcapsule. Two million viable SN12C tumor cells were injected in a volume of 0.05 ml HBSS. Visible bulla formation between the renal parenchyma and the capsule was the criterion for a successful injection. The needle was then carefully removed and animals checked for local bleeding and extra-renal leakage of tumor cell suspension. If leakage or severe bleeding was found, the animal was eliminated. Reopening the abdomen was performed to check the existing bulla under the renal capsule after the animals recovered from anesthesia and started to move. In this study, only three mice were found to have leakage and one mouse had bleeding. They were all replaced with new animals. After the injection, the kidney was wrapped with the surrounding soft tissue with an 8-0 nylon suture. The abdominal wall was closed with a 6-0 silk suture. All procedures were carried out under a 5X-dissection microscope.

Subcutaneous tumor growth

Cells suspended as above were injected subcutaneously at 2×10^6 per nude mouse. The purpose of growing the subcutaneous tumor was for stock tumor tissue to be used in SOI. When the tumors were growing in the log phase, they were harvested. The periphery of the tumors was collected following removal of necrotic and less viable tissue near the center of the tumor. Tumor tissue was cut into small pieces of one cubic millimeter each, which were mixed thoroughly during implantation to insure that all the mice were transplanted with equally viable tissue. The use of stock tumor tissue for SOI grown at the subcutaneous site was for experimental convenience and for tumor tissue of high malignant potential when transplanted by SOI in the renal capsule.

Renal subcapsule surgical orthotopic implantation (SOI) of tumor fragments

Mice were anesthetized by isoflurane and positioned laterally. A small incision was made along the left flank of the mice. The kidney was exposed with a small retractor. A small cut was made on the renal subcapsule. One piece of tumor tissue was inserted into the capsule. The cut was covered with surrounding soft tissue using an 8-0 nylon suture. The abdomen was closed with a 6-0 silk suture. All procedures were carried out under a 5X-dissection microscope.

Evaluation of tumor growth and metastasis

All mice from both transplantation procedures were closely observed and allowed to live through their natural course of disease after tumor cell implantation. At time of death, one fragment of the primary tumor and two fragments from each lobe of the lung and the liver as well as all detectable mediastinal lymph nodes were sampled and immersed in 10% formalin for fixation. The sampled tissues were dehydrated, embedded, sectioned and then stained with standard hematoxylin and eosin staining procedure for microscopic examination.

Statistical analysis

The incidence of survival at defined time points and the incidence of metastasis in both cell injection and tissue implantation were analyzed using the Fisher Exact test. The median survival was analyzed using the Wilcoxon Rank-Sum test.

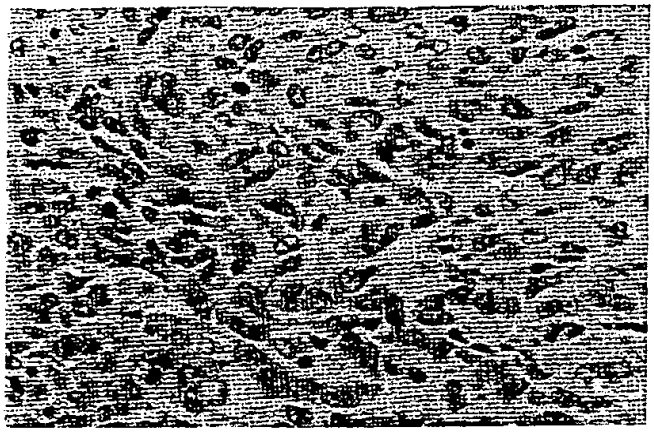

Figure 1. Histology of the primary tumor from the SOI model. Note the bizarre nuclei and polygonal shapes of the cells.

Figure 2. Gross picture of primary tumor in the SOI model. Note that the liver and the spleen (hollow arrows) are adhered to by the primary tumor (black arrows).

Results

Primary tumor growth

The human renal carcinoma cell line SN12C implanted by SOI with intact tumor tissue grew very aggressively in the renal subcapsule of nude mice. The take rate was 100%, compared with 75% for COI. In the SOI and COI models, the tumor cells were polygonal and contained large bizarre nuclei (Figure 1). In the SOI model, all primary tumors destroyed most of the renal parenchyma and disfigured the abdomen (Figure 2). The local invasion was extensive, with the abdominal wall, the pancreas, the spleen, the liver and a large portion of the intestine adhering to the primary tumor (Figure 2). In contrast, COI generated relatively small primary tumors with less severe local invasion, i.e. the spleen and the liver were usually spared (Figure 3).

Vascularity of the primary tumor

Close examination of the histology of the primary tumor revealed that the primary tumors in the SOI model were rich in blood vessels. In contrast in the COI model, blood vessels were sparse (Figure 4).

Figure 3. Gross picture of the primary tumor in the COI model. The liver and the spleen (hollow arrows) are free of invasion from the tumor (black arrows).

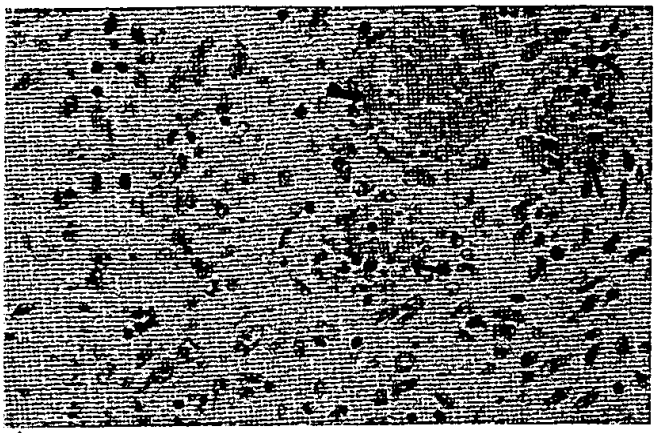

A

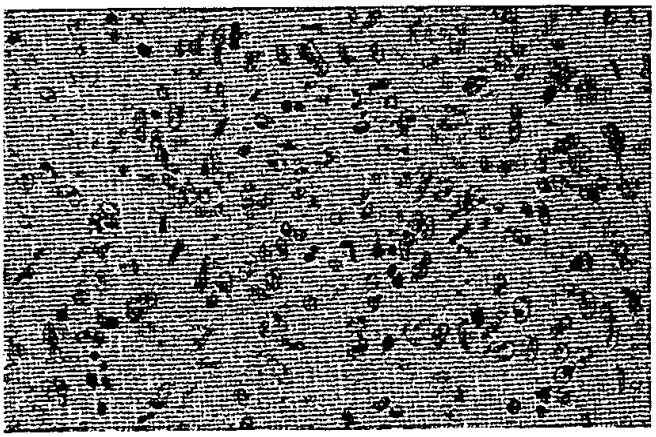

B

Figure 4. A. Photomicrograph shows the rich vasculature (arrows) in the primary tumor of the SOI model. B. Photomicrograph shows apparent lack of vasculature in the COI model.

Systemic metastasis

Both models demonstrated metastases in the lung, the liver and the mediastinal lymph nodes. However, the metastatic rate for lung, liver and mediastinal lymph nodes was 2–3 fold higher in SOI compared to COI. This difference in incidence was statistically significant ($P < 0.05$ by the Fisher-Exact test) (Table 1).

Table 1. Comparison of metastatic and survival rates of human renal carcinoma SN12C in SOI and COI models of renal carcinoma

Orthotopic model	Take rate	Median survival*	Site and incidence of metastasis**		
			Lung	Liver	MLN***
Tissue implant (SOI)	100%	40 days	12/20	8/20	19/20
Cell injection (COI)	75%	68 days	4/15	2/15	7/15

*$P < 0.001$ by the Wilcoxon Rank-Sum test. **$P < 0.05$ when the incidence of metastasis in all the three organs listed was compared between the two models by the Fisher Exact Test. ***MLN – mediastinal lymph node.

Mediastinal lymph nodes were usually exceedingly enlarged upon autopsy of mice with the SOI model. Some modified lymph nodes were as large as 0.5 cm. Microscopically, widespread infiltration of tumor cells was found in the subcapsular, the cortical, and medullary areas. Some tumor cells formed large nests that totally replaced the nodal parenchyma. In many of the nodes analyzed, tumor cells occupied the whole node and the lymphatic cells could be barely seen. In contrast in the COI model, lymph node metastases were relatively small and constricted. Clusters of metastatic cells were spotted within the nodes but did not form large nests and seldom totally replaced large areas of nodal parenchyma (Figure 5).

The lung metastases were disseminated in the SOI models. Large nests of tumor cells usually squeezed the nearby alveoli. In contrast, in the COI model, lung metastases were small and less diffuse (Figure 6).

Liver metastases were observed in both the SOI and COI models (Table 1). There was a significant higher liver metastatic rate in the SOI model compared to the COI. However, no morphological differences in the liver metastases lesions were observed (Figure 7).

Survival of animals

The SOI model demonstrated a shorter median survival (40 days) compared to the COI model (68 days) ($P < 0.001$ by the Wilcoxon Rank-Sum test) (Table 1 and Figure 8). When all the animals in the SOI group had died, 80% of the mice in COI group were still alive ($P < 0.001$ by the Fisher Exact Test). When the metastatic rates in different organs were taken into account, it was probable that the SOI model succumbed mostly due to distant metastases while in the COI model death was due to primary tumor burden.

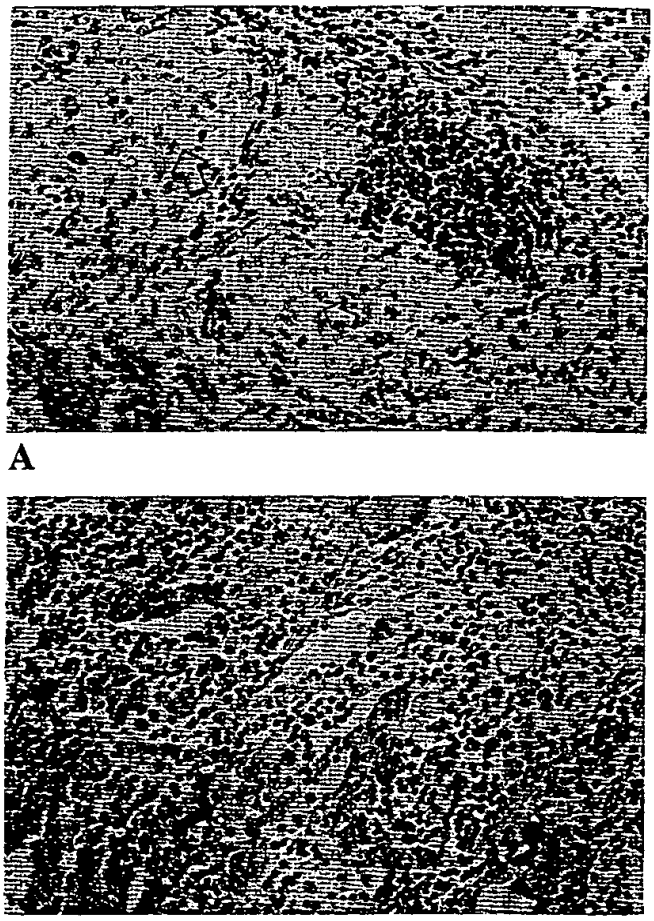

Figure 5. A. Lymph node from SOI model. Note the large tumor nests (arrows). B. Lymph node from the COI model showing metastatic cells are sparse and do not form large nests (arrows).

Discussion

The purpose of this study was to determine if surgical orthotopic implantation (SOI) of histologically intact tumor tissue could allow higher expression of the biological nature of a human renal cell carcinoma in nude mice than cellular orthotopic injection (COI) of cell suspensions.

The technique of using histologically intact tumor tissue to construct orthotopic models of human cancer in nude mice was based on the idea that the supportive stromal tissue architecture in a tumor mass plays a role in the growth and spread of human cancer. It has been shown that the proliferation of tumor cells implanted in nude mice was preceded by the penetration of host stromal cells into the tumor [15, 16]. The supportive stromal cells maintain the three-dimensional architecture of the tumor and allow growth factors, angiogenic factors and other stimulating factors to interact between the tumor cells and stroma. Previous studies with other human cancer types support these ideas [17–21].

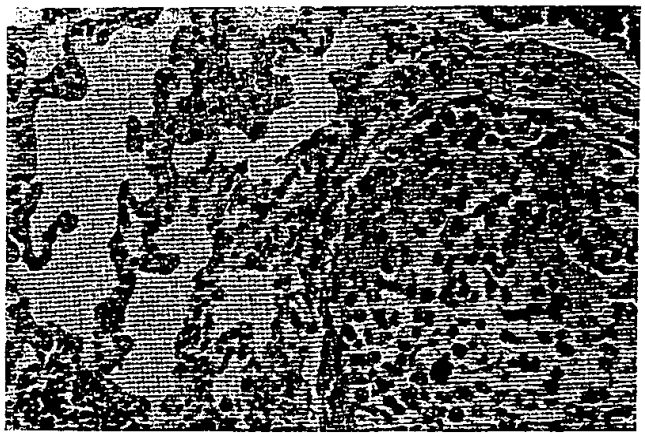

A

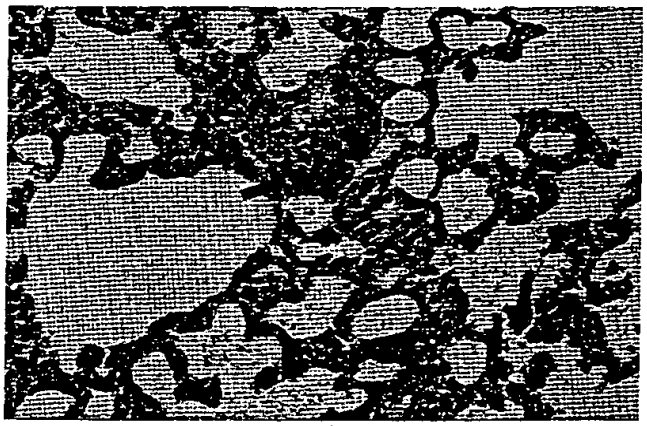

B

Figure 6. A. Lung metastasis in SOI model containing large nests of tumor cells (arrows). B. Lung metastasis in COI model containing small nests of tumor cells (arrows).

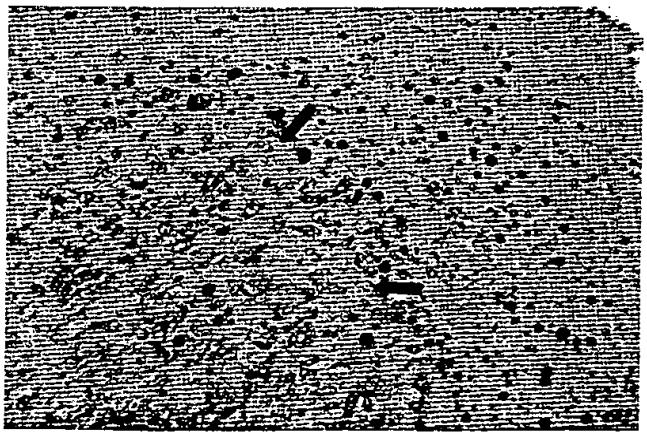

Figure 7. Liver metastasis in the SOI model (arrows).

Since the first isolation of the SN12C cell line [8], several laboratories have reported the metastatic nature of this human renal cell carcinoma in nude mice. Those studies were all conducted using the COI model [1, 5–26]. This is the first report on SOI of this line into the kidney of nude mice.

Since metastatic properties of a cancer cell line such as SN12C may change between laboratories or even in a single laboratory [8, 26] and make the results difficult to compare, we conducted a head-to-head study. Both cell suspensions

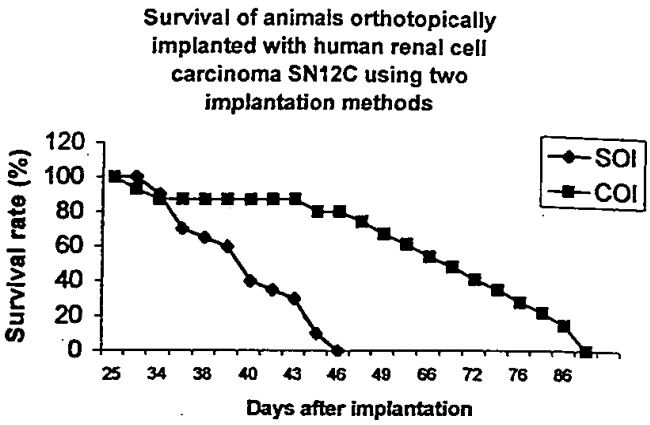

Figure 8. Survival curve of SOI and COI models of human renal cell carcinoma SN12C.

and tumor tissue of SN12C were derived from the same *in vitro* passage. The tumor tissue implanted orthotopically was harvested from a subcutaneous tumor. The tumor tissue fragments used for SOI were 1 mm^3 which we estimated contained the same amount of viable cells, 2×10^6, that was used for COI in each mouse.

Our results indicated SOI expressed significantly more metastasis as compared with orthotopic injection of cell suspensions. The survival of SOI mice was significantly shorter than that of the COI mice, indicating much earlier and more aggressive metastases in the SOI model

Tumor cells are thought to grow better in injured tissue than healthy ones. The SOI procedure caused only minimal trauma to the renal parenchyma, since only a small cut was made in the capsule and the renal parenchyma was not injured. In contrast, in COI, a syringe needle was used to penetrate the renal parenchyma to reach the subcapsule space, where tumor cells were injected. In both SOI and COI, the abdomen was opened to expose the kidney. Therefore, the lesser tumor growth and extent of metastasis of COI compared to SOI is not explainable by less surgical trauma.

The primary tumors from SOI were richer in blood vessels than those from COI, suggesting the three-dimensional tumor-stromal architecture of implanted tumor tissue might function in tumor angiogenesis. The SOI model resembled the primary renal tumor in the patient, which is also rich in blood vessels.

A recent study by Cowen *et al.* showed that the metastatic lesions resulting from SOI of a mouse colon adenocarcinoma had rich and functional networks of blood vessels. The vascularity was much different from the organ deposits of this tumor after i.v. injection of cell suspensions, which had poor vascular development [21]. This result agreed with our suggestion as to the function of three-dimensional tumor-stromal architecture in histologically intact tissue to promote tumor growth and progression, including tumor angiogenesis. It is believed that there are two stages in the development of a tumor: the prevascular stage and the vascular stage. The vascular stage is usually demarcated by rapid tumor growth and the potential for metastasis [22, 23]. Therefore earlier metastasis usually indicates faster and earlier angiogenesis. There is also evidence that intensity of an-

giogenesis correlates well with the rate of metastasis [24]. Future studies will focus on new vessel formation in the primary and metastatic tumors in the SOI compared to the COI models to confirm the hypothesis of the relationship of angiogenesis to increased metastatic potential in the SOI models. These studies will involve precise immunohistochemical staining for the presence of microvasculature in the tumors and metastases developed in the SOI and COI models.

In the present study, early death was thought to be mainly due to early distant metastasis and the high metastatic rates in the SOI model.

The organ microenvironment can have a profound influence on the growth and expression of metastatic potential of implanted human tumors [2–4, 8, 25, 26]. The SOI model allows optimal expression of the biological nature of the implanted tumor, including angiogenesis, primary tumor growth, and distant metastases. This study demonstrated the quantitative and qualitative differences in the resulting primary tumor growth, distant metastases, and survival of the SOI model, compared to the COI model.

SOI of histologically intact human tumor tissue provides a more suitable microenvironment for the tumor. The SOI model developed in this study thus provides an accurate model of renal carcinoma to investigate mechanisms of metastasis and for drug discovery and development. The present study has revealed the high metastatic potential of human renal carcinoma SN12C. SOI models of cell lines from other tumor types have also revealed a high metastatic potential [9–14, 17–20] that was not apparent in other model types. It is, therefore, possible that many tumor cell lines will be found to have interesting and important metastatic properties when investigated in SOI models. The SOI models should make an important contribution to our understanding of the mechanisms and therapy of metastasis of many types of cancer.

Acknowledgements

This study was supported in part by U.S. National Cancer Institute Grant R44 CA53963.

References

1. Marutsuka K, Hasui Y, Asada Y et al. Effects of suramin on metastatic ability, proliferation, and production of urokinase-type plasminogen activator and plasminogen activator inhibitor type 2 in human renal cell carcinoma cell line SN12C-PM6. Clin Exp Metastasis 1995; 13: 116–22.
2. Morikawa K, Walker SM, Jessup JM, Fidler IJ. *In vivo* selection of highly metastatic cells from surgical specimens of different primary human colon carcinoma implanted into nude mice. Cancer Res 1988; 48: 1943–8.
3. Nakajima M, Morikawa K, Fabra A et al. Influence of organ microenvironment on extracellular matrix degradative activity and metastasis of human colon carcinoma cells. J Natl Cancer Inst 1990; 82: 1890–8.
4. Vieweg J, Heston WDW, Gilboa E, Fair WR. An experimental model simulating local recurrence and pelvic lymph node metastasis following orthotopic induction of prostate cancer. Prostate 1994; 24: 291–8.
5. Singh RK, Bucana CD, Gutman M et al. Organ site-dependent expression of basic fibroblast growth factor in human renal cell carcinoma cells. Am J Pathol 1994; 145: 365–74.
6. Naito S, Walker SM, von Eschenbach AC, Fidler IJ. Evidence for metastasis heterogeneity of human renal cell carcinoma. Anticancer Res 1988; 8: 1163–7.
7. Burgers JK, Marshall FF, Isaacs JT. Enhanced anti-tumor effects of recombinant human tumor necrosis factor plus VP-16 on metastatic renal cell carcinoma in a xenograft model. J Urol 1989; 142: 160–4.
8. Naito S, von Eschenbach AC, Fidler IJ. Different growth pattern and biologic behavior of human renal cell carcinoma implanted into different organs of nude mice. JNCI 1987; 78: 377–85.
9. Fu X, Besterman JM, Monosov A and Hoffman RM. Models of human metastatic colon cancer in nude mice orthotopically constructed by using histologically intact patient specimens. Proc Natl Acad Sci USA 1991; 88: 9345–9.
10. Fu X, Guadagni F and Hoffman RM. A metastatic nude-mouse model of human pancreatic cancer constructed orthotopically from histologically intact patient specimens. Proc Natl Acad Sci USA 1992; 89: 5645–9.
11. Hoffman RM. Patient-like models of human cancer in mice. Current Perspectives Molecular Cellular Oncol 1992; 1(B): 311–26.
12. Wang X, Fu X, Hoffman RM. A new patient-like metastatic model of human lung cancer constructed orthotopically with intact tissue via thoractomy in immunodeficient mice. Int J Cancer 1992; 51: 992–5.
13. Astoul P, Colt HG, Wang X, Hoffman RM. Metastatic human pleural ovarian cancer model constructed by orthotopic implantation of fresh histologically intact patient carcinoma in nude mice. Anticancer Res 1993; 13: 1999–2002.
14. An Z, Wang X, Kubota T et al. A clinical nude mouse metastatic model for highly malignant human pancreatic cancer. Anticancer Res 1996; 16: 627–32.
15. Kopf-Maier P, Jackel M. Proliferation behavior of xenografted human tumors: A flow cytometric study. Anticancer Res 1988; 8: 1355–60.
16. Kopf-Maier P. Dying and regeneration of human tumor cells after heterotransplantation to athymic mice. Histol Histopathol 1986; 1: 383–90.
17. An Z, Wang X, Geller J et al. Surgical orthotopic implantation allows high lung and lymph node metastatic expression of human prostate carcinoma cell line PC-3 in nude mice. Prostate 1998; 34: 169–74.
18. Fu X, Hoffman RM. Human RT-4 bladder carcinoma is highly metastatic in nude mice and comparable to rasH-transformed RT-4 when orthotopically onplanted as histologically intact tissue. Int J Cancer 1992; 51: 989–91.
19. Fu X, Theodorescu D, Kerbel RS, Hoffman RM. Extensive multiorgan metastasis following orthotopic onplantation of histologically-intact human bladder carcinoma tissue in nude mice. Int J Cancer 1991; 49: 938–9.
20. Furukawa T, Fu X, Kubota T et al. Nude mouse metastatic models of human stomach cancer constructed using orthotopic implantation of histologically intact tissue. Cancer Res 1993; 53: 1204–8.
21. Cowen SE, Bibby MC, Double JA. Characterization of the vasculature within a murine adenocarcinoma growing in different sites to evaluate the potential of vascular therapies. Acta Oncologica 1995; 34: 357–60.
22. Folkman J, Watson K, Ingber D, Hanahan D. Induction of angiogenesis during the transition from hyperplasia to neoplasia. Nature 1989; 339: 58–61.
23. Folkman J. Angiogenesis. In: Verstraete M, Vermylen J, Lijnan R, Arnout J (eds) Thombosis and haemostasis. Leuven: Leuven University Press, 1987; 583–96.
24. Weidner N, Semple JP, Welch WR, Folkman J. Tumor angiogenesis and metastasis-correlation in invasive breast carcinoma. N Engl J Med 324 1991; 1–8.
25. Togo S, Shimada H, Kubota T, Moossa AR, Hoffman RM. Host organ specifically determines cancer progression. Cancer Res. 1995; 55: 681–4.
26. Naito S, von Eschenbach AC, Giavazzi R, Fidler IJ. Growth and metastasis of tumor cells isolated from a human renal cell carcinoma implanted into different organs of nude mice. Cancer Res 1986; 46: 4109–15.

[CANCER RESEARCH 58, 4217–4221, October 1, 1998]

Advances in Brief

Widespread Skeletal Metastatic Potential of Human Lung Cancer Revealed by Green Fluorescent Protein Expression[1]

Meng Yang, Satoshi Hasegawa, Ping Jiang, Xiaoen Wang, Yuying Tan, Takashi Chishima, Hiroshi Shimada, A. R. Moossa, and Robert M. Hoffman[2]

AntiCancer, Inc., San Diego, California 92111 [M. Y., S. H., P. J., X. W., Y. T., T. C., R. M. H.]; Department of Surgery, Yokohama City University School of Medicine, Yokohama, Japan [M. Y., S. H., T. C., H. S.]; and Department of Surgery, University of California, San Diego, California 92103-8220 [M. Y., S. H., T. C., A. R. M., R. M. H.]

Abstract

To understand the skeletal metastatic pattern of non-small cell lung cancer, we developed a stable high-expression green fluorescent protein (GFP) transductant of human lung cancer cell line H460 (H460-GFP). The GFP-expressing lung cancer was visualized to metastasize widely throughout the skeleton when implanted orthotopically in nude mice. H460 was transduced with the pLEIN retroviral expression vector containing the enhanced GFP and the neomycin (G418) resistance gene. A stable high GFP-expressing clone was selected *in vitro* using 800 μg/ml G418. Stable high-level expression of GFP was maintained in s.c.-growing tumors formed after injecting H460-GFP cells in nude mice. To use H460-GFP for visualization of metastasis, fragments of s.c.-growing H460-GFP tumors were implanted by surgical orthotopic implantation in the left lung of nude mice. Subsequent micrometastases were visualized by GFP fluorescence in the contralateral lung, plural membrane, and widely throughout the skeletal system including the skull, vertebra, femur, tibia, pelvis, and bone marrow of the femur and tibia. The use of GFP-expressing H460 cells transplanted by surgical orthotopic implantation revealed the extensive metastatic potential of lung cancer in particular to widely disseminated sites throughout the skeleton. This new metastatic model can play a critical role in the study of the mechanism of skeletal and other metastasis in lung cancer and in screening of therapeutics that prevent or reverse this process.

Introduction

Lung cancer is the leading cause of cancer death in the United States with metastasis being the principal cause (1–3). The skeleton is one of the most common sites of metastasis in lung cancer. However, the biology of bone metastasis is poorly understood because of a lack of a bone-metastasis animal model of lung cancer (4).

Models including s.c.-implant models (5, 6) and renal capsule-implant models (7–9) have been developed for human lung cancer, which have been useful. However, these models are not sufficiently representative of the clinical situation (10). In the past 10 years, orthotopic-implant models, such as the intrapulmonary-injection model and the SOI[3] model (10–13), have been established. The SOI model allows extensive lung cancer metastasis due to the maintenance of tissue architecture during the orthotopic implant process. The SOI model of lung cancer required the development of an open thoracotomy procedure in the mouse to suture histologically intact tumor tissue onto the lung (12, 13).

However, the early stages of tumor progression and micrometastasis formation have been difficult to analyze because of the inability to identify small numbers of tumor cells against a background of host tissue. Bone involvement of lung cancer has been observed when cells were injected into the cardiac ventricle of nude mice (14). However, this model does not represent the clinical metastatic process.

To develop a representative experimental model of human lung cancer that could closely represent the clinical situation, we designed an SOI model of GFP-expressing H460 human lung cancer. These models involved the stable transduction of tumor cells *in vitro* with the jellyfish *Aequorea victoria* GFP gene that was stably and highly expressed *in vivo* (15, 16). Our previous studies had shown that high GFP expression in the tumor cells allowed the visualization of tumor cell emboli, micrometastases, and their progression during the course of the disease (15, 16). In the present investigation, GFP expression in the SOI model has revealed the very extensive and widespread skeletal metastatic potential of lung cancer.

Materials and Methods

DNA Expression Vector. The RetroXpress vector pLEIN was purchased from Clontech Laboratories, Inc. (Palo Alto, CA). The pLEIN vector expresses enhanced GFP and the neomycin resistance gene on the same bicistronic message, which contains an IRES site.

Cell Culture, Vector Production, Transduction, and Subcloning. PT67, an NIH3T3-derived packaging cell line expressing the 10 A1 viral envelope, was purchased from Clontech Laboratories, Inc. PT67 cells were cultured in DMEM (Irvine Scientific, Santa Ana, CA) supplemented with 10% heat-inactivated fetal bovine serum (Gemini Bio-products, Calabasas, CA). For vector production, packaging cells (PT67), at 70% confluence, were incubated with a precipitated mixture of DOTAP reagent (Boehringer Mannheim) and saturating amounts of pLEIN plasmid for 18 h. Fresh medium was replenished at this time. The cells were examined by fluorescence microscopy after 48 h. For selection of GFP transductants, the cells were cultured in the presence of 500-2000 μg/ml of G418 (Life Technologies, Inc., Grand Island, NY) for 7 days.

Retroviral Transduction of H460 Cells. For GFP gene transduction, 20% confluent H460 cells were incubated with a 1:1 precipitated mixture of retroviral supernatants of PT67 cells and RPMI 1640 (Life Technologies, Inc.) containing 10% fetal bovine serum (Gemini Bio-Products, Calabasas, CA) for 72 h. Fresh medium was replenished at this time. H460 cells were harvested by trypsin/EDTA 72 h after infection and subcultured at a ratio of 1:15 into selective medium that contained 200 μg/ml of G418. The level of G418 was increased to 800 μg/ml gradually. H460 clones expressing GFP (H460-GFP) were isolated with cloning cylinders (Bel-Art Products, Pequannock, NJ) by trypsin/EDTA and were amplified and transferred by conventional culture methods.

Doubling Time of Stable GFP Clones. H460-GFP or nontransduced cells were seeded at 5.5×10^4 in 60-mm culture dishes. The cells were harvested and counted every 24 h using a hemocytometer (Reichert Scientific Instruments, Buffalo, NY). The doubling time was calculated from the cell growth curve over 6 days.

s.c. Tumor Growth. Three BALB/c *nu/nu* female mice, 6 weeks of age, were injected s.c. with a single dose of 5×10^6 H460-GFP cells. Cells were first harvested by trypsinization and washed three times with cold serum-free medium and then injected in a total volume of 0.2 ml within 40 min of harvesting.

SOI. Tumor fragments (1 mm^3) derived from the H460-GFP s.c. tumor growing in the nude mouse were implanted by SOI on the left lung in eight nude

Received 6/19/98; accepted 8/14/98.

The costs of publication of this article were defrayed in part by the payment of page charges. This article must therefore be hereby marked *advertisement* in accordance with 18 U.S.C. Section 1734 solely to indicate this fact.

[1] This study was supported in part by U. S. National Cancer Institute Grant R44 CA53963.

[2] To whom requests for reprints should be addressed, at AntiCancer, Inc., San Diego, CA 92111. Phone: (619) 654-2555; Fax: (619) 268-4175; E-mail: all@anticancer.com.

[3] The abbreviations used are: SOI, surgical orthotopic implantation; GFP, green fluorescent protein.

Exhibit 4RMH

THIS PAGE BLANK (USPTO)

mice (12, 13). The mice were anesthetized by isofluran inhalation. The animals were put in a position of right lateral decubitus, with four limbs restrained. A 0.8-cm transverse incision of skin was made in the left chest wall. Chest muscles were separated by sharp dissection, and costal and intercostal muscles were exposed. A 0.4–0.5-cm intercostal incision between the third and fourth rib on the chest wall was made, and the chest wall was opened. The left lung was taken up by a forceps, and tumor fragments were sewn promptly into the upper lung by one suture. The lung was then returned into the chest cavity. The incision in the chest wall was closed with a 6-0 surgical suture. The closed condition of the chest wall was examined immediately and, if a leak existed, it was closed by additional sutures. After closing the chest wall, an intrathoracic puncture was made by using a 3-ml syringe and 25-gauge 1/2 needle to withdraw the remaining air in the chest cavity. After the withdrawal of air, a completely inflated lung could be seen through the thin chest wall of the mouse. Then the skin and chest muscle were closed with a 6-0 surgical suture in one layer. All procedures of the operation described above were performed with a ×7 microscope (Olympus).

Analysis of Metastases. After tumor progression in the SOI animals, the performance status of the mice began to decrease, at which time the animals were sacrificed and autopsied. The orthotopic primary tumor and all major organs as well as the whole skeleton were explored. The fresh samples were sliced at ~1 mm thickness and observed directly under fluorescence microscopy.

Microscopy. Light and fluorescence microscopy were carried out using a Nikon microscope equipped with a Xenon lamp power supply. A Leica stereo fluorescence microscope model LZ12 equipped with a mercury lamp power supply was also used. Both microscopes had a GFP filter set (Chroma Technology, Brattleboro, VT).

Results and Discussion

Isolation of Stable High-Level Expression GFP Transductants of H460 Cells. The retroviral-vector transduced cells were able to grow *in vitro* at levels of G418 up to 800 μg/ml. The selected G418-resistant H460-GFP cells had bright GFP fluorescence (Fig. 1). There was no difference in the cell proliferation rates of parental cells and the GFP transductants as determined by comparing their doubling times *in vitro* (data not shown).

Stable High-Level Expression of GFP in H460 Tumors in Nude Mice. Three weeks after s.c. injection of H460-GFP cells, the mice were sacrificed. All three mice had a s.c. tumor, which ranged in diameter from 1.5 to 2.1 cm (mean, 1.82 ± 0.3). The tumor tissue was strongly GFP fluorescent, thereby demonstrating stable high-level GFP expression *in vivo* during s.c. tumor growth. Lung metastases were found, but no metastases were found in systemic organs in the s.c. tumor model of H460-GFP (data not shown).

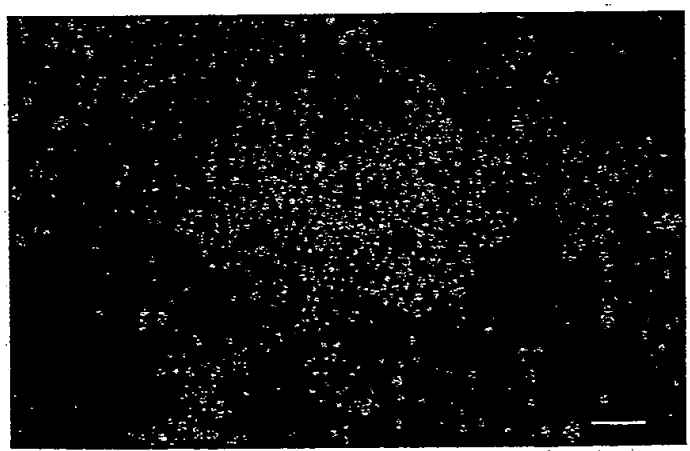

Fig. 1. Stable high-level expression GFP transductants *in vitro*. The human non-small lung cancer cell line H460 was transduced with the RetroXpress vector pLEIN that expresses enhanced GFP and the neomycin resistance gene on the same bicistronic message. The stable high expression clone was selected in 800 μg/ml of G418. *Bar*, 80 μm.

GFP-expressing Lung and Bone Metastases in Nude Mice. Eight nude mice were implanted in the left lung by SOI with 1-mm^3 cubes of H460-GFP tumor tissue derived from the H460-GFP s.c. tumor. The implanted mice were sacrificed at 3–4 weeks at the time of significant decline in performance status. All mice had tumors in the left lung weighing from 0.985 to 2.105 g (mean, 1.84 ± 0.4; Fig 2A, *a*). All tumors (eight of eight) metastasized to the contralateral lung and chest wall (Fig. 2*B*, *C* and *c*; Table 1). Seven of eight tumors metastasized to the skeletal system (Fig. 3; Table 1).

In the present investigation, it was determined that the vertebrae were the most involved skeletal site of metastasis, because seven of eight mice had vertebral metastasis. Fig. 3, *A* and *B*, are examples of tumor metastasis in the lumbar vertebrae visualized by GFP. Fig. 3*A* shows ~0.38 mm^2 of a vertebral body involved with tumor. Fig. 3*C* shows a tumor metastasis in the pelvis. Approximately 0.32 mm^2 of the pelvis was involved with tumor.

Three of seven mice had skull metastases visualized by GFP. Fig 3*D* shows very strong GFP fluorescence in the skull of one mouse, which was involved with tumor of ~0.46 mm^2.

Metastasis could be visualized in the tibia and femur marrow by GFP fluorescence. Fig. 3*E* shows the bone marrow of the tibia under bright-field microscopy. Fig. 3, *F* and *G*, show the same fields as *E* under fluorescence microscopy. A strong GFP-fluorescing metastasis could be detected in the tibia bone marrow. Fig. 3*H* shows tumor metastasis in the bone marrow of the femur visualized under fluorescence microscopy. The tumor lodged in the bone marrow and seemed to begin to involve the bone as well.

Fig. 3*I* shows the surface of the femur. No metastatic lesion was detected on the surface under bright-field microscopy. Fig. 3*J* shows the same field as Fig. 3*I* under fluorescence microscopy, where a strongly GFP-fluorescent metastasis could be visualized on the surface of the femur.

Fig. 3*K* shows the tibia. No metastatic lesion was detected on the bone under bright-field microscopy. Fig. 3*L* shows the same field as Fig. 3*K* under fluorescence microscopy, where a strongly GFP-fluorescent metastasis was visualized on the tibia with an area of ~0.24 mm^2.

Table 1 summarizes the metastatic pattern of human lung tumor H460-GFP. All of the experimental animals were found with contralateral lung metastases. Extensive and widespread skeletal metastasis, visualized by GFP expression, were found in ~90% of the animals explored. Thus, the H460-GFP SOI model revealed the extensive skeletal metastasizing potential of lung cancer. Such a high incidence of skeletal metastasis could not have been visualized previously before the development of the GFP-SOI model described here, which provided the necessary tools. Although previous studies have suggested that bone is one of the three most favored sites of solid tumor metastasis, the present study revealed that the bone microenvironment provides a highly fertile soil for lung cancer. Patients with other common solid tumors, such as breast and prostate cancer, also may have a major portion of the tumor burden present in bone at the time of death (17).

Our previous studies have shown that GFP expression allowed the visualization of tumor cell emboli, micrometastases, and their progression in fresh tissue down to the single-cell level (15, 16). These models provided a powerful and convenient tool for the study of micrometastasis in experimental animal models.

In the present investigation, an extensive metastatic process, involving the bone marrow and bone, were visualized by GFP directly under fluorescence microscopy. This method has higher resolution and is much more facile than the traditional cumbersome pathological examination procedures, such as histology and immunohistochemistry. A major advantage of GFP-expressing tumor cells is that they can be visualized in fresh live tissue. It is possible that when GFP-expressing cells undergo apoptosis, they could be engulfed by macrophages. However, when

THIS PAGE BLANK (USPTO)

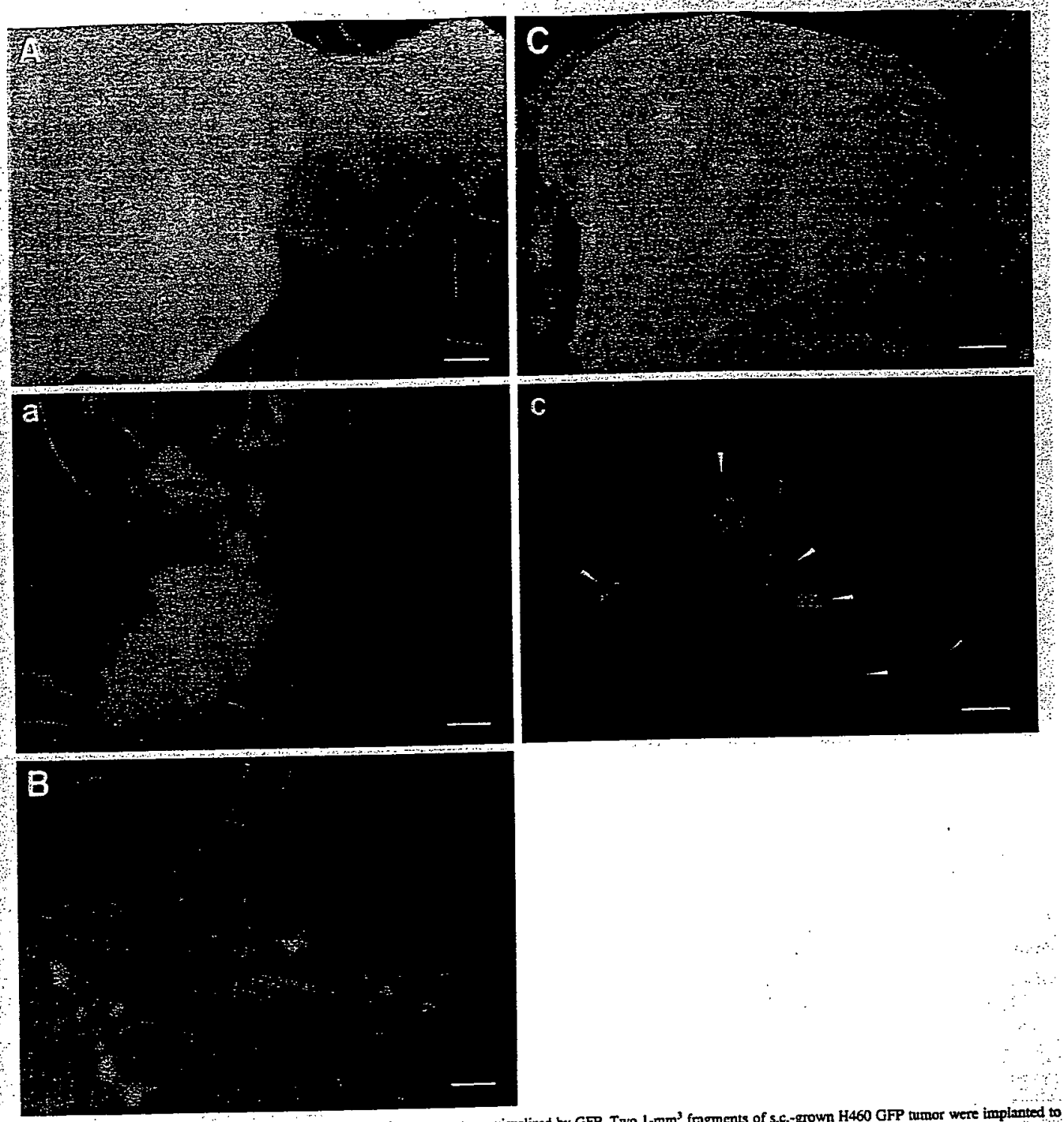

Fig. 2. Orthotopic growth and contralateral lung and plural membrane metastases visualized by GFP. Two 1-mm^3 fragments of s.c.-grown H460 GFP tumor were implanted to the left lung of nude mice by SOI. *A*, the primary tumor formed in the left lung visualized under bright-field microscopy. *Bar*, 1280 μm. *a*, same as *A*, but the tumor is visualized by intense expression of GFP under fluorescence microscopy. *Bar*, 1280 μm. *B*, numerous metastases and micrometastases can be visualized by GFP in the contralateral lung of the nude mouse. *Bar*, 200 μm. *C*, metastases in the contralateral plural membrane under bright-field microscopy. *Bar*, 1280 μm. *c*, same as *C*, but visualized by GFP under fluorescence microscopy (*white arrowheads*). *Bar*, 1280 μm.

Table 1 *Metastasis of GFP-expressing H460 cells after SOI in nude mice*

Eight nude mice were implanted in the left lung by SOI with 1-mm^3 cubes of H460-GFP tumor tissue derived from the H460-GFP sc. tumor grown previously in a nude mouse. The implanted mice were sacrificed at 3–4 weeks at the time of significant decline in performance status. All transplanted mice (eight of eight) had metastases to the contralateral lung and chest wall. Seven of eight tumors metastasized to the skeletal sytem including skull, vertebra, femur, tibia, pelvis, and bone marrow of the femur as well as the tibia.

Mouse #	Primary Tumor Weight (mg)	Brain	Contralateral Lung	Pleural Membrane	Liver	Spleen	Kidney	Adrenal Gland	Bone
1	1370	–	+	+	–	–	–	–	+ (vertebra, pelvis, bone marrow of tibia)
2	1388	–	+	+	–	–	–	–	+ (vertebra)
3	1132	–	+	+	–	–	–	–	+ (vertebra)
4	985	–	+	+	–	–	–	–	+ (vertebra, tibia, bone marrow of femur)
5	1710	–	+	+	–	–	–	–	–
6	2105	–	+	+	–	–	–	–	+ (vertebra, skull, femur)
7	1221	–	+	+	–	–	–	–	+ (vertebra, skull)
8	1960	–	+	+	–	–	–	–	+ (vertebra, femur)

THIS PAGE BLANK

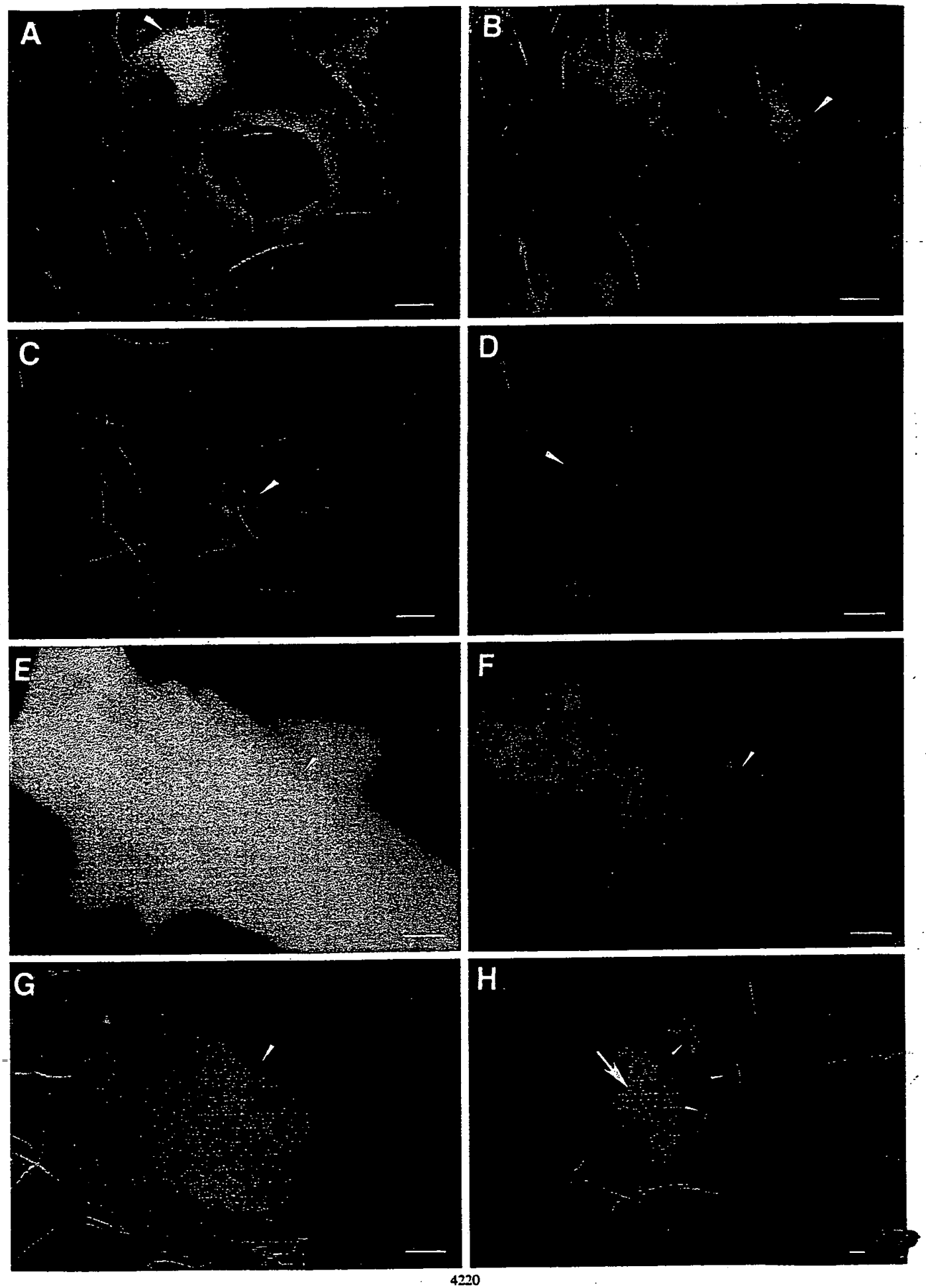
A
B
C
D
E
F
G
H

THIS PAGE BLANK (US

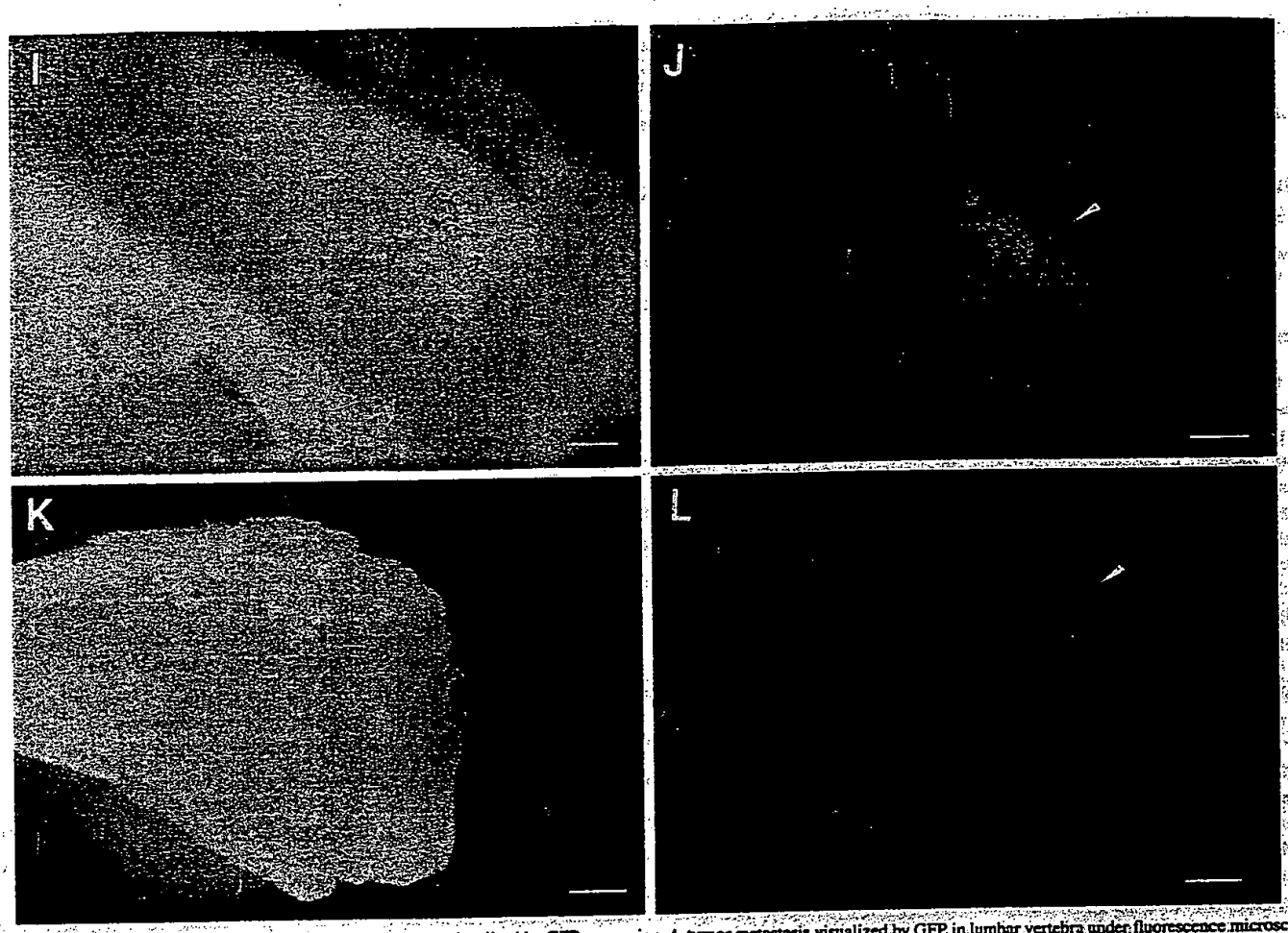

Fig. 3. Bone metastases of human lung cancer cell line H460 visualized by GFP expression. *A*, tumor metastasis visualized by GFP in lumbar vertebra under fluorescence microscopy (*white arrowhead*). *Bar*, 320 μm. *B*, tumor metastasis visualized by GFP in lumbar vertebra under fluorescence microscopy (*white arrowhead*). *Bar*, 200 μm. *C*, tumor metastasis visualized by GFP in the pelvis under fluorescence microscopy (*white arrowhead*). *Bar*, 200 μm. *D*, tumor metastasis visualized by GFP in lumbar skull under fluorescence microscopy (*white arrowhead*). *Bar*, 200 μm. *E*, bone marrow of tibia. No metastatic lesion was detected on the bone marrow under bright-field microscopy (*white arrowhead*). *Bar*, 200 μm. *F*, same fields as *E* under fluorescence microscopy (*white arrowhead*). Strong GFP-fluorescent metastasis was visualized in the bone marrow of the tibia. *Bar*, 200 μm. *G*, same as *E*. high magnification (*white arrowhead*). *Bar*, 80 μm. *H*, tumor metastasis in bone marrow of the femur was visualized by GFP under fluorescence microscopy. The tumor lodged in the bone marrow (*large white arrow*) and also involved the bone as well (*small white arrowheads*). *Bar*, 200 μm. *I*, the surface of the femur. No metastatic lesion was detected on the surface under bright-field microscopy. *Bar*, 200 μm. *J*, same fields as *I* under fluorescence microscopy. Strong GFP-fluorescent metastasis was visualized in the surface of the femur (*white arrowhead*). *Bar*, 200 μm. *K*, no metastatic lesion was detected on the bone of the tibia under bright-field microscopy. *Bar*, 320 μm. *L*, same fields as *K* under fluorescence microscopy. Strong GFP-fluorescent metastasis was visualized in the tibia (*white arrowhead*). *Bar*, 320 μm.

GFP-expressing cells die, they lose their fluorescence, such as in necrotic areas of tumors, suggesting that these macrophages would not interfere with detection of metastases.

The data presented here reveal the extensive, widespread skeletal metastatic potential of lung cancer. This new metastasis model will be relevant for the study of the mechanism of skeletal and other metastasis in lung cancer and for their therapy.

References

1. Silverberg, E. Cancer statistics. CA Cancer J. Clin., *35:* 19–35, 1985.
2. Horn, J. W., Asire, A. J., Young, J. L., and Pollack, E. S. SEER Program: Cancer incidence and Mortality in the United States, 1973–1981. NIH Publication 85-1837. Bethesda, MD: Department of Health and Human Services, 1984.
3. Loeb, L. A., Ernster, V. L., Warner, K. E., Abbotts, J., and Laszlo, J. Smoking and lung cancer: an overview. Cancer Res., *44:* 5940–5958, 1984.
4. Arguello, F., Baggs, R. B., and Frantz, C. N. A murine model of experimental metastasis to bone and bone marrow. Cancer Res., *48:* 6876–6881, 1988.
5. Fidler, I. J. Rationale and methods for the use of nude mice to study the biology and therapy of human cancer metastasis. Cancer Metastasis Rev., *5:* 29–49, 1986.
6. Sharkey, F. E., and Fogh, J. Considerations in the use of nude mice for cancer research. Cancer Metastasis Rev., *3:* 341–360, 1984.
7. Aamdal, S., Fodstad, O., and Pihl, A. Human tumor xenografts transplanted under the renal capsule of conventional mice. Growth rates and host immune response. Int. J. Cancer, *34:* 725–730, 1984.
8. Aamdal, S., Fodstad, O., and Pihl, A. Methodological aspects of the 6-day subrenal capsule assay for measuring response of human tumors to anticancer agents. Anticancer Res., *5:* 329–338, 1985.
9. Bogden, A. E., Haskell, P. M., LePage, D. J., Kelton, D. E., Cobb, W. R., and Esber, H. J. Growth of human tumor xenografts implanted under the renal capsule of normal immunocompetent mice. Exp. Cell Biol., *47:* 281–293, 1979.
10. McLemore, T. L., Eggleston, J. C., Shoemaker, R. H., Abbott, B. J., Bohlman, M. E., Liu, M. C., Fine, D. L., Mayo, J. G., and Boyd, M. R. Comparison of intrapulmonary, percutaneous intrathoracic, and subcutaneous models for the propagation of human pulmonary and nonpulmonary cancer cell lines in athymic nude mice. Cancer Res., *48:* 2880–2886, 1988.
11. McLemore, T. L., Liu, M. C., Blacker, P. C., Gregg, M., Alley, M. C., Abbott, B. J., Shoemaker, R. H., Bohlman, M. E., Litterst, C. C., Hubbard, W. C., Brennan, R. H., McMahon, J. B., Fine, D. L., Eggleston, J. C., Mayo, J. G., and Boyd, R. Novel intrapulmonary model for orthotopic propagation of human lung cancers in athymic nude mice. Cancer Res., *47:* 5132–5140, 1987.
12. Wang, X., Fu, X., and Hoffman, R. M. A new patient-like metastatic model of human lung cancer constructed orthotopically with intact tissue via thoracotomy in immunodeficient mice. Int. J. Cancer, *51:* 992–995, 1992.
13. Wang, X., Fu, X., and Hoffman, R. M. A patient-like metastasizing model of human lung adenocarcinoma constructed via thoracotomy in nude mice. Anticancer Res., *12:* 1399–1402, 1992.
14. Aiguchi, H., Tanaka, S., Ozawa, Y., Kashiwakuma, T., Kimura, T., Hiraga, T., Ozawa, H., and Kono, A. An experimental model of bone metastasis by human lung cancer cells: the role of parathyroid hormone-related protein in bone metastasis. Cancer Res., *56:* 4040–4043, 1996.
15. Chishima, T., Miyagi, Y., Wang, X., Yamaoka, H., Shimada, H., Moossa, A. R., and Hoffman, R. M. Cancer invasion and micrometastasis visualized in live tissue by green fluorescent protein expression. Cancer Res., *57:* 2042–2047, 1997.
16. Chishima, T., Miyagi, Y., Wang, X., Yang, M., Tan, Y., Shimada, H., Moossa, A. R., and Hoffman, R. M. Metastatic patterns of lung cancer visualized live and in process by green fluorescent protein expression. Clin. Exp. Metastasis, *15:* 547–552, 1997.
17. Mundy, G. R. Mechanisms of bone metastasis. Cancer (Phila.), *80:* 1546–1556, 1997.

THIS PAGE BLANK (USP

Clinical & Experimental Metastasis **18**: 57–60, 2000.

A highly metastatic Lewis lung carcinoma orthotopic green fluorescent protein model

Babak Rashidi[1,2], Meng Yang[1], Ping Jiang[1], Eugene Baranov[1], Zili An[1], Xiaoen Wang[1], A. R. Moossa[2] & R. M. Hoffman[1,2]

[1]*AntiCancer, Inc., San Diego, California, USA,* [2]*Department of Surgery, University of California, San Diego, California, USA*

Received 11 March 2000; accepted in revised form 6 July 2000

Abstract

The Lewis lung carcinoma has been widely used for many important studies. However, the subcutaneous transplant or orthotopic cell-suspension injection models have not allowed the expression of its full metastatic potential. A powerful new highly metastatic model of the widely-used Lewis lung carcinoma is reported here using surgical orthotopic implantation (SOI) of tumor fragments and enhanced green fluorescent protein (GFP) transduction of the tumor cells. To achieve this goal, we first developed *in vitro* a stable high-expression GFP transductant of the Lewis lung carcinoma with the pLEIN retroviral expression vector containing the enhanced *Aequorea victoria* GFP gene. Stable high-level expression of GFP was found maintained *in vivo* in subcutaneously-growing Lewis lung tumors. The *in vivo* GFP-expressing tumors were harvested and implanted as tissue fragments by SOI in the right lung of additional nude mice. This model resulted in rapid orthotopic growth and extensive metastasis visualized by GFP-expression. 100% of the animals had metastases on the ipsilateral diaphragmatic surface, contralateral diaphragmatic surface, contralateral lung parenchima, and in mediastinal lymph nodes. Heart metastases were visualized in 40%, and brain metastases were visualized in 30% of the SOI animals. Mice developed signs of respiratory distress between 10–15 days post-tumor implantation and were sacrificed. The use of GFP-transduced Lewis lung carcinoma transplanted by SOI reveals for the first time the high malignancy of this tumor and provides an important useful model for metastasis, angiogenesis and therapeutic studies.

Introduction

The Lewis lung carcinoma was first isolated by Dr Margaret R. Lewis in 1951 from a spontaneous epidermoid carcinoma of the lung in mouse [1]. The Lewis lung carcinoma has been an important tumor model for metastatic and angiogenesis studies and neoadjuvant chemotherapy [2–5]. Folkman's group demonstrated that removal of the subcutaneously implanted Lewis lung carcinoma tumor increases metastatic growth [2].

Li et al. reported that orthotopic implantation of Lewis lung cell suspension did not increase tumorigenicity [12]. Doki et al. demonstrated, after an orthotopic injection of tumor cells, limited metastasis localized only in mediastinal lymph nodes [13].

We have previously demonstrated, however, that orthotopic potential of implantation of tumor fragments allows the full metastatic potential of tumors to be expressed [6–11]. Our hypothesis was that the Lewis lung carcinoma had far greater metastatic potential than has previously demonstrated. In order to investigate the metastatic potential of Lewis lung carcinoma, the tumor was transplanted to nude mice using SOI in the present study. To fully visualize metastases in the SOI Lewis lung carcinoma model, it was transduced with the jellyfish *Aequorea victoria* green fluorescent protein (GFP) gene [14, 15].

Correspondence to: Robert M. Hoffman. AntiCancer, Inc., 7917 Ostrow Street, San Diego. CA 92111. USA. Tel: +1-858-654-2555; Fax: +1-858-268-4175; E-mail: all@anticancer.com

Materials and methods

GFP DNA expression vector [13]

The retroXpress vector GFP pLEIN was purchased from Clontech Laboratories, Inc. (Palo Alto, California). The pLEIN vector expresses enhanced GFP and the neomycin resistance gene on the same bicistronic message, which contains an IRES site [13].

GFP vector production [13]

PT67, an NIH3T3-derived packaging cell line expressing the 10 Al viral envelope, was purchased from Clontech Laboratories, Inc. PT67 cells were cultured in DMEM (Irvine Scientific, Santa Ana, California) supplemented with 10% heat-inactivated fetal bovine serum (Gemini Bioproducts, Calabasas, California). For vector production, packaging cells (PT67), at 70% confluence, were incubated with a precipitated mixture of DOTAP reagent (Boehringer Mannheim) and saturating amounts of pLEIN plasmid for 18 h. Fresh medium was replenished at this time. The cells

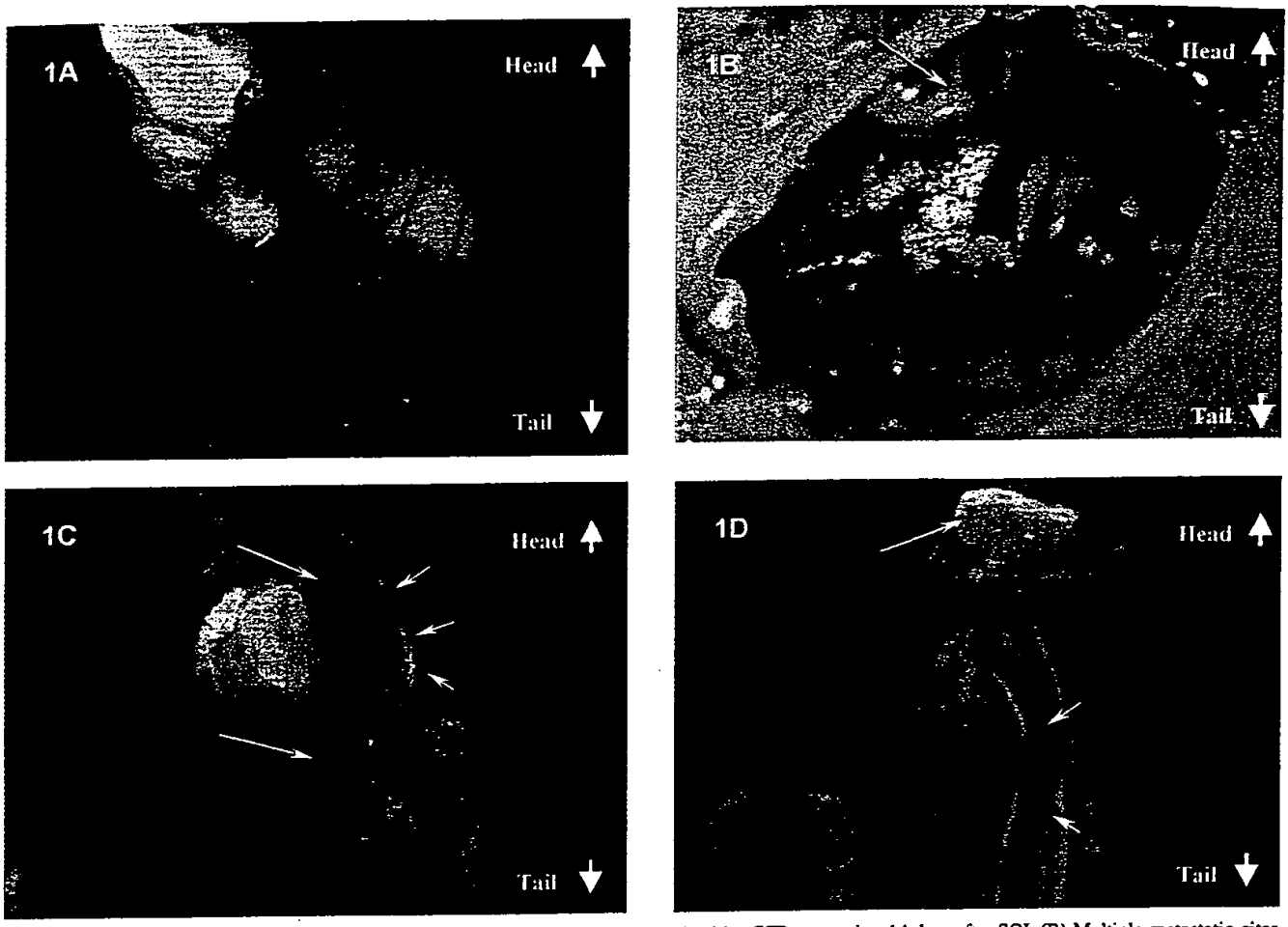

Figure 1. (A) Primary GFP-Lewis lung tumor implanted in the right lung visualized by GFP expression 14 days after SOI. (B) Multiple metastatic sites of the GFP-Lewis lung carcinoma in the contralateral lung by GFP expression through a window in the thoracic wall 14 days after SOI (white arrow indicates the heart). (C) Superior mediastinal lymph nodes involved with GFP-Lewis lung carcinoma metastases around a thoracic vein (large white arrows) visualized by GFP expression 14 days after SOI. Tumor cells in the lymphatic duct (small white arrows) connected to a metastatic lymph node are clearly visualized by GFP expression. (D) A lymph node in the superior mediastinum massively involved with GFP Lewis lung carcinoma metastasis (large white arrow), close to the great vessels (small white arrows), visualized by GFP expression 14 days after SOI.

were examined under fluorescence microscopy after 48 h. For the selection of the GFP transductants, the cells were cultured in the presence of 500–2000 μg/ml of G418 (Life Technologies, Inc, Grand Island, New York) for 7 days.

GFP transduction of Lewis lung carcinoma cells

Confluent Lewis lung carcinoma cells from the National Cancer Institute were incubated with a 1–1 precipitated mixture of retroviral supernatants of PT67 cells and RPMI 1640 (Life Technologies, Inc.) containing 10% fetal bovine serum (Gemini Bio-products, Calabasas, California) for 72 h. Fresh medium was replenished at this time. Lewis lung carcinoma cells were harvested by trypsin/EDTA 72 h after infection and subcultured at a ratio of 1:15 into selective medium that contained 200 μg/ml of G418. The level of G418 was increased to 400 μg/ml gradually. Lewis lung carcinoma clones highly expressing GFP were isolated with cloning cylinders (Bel-Art products, Pequannock, New Jersey) by trypsin EDTA and were amplified and transferred by conventional culture methods.

Subcutaneous tumor transplantation of GFP-Lewis lung cells

Three BALB/c nu/nu female mice, 6 weeks of age, were injected s.c. with a single dose of 5×10^6 of Lewis lung–GFP cells that were previously selected in G418 as described above. Cells were first harvested by trypsinization and washed three times with cold serum free medium and then injected in a total volume of 0.2 ml within 40 min of harvesting.

Surgical orthotopic implantation (SOI) of GFP-Lewis lung tissue fragments

Tumor fragments (1 mm) derived from the Lewis lung-GFP s.c. tumors growing in nude mice were implanted by SOI on the right lung in ten nude mice [10, 11]. The mice were anesthetized by isofluran inhalation. The animals were put in a position of left lateral decubitus. A 0.8-cm transverse incision of skin was made in the right chest wall. Chest muscles were separated by sharp dissection, and costal and intercostal muscles were exposed. A 0.5-cm intercostal incision between the third and fourth rib on the chest wall was

THIS PAGE BLANK (USPTO)

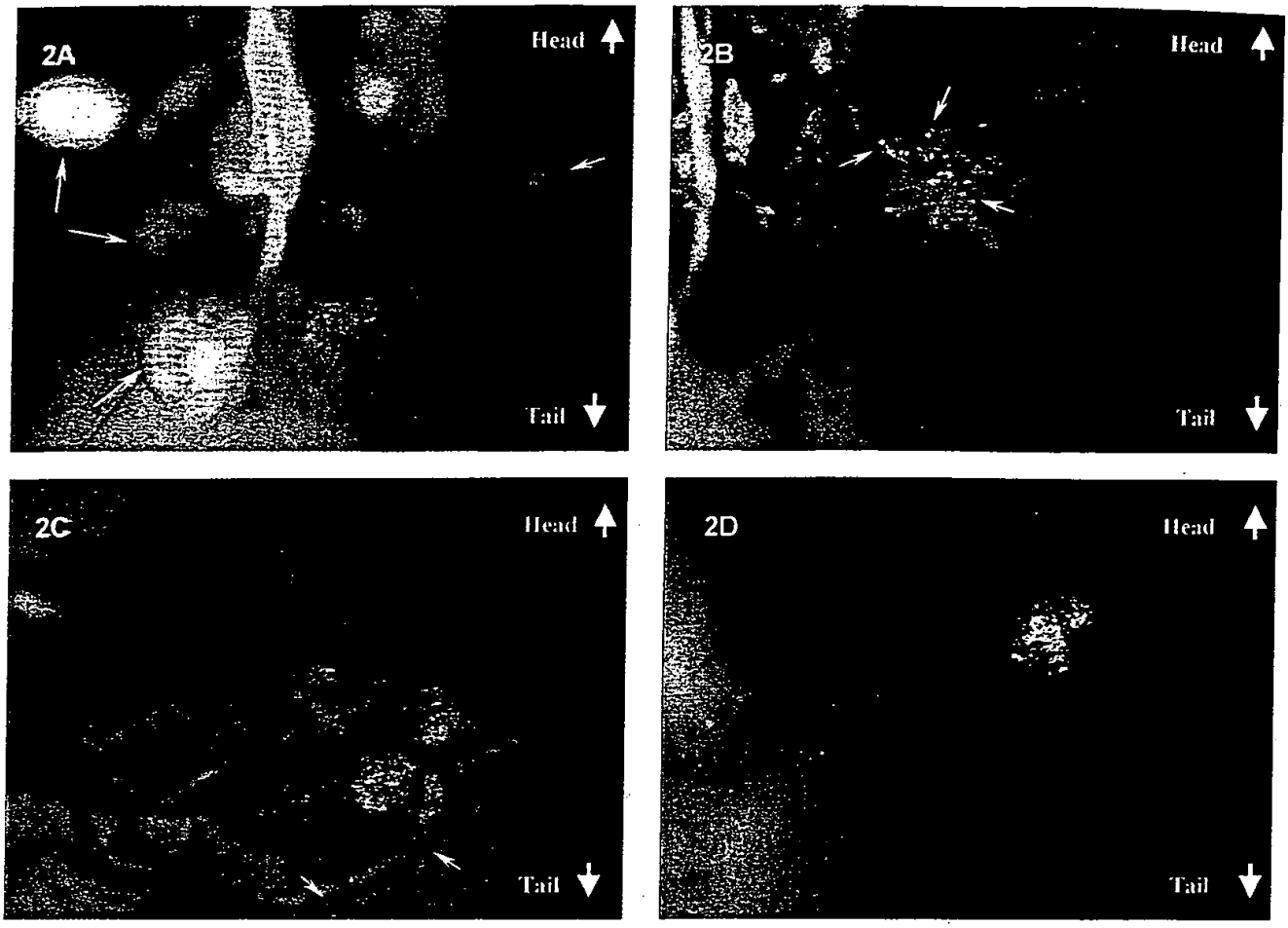

Figure 2. (A) The inferior mediastinum is massively involved with GFP-Lewis lung carcinoma metastases visualized by GFP expression 14 days after SOI. Large arrows indicate ipsilateral diaphragmatic surface metastases. Small arrows indicate the contralateral diaphragmatic surface involved with metastases. (B) Contralateral diaphragmatic surface involved with GFP-Lewis lung carcinoma metastases visualized by GFP expression 14 days after SOI (white arrows). (C) The heart is involved with GFP-Lewis lung carcinoma metastases around the posterior coronary artery visualized by GFP expression 14 days after SOI (white arrows). (D) Lewis lung carcinoma brain metastasis visualized by GFP expression 14 days after SOI.

made, and the chest wall was opened. The right lung was taken up by a forceps, and one tumor fragment was sewn promptly into the upper lung using one 8–0 suture. The lung was then returned into the chest cavity. The incision of the chest wall was closed with a 6–0 surgical suture. Closure of the chest wall was examined immediately and, if a leak existed, it was closed by additional sutures. After closing the chest wall, an intrathoracic puncture was made by using a 3-ml syringe and 25-gauge 1/2 ml needle to withdraw the remaining air in the chest cavity. After the withdrawal of air, a completely inflated lung could be seen through the thin chest wall of the mouse. The skin and chest muscles were then closed using a 6–0 surgical suture in one layer. All procedures of the operation described above were performed under a 7X microscope (Olympus).

Analysis of GFP-Lewis lung carcinoma metastases

After tumor progression in the SOI animals, the performance of the mice began to decrease, at which time the animals were sacrificed and autopsied. The orthotopic primary tumor and all major organs were explored under fluorescence microscopy.

Fluorescence microscopy of GFP-Lewis lung carcinoma

Light and fluorescent microscopy were carried out using a Nikon microscope equipped with a xenon lamp power supply. A Leica stereo fluorescent microscope model LZ12 equipped with a mercury lamp power supply was also used. Both microscopes had a GFP filter set (Chroma Technology, Brattleboro, Vermont).

Results and discussion

Isolation of stable high-level expression GFP transductants of Lewis lung carcinoma cells

The retroviral-vector GFP-transduced Lewis lung carcinoma cells were able to grow *in vitro* at levels of G418 up to 400 μg/ml. The selected G418-resistent Lewis lung-GFP cells had very bright GFP fluorescence (data not shown).

Stable high-level expression of GFP in Lewis lung carcinoma subcutaneous tumors in nude mice

Three weeks after s.c. injection of Lewis lung-GFP cells, the mice were sacrificed. Tumor tissue was strongly GFP

THIS PAGE BLANK

Table 1. Metastasis of GFP-Lewis lung carcinoma after SOI in nude mice.

% of the animals involved with metastases	Bilateral lung	Bilateral diaphragmatic surface	Heart	Brain	Mediastinal L.N.
	100% (10 of 10)	100% (10 of 10)	40% (4 of 10)	30% (3 of 10)	100% (10 of 10)

Ten mice were implanted in the right lung by SOI with one piece each of GFP-Lewis lung carcinoma tissue (1 mm^3) derived from the GFP-Lewis lung tumor previously grown s.c. in a nude mouse. The implanted mice were sacrificed at 10–14 days post-SOI at the time of significant decline of performance status.

fluorescent, demonstrating stable high-level GFP expression *in vivo* during s.c tumor growth (data not shown). Lung metastases were visualized by GFP-expression in these mice (data not shown). The median survival of these mice was approximately 27 days.

Orthotopic growth of GFP-Lewis lung carcinoma

Beginning 10 days after SOI, the mice started to decline in performance. All animals were sacrificed by day 15 post tumor implantation. All sacrificed animals had highly fluorescent tumors (Figure 1A) in the right lung weighing from 144 mg to 466 mg.

Metastatic pattern of the SOI Lewis lung carcinoma

Table 1 summarizes the metastatic pattern of the Lewis lung-GFP carcinoma. One-hundred percent of the animals (10 of 10) had disseminated contralateral lung metastases (Figure 1B); mediastinal lymph node metastases (Figures 1C, 1D); and ipsilateral (Figure 2A) and contralateral (Figures 2A, 2B) diaphragmatic surface metastases. The heart was involved with metastases in 40% (4 of 10) of the animals (Figure 2C) and the brain in 30% (3 of 10) of the animals (Figure 2D). Metastases in the contralateral lung, contralateral diaphragmatic surface, heart, and brain were only detectable by GFP expression and not detectable under bright-field microscopy in fresh tissue. A major advantage of GFP-expressing tumor cells is that they can be visualized in fresh live tissue [14–16].

The Lewis lung-GFP carcinoma implanted by SOI diffusely metastasized locally and distantly and decreased the mean survival of the animals to approximately 12 days, far shorter than the mean survival of 27 days in the subcutaneous transplant model.

The developments described here have enabled the widely-used Lewis lung carcinoma to become a far more powerful model to study the mechanism of tumor progression including regional and distant metastasis representative of lung cancer. The data obtained in this study confirmed our hypotheses that SOI allowed the Lewis lung carcinoma to express its enormous metastatic potential. The new model should be of greater use to study metastasis, the role of angiogenesis, and for the discovery of agents which inhibit or reverse these processes.

References

1. Sugiura K, Stock CC. Studies in a tumor spectrum. III. The effect of phosphoramides on the growth of a variety of mouse and rat tumors. Cancer Res 1955; 15: 38–51.
2. O'Reilly M, Holmgren L, Shing Y et al. Angiostatin: A novel angiogenesis inhibitor that mediates the suppression of metastases by a Lewis lung carcinoma. Cell 1994; 79: 315–25.
3. Fichtner I, Tanneberger S. Preoperative (neoadjuvant) chemotherapy in the murine Lewis lung carcinoma and possible implications for clinical use. Anticancer Research 1987; 7: 227–33.
4. Himmele JC, Rabenhorst B, Werner D. Inhibition of Lewis lung tumor growth and metastases by Ehrlich ascites tumor growth in the same host. J Cancer Res *Clin. Oncol.* 1986; 111: 160–165.
5. Gorelik E, Segal S, Feldman M. Control of lung metastases progression in mice: role of growth kinetic of 3LL Lewis lung carcinoma and host immunity reactivity. J Natl Cancer Inst 1980; 65: 1257–64.
6. Rashidi B, An Z, Sun F-X et al. Minimal liver resection strongly stimulates the growth of human colon cancer in the liver of nude mice. Clin Exp Metastasis 1999; 17: 497–500.
7. An Z, Jiang P, Wang X, Moossa AR, Hoffman RM. Development of a high metastatic orthotopic model of human renal cell carcinoma in nude mice: benefits of fragment implantation compared to cell-suspension injection. Clin Exp Metastasis 1999; 17: 265–270.
8. Hoffman RM. Orthotopic metastatic mouse models for anticancer drug discovery evaluation: a bridge to the clinic. Invest New Drugs 1999; 17: 343–59.
9. Hoffman RM. Orthotopic is orthodox: Why are orthotopic transplant metastatic models different from all other models? J Cell Biochem 1994; 56: 1–3.
10. Wang X, Fu X, Hoffman RM. A new patient-like metastatic model of human lung cancer constructed orthotopically with intact tissue via thoracotomy in immunodeficient mice. Int J Cancer 1992; 51: 992–5.
11. Wang X, Fu X, Hoffman RM. A patient-like metastasizing model of human lung adenocarcinoma constructed via thoracotomy in nude mice. Anticancer Res 1992; 12: 1399–1402.
12. Li L, Shin DM, Fidler IJ. Intrabronchial implantation of the Lewis lung tumor cell does not favor tumorigenocity and metastasis. Invasion Metastases 1990; 10: 129–41.
13. Doki Y, Murakami K, Yamamura T. et al. Mediastinal lymph node metastasis model by orthotopic intrapulmonary implantation of Lewis lung carcinoma cells in mice. Br J Cancer 1999; 79: 1121–6.
14. Chishima T, Miyagi Y, Wang X et al. Cancer invasion and micrometastasis visualized in live tissue by green fluorescent protein expression. Cancer Res 1997; 57: 2042–7.
15. Chishima T, Miyagi Y, Wang X et al. Metastatic patterns of lung cancer visualized live and in process by green fluorescent protein expression. Clin Exp Metastasis 1997; 15: 547–52.
16. Yang M, Hasegawa S, Jiang P et al. Widespread skeletal metastatic potential of human lung cancer revealed by green fluorescent protein expression. Cancer Res 1998; 58: 4217–21.

THIS PAGE BLANK

Investigational New Drugs 17: 343–359, 1999.

Invited Review

Orthotopic metastatic mouse models for anticancer drug discovery and evaluation: a bridge to the clinic

Robert M. Hoffman
AntiCancer, Inc., San Diego, CA, USA

Key words: metastasis, surgical orthotopic implantation, immunodeficient mice, green fluorescent protein, tumor imaging, clinically-relevant models

Summary

Currently used rodent tumor models, including transgenic tumor models, or subcutaneously-growing human tumors in immunodeficient mice, do not sufficiently represent clinical cancer, especially with regard to metastasis and drug sensitivity. In order to obtain clinically accurate models, we have developed the technique of surgical orthotopic implantation (SOI) to transplant histologically-intact fragments of human cancer, including tumors taken directly from the patient, to the corresponding organ of immunodeficient rodents. It has been demonstrated in 70 publications describing 10 tumor types that SOI allows the growth and metastatic potential of the transplanted tumors to be expressed and reflects clinical cancer. Unique clinically-accurate and relevant SOI models of human cancer for antitumor and antimetastatic drug discovery include: spontaneous SOI bone metastatic models of prostate cancer, breast cancer and lung cancer; spontaneous SOI liver and lymph node ultra-metastatic model of colon cancer, metastatic models of pancreatic, stomach, ovarian, bladder and kidney cancer. Comparison of the SOI models with transgenic mouse models of cancer indicate that the SOI models have more features of clinical metastatic cancer. Cancer cell lines have been stably transfected with the jellyfish *Aequorea victoria* green fluorescent protein (GFP) in order to track metastases in fresh tissue at ultra-high resolution and externally image metastases in the SOI models. Effective drugs can be discovered and evaluated in the SOI models utilizing human tumor cell lines and patient tumors. These unique SOI models have been used for innovative drug discovery and mechanism studies and serve as a bridge linking pre-clinical and clinical research and drug development.

Abbreviations: SOI, surgical orthotopic implantation, GFP, green fluorescent protein, G418, geneticin, 5-FU, 5-fluorouracil, SCLC, small cell lung cancer

Introduction

A. Background of surgical orthotopic implantation (SOI) mouse models of human cancer

In the past 10 years, we have developed a new approach to the development of a clinically-accurate rodent model for human cancer based on our invention of surgical orthotopic implantation (SOI). The SOI models have been described in approximately 70 publications [1–71] and in four patents[1]. SOI allows human tumors of all the major types of human cancer to reproduce clinical-like tumor growth and metastasis in the transplanted rodents [1–71]. The major features of the SOI models are reviewed here and also compared to transgenic mouse models of cancer.

B. Previous in vivo screening systems

1. *Early screening systems.* Early screening *in vivo* systems for drug discovery included the L1210 mouse leukemia [72]. A more sensitive mouse leukemia, P388, was introduced somewhat later [73]. The possibility of more relevant screening was expanded when

[1] U.S. Patent Nos. 5,569,812 and 5,491,284; European Patent No. 0437488; Japanese Patent No. 2664261.

Exhibit 6 RMH

Rygaard utilized the newly-isolated athymic nude mouse to transplant human tumors [74]. Screening with human xenografts started with the colon CX-1, lung LX-1 and breast MX-1 tumors [75]. The U.S. National Cancer Institute (NCI) and the Central Institute of Experimental Animals of Japan have greatly expanded the number of human tumor cell lines which can grow in nude mice. However the early nude mouse models were quite distinct from clinical cancer. The human tumors were implanted subcutaneously, which is a very different micro-environment from the tissue of origin of the tumors. The subcutaneous environment usually precludes the tumors from metastasizing. Workers such as Sordat and Fidler [76] have partly addressed this point, by introducing orthotopic transplantation of suspensions of tumor cell lines in nude mice as detailed below.

2. *Orthotopic injection of suspensions of established cell lines.* Fidler [76] noted that the subcutaneous micro-environment for human visceral tumors is very different from their original milieu. He postulated that this difference may result in the lack of metastases and the altered drug responses seen in the subcutaneous models. Indeed radical differences have been noted by Fidler [77] and us [20] in the drug responses of tumors in the orthotopically-transplanted site vs. the tumor growing subcutaneously. Despite species difference, the corresponding nude mouse organ more closely resembles the original patient micro-environment than the subcutaneous milieu.

Injecting tumor cell suspensions into the analogous or orthotopic mouse sites occasionally allowed relevant metastases. For example, disaggregated human colon-cancer cell lines injected into the cecum of nude mice produced tumors that eventually metastasized to the liver [76]. Although orthotopic injection of cell suspensions is an improvement over simple subcutaneous implantation, the technique has several major drawbacks. Orthotopic cell injection so far has been shown to work essentially only with established cell lines which greatly restricts its utility. The tumors resulting from orthotopic transplantation of cell suspensions often showed relatively low rates of metastasis compared to the original tumor in the patient and to SOI [1–71].

C. Surgical orthotopic implantation (SOI) of tumor fragments

The SOI models circumvent the cell disaggregation step used in previous orthotopic models. Instead of injecting cell suspensions into the orthotopic site, we have developed micro-surgical technology to transplant tumor fragments orthotopically [1–71]. The development of SOI technology led to a profound improvement in the results achieved in that the metastatic rates and sites in the transplanted mice reflect the clinical pattern after SOI. The advantages of SOI appear quite general having been seen in comparison to orthotopic implantation of cell suspensions for bladder [2,3], lung [4,9,10,24,26,27], stomach [5,14,18], kidney [78], and colon cancers [1,6,8,16,32,66–70].

In a head-to-head comparison of SOI with orthotopic transplantation of cell suspensions, SOI of stomach cancer tissue fragments resulted in metastases in 100% of the nude mice with extensive primary growth. Metastases were found in the regional lymph nodes, liver, and lung as is characteristic of this cancer [5]. In contrast, orthotopic injection of suspensions of stomach cancer cells to the nude-mouse stomach resulted in lymph node metastases in only 6.7% of those mice bearing tumors and no distant metastases.

We also compared the metastatic rate of human renal cell carcinoma SN12C in the two orthotopic nude mouse models [78] SOI of tumor tissue and orthotopic injection of cell suspensions in the kidney. The primary tumors resulting from SOI were larger and much more locally invasive than primary tumors resulting from orthotopic transplantation of cell suspension. SOI generated higher metastatic rates than orthotopic transplantation of cell suspensions. The differences in metastatic rates in the involved organs (lung, liver, and mediastinal lymph nodes) were 2–3 fold higher in SOI compared to orthotopic transplantation of cell suspensions ($p < 0.05$). Median survival time in the SOI model was 40 days, which was significantly shorter than that of orthotopic transplantation of cell suspensions (68 days) ($p < 0.001$). Histological observation of the primary tumors from the SOI model demonstrated a much richer vascular network than the orthotopic transplantation of cell suspension. Lymph node and lung metastases were larger and more cellular in the SOI model compared to the orthotopic transplantation of cell suspension models.

We conclude that the tissue architecture of the implanted tumor tissue in the SOI model plays an important role in the initiation of primary tumor growth,

invasion, and distant metastasis. These studies directly demonstrate that the implantation of histologically intact tumor tissue orthotopically allows accurate expression of the clinical features of human cancer in nude mice. Experiments showed that distant tumor growth in the SOI models were true time-dependent metastases resulting from clinical-like routes and not due to cells shed in transplantation [17]. Thus the SOI models are a significant improvement allowing the full metastatic potential of human tumors to be expressed in a rodent model. A limitation to the SOI technique is the high level of surgical skill necessary for the implantation procedures.

D. Drug discovery with SOI models

The antitumor and antimetastatic efficacy of the following new agents have been demonstrated in SOI models:

1) The metalloproteinase inhibitor Batimastat: Found to be active against an SOI human-patient colon tumor model [28] including:
   a. inhibition of primary tumor growth
   b. inhibition of metastatic events,
   c. extension of survival.
2) The metalloproteinase inhibitor CT1746: Found to be active against an SOI human colon tumor xenograft model [79] including:
   a. arrest of primary tumor growth
   b. inhibition of metastatic events, and
   c. a large increase in survival.
3) IFN-γ: Found to be active against a patient pleural cancer SOI model [45] including:
   a. elimination of metastatic events
   b. decrease in cachexia, and
   c. extension of survival.
4) Angiogenesis inhibitor TNP-470: Found to be active in patient colon and stomach tumor SOI models [66–70] including:
   a. inhibition of liver metastasis in colon cancer
   b. minimal or no effect on primary tumor

Feasibility for the drug discovery in the SOI models has been demonstrated with colon, pancreatic, stomach and lung cancer whose chemotherapy has resulted in dose-response, differential sensitivity of primary and metastatic tumors, reproducibility and correlation to historical clinical activity of the drugs [16,18–20,22–26,28,66–71]. Ongoing clinical studies with the new agents listed above will provide further correlative information.

E. Discovery of basic aspects of metastasis and possible new therapeutic targets

It was shown with the SOI colon cancer models that liver colonization is the governing process of colon cancer liver metastasis [32]. This study further confirmed Paget's seed and soil hypothesis and demonstrated that the liver colonization event is a potential therapeutic target to prevent metastasis.

We have developed a new antimetastatic chemotherapeutic strategy for combination with hepatic resection of human colon cancers in nude mice. The procedure involves i.p. administration of 5-FU two hours before hepatic resection of the colon tumors. Therapy was then continued for four consecutive days. We termed this strategy neo-neoadjuvant chemotherapy. The regime was tested in the AC3488 nude mice model of highly malignant human colon cancer [62] and significantly prolonged animal survival compared to 5-FU adjuvant chemotherapy; surgery alone; 5-FU without surgery; or the untreated control. The 5-FU neo-neoadjuvant chemotherapy had a 50% survival of 68 days compared to 41 days for 5-FU neo-adjuvant treatment; 32 days for 5-FU adjuvant therapy; 30 days for surgery only; 28 days for 5-FU without surgery; and 26 days for control. Two animals in the neo-neoadjuvant group were free of tumor when sacrificed at day-165 post-surgically. The results in this study indicate that new treatment strategies for resecting colon cancer liver metastasis should be further explored and the novel regimes introduced in the study of the model could be of great value for designing further clinical trials (Rashidi B, Hoffman RM, unpublished data).

F. Development of patient-tumor SOI models

The first model developed with SOI was for human patient colon cancer [1]. The human patient and human xenograft colon tumors transplanted by SOI resulted in clinically relevant courses such as liver metastasis, lymph node metastasis and peritoneal carcinomatosis (1). The initial "take" rates for human patient colon tumors transplanted by SOI were greater than 80%. In a study of colorectal cancer with the University of California, San Diego (UCSD), Department of Surgery, we have successfully transplanted colon rectal cancer specimens from 16 patients using SOI. In each case, we have been able to passage the tumor to form large cohorts. The tumors have demonstrated liver metastasis,

lymph node metastasis and other clinically-relevant events. Both primary tumors and liver metastasis from patients have been used for SOI (Table 1). In a recent study, we have developed an ultra-metastatic SOI model of human colon cancer with all animals having liver and lymph node metastases by day 10 [62]. Banks of patient tumors which are established in the SOI models are being developed of all the major tumor types (see section G below).

G. Establishment and expansion of SOI tumor models

Patient-derived tumors can be established by SOI with take rates of up to 100% [1,5,62,66–70]. It has been shown to be straightforward to expand an SOI tumor population by serial passage to produce large cohorts of 100 or more SOI animals with the tumor phenotype remaining stable. Established tumors can be serially passaged with nearly 100% efficiency [1,8,62,66–70]. Such expansion allows the SOI models to serve as an important research and development tool. Making large mouse cohorts with identical tumors available is essential for drug discovery and development and has been achieved [1,8,62,66–70].

The SOI technology is effective with a wide variety of patient cancers. We have constructed SOI models of patient cancers of the colon [1,8], lung [4,24,26,27], head and neck (unpublished data), pancreas [5], stomach [4], ovarian [15], liver [37] and breast [22]. Regardless of whether the tumors are passaged subcutaneously or orthotopically, once implanted orthotopically they resemble the donor tissue in detailed morphology, and pattern of growth and metastatic behavior.

The SOI models solve two very major problems in cancer research. Provision of animal models that are more representative of clinical cancer for antitumor and antimetastatic drug discovery and research. The SOI models are also used for producing human primary and metastatic tumor tissue, on demand, with precisely defined characteristics and in large amounts for study of tumor biology, diagnostics development and pharmacogenomics studies.

H. Validation of the SOI models

The SOI tumors have demonstrated a close replication of the original tumor. Apparently the analogous mouse host tissue closely replicates the original patient micro-environment which affects tumor progression and chemosensitivity. For example, an orthotopic model of human small cell lung carcinoma (SCLC) demonstrates sensitivity to cisplatin and resistance to mitomycin C, reflecting the clinical situation [20]. In contrast, the same tumor xenograft implanted subcutaneously responded to mitomycin and not to cisplatin, thus failing to match clinical behavior for SCLC [20]. These data suggest that the orthotopic site is essential to achieve clinically-relevant drug response. Other laboratories have observed similar phenomena indicating the effect of the micro-environnent on drug sensitivity [77].

In order to further understand the role of the host organ in tumor progression, we have transplanted into nude mice histologically-intact human colon cancer tissue on the serosal layers of the stomach (heterotopic site) and the serosal layers of the colon (orthotopic site) [31]. Human colon tumor, Co-3, which is well differentiated, and COL-3-JCK which is poorly differentiated were used for transplantation. After orthotopic transplantation of the human colon tumors on the nude mouse colon, the growing colon tumors resulted in macroscopically extensive invasive local growth in 4 of 10 mice, serosal spreading in 9 of 10 mice, musclaris propria invasion in 1 of 10 mice, submucosal invasion in 3 of 10 mice, mucosal invasion in 3 of 10 mice, lymphatic duct invasion in 4 of 10 mice, regional lymph node metastasis in 4 of 10 mice, and liver metastasis in 1 of 10 mice. In striking contrast, after heterotopic transplantation of the human colon tumor on the nude mouse stomach, a large growing tumor resulted but with only limited invasive growth and without serosal spreading lymphatic duct invasion, or regional lymph node metastasis. It has become clear from these studies that the orthotopic site, in particular the serosal and subserosal transplant surface, is critical to the growth, spread, and invasive and metastatic capability of the implanted colon tumor in nude mice. These studies suggest that the original host organ plays a critical role in tumor progression.

Established human colon and stomach tumors were transplanted by SOI to nude mice and tested for response to 5-FU and mitomycin-C, the standard treatments for these tumors [16,18]. The tumors responded to a dose level that was the mouse equivalent of typical clinical doses. The primary tumors responded as would be expected in the clinic for these agents. The metastases of these tumors were drug-insensitive which replicates the usual clinical situation [16,18]. It was demonstrated that antineoplastic agents can exhibit differential activity against metastases versus primary tumors in SOI models for pancreatic [19], colon [16] and stomach cancer [18]. Importantly,

Table 1. Human patient colon cancer SOI models

Case	Site	Stage	Grade
AC 3438	Colon	T3N0M0	Well diff
AC 3445	Right Colon	Stage II – T3N0M0	Well diff
AC 3488	Sigmoid Colon	Stage IV – T3N1M1	Poorly diff
AC 3508	Sigmoid Colon	Stage IV – T3N1M1	Mod well diff
AC 3518	Sigmoid Colon	Stage III – T3N1M0	Well diff
AC 3521	Cecal Area	Stage III – T2N1M0	Well diff
AC 3528	Polyposis coli	Stage IV – T3N2M1 (liver)	Mod diff
AC 3557	Sigmoid Colon	Stage II – T2N0M0	Welldiff
AC 3603	Transverse Colon	Stage I – TIN0M0	Well diff
AC 3609	Rectal	Stage III – T3N1M0	Mod poor diff
AC 3612	Ascending Colon	Stage II – T3N0M0	Mod diff
AC 3624	Rectal	Stage II – T3N0M0	Well diff
AC 3625	Rectal	Stage III – T3N2M0	Mod diff
AC 3653	Ascending Colon	Stage III –T4N2M0	Well diff

we have demonstrated that very low passage patient colon tumors transplanted by SOI can respond to 5-FU, the standard drug of treatment for this disease (unpublished data).

A correlative clinical trial was carried out to compare the course of stomach tumors in patients and in SOI models after orthotopic transplantation [14]. Of the twenty patient cases whose tumors grew in the nude mice, 6 had clinical peritoneal involvement of their tumor, and of these, 5 resulted in peritoneal metastases in the nude mice. Of the 14 patients without peritoneal involvement whose primary tumors grew locally in the mice, none gave rise to peritoneal involvement in the mice. Of the twenty patient cases, 5 had clinical liver metastases and 15 did not. After SOI of the patient's primary tumors, all 5 primary tumors from the patients with clinical liver metastases gave rise to liver metastases in the nude mice. In contrast, of the 15 primary tumors from patients without liver metastases, only one primary tumor gave rise to liver metastases in the nude mice after SOI. There was a statistical correlation ($p < 0.01$) for both liver metastases and peritoneal involvement between patients and SOI mice. These results indicate that, after surgical orthotopic transplantation of histologically intact gastric cancers from patients to nude mice, the subsequent local and metastatic behavior of the tumor in the mice closely correlated with the course of the tumors in the patients. The histology of both the local and metastatic tumors in the mice closely resembled the original local and metastatic tumors in the patient. These results indicate that the SOI models resemble clinical cancer and correlate with the patient's clinical course and should be useful for drug discovery for both antitumor and antimetastatic agents [14].

I. Bone metastasis in SOI models

1. Breast cancer

The mechanisms of breast cancer metastasizing to bone have been extensively studied [80–82], but remain poorly understood. One of the major impediments is the lack of an accurate animal model [83]. Although human breast cancer cells injected into the mammary fat pad of nude mice can metastasize to the soft organs such as the lung and lymph nodes, spontaneous metastasis of non-selected tumor cell lines to bone has not been reported [84–88]. Bone metastasis thus far has been achieved by injecting breast cancer cells into the left ventricle [89–93] or directly into the bone of nude mice [94]. An orthotopic cell-suspension model of a fgf-transformed MCF-7 human breast cancer cell line demonstrated some bone metastasis [87].

We have developed a spontaneous, highly metastatic nude mice model of human breast cancer, MDA-MB-435, with SOI. Histologically intact MDA-MB-435 tumor tissues were implanted into the mammary fat pads of female nude mice. The results showed extensive metastasis to numerous soft organs and throughout the skeletal system in every transplanted

animal. Orthotopic tumor growth and metastasis occurred throughout the axial skeleton at very high incidence (vertebra 96%, femur 88%, tibia 88%, fibula 64%, humerus 88%, sternum 76%, scapula 40%, skull 24%, rib 44%, pelvis 24% and maxillofacial region 20%) in the SOI animals. Bone metastasis occurred in 25 of 25 transplanted animals. Extensive metastasis also involved numerous visceral organs including lung, lymph node, heart, spleen, diaphragm, adrenal gland, spinal cord, skeletal muscles, parietal pleural membrane, peritoneal cavity, pancreas, liver and kidney. Histologically, the involved bones had obvious osteolytic changes, mimicking clinical bone metastasis in breast cancer. To our knowledge, this is the first report demonstrating extensive spontaneous bone metastasis of human breast cancer from the orthotopic site in nude mice. This clinically accurate model of human estrogen-receptor-negative, advanced breast cancer should be of significant value for the study and development of effective treatment of bone and other metastasis of human breast cancer (An, Z. and Hoffman, R.M., unpublished data).

2. Prostate cancer

We have developed new models of human and animal cancer by transfer of the *Aequorea victoria* jellyfish green fluorescent protein (GFP) gene to tumor cells that enabled visualization of fluorescent tumors and metastases at the microscopic level in fresh viable tissue after transplantation [49,51–53,55,61] (see section K below). We have now developed a fluorescent spontaneous bone metastatic SOI model of human prostate cancer. Fragments of a fluorescent subcutaneously-growing tumor were implanted by SOI in the prostate of a series of nude mice. Subsequent micro-metastases and metastases were visualized by GFP fluorescence throughout the skeleton including the skull, rib, pelvis, femur and tibia. The central nervous system was also involved with tumor, including the brain and spinal cord, as visualized by GFP fluorescence. Systemic organs including the lung, plural membrane, liver, kidney, adrenal gland also had fluorescent metastases. The metastasis pattern in this model accurately reflects the bone and other metastatic sites of human prostate cancer [64]. In previous orthotopic transplant models of human prostate cancer, Stephenson et al. [95], Fu et al. [11], Pettaway et al. [96], Saito et al. [97], Rembrink et al. [98] An et al. [58] and Wang et al. [65] have observed prostate cancer metastasis but only in the lymph nodes and the lung. Thalmann et al. reported a spontaneous bone metastasis model of androgen-independent human prostate cancer LNCaP sublines. The animals developed bone metastasis in 10% and 21.5% of intact and castrated hosts, respectively, after orthotopic injection of cell suspensions [99].

3. Lung cancer

In order to understand the skeletal metastatic pattern of non-small-cell lung cancer, we developed a stable high-expression GFP transductant of human lung cancer cell line H460 (H460-GFP) (see section K below). The GFP-expressing lung cancer was visualized to metastasize widely throughout the skeleton when implanted orthotopically in nude mice. Micrometastases were visualized by GFP fluorescence in the contralateral lung, plural membrane and widely throughout the skeletal system including the skull, vertebra, femur, tibia, pelvis and bone marrow of the femur and tibia. This new metastatic model can play a critical role in the study of the mechanism of skeletal and other metastasis in lung cancer and in screening of therapeutics which prevent or reverse this process [61].

J. Ultrametastatic SOI model of colon cancer

An ultra-high metastatic SOI model of human colon cancer was established from a histologically intact liver metastasis fragment derived from a surgical specimen of a patient with metastatic colon cancer [62]. The stably ultra-metastatic SOI model is termed AC3488UM. 100% of mice transplanted with AC3488UM with SOI to the colon exhibited local growth, regional invasion, and spontaneous metastasis to the liver and lymph nodes. Liver metastases were detected by the tenth day after transplantation in all animals. Half the animals died of metastatic tumor 25 days after transplantation. Histological characteristics of AC3488UM tumor were poorly differentiated adenocarcinoma of colon. Mutant p53 is expressed heterogeneously in the primary tumor and more homogeneously in the liver metastasis suggesting a possible role of p53 in the liver metastasis. The human origin of AC3488UM was confirmed by positive fluorescence staining for *in situ* hybridization of human DNA. The AC3488 human colon tumor model with its ultra-high metastatic capability in each transplanted animal, short latency and a short median survival period is different from any known human colon cancer model and will be an important tool for the study of and development of new therapy for highly metastatic human colon cancer [62].

Future studies will be done to develop SOI models of CNS malignancies and pediatric tumors.

K. Stable expression of the green fluorescent protein (GFP) in cancer cells and tissue to visualize metastasis

The visualization of tumor cell emboli, micrometastases and their progression over real-time during the course of the disease has been difficult in current models of metastasis. Previous studies used transfection of tumor cells with the *Escherichia coli* beta-galactosidase (lacZ) gene to detect micrometastases [100,101]. However, detection of lacZ requires extensive histological preparation, and therefore it is impossible to detect and visualize tumor cells in viable fresh tissue or the live animal at the microscopic level. The visualization of tumor invasion and micrometastasis formation in viable fresh tissue or the live animal is necessary for a critical understanding of tumor progression and its control.

To enhance the resolution of the visualization of micrometastases in fresh tissue, we have utilized the green fluorescent protein (GFP) gene, cloned from the bioluminescent jellyfish *Aequorea victoria* [102–116]. GFP has demonstrated its potential for use as a marker for gene expression in a variety of cell types [103,104]. The GFP cDNA encodes a 283 amino acid polypeptide with molecular weight of 27 kD [105,106]. The monomeric GFP requires no other *Aequorea* proteins, substrates, or cofactors to fluoresce [107]. Recently, GFP gene gain-of-function mutants have been generated by various techniques [108,110]. For example, the GFP-S65T clone has the serine-65 codon substituted with a threonine codon which results in a single excitation peak at 490 nm [108,109]. Moreover, to develop higher expression in human and other mammalian cells, a humanized hGFP-S65T clone was isolated [111]. The much brighter fluorescence in the mutant clones allows for easy detection of GFP expression in transfected cells.

We have isolated 50 GFP transfectants of human and animal cancer cells that are stable *in vitro* and *in vivo* [49,51,52]. The transfectants are highly fluorescent *in vivo* in tumors formed from the cells. Using these fluorescent transfectants, orthotopic-transplant animal models [26,61,64,112] were utilized for visualizing the metastatic processes in fresh tissue down to the single cell level that heretofore was not possible.

L. GFP-expressing macro- and micrometastases of CHO-K1 in nude mice in SOI models

Nude mice were implanted with 1-mm^3 cubes of GFP-CHO-K1 tumor into the ovary and were sacrificed at four weeks [49]. All mice had tumors in the ovaries. The tumor had also seeded throughout the peritoneal cavity, including the colon, cecum, small intestine, spleen, and peritoneal wall. The primary tumor and peritoneal metastases were strongly fluorescent. Numerous micrometastases were detected by fluorescence on the lungs of all mice. Multiple micrometastases were also detected by fluorescence on the liver, kidney, contralateral ovary, adrenal gland, para-aortic lymph node, and pleural membrane at the single-cell level. Single-cell micrometastases could not be detected by standard histological techniques. Even multiple-cell small colonies were difficult to detect by hematoxylin and eosin staining, but they could be detected and visualized clearly by GFP fluorescence. Some colonies were observed under confocal microscopy. As these colonies developed, the density of tumor cells was markedly decreased in the center of the colonies.

M. Patterns of lung tumor metastases of human lung tumors visualized by GFP expression in SOI models

Primary tumor grew in the operated left lung in all mice after SOI of human lung tumor GFP-ANIP-973. GFP expression allowed visualization of the advancing margin of the tumor spreading in the ipsilateral lung. All animals explored had evidence of chest wall invasion and local and regional spread. Metastatic contralateral tumors involved the mediastinum, contralateral pleural cavity, the contralateral visceral pleura. While the ipsilateral tumor had a continuous and advancing margin, the contralateral tumor seems to have been formed by multiple seeding events. These observations were made possible by GFP fluorescence of the fresh tumor tissue [51,52]. Contralateral hilar lymph nodes were also involved as well as cervical lymph nodes shown by GFP expression. A cervical lymph node metastasis was brightly visualized by GFP in fresh tissue [51,52]. When non-GFP-transfected ANIP-973 was compared with GFlP-transformed ANIP-973 for metastatic capability similar results were seen [51].

Nude mice were implanted in the left lung by SOI with 1-mm^3 cubes of human H460-GFP tumor tissue derived from the H460-GFP subcutaneous tumor [61]. The implanted mice were sacrificed at three to

four weeks at the time of significant decline in performance status. All mice had tumors in the left lung. All tumors (8/8) metastasized to the contralateral lung, and chest wall. Seven of eight tumors metastasized to the skeletal system. It was determined that the vertebrae were the most involved skeletal site of metastasis, since 7 of 8 mice had vertebral metastasis. Three of seven mice had skull metastases visualized by GFP. Metastasis could also be visualized in the tibia and femur marrow by GFP fluorescence. The tumor lodged in the bone marrow and seemed to begin to involve the bone as well. All of the experimental animals were found with contralateral lung metastases [61]. Extensive and widespread skeletal metastasis, visualized by GFP expression, were found in approximately 90% of the animals explored. Thus, the H460-GFP SOI model revealed the extensive skeletal metastasizing potential of lung cancer. Such a high incidence of skeletal metastasis could not have been previously visualized before the development of the GFP-SOI model described here which provided the necessary tools.

N. Bone and visceral metastasis of human prostate cancer PC-3 visualized by GFP in SOI models

Five of five mice developed strongly fluorescent orthotopic tumors. Three of five tumors metastasized to the skeletal system. The skeletal metastasis included the skull, rib, pelvis, femur, and tibia. All the tumors metastasized to the lung, pleural membrane and kidney. Four of five tumors metastasized to liver and two of five tumors metastasized to the adrenal gland. In two mice, cancer cells or small colonies were seen in the brain and in one mouse a few cells were in the spinal cord by GFP fluorescence [64].

O. In vivo *videomicroscopy to follow steps of metastasis*

We took advantage of stable GFP-transfected cells for monitoring and quantifying sequential steps in the metastatic process [113]. Using GFP-CHO-K1, the visualization of sequential steps in metastasis within mouse liver, from initial arrest of cells in the microvasculature to the growth and angiogenesis of metastases were quantified by intravital videomicroscopy. Individual, non-dividing cells, as well as micro- and macrometastases could clearly be detected and quantified, as could fine cellular details such as pseudopodial projections, even after extended periods of *in vivo* growth. The GFP-fluorescent tumor cells had preferential growth and survival of micrometastases near the liver surface. Furthermore, we observed a small population of single cells that persisted over the 11-day observation period, which may represent dormant cells with potential for subsequent proliferation. This study demonstrated the advantages of GFP-expressing cells, coupled with real-time high resolution videomicroscopy, for long-term *in vivo* studies to visualize and quantify sequential steps of the metastatic process.

GFP-transfected murine mammary adenocarcinoma cells inoculated into various sites of the rat were visualized colonizing various organs by video microscopy [114].

P. Transgenic mouse models of cancer

Examples of transgenic mouse cancer models are outlined below for comparison with SOI models:

1. Breast cancer

Stewart et al. [115] and Sinn et al. [116] developed transgenic mice in which expression of the c-*myc* or v-Ha-*ras* oncogenes or both were targeted to mammary tissue using the MMTV (mouse mammary tumor virus) long terminal repeat promoter. Both lines of mice, MMTV-myc [115,116] and MMTV-ras [116], were found to have mammary tumors after several months of life. In lines with both oncogenes, tumors developed more rapidly than either of the single transgenic lines [116]. In one strain, all surviving F1 female progeny that inherited the MTV/*myc* fusion gene developed breast tumors at 5 to 6 months of age during their second or third pregnancies [115]. The tumors in the double transgenics arose in a stochastic fashion, as solitary adenocarcinomas or as monoclonal B cell lymphomas [116].

Mice expressing the polyomavirus middle T-antigen (MTAg) under the control of the MMTV promoter/enhancer (MMTV-MTAg mice) had synchronous multifocal mammary adenocarcinoma with a short latency period and a high rate of metastasis to lung. Not all tumors in MMTV-MTAg mice are uniform or synchronous. All mice with established primary mammary tumors did not have metastatic disease [117,118].

MMTV-*neu* transgenic mice overexpress *neu* in the mammary epithelium and develop focal, frequently metastatic mammary adenocarcinoma after a relatively long latency period [119].

A transgenic mouse strain was constructed with the mammary tumor virus LTR/c-*myc* fusion gene. The glucocorticoid inducible c-*myc* transgene led to an

increased incidence of breast, testicular, and lymphocytic (B-cell and T-cell), and mast cell tumors [120].

2. Prostate cancer

A recombinant probasin (PB)-SV40 Tag (T antigen) transgenic mouse was developed [121,122]. These transgenic animals were termed TRAMP (transgenic adenocarcinoma mouse prostate) [121,122]. In TRAMP mice, expression of the PB-Tag transgene is restricted to the dorsolateral lobes of the prostate. TRAMP mice have high-grade PIN (prostatic intraepithelial neoplasia) and/or well-differentiated prostate cancer by the age of 10–12 weeks [123]. TRAMP mice spontaneously develop invasive primary tumors that routinely metastasize to the lymph nodes and lungs and less frequently metastasize to the spinal column, kidneys, and adrenal glands [122]. Hind limb paraplegia was observed in a single TRAMP mouse at the age of 22 weeks. Histological examination of decalcified sections of the spine at the level of the thoracolumbar vertebrae demonstrated that the spinal canal was filled with metastatic tumor. The tumor appeared to have destroyed the spinal cord through pressure atrophy rather than by invasion and destruction of the adjacent vertebral bone as typically seen with osteolytic metastatic tumors [122]. Lymph node metastases were found in 31% (5 of 16) of TRAMP mice between 18 and 24 weeks of age. Pulmonary metastases were found in 4 of 11 (36%) by 24 weeks. A metastasis in the kidney has been found in one mouse at 12 weeks. Two metastases to the adrenal gland were found [122]. At 30–36 weeks of age, 100% of TRAMP animals have primary tumors and metastatic disease [122,123].

3. Colon cancer

The Smad3 gene was inactivated in mice by homologous recombination. Homozygous mutants were viable and spontaneously formed colorectal adenocarcinomas [124]. Between 4 and 6 months of age, the Smad3 mutant mice became moribund with the colorectal adenocarcinomas. The colorectal cancers penetrated through all layers of the intestinal wall and metastasized to lymph nodes [124].

4. p53 knockouts

Homozygote p53-deficient mice, and normal littermates (with wild-type p53 genes) were monitored for spontaneous neoplasms [125]. Wild-type mice (95 animals) by the age of 9 months did not develop tumors. By 9 months, only 2 of 96 heterozygote animals developed tumors. One heterozygote mouse developed an embryonal carcinoma of the testis at 5 months and another developed a malignant lymphoma at the age of 9 months [125]. Of 35 homozygote animals, 26 (74%) developed neoplasms by 6 months of age. Some tumors appeared before 10 weeks of age, and tumor occurrence increased rapidly between 15 and 25 weeks of age [125]. Multiple primary neoplasms of different origin were observed in 9 of the 26 homozygote mice with tumors. Malignant lymphomas were found in 20 of 26 animals. Sarcomas also occurred with some frequency. There were seven hemangiosarcomas, three undifferentiated sarcomas, and one osteosarcoma. Only one female mouse developed a mammary adenocarcinoma [125].

It can be clearly seen that the transgenic mouse models of breast, prostate and colon cancer do not reflect human clinical cancer as do the SOI models. For example, the transgenic breast cancer models to not metastasize to the bone; the prostate cancer transgenic model metastasized to the bone in only one reported animal; the colon cancer transgenic model did not metastasize to the liver, and in the p53 knockout models only one animal had breast cancer. The SOI models thus offer unique and critically important features for antitumor and antimetastatic drug discovery.

Materials and methods

A. General construction of models

1. Mice

Four-to-six-week old outbred nu/nu mice of both sexes are used for the orthotopic transplantation. All the mice are maintained in a pathogen-free environment. Cages, bedding, food and water are autoclaved and changed regularly. All the mice are maintained in a daily cycle of 12 hour period of light and darkness. Bethaprim Pediatric Suspension (containing sulfamethoxazole and trimethoprim) is added to the drinking water. Mice are periodically sent to the University of Missouri to test for pathogens. All animal studies were conducted in accordance with the principles and procedures outlined in the National Institutes of Health Guide for the Care and Use of Laboratory Animals under assurance number A3873-1.

2. Specimens

Fresh surgical specimens are kept in Earle's MEM at 4°C and obtained as soon as possible from hospitals.

Transplantation should take place within 24 hours of surgical excision. Before transplantation, each specimen is inspected, and all necrotic and suspected necrotic tumor tissue is removed. To take into account tumor heterogeneity, each specimen is equally divided into 5 parts, separated and each part is subsequently cut into small pieces of about 1 mm^3 size. Tumor pieces for each transplantation are taken from 5 parts of each specimen equally. In our experience, a typical colon tumor specimen of 1–2 grams provides sufficient material for initial surgical orthotopic implantation of more than 20 mice. Additional SOI models of this same tumor can subsequently be generated by a single passage using SOI. It should be noted that patient tumors are routinely passaged orthotopically to produce large cohorts. One hundred mice or more can be readily transplanted in the first passage which are more than sufficient for treatment studies.

B. Examples of surgical orthotopic implantation (SOI)

1. Colon cancer

Colonic transplantation For transplantation, nude mice are anesthetized, and the abdomen is sterilized with iodine and alcohol swabs. A small midline incision is made and the colorectal part of the intestine is exteriorized. Serosa of the site where tumor pieces are to be implanted is removed. Eight pieces of 1-mm^3 size tumor are implanted on the top of the animal intestine. An 8-0 surgical suture is used to penetrate these small tumor pieces and attach them on the wall of the intestine. The intestine is returned to the abdominal cavity, and the abdominal wall is closed with 7-0 surgical sutures (Figure 1). Animals are kept in a sterile environment. Tumors of all stages and grades can be utilized [1].

Intrahepatic transplantation An incision is made through the left upper abdominal pararectal line and peritoneum. The left lobe of the liver is carefully exposed and the liver is cut about 3 mm with scissors. Two to three tumor pieces of 1–2 mm^3 size are put on the nude mouse liver and attached immediately with double sutures using 8-0 nylon with an atraumatic needle. After confirmation that no bleeding is occurring, the liver is then returned to the peritoneal cavity. The abdomen and skin are then closed with 6-0 back silk sutures [30].

2. Prostate cancer

Tumor fragments are prepared as for colon and breast tumors. Two tumor fragments (1 mm^3) are implanted by SOI in the dorsolateral lobe of the prostate. After proper exposure of the bladder and prostate following a lower midline abdominal incision, the capsule of the prostate is opened and the two tumor fragments are inserted into the capsule. The capsule is then closed with an 8-0 surgical suture. The incision in the abdominal wall is closed with a 6-0 surgical suture in one layer [11,64,65].

3. Lung cancer

The mice are anesthetized by isoflurane inhalation. The animals are put in a position of right lateral decubitus, with four limbs restained. A 0.8 cm transverse incision of skin is made in the left chest wall. Chest muscles are separated by sharp dissection and costal and intercostal muscles are exposed. A 0.4–0.5 cm intercostal incision between the third and fourth rib on the chest wall is made and the chest wall is opened. The left lung is taken up with a forceps and tumor fragments are sewn promptly into the upper lung with one suture. The lung is then returned into the chest cavity. The incision in the chest wall is closed by a 6-0 surgical suture. The closed condition of the chest wall is examined immediately and if a leak exists, it is closed by additional sutures. After closing the chest wall, an intrathoracic puncture is made by using a 3-ml syringe and 25G ½ needle to withdraw the remaining air in the chest cavity. After the withdrawal of air, a completely inflated lung can be seen through the thin chest wall of the mouse. Then the skin and chest muscle are closed with a 6-0 surgical suture in one layer [61] (Figure 2).

C. Cohorts of transplanted animals for treatment

Cohorts of over 100 SOI models have been constructed from many SOI models. The "take rate" for transplantation after the first passage is generally 100%. Cohorts of 100 mice per case can be easily constructed [62].

D. Determination and characterization of xenografted tumors

Complete autopsy with histological examination is performed on all mice at time of death. All of the major organs are examined carefully and routinely sampled, along with any tissues showing gross abnormalities.

SOI OF COLON TUMORS

1. A 0.5 cm incision is made on the left lower abdomen

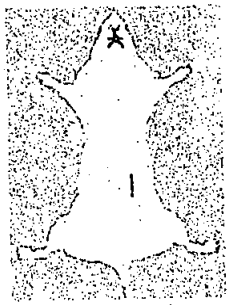

2. The cecum and ascending colon are exposed with forceps

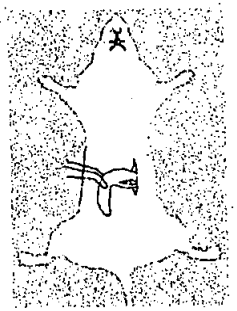

3. Serosa of the ascending colon is scraped with two forceps

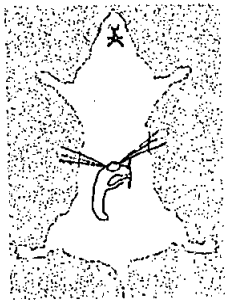

4. The first suture is made on the right edge of the scraped serosa area of the ascending colon

5. The tumor pieces are penetrated with the suture

6. The second suture is made on the left edge of the scraped area of the serosa of the ascending colon

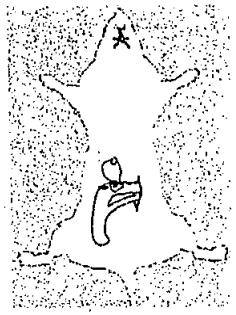

7. Three knots are made to fix the tumor pieces on the ascending colon

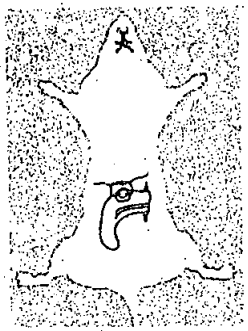

8. The ascending colon and cecum are returned into the abdominal cavity

9. The abdominal wound is closed in one layer

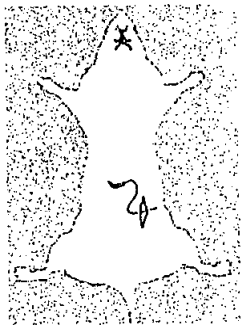

Figure 1.

SOI OF LUNG TUMORS

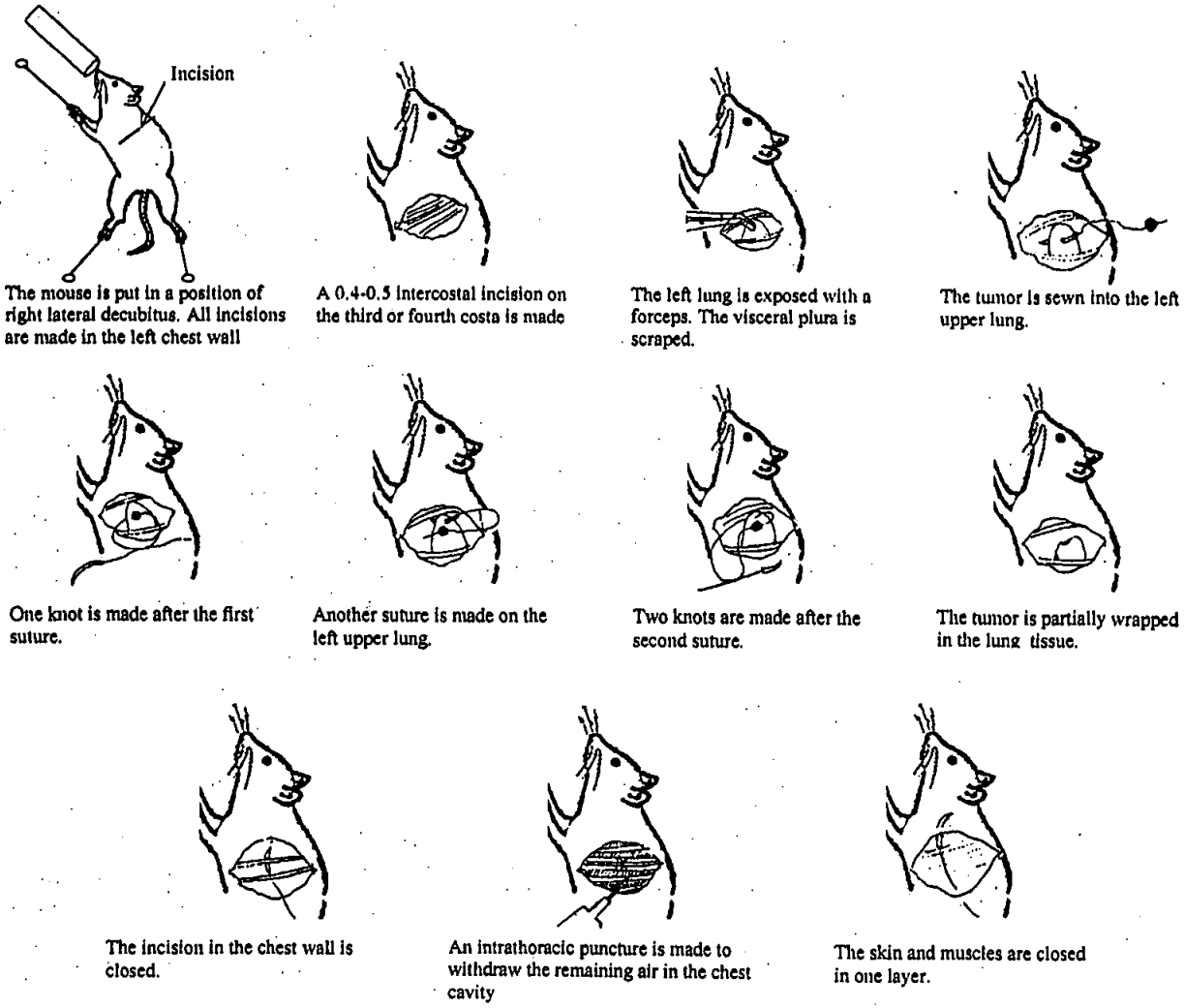

Figure 2.

E. Evaluation of growth and metastasis of orthotopically transplanted tumors

The mice are autopsied and analyzed histologically for the presence of local growth and metastases upon sacrifice after they become moribund. Mice are killed if they develop signs of distress. For example, in the colon tumor models the distress symptoms include a decline in performance status and weight loss due to cachexia or drug treatment. At autopsy, the colon and all peritoneal organs, lymph nodes, liver and lungs are resected and processed for routine histological examination for tumors after careful microscopic examination. Metastases are considered to have occurred if at least one microscopic metastatic lesion is found in any of the animals. The growth of locally growing tumors is determined by caliper measurement of the locally growing tumor which is possible for colon tumors, since the body wall is so thin, and by weighing the tumors that are removed at autopsy. Caliper measurements of the primary tumor can also allow determination of tumor regression. The primary tumor is weighed at autopsy.

1. Isolation of stable high expression GFP tumor cells

The GFP expression vector RetroXpress vector pLEIN is purchased from CLONTECH Laboratories, Inc. (Palo Alto, CA). The pLEIN vector expresses enhanced green fluorescent protein (EGFP) and the neomycin resistance gene on the same bicistronic message which contains an IRES site [61,64]. For GFP gene transduction, 20%-confluent cancer cells are incubated with a 1:1 precipitated mixture of retroviral supernatants of PT67 packaging cells and RPMI 1640 (GIBCO) containing 10% fetal bovine serum (FBS) (Gemini Bio-products, Calabasas, CA) for 72 hours. Fresh medium is replenished at this time. Cells are harvested by trypsin/EDTA 72 hours post-infection, and subcultured at a ratio of 1:15 into selective medium which contains 200 μg/ml of G418. The level of geneticin (G418) (Life Technologies, Grand Island, NY) is increased to 800–1000 μg/ml gradually. Clones expressing GFP are isolated with cloning cylinders (Bel-Art Products, Pequannock, NJ) by trypsin/EDTA and are amplified and transferred by conventional culture methods [61,64].

2. Analysis of GFP-expressing metastases

Mice are sacrificed when their performance status begins to decline and the systemic organs are removed. The orthotopic primary tumor and all major organs as well as the whole skeleton are explored. The fresh samples are sliced at approximately 1 mm thickness and observed directly under fluorescence microscopy. The samples are also processed for histological examination for fluorescence in frozen sections. The slides are then rinsed with phosphate-buffered saline (PBS) and then fixed for 10 minutes at 4°C in 2% formaldehyde plus 0.2% gluteraldehyde in PBS. The slides are washed with PBS and stained with hematoxylin and eosin using standard techniques.

3. Microscopy

Light and fluorescence microscopy are carried out using a Nikon microscope equipped with a Xenon lamp power supply. A Leica stereo fluorescence microscope model LZ12 equipped with a mercury lamp power supply are also used. Both microscopes have a GFP filter set (Chroma Technology, Brattleboro, VT). An MRC-600 confocal imaging system (Bio-Rad) mounted on a Nikon microscope with an argon laser is also used. Photomicrographs are processed for brightness and contrast with Image Pro Plus, Version 3.0, software (Media Cybernetics, Silver Springs, MD).

References

1. Fu X, Besterman JM, Monosov A, Hoffman RM: Models of human metastatic colon cancer in nude mice orthotopically constructed by using histologically-intact patient specimens. Proc Natl Acad Sci USA 88: 9345–9349, 1991
2. Fu X, Theodorescu D, Kerbel RS, Hoffman RM: Extensive multi-organ metastasis following orthotopic on plantation of histologically-intact human bladder carcinoma tissue in nude mice. Int J Cancer 49: 938–939, 1991
3. Fu X, Hoffman RM: Human RT-4 bladder carcinoma is highly metastatic in nude mice and comparable to ras-H-transformed RT-4 when orthotopically onplanted as histologically-intact tissue. Int J Cancer 51: 989–991, 1992
4. Wang X, Fu X, Hoffman RM: A new patient-like metastatic model of human lung cancer constructed orthotopically with intact tissue via thoracotomy in immunodeficient mice. Int J Cancer 51: 992-995, 1992
5. Fu X, Guadagni F, Hoffman RM: A metastatic nude-mouse model of human pancreatic cancer constructed orthotopically from histologically-intact patient specimens. Proc Natl Acad Sci USA 89: 5645–5649, 1992
6. Hoffman RM: Patient-like models of human cancer in mice. Current Perspectives on Molecular & Cellular Oncology 1(B): 311–326, 1992
7. Kuo, T-H, Kubota T, Watanabe M, Furukawa T, Kase S, Tanino H, Nishibori K, Saikawa Y, Teramoto T, Ishibiki K, Kitajima M, Hoffman RM: Orthotopic reconstitution of human small-cell lung carcinoma after intravenous transplantation in SCID mice. Anticancer Res 12: 1407–1410, 1992
8. Fu X, Herrera H, Kubota T, Hoffman RM: Extensive liver metastasis from human colon cancer in nude and scid mice

after orthotopic onplantation of histologically-intact human colon carcinoma tissue. Anticancer Res 12: 1395–1398, 1992
9. Wang X, Fu X, Hoffman RM: A patient-like metastasizing model of human lung adenocarcinoma constructed via thoracotomy in nude mice. Anticancer Res 12: 1399–1402, 1992
10. Wang X, Fu X, Kubota T, Hoffman RM: A new patient-like metastatic model of human small-cell lung cancer constructed orthotopically with intact tissue via thoracotomy in immunodeficient mice. Anticancer Res 12: 1403–1406, 1992
11. Fu X, Herrera H, Hoffman RM: Orthotopic growth and metastasis of human prostate carcinoma in nude mice after transplantation in nude mice. Int J Cancer 52: 987–990, 1992
12. Hoffman RM: Histoculture and the immunodeficient mouse come to the cancer clinic: rational approaches to individualizing cancer therapy and new drug evaluation review). Int J Oncol 1: 467–474, 1992
13. Furukawa T, Fu X, Kubota T, Watanabe M, Kitajima M, Hoffman RM: Nude mouse metastatic models of human stomach cancer constructed using orthotopic implantation of histologically-intact tissue. Cancer Research 53: 1204–1208, 1993
14. Furukawa T, Kubota T, Watanabe M, Kitajima M, Fu X, Hoffman RM: Orthotopic transplantation of histologically-intact clinical specimens of stomach cancer to nude mice: Correlation of metastatic sites in mouse and human. Int J Cancer 53: 608–612, 1993
15. Fu X, Hoffman RM: Human ovarian carcinoma metastatic models constructed in nude mice by orthotopic transplantation of histologically-intact patient specimens. Anticancer Res 13: 283–286, 1993
16. Furukawa T, Kubota T, Watanabe M, Kuo PH, Kase S, Saikawa Y, Tanino H, Teramoto T, Ishibiki K, Kitajima M, Hoffman RM: Immunochemotherapy prevents human colon cancer metastasis after orthotopic onplantation of histologically-intact tumor tissue in nude mice. Anticancer Res 13: 287–291, 1993
17. Kuo T-H, Kubota T, Watanabe M, Fujita S, Furukawa T, Teramoto T, Ishibiki K, Kitajima M, Hoffman RM: Early resection of primary orthotopically-growing human colon tumor in nude mouse prevents liver metastasis: Further evidence for patient-like hematogenous metastatic route. Anticancer Res 13: 293–298, 1993
18. Furukawa T, Kubota T, Watanabe M, Kitajima M, Hoffman RM: Differential chemosensitivity of local and metastatic human stomach cancer after orthotopic transplantation of histologically-intact tumor tissue in nude mice. Int J Cancer 54: 397–401, 1993
19. Furukawa T, Kubota T, Watanabe M, Kitajima M, Hoffman RM: A novel "patient-like" treatment model of human pancreatic cancer constructed using orthotopic transplantation of histologically-intact human tumor-tissue in nude mice. Cancer Res 53: 3070–3072, 1993
20. Kuo T-H, Kubota T, Watanabe M, Furukawa T, Kase S, Tanino H, Nishibori H, Saikawa Y, Ishibiki K, Kitajima M, Hoffman RM: Site-specific chemosensitivity of human small-cell lung carcinoma growing orthotopically compared to subcutaneously in SCID mice: The importance of orthotopic models to obtain relevant drug evaluation data. Anticancer Res 13: 627–630, 1993
21. Furukawa T, Kubota T, Watanabe M, Kuo T-H, Nishibori H, Kase S, Saikawa Y, Tanino H, Teramoto T, Ishibiki K, Kitajima M: A metastatic model of human colon cancer constructed using cecal implantation of cancer tissue in nude mice. Jpn J Surg 23: 420–423, 1993
22. Fu X, Le P, Hoffman RM: A metastatic orthotopic transplant nude-mouse model of human patient breast cancer. Anticancer Res 13: 901–904, 1993
23. Astoul P, Colt HG, Wang X, Hoffman RM: Metastatic human pleural ovarian cancer model constructed by orthotopic implantation of fresh histologically-intact patient carcinoma in nude mice. Anticancer Res 13: 1999–2002, 1993
24. Astoul P, Wang X, Hoffman RM: "Patient-Like" nude mouse models of human lung and pleural cancer (Review). Int J Oncology 3: 713–718, 1993
25. Kubota T, Inoue S, Furukawa T, Ishibiki K, Kitajima M, Kawamura E, Hoffman RM: Similarity of Serum – Tumor Pharmacokinetics of Antitumor Agents in Man and Nude Mice. Anticancer Research 13: 1481–1484, 1993
26. Astoul P, Colt HG, Wang X, Hoffman RM: A "patient-like" nude mouse model of parietal pleural human lung adenocarcinoma. Anticancer Res 14: 85–92, 1994
27. Astoul P, Colt HG, Wang X, Boutin C, Hoffman RM: A "patient-like" nude mouse metastatic model of advanced human pleural cancer. J Cell Biochem 56: 9–15, 1994
28. Wang X, Fu X, Brown PD, Crimmin MJ, Hoffman RM: Matrix metalloproteinase inhibitor BB-94 (Batimastat) inhibits human colon tumor growth and spread in a patient-like orthotopic model in nude mice. Cancer Res 54: 4726–4728, 1994
29. Hoffman RM: Orthotopic is orthodox: why are orthotopic-transplant metastatic models different from all other models? J Cell Biochem 56: 1–4, 1994
30. Togo S, Shimada H, Kubota T, Moossa AR, Hoffman RM: Seed to soil is a return trip in metastasis. Anticancer Res 15: 791–794, 1995
31. Togo S, Shimada H, Kubota T, Moossa AR, Hoffman RM: Host organ specifically determines cancer progression. Cancer Res 55: 681–684, 1995
32. Kuo T-H, Kubota T, Watanabe M, Furukawa T, Teramoto T, Ishibiki K, Kitajimi M, Moossa AR, Penman S, Hoffman RM: Liver colonization competence governs colon cancer metastasis. Proc Natl Acad Sci USA 92: 12085–12089, 1995
33. Togo S, Wang X, Shimada H, Moossa AR, Hoffman RM: Cancer seed and soil can be highly selective: Human-patient colon tumor lung metastasis grows in nude mouse lung but not colon or subcutis. Anticancer Res 15: 795–798, 1995
34. Dutton G: AntiCancer Inc. scientists identify a key governing step in the metastasis of cancer. Genetic Engineering News 16: 1, January 15, 1996
35. Holzman D: Of mice and metastasis: a new for-profit model emerges J Natl Cancer Inst 88: 396–397, 1996
36. Leff DN: MetaMouse models colon cancer metastasis with clinical potential. BioWorld Today 7, 1 (January 8), 1996
37. Sun FX, Tang ZY, Liu KD, Ye SL, Xue Q, Gao DM, Ma ZC: Establishment of a metastatic model of human hepatocellular carcinoma in nude mice via orthotopic implantation of histologically intact tissues. Int J Cancer 66: 239–243, 1996
38. An Z, Wang X, Kubota T, Moossa AR, Hoffman RM: A clinical nude mouse metastatic model for highly malignant human pancreatic cancer. Anticancer Res 16: 627–632, 1996
39. Riordan T: A technique is said to ease attachment of tumors to mice, making them "little cancer patients". New York Times, "Patents" Column, March 4, 1996
40. Murray G, Duncan M, O'Neil P, Melvin W, Fothergill J: Matrix metalloproteinase-1 is associated with poor prognosis in colorectal cancer. Nature Med 2: 461–462, 1996

41. Hoffman RM: Fertile seed and rich soil: development of patient-like models of human cancer by surgical orthotopic implantation of intact tissue. Update Series: Comprehensive Textbook of Oncology 3: 1–10, Schimpff, S.C, et al, eds. Williams & Williams, Baltimore, 1996
42. Sun F-X, Tang Z-Y, Liu K-D, Xue Q, Gao D-M, Yu Y-Q, Zhou X-D, Ma Z-C: Metastatic models of human liver cancer in nude mice orthotopically constructed by using histologically intact patient specimens. J Cancer Res Clin Oncol 122: 397-402, 1996
43. Astoul P, Wang X, Colt HG, Boutin C, Hoffman RM: A patient-like human malignant pleural mesothelioma nude-mouse model. Oncology Reports 3: 483–487, 1996
44. Colt HG, Astoul P, Wang X, Yi ES, Boutin C, Hoffman RM: Clinical course of human epithelial-type malignant pleural mesothelioma replicated in an orthotopic-transplant nude mouse model. Anticancer Res 16: 633–640, 1996
45. An Z, Wang X, Astoul P, Danays T, Hoffman RM: Interferon gamma is highly effective against orthotopically-implanted human pleural adenocarcinoma in nude mice. Anticancer Res 16: 2545–2551, 1996
46. Olbina G, Cieslak D, Ruzdijic S, Esler C, An Z, Wang X, Hoffman RM, Seifert W, Pietrzkowski Z: Reversible inhibition of IL-8 receptor B mRNA expression and proliferation in non-small cell lung cancer by antisense oligonucleotides. Anticancer Res 16: 3525–3530, 1996
47. An Z, Wang X, Willmott N, Chander SK, Tickle S, Docherty AJP, Mountain A, Millican AT, Morphy R, Porter JR, Epemolu RO, Kubota T, Moossa AR, Hoffman RM: Conversion of highly malignant colon cancer from an aggressive to a controlled disease by oral administration of a metalloproteinase inhibitor. Clin Exp Metastasis 15: 184–195, 1997
48. Hoffman RM: Fertile seed and rich soil: The development of clinically relevant models of human cancer by surgical orthotopic implantation of intact tissue. In: Teicher B (ed) Anticancer Drug Development Guide: Preclinical Screening Clinical Trials, and Approval. Totowa, NJ: Humana Press Inc., 127–144, 1997
49. Chishima T, Miyagi Y, Wang X, Yamaoka H, Shimada H, Moossa AR, Hoffman RM: Cancer invasion and micrometastasis visualized in live tissue by green fluorescent protein expression. Cancer Res 57: 2042–2047, 1997
50. Inada T, Ichikawa A, Kubota T, Ogata Y, Moossa AR, Hoffman RM: 5-FU-induced apoptosis correlates with efficacy against human gastric and colon cancer xenografts in nude mice. Anticancer Res 17: 1965–1972, 1997
51. Chishima T, Miyagi Y, Wang X, Baranov E, Tan Y, Shimada H, Moossa AR, Hoffman RM: Metastatic patterns of lung cancer visualized live and in process by green fluorescent protein expression. Clin Exp Metastasis 15: 547–552, 1997
52. Chishima T, Miyagi Y, Wang X, Tan Y, Shimada H, Moossa AR, Hoffman RM: Visualization of the metastatic process by green fluorescent protein expression. Anticancer Res 17: 2377–2384, 1997
53. Chishima T, Yang M, Miyagi Y, Li L, Tan Y, Baranov E, Shimada H, Moossa AR, Penman S, Hoffman RM: Governing step of metastasis visualized *in vitro*. Proc Natl Acad Sci USA 94: 11573–11576, 1997
54. Tomikawa M, Kubota T, Matsuzaki SW, Takahasi S, Kitajima M, Moossa AR, Hoffman RM: Mitomycin C and cisplatin increase survival in a human pancreatic cancer metastatic model. Anticancer Res 17: 3623–3626, 1997
55. Chishima T, Miyagi Y, Li L, Tan Y, Baranov E, Yang M, Shimada H, Moossa AR, Hoffman RM: The use of histoculture and green fluorescent protein to visualize tumor cell host interaction. In Vitro Cell Dev Biol 33: 745–747, 1997
56. Chang S-G, Kim JI, Jung J-C, Rho Y-S, Lee K-T, An Z, Wang X, Hoffman RM: Antimetastatic activity of the new platinum analog {Pt(cis-dach)(DPPE)·$2NO_3$} in a metastatic model of human bladder cancer. Anticancer Res 17: 3239–3242, 1997
57. Dev SB, Nanda GS, An Z, Wang X, Hoffman RM, Hofmann GA: Effective electroporation therapy of human pancreatic tumors implanted in nude mice. Drug Delivery 4: 293–299, 1997
58. An Z, Wang X, Geller J, Moossa AR, Hoffman RM: Surgical orthotopic implantation allows high lung and lymph node metastatic expression of human prostate carcinoma cell line PC-3 in nude mice. Prostate 34: 169–174, 1998
59. Nanda GS, Sun FX, Hofmann GA, Hoffman RM, Dev SB: Electroporation therapy of human larynx tumors HEp-2 implanted in nude mice. Anticancer Res 18: 999–1004, 1998
60. Nanda GS, Sun FX, Hofmann GA, Hoffman RM, Dev SB: Electroporation enhances therapeutic efficacy of anticancer drugs: Treatment of human pancreatic tumor in animal model. Anticancer Res 18: 1361–1366, 1998
61. Yang M, Hasegawa S, Jiang P, Wang X, Tan Y, Chishima T, Shimada H, Moossa AR, Hoffman RM: Widespread skeletal metastatic potential of human lung cancer revealed by green fluorescent protein expression. Cancer Res 58: 4217–4221, 1998
62. Sun F-X, Sasson AR, Gamagami R, Jiang P, Moossa AR, Hoffman RH: An ultra-metastatic model of human colon cancer in nude mice. Clin Exp Metastasis 17(1): 41–48, 1999
63. Kiguchi K, Kubota T, Aoki D, Udagawa Y, Tamanouchi S, Saga M, Amemiya A, Sun F-X, Nozawa S, Moossa AR, Hoffman RM: A patient-like orthotopic implantation nude mouse model of highly metastatic human ovarian cancer. Clin Exp Metastasis 16: 75 1–756, 1999
64. Yang M, Jiang P, Sun FX, Hasegawa S, Baranov E, Chishima T, Shimada H, Moossa AR, Hoffman RM: A fluorescent orthotopic bone metastasis model of human prostate cancer. Cancer Res 59: 781–786, 1999
65. Wang X, An Z, Geller J, Hoffman RM: A high malignancy orthotopic nude mouse model of the human prostate cancer LNCaP. Prostate 39: 182–186, 1999
66. Kanai T, Konno H, Tanaka T, Matsumoto K, Baba M, Nakamura S, Baba S: Effect of angiogenesis inhibitor TNP-470 on the progression of human gastric cancer xenotransplanted into nude mice. Int J Cancer 71: 838–841, 1997
67. Konno H, Tanaka T, Kanai T, Masuyama K, Nakamura S, Baba S: Efficacy of an angiogenesis inhibitor, TNP-470, in xenotransplanted colorectal cancer with high metastatic potential. Cancer 77(8): 1736–1740, 1996
68. Konno H, Tanaka T, Matsuda I, Kanai T, Maruo Y, Nishino N, Nakamura S, Baba S: Comparison of the inhibitory effect of the angiogenesis inhibitor, TNP-470 and mitomycin C on the growth and liver metastasis of human colon cancer. Int J Cancer 11: 268–271, 1995
69. Konno H, Tanaka T, Baba M, Matsumoto K, Kamiya K, Nakamura S, Baba S, Arai T, Asano M, Suzuki H: Antitumor effect of angiogenesis inhibitors on colon cancer. Biotherapy 11: 993–996, 1997
70. Tanaka T, Konno H, Matsuda I, Nakamura S, Baba S: Prevention of hepatic metastasis of human colon cancer by angiogenesis inhibitor TNP-470. Cancer Res 55: 836–839, 1995
71. Konno H, Arai T, Tanaka T, Baba M, Matsumoto K, Kanai T, Nakamura S, Baba S, Naito T, Sugimura H, Yukita A, As-

ano M, Suzuki H: Antitumor effect of neutralizing antibody to vascular endothelial growth factor on liver metastasis of endocrine neoplasm. Jpn J Cancer Res 89: 933–939, 1998
72. Schabel FM: Animal Models as Predictive Systems in Cancer Chemotherapy Fundamental Concepts and Recent Advances, Year Book Publishers, pp. 323–355, 1975
73. Goldin A, Serpick AA, Mantel N: Experimental screening procedures and clinical predictability value. Cancer Chemother Rep 50: 173–218, 1966
74. Rygaard J, Povlsen CO: Heterotransplantation of a human malignant tumor to "nude" mice. Acta Pathol Microbiol Scan 77: 758–760, 1969
75. Ovejera A: The use of human tumor xenografts in large-scale drug screening. In Kalimann RF (ed) Rodent Tumor Model in Experimental Cancer Therapy, pp 218–220. Pergamon Press, NY, 1987
76. Fidler IJ: Critical factors in the biology of Human Cancer Metastases: twenty Eighth G.H.A Clowes memorial Award Lecture. Cancer Res 50: 6130–6138, 1990
77. Wilmans C, Fan D, O'Brian CA, Bucana CD, Fidler IJ: Orthotopic and ectopic organ environments differentially influence the sensitivity of murine colon carcinoma cells to doxorubicin and 5-fluorouracil. Int J Cancer 52: 98–104, 1992
78. An Z, Jiang P, Wang X, Moossa AR, Hoffman RM: Development of a high metastatic orthotopic model of human renal cell carcinoma in nude mice: Benefits of fragment implantation compared to cell-suspension injection. Clin Exp Metastasis 17: 265–270, 1999
79. Tanizawa A, Fujimori A, Fujimori Y et al.: Comparison of topoisomerase I inhibition, DNA damage, and cytotoxicity of camptothecin derivatives presently in clinical trials. J Natl Cancer Inst 86: 836–842, 1994
80. Cifuentes N, Pickren JW: Metastasis from carcinoma of mammary gland: an autopsy study. J Surg Oncol 11: 193–205, 1979
81. Mundy GR, Yoneda T: Facilitation and suppression of bone metastasis. Clin Orthop 312: 34–82, 1995
82. Guise TA: Parathyroid hormone-related protein and bone metastases. Cancer 80: 1572–1580, 1997
83. Olden K: Human tumor bone metastasis model in athymic nude rats. J Natl Cancer Inst 82: 340–341, 1990
84. Price JE, Polyzos A, Zhang RD, Daniels LM: Tumorigenicity and metastasis of human breast carcinoma cell lines in nude mice. Cancer Res 50: 717–721, 1990
85. Jia T, Liu YE, Liu J, Shi YE: Stimulation of breast cancer invasion and metastasis by synuclein-Γ. Cancer Res 5959: 742–747, 1999
86. Bagheri-Yarmand R, Kourbali Y, Rath AM, Vassy R, Martin A, Jozefonvicz J, Soria C, Lu H, Crepin, M: Carboxymethyl benzylamide dextran blocks angiogenesis of MDA-MB435 breast carcinoma xenograft in fat pad and its lung metastases in nude mice. Cancer Res 59: 507–510, 1999
87. Kurebayashi J, Nukatsuka M, Fujioka A, Saito H, Takeda S, Unemi N, Fukumori N, Kurosumi M, Sonoo H, Dickson RB: Postsurgical oral administration of uracil and tegafur inhibits progression of micrometastasis of human breast cancer cells in nude mice. Clin Cancer Res 3: 653–659, 1997
88. Thompson EW, Brunner N, Torri J, Johnson MD, Boulay V, Wright A, Lippman ME, Steeg PS, Clarke R: The invasive and metastatic properties of hormone-independent but hormone-responsive variants of MCF-7 human breast cancer cells. Clin Exp Metastasis 11: 15–26, 1993
89. Arguello FB, Baggs RB, Frantz CN: A murine model of experimental metastasis to bone and bone marrow. Cancer Res 48: 6876–6881, 1988
90. Sasaki A, Boyce BF, Story B, Wright KR, Chapman M, Boyce R, Mundy GR, Yoneda T: Bisphosphonate risedronate reduces metastatic human breast cancer burden in bone in nude mice. Cancer Res 55: 3551–3557, 1995
91. Morinaga Y, Fujita N, Ohishi K, Tsuruo T: Stimulation of interleukin-11 production from osteoblast-like cells by transforming growth factor-P and tumor cell factors. Int J Cancer 71: 422–428, 1997
92. Guise TA, Yin JJ, Taylor SD, Kumagai Y, Dallas M, Boyce BF, Yoneda T, Mundy GR: Evidence of causal role of parathyroid hormone-related protein in the pathogenesis of human breast cancer-mediated osteolysis. J Clin Invest 98: 1544–1549, 1996
93. Sung V, Gilles C, Murray A, Clarke R, Aaron AD, Azumi N, Thompson EW: The LCC1S-MB human breast cancer cell line expresses osteopontin and exhibits an invasive and metastatic phenotype. Exp Cell Res 241: 273–284, 1998
94. Wang CY, Chang YW: A model for osseous metastasis of human breast cancer established by intrafemur injection of the MDA-MB-435 cells in nude mice. Anticancer Res 17: 2471–2474, 1997
95. Stephenson RA, Dinney CPN, Gohji K, Ordonez NC, Kilion JJ, Fidler IJ: Metastasis model for human prostate cancer using orthotopic implantation in nude mice. J Natl Cancer Inst 84: 951–957, 1992
96. Pettaway CA, Pathak S, Greene G, Ramirez E, Wilson MR, Killion JJ, Fidler IJ: Selection of highly metastatic variants of different human prostatic carcinomas using orthotopic implantation in nude mice. Clin Cancer Res 2: 1627-1636, 1996
97. Saito N, Gleave ME, Bruchovshy N, Rennie PS, Beraldi E, Sullivan LD: A metastatic and androgen-sensitive human prostate cancer model using intraprostatic inoculation of LNCaP cells in SCID mice. Cancer Res 57: 1584–1589, 1997
98. Rembrink K, Romijn JC, van der Kwast TH, Rubben H, Schroder FH: Orthotopic implantation of human prostate cancer cell lines: a clinically-relevant animal model for metastatic prostate cancer. Prostate 31: 168–174, 1997
99. Thalmann GN, Anezinis PE, Chang SM, Zhau HE, Kim EE, Hopwood VL, Pathak S, Eschenbach ACV, Chung WK: Androgen-independent cancer progression and bone metastasis in the LNCaP model of human cancer. Cancer Res 54: 2577–2581, 1994
100. Lin WC, Pretlow TP, Pretlow TG, Culp LA: Bacterial lacZ gene as a highly sensitive marker to detect micrometastasis formation during tumor progression. Cancer Res 50: 2808–2817, 1990
101. Lin WC, Culp LA: Altered establishment/clearance mechanisms during experimental micrometastasis with live and/or disabled bacterial lacZ-tagged tumor cells. Invasion & Metastasis 12: 197–209, 1992
102. Morin J, Hastings J: Energy transfer in a bioluminescent system. J Cell Physiol 77: 313–318, 1972
103. Chalfie M, Tu Y, Euskirchen G, Ward, WW, Prasher DC: Green fluorescent protein as a marker for gene expression. Science 263: 802–805, 1994
104. Cheng L, Fu J, Tsukamoto A, Hawley RG: Use of green fluorescent protein variants to monitor gene transfer and expression in mammalian cells. Nature Biotechnol 14: 606–609,1996

105. Prasher DC, Eckenrode VK, Ward WW, Prendergast FG, Cormier MJ: Primary structure of the Aequorea victoria green-fluorescent protein. Gene 111: 229-233, 1992
106. Yang F, Miss LG, Phillips GN Jr: The molecular structure of green fluorescent protein. Nature Biotechnol 14: 1252–1256, 1996
107. Cody CW, Prasher DC, Welstler VM, Prendergast FG, Ward WW: Chemical structure of the hexapeptide chromophore of the Aequorea green fluorescent protein. Biochemistry 32: 1212–1218, 1993
108. Heim R, Cubitt AB, Tsien RY: Improved green fluorescence. Nature 373: 663–664, 1995
109. Delagrave S, Hawtin RE, Silva CM, Yang MM, Youvan DC: Red-shifted excitation mutants of the green fluorescent protein. Bio/Technology 13: 151–154, 1995
110. Cormack B, Valdivia R, Falkow S: FAGS-optimized mutants of the green fluorescent protein (GFP). Gene 173: 33–38, 1996
111. Zolotukhin S, Potter M, Hauswirth WW, Guy J, Muzycka N: 'Humanized' green fluorescent protein cDNA adapted for high-level expression in mammalian cells. J Virology 70: 4646–4654, 1996
112. Wang X, Fu X, Hoffman RM: A new patient-like metastatic model of human lung cancer constructed orthotopically with intact tissue via thoracotomy in immunodeficient mice. Int J Cancer 51: 992–995, 1992
113. Naumov GN, Wilson SM, MacDonald IC, Schmidt EE, Morris VL, Groom AC, Hoffman RM, Chambers AF: Cellular expression of green fluorescent protein, coupled with high-resolution *in vivo* videomicroscopy, to monitor steps in tumor metastasis. J Cell Sci 112: 1835–1842, 1999
114. Kan Z, Liu T-J: Video microscopy of tumor metastasis: using the green fluorescent protein (GFP) gene as a cancer-cell-labeling system. Clin Exp Meta 17: 49–55, 1999
115. Stewart TA, Pattengale PK, Leder P: Spontaneous mammary adenocarcinomas in transgenic mice that carry and express MTV/myc fusion genes. Cell 38: 627–637, 1984
116. Sinn E, Muller W, Pattengale P, Tepler I, Wallace R, Leder P: Coexpression of MMTV/v-Ha-ras and MMTV/c-myc genes in transgenic mice: synergistic action of oncogenes *in vivo*. Cell 49: 465–475, 1987
117. Guy CT, Cardiff RD, Muller WJ: Induction of mammary tumors by expression of polyomavirus middle T oncogene: a transgenic mouse model for metastatic disease. Mol Cell Biol 12: 954–961, 1992
118. Ritland SR, Rowse GJ, Chang Y, Gendler SJ: Loss of Heterozygosity Analysis in Primary Mammary Tumors and Lung Metastases of MMTV-MTAg and MMTV-*neu* Transgenic Mice. Cancer Res 57: 3520–3525, 1997
119. Guy CT, Webster MA, Schaller M, Parsons TJ, Cardiff RD, Muller, WJ: Expression of the *neu* protooncogene in the mammary epithelium of transgenic mice induces metastatic disease. Proc Natl Acad Sci USA 89: 10578–10582, 1992
120. Leder A, Pattengale PK, Kuo A, Stewart TA, Leder P: Consequences of Widespread Deregulation of the *c-myc* Gene in Transgenic Mice: Multiple Neoplasms and Normal Development. Cell 45: 485–495, 1986
121. Greenberg NM, DeMayo F, Finegold MJ, Medina D, Tilley WD, Aspinall JO, Cunha GR, Donjacour AA, Matusik RJ, Rosen JM: Prostate cancer in a transgenic mouse. Proc Natl Acad Sci USA 92: 3439–3443, 1995
122. Gingrich JR, Barrios RJ, Morton RA, Boyce BF, DeMayo FJ, Finegold MJ, Angelopoulou R, Rosen JM, Greenberg NM: Metastatic prostate cancer in a transgenic mouse. Cancer Res 56: 4096–4102, 1996
123. Gingrich JR, Barrios RJ, Kattan MW, Nahm HS, Finegold MJ, Greenberg NM: Androgen-independent Prostate Cancer Progression in the TRAMP Model Cancer Res 57: 4687–4691, 1997
124. Zhu Y, Richardson JA, Parada LF, Graff JM: Smad3 Mutant Mice Develop Metastatic Colorectal Cancer. Cell 94: 703–714, 1998
125. Donehower LA, Harvey M, Slagle BL, McArthur MJ, Montgomery CA Jr, Butel JS, Bradley A: Mice deficient for p53 are developmentally normal but susceptible to spontaneous tumors. Nature 356: 215–221, 1992

Address for offprints: Robert M. Hoffman, AntiCancer, Inc., 7917 Ostrow Street, San Diego, CA 92111, USA; Fax: 858-268-4175; e-mail: all@anticancer.com

THIS PAGE BLANK (USP